Microbial Desulphurization of Combustion Coal and Environmental Control in Carbonization Coal: Emissions Reduction Techniques

Submitted By

Seshibe Stanford Makgato

A thesis submitted to the Faculty of Engineering, Built Environment and Information Technology in the fulfilment of the requirements for the degree

Doctor of Philosophy (Chemical Engineering)

at the

UNIVERSITY OF PRETORIA

Supervisor

Prof Evans M.N. Chirwa

April 2020

Microbial Desulphurization of Combustion Coal and Environmental Control in Carbonization Coal: Emissions Reduction Techniques

Author : Seshibe Stanford Makgato

Supervisor : Professor Evans M. N. Chirwa

Department : Chemical Engineering

University : University of Pretoria

Degree : Doctor of Philosophy (Chemical Engineering)

Coal use in electricity generation has attracted much attention recently mainly due to the sector been identified as the main source of sulphur dioxide (SO_2) emissions globally. The combustion of coal releases sulphur dioxide emissions into the atmosphere that create air pollution and cause harmful effects on the ecosystem. In the current study, biodesulphurization of Waterberg steam coal was investigated using a bacterial consortium isolated from coal. Coal samples were obtained from the coal feed into the power plant mills, by auto sampling equipment. Coal samples with various particle size fraction of +4.60 mm, −4.60 + 2.30 mm, −2.30 + 1.00 mm and −0.85 mm were used in the biodesulphurization experiments. The characteristic properties of the coal samples were analysed by means of a number of techniques, including Leco S-628 Elemental analyser, UV Spectrophotometry, bomb calorimeter and X-Ray Fluorescence. The contribution of this study to the country's minimum emissions requirements and compliance could be outlined as follows: Coal was classified as medium sulphur coal when the sulphur content was detected in the range 1.15 – 1.49 wt.%. Four forms of sulphur - pyrite, mineral/sulphide sulphur, inorganic sulphates and organic sulphur were present in Waterberg coal with pyritic sulphur (≥ 0.51 wt.%) and organic sulphur (≥ 0.49 wt.%) accounting for the bulk of the total sulphur in coal.

Results from biodesulphurization treatment study showed reduction efficiencies of 70.3%, 51.0% and 43.8% for pyritic sulphur, organic sulphur and sulphide sulphur respectively with

18 days treatment. However, as the temperature increased from 23 ± 3 °C to 30 ± 2 °C, biodesulphurization efficiencies of 81%, 44%, and 67% were achieved for pyritic sulphur, sulphide sulphur and organic sulphur form respectively. On the other hand, the overall biodesulphurization efficiencies for – 0.85 mm, – 2.30 +1.00 mm, – 4.60 +2.30 mm and +4.60 mm particle sizes were found to be 65.4%, 53.8%, 49.2% and 23.6% respectively being reached after 18 days. When the temperature was increased from 23 ± 3 °C to 30 ± 2 °C, overall process efficiency for – 0.85 mm particle size fraction improved further to 72.4 %. The process of biodesulphurization reduced the ash content by some 33% and concomitantly improved the calorific value by 19%. The decrease in ash content due to biodesulphurization treatment is desirable given that improved combustion of the coal would be expected, and a lower amount of ash will need to be discarded, thus imparting a positive impact on the environment, and a reduction in operational costs such as the transportation of ash to dump site.

Maceral analyses of coal showed that inertinite was the dominant maceral (up to 48 vol.%), whereas vitrinite and liptinite occurred in proportions of 22 vol.% and 4 vol.% respectively. Theoretical calculations were developed, verified at the existing plant and used to predict the resultant SO_2 emissions from the combustion of the Waterberg coal in a typical power plant. The sulphur content requirements for Waterberg coal to comply with the minimum emissions standards of 3500 mg/Nm^3 and 500 mg/Nm^3 were established to be ≤1.37 wt.% and ≤0.20 wt.%, respectively. Microbial growth solution pH varied in the range of 3.0 – 6.5. Seven isolates after purification of the most dominant colonies, viz: *Pseudomonas sp, Pseudomonas aeruginosa, Pseudomonas putida; Pseudomonas stutzeri, Bacillus sp., Pseudomonas rhizosphaerae and Pseudomonas alcaligenes* were identified. The achieved sulphur reduction of 0.50 wt.%, 0.65 wt.%, 0.73 wt.% and 1.1 wt.% for – 0.85 mm, – 2.30 + 1.00 mm, – 4.60 + 2.30 mm and +4.60 mm particle sizes respectively shows that reduction of total sulphur by biodesulphurization is possible, and significantly so.

The last part of the part one of the studies involved the development of a kinetic model based on the simulation of the microbial desulphurization process in a CSTR reactor setup. The model was then validated under various experimental conditions. The values of the kinetic parameters (K_s *and* k_{mc}) in the batch study were determined from the experimental data. These results are statistical correct since the regression coefficients R are above 97 % and all

R^2 are above 95 %. However, the biodesulphurization rate coefficient, k_{mc} was determined to be very low. This indicates that sulphur reduction happened faster during exponential phase. These kinetic parameters could not generate a unique representative model for all studied coal particle sizes. The results also show that K_c values obtained from the non-linear regression were not constant and were shown to be much higher than S_T values (Kc >> Co). From these results, it can be noticed that the fitting between the model-simulated and the experimental data is satisfactory. Though different from the sulphur and the ash contents, the experimental data for CV values were found to correlate well with a second-order rate equation.

Part two of the study focused on carbonization tar waste minimization and dust reduction during coke production. The use of coal fines in coke making process has lately become a problem worth addressing due to its negative impact on ecosystems, its tendency to ignite explosively causing coal losses and plant equipment damages. In addition, the use of coal fines is becoming an issue due to high Quinoline Insoluble formation during the carbonization process as well as carryover or enhancement of carbon deposition in the upper parts of the coke ovens. In this study, the effect of carbonization tar addition over a range of 2.0 – 8.0 wt.% was evaluated as a probable partial substitute for expensive coking coals by assessing coal fines reduction, coal blend cost analysis, extended coke production and coke quality. At the optimum condition of adding 6.0 wt.% carbonization tar, key coke qualities were improved. Coke quality results obtained in this study were comparable to international benchmarks. Furthermore, a 56.8 wt.% reduction in coal fines (powder) was observed. By reducing coal fines, there is a considerable reduction in coal dust that personnel are exposed to and a reduction in acid mine drainage as well as a decreased likelihood of spontaneous combustion. In addition, coal dust can cause pneumoconiosis and other health – related conditions. Savings of up to USD 1.7 million per year were postulated and supported by mathematical models used to calculate the cost-effectiveness of such a project. Vital factors for coking pressure such as maximum dilatation and maximum contraction increased within the acceptable range of <30 and < 20 respectively. High coking pressures cause operational problems such as stickers and heavy-pushes, which result in the deterioration of the brick lining of the coke oven walls. Therefore, it is desirable that carbonization tar increase coking pressure within the acceptable range so that the life span of the coke ovens is not shortened.

Therefore, recycling carbonization tar has a great realistic significance in saving coal resources and protecting personnel, process safety and the environment.

Keywords: Emissions; Sulphur dioxide; Desulphurization; Coal; Carbonization; Oven charging

DECLARATIONS

I Seshibe Stanford Makgato, declare that the thesis to which I hereby submit for a Doctor of Philosophy in Chemical Engineering at the University of Pretoria is my own work and has not been previously submitted by me for any degree at this or any other institution.

Makgato Seshibe Stanford Date

DEDICATION

This thesis is lovingly dedicated to my wife, Malebo - who has encouraged me all the way to ensure that I give it all it takes to finish that which I have started. Honey, my love for you can never be quantified. I'm a lucky man - I hope to return the favor when you pursue your own doctorate;

This thesis is also dedicated to both my parents - My father, the late Mothibi Alfred Makgato who did not only raise and nurture me but also taxed himself dearly over the years for my education and intellectual development. Robala ka khutso Tau! My mother, Moyahabo Legina Makgato - her support, encouragement, and constant love has sustained me throughout my life. You have actively supported me in my determination to find and realize my potential, and to make this contribution to our world. Kea leboga Mokwena!

Furthermore, I am dedicating this thesis to five beloved people who have meant and continue to mean so much to me. Although they are no longer of this world, their memories continue to regulate my life.

- To my two late brothers Mothabela Jackson Makgato and Mohololo Abram Makgato who left a void never to be filled in my life. I always feel their presence that used to urge me to strive to achieve my goals in life. Ditau, you have always had confidence in me and offered me encouragement and support in all my endeavours. Robalang ka khutso Ditau.
- To my late maternal grandmother, Mahlodi Ester Ramaotswa who raised me, loved me unconditionally and has taught me to work hard for the things that I aspire to achieve. She taught me to persevere and prepared me to face the challenges with faith and humility. You have been a constant source of inspiration to my life. Robala ka khutso Tau!
- My gratitude is also extended to my late paternal grandmother, Rosina Mampai Makgato, Koko, you have been a source of encouragement and inspiration to me throughout. Robala ka khutso Tlou.
- To the late Maphuti Regina Moja, whose words of encouragement and push for tenacity ring in my ears. You were one in a million and may your soul rest in peace.

ACKNOWLEDGEMENT

Without the strength, wisdom, and grace bestowed upon me by my God, this thesis would not have been possible. Through His grace, I can do all things through Christ who gives me the strength.

Without the support of many people the completion of this project would never have occurred. I wish to express my sincere appreciation and thanks to the following people:

- My thanks and appreciation to my supervisor, Prof Evans. M. Nkhalambayausi Chirwa who challenged me to do the best that I could do. His brilliant mind, razor-sharp wit, and unflagging willingness to help did make this project fun. Thank you Prof Chirwa, now and always.

- To my children (Neo Kwena, Lethabo Victoria, Moyahabo Praise and Mothabela Tshegofatso), who have been affected in every way possible by this quest to complete a Ph.D, may you also be encouraged to reach your dreams.

- I am most grateful to the Management Committee of Eskom Medupi Power Station Generation for allowing me to conduct my research and providing me with permission to use the power station coal samples for study purposes.

- Special thanks go to the University of Pretoria, South Campus colleagues for their continued support while carrying out this research.

- Special thanks go to Dr Nthabiseng Maledi of the University of The Witwatersrand who always gave excellent suggestions and lots of support. Thank you Dr Maledi for your willing help and encouragement during this process and over the years.

- I would like to express my special thanks to Dr Nandi Malumbazo and her team at the Council of Geoscience and Dr Samson Bada of the University of The Witwatersrand for conducting both proximate and ultimate analyses.

- Special thanks go to Prof Venus Venter of the Department of Microbiology and Inqaba Biotechnical Industries for carrying out 16SrRNA gene sequencing for bacterial identification.

- I am extremely grateful to Prof Nicola Wagner of the University of Johannesburg for carrying out coal petrography analyses.

- I would like to express my special thanks to Mr Vongani Chabalala and his team at SABS, Minerals and Mining Division for conducting coal petrography, proximate and ultimate analyses as well as sulphur forms analyses.

- Thanks also to my friends and colleagues who I have not mentioned by name, I am grateful for the innumerable demonstrations of kindness and encouragement you have shown me.

- Last, but never least, my siblings, Mr Motlatso Lawrence Makgato, Ms Mosima Francinah Makgato and Mr Llema Martin Makgato who were always there for me when I needed them. Thank you for your help, support, and love. I am the luckiest person in the world to have you in my life.

TABLE OF CONTENTS

LIST OF FIGURES

LIST OF TABLES

LIST OF ABBREVIATIONS AND ACRONYMS

A	Ash
ASTM	American Society for Testing and Materials
B_E	Break-even
BMM	Basal mineral medium
c	constant
C	Carbon
C	Maximum Contraction
CRI	Coke Reactivity Index
CSR	Coke Strength after Reaction
CSTR	completely stirred tank reactor
CV	Calorific Value
D	Maximum Dilatation
db	Dry Basis
DBT	dibenzothiophene
Ddpm	Dial Division per Minute
DszA	DBT-sulfone monooxygenase
DszB	hydroxybiphenyl desulphinase
DszC	Sulphoxide monooxygenase
DszD	flavin reductase
F_C	fixed cost
FC	Fixed Carbon
FGD	Flue Gas Desulphurization
FID	flame ionization detector
FMN	flavin mononucleotide
$FMNH_2$	flavin mononucleotide reduced form
FSI	Free Swelling Index
GC-MS	Gas Chromatograph coupled with Mass Detector
H	Hydrogen
h	hour
i.d	internal diameter
ISO	International Organization for Standardization
j	analysis year

LB	Luria-Bettani
N	Nitrogen
NCBI	National Centre for Biotechnology Information
NPV	net present value of the capital investment
O	Oxygen
SG	Specific Gravity
min	minutes
MIT	Matter Insoluble in Tar
Mw	Molecular Weight
MW	Megawatt
n	the number of coals blended
n.a	not available
NZ	New Zealand
NPV	net present value of the capital investment
PSD	The particle size distribution
QI	Quinoline Insoluble
r.p.m	revolution per minute
RSA	Republic of South Africa
RSF	Reactive semifusinite
RT	Retention Time
RT–PCR	reverse transcriptase-polymerase chain reaction
R_oVr	Reflectance
RXN	Reaction
S	Sulphur content in the coal (wt.%, db)
SANS	South African National Standard
SD	Standard Deviation of Reflectance
SG	Specific Gravity
S_j	cash flows received at time *j*
S_P	Selling price
$S_{Untreated\ coal}$	the total sulphur, an ash content of untreated coal
$S_{Treated\ coal}$	is the total sulphur, an ash content of treated coal
S_{IN}	Sulphide/ mineral sulphur (wt.%, db)
S_{PYR}	Pyritic sulphur (wt.%, db)

S_S	Sulphate sulphur (wt.%, db)
S_{ORG}	Organic sulphur (wt.%, db)
S_T	Total sulphur (wt.%, db)
T, n	Time in any day
T_1	Softening Temperature
T_2	Maximum Contraction Temperature
T_3	Maximum Dilatation Temperature
USA	United States of America
USD	United States Dollar
UV	Ultraviolet
V	Vitrinite
VM	Volatile Matter
vol.%	Volume percentage
V_P	variable price
wt.%	Weight percentage
XRF	X-ray Fluorescence

Symbols:

c	rate that equates the present value of positive and negative cash flows
η	Efficiency (%)
σ	Coefficient of CV variation (MJ/kg)
μ	mass of coal burnt (kg/h)
$\sum F$	Sum of Flue Gas Product or the emissions of total flue gas (Sm^3/h)
Y	form of sulphur
z	distribution factor/ gradient

$\sum F(a,b,c...n)$ the sum of Flue Gas products (in Sm^3/h)

$\sum(a,T_1;b,T_2;c,T_3...k,T_{11})$ sum of daily ash decrease over the biodesulphurization period

m	gradient or distribution factor
k	the first-order rate constant
S_{Feed}	sulphur form in the coal feed (wt.%)

vol.%	Volume percentage
wt.%	Weight percentage
Y	Form of sulphur (wt.%)
t	Time in days
w	The initial amount of total sulphur in the coal
k_{ms}	Maximum specific reaction rate coefficient
Kc	Half velocity concentration
X_0	Initial viable cells concentration in the reactor
Z_i	The property such as ash content, sulphur content and volatile matter content of the coal blend
Z_a and x_i	The property and the percentage mass fraction of coal i respectively
Z	The experimental value
Z'	The predicted

CONTRIBUTIONS

1. Makgato S. S., Chirwa E. M. N. (2017). Characteristics of Thermal Coal used by Power Plants in Waterberg Region of South Africa. **Chemical Engineering Transactions, ISSN 2283-9216**, Vol. 57: 511 – 516.

2. Makgato Stanford. S., Chirwa Nkhalambayausi. E. M. (2017), Waterberg Coal Characteristics and SO_2 Minimum Emissions Standards in South African Power Plants. **Journal of Environmental Management, ISSN 0301-4797.** Vol 201: 294 – 302.

3. Makgato S., Chirwa E. (2018), Desulphurization of Medium Sulphur Waterberg Steam Coal in a Batch Operated Scale: Microbial Solution. **Chemical Engineering Transactions, ISSN 2283-9216,** Vol. 64: 523 – 528.

4. Makgato S.S., Chirwa E.M.N. (2018), Pre-Combustion Technique for Desulphurization of Waterberg Coalfield: Biological Treatment. Oral Presentation – WM2018 Conference, March 18 – 22, 2018, Phoenix, Arizona, USA, pp. 1 – 9.

5. Chirwa E.M.N., Makgato S.S., Tikilili P.V., Lutsinge T.B. (2018). Bioremediation of Chlorinated and Aromatic Petrochemical Pollutants in Multi-Phase Media and Oily Sludge. In Bharagava R.N., (Ed.), Environmental Pollution and Mitigation, **Book Chapter. 16,** pp. 367– 384, CRC Press, Springer International, New York, NY, USA.

6. Makgato Stanford S., Chirwa Evans M.N. (2018), Performance Evaluation of Microbial Desulphurization of Waterberg Steam Coal as a Pre-Combustion Technique. **Chemical Engineering Transactions, ISSN 2283-9216**, Vol. 70: 553 – 558.

7. Evans M. N. Chirwa, Pulane E. Molokwane, Phumza V. Tikilili, Stanford S. Makgato, Emomotimi E. Bamuza-Pemu, Lindelwa Jay. (2018), Biological remediation and removal of radioactive metals and complex aromatic compounds from nuclear and radioactive waste. **Chemical Engineering Transactions, ISSN 2283-9216**, Vol. 70: 85 – 90.

8. S.S. Makgato, R.M.S. Falcon, E.M.N. Chirwa, (2019), Reduction in coal fines and extended coke production through the addition of carbonization tar: Environmentally clean process technology. **Journal of Cleaner Production, ISSN 0959-6526**, Vol. 221: 684 – 694.

9. S.S. Makgato, R.M.S. Falcon, E.M.N. Chirwa, (2019), The effect of recycling carbonization tar on environmental pollution, coke quality, personnel and process safety. **Journal of Process Safety and Environmental Protection, ISSN: 0957-5820**, Vol. 126: 141 – 149.

10. Seshibe S. Makgato, Evans M. N. Chirwa (2019), Modeling Performance Evaluation of Microbial Desulphurization of Waterberg Steam Coal in CSTR. **Chemical Engineering Transactions, ISSN 2283-9216**, Vol. 76: 145 – 150.

11. S.S. Makgato, E.M.N. Chirwa, (2020), The Desulphurization Potential of Waterberg Steam Coal using Bacteria Isolated from Coal: The SO_2 Emissions Control Technique. **Journal of Cleaner Production, ISSN 0959-6526**, Vol. 263: 121051.

12. S.S. Makgato, E.M.N. Chirwa, (2020), Recent Developments in Reduction of Sulphur Emissions from Selected Waterberg Coal Samples used in South African Power Plants. **Journal of Cleaner Production, ISSN 0959-6526**, Vol. 276: 123192.

CHAPTER 1
INTRODUCTION

1.1 Background

The supply of energy in South Africa depends significantly on coal as the dominant primary energy source and will continue to do so for the near future. The deployment of renewables to replace coal is hindered by their unreliability and concerns over present power lines and infrastructure needed to move electricity to consumers. The current power lines and infrastructure were built to receive and transmit power generated in coal-fired mainly situated in the Highveld areas, Mpumalanga, Gauteng and the North West provinces. Since the early 1900's, coal has remained the driving force of the South African economy. According to Ozonoh et al. (2018), almost about 95% of electricity generation in South Africa is from coal-fired power plants. Coal use in electricity generation has attracted much attention recently mainly due to the sector been identified as the main source of Sulphur dioxide (SO_2) emissions globally (Barreira et al., 2017). During combustion, organic and pyrolytic sulphur compounds in coal are readily oxidized to SO_X species due to the presence of oxygen in the air and high temperatures. The SO_X species such as SO_2 readily react with H_2O in the atmosphere to form acid rain that is detrimental to plant, animal life (Ozonoh et al., 2018) and water pollution (Hu et al., 2018). Additional issues including human health such as chronic respiratory illnesses (Mketo et al., 2016), sulphate aerosols from S (0)/S (-2) oxidation causing corrosion (Zhao et al., 2008), abrasion, fouling and slagging of metal bodies (Mketo et al., 2016) as well as and boiler tubes leaks (Saikia et al., 2013) also add to the list of concerns

The development of alternative technologies that can desulphurize coal has been a focused topic among the scientific community. Among the microbial, chemical and physical methods for coal desulphurization, microbial treatment emerges as a clean, less energy – intensive, efficient and environmentally reasonable technique with low capital and operating costs (Gonsalvesh et al., 2012). Microbial treatment is based on certain microorganism's ability to metabolize some stable sulphur – containing compounds or degradation of sulphur compounds by microorganisms. Therefore, it is noticeable that certain bacteria exist with demonstrated strong abilities to oxidation and metabolism of sulphur content in the coal and to use the energy released to support their growth (Ghosh and Dam, 2009). Among all the reported work on coal desulphurization, only one microbial treatment of coal has been

successful - the removal of pyritic sulphur. Various authors (Huifang and Yagin, 1993; Dong-chen et al., 2009; Mishra et al., 2014) have reported the reduction of pyritic Sulphur using several bacterial and fungal strains. Although pyritic sulphur is the dominant sulphide mineral in the Waterberg coals, organic sulphur also exist in a greater proportion (Wagner and Tlotleng, 2012).

Very few attempts were made on desulphurization of other forms of sulphur content like organic sulphur. Most of the organic sulphur reduction studies were carried out using a model compound such as dibenzothiophene (Gonsalvesh et al., 2012; Mishra et al., 2014; Han et al., 2018) which is recognized to behave differently to the actual sulphur in the coal. Of the little simultaneous microbial desulphurization of sulphur forms attempted, the application has been on lignite type only (Aytar et al. 2011). The main difference between lignite and the Waterberg steam coal lies in the rank of the coal, with the Waterberg coal being a bituminous coal, higher in rank than the lignite. In addition, the Waterberg coal studied reported comparatively higher in calorific value (CV), ash, sulphur and nitrogen contents. Therefore, despite the plethora of desulphurization studies that have made epigrammatic progress, there is still limited information provided by the current literature for biodesulphurization application of all sulphur forms in coal studies. The novelty of the current study compared to the state of the art consists of bacteria isolated from coal been used for the first time towards simultaneous biodesulphurization of various forms of sulphur in the Waterberg steam coal. Waterberg steam coal is unique in various aspects on high sulphur Indian coals dominating the literature (Saikia et al., 2013, 2014a; 2014b). Furthermore, the Waterberg steam coal is one of the remaining large resources of South Africa's remaining coal reserves (Eberhard, 2011). Therefore, biodesulphurization of Waterberg steam coal is a new contribution to clean coal technologies research with the intention to reduce SO_2 emissions spikes from the power plant.

1.2. Problem Statement

Currently, the minimum emissions standards (MES) which are being applied in several countries have put combustion, metallurgical industries and gasification coal users under increasing pressure to decrease high SO_2 emissions level in their operations. According to Dahiya and Myllyvirta (2019), the Mpumalanga area in South Africa is the second highest SO_2 emissions hotspot in the world after giant nickel smelters at Norilsk in Russia, (Fig.1.1).

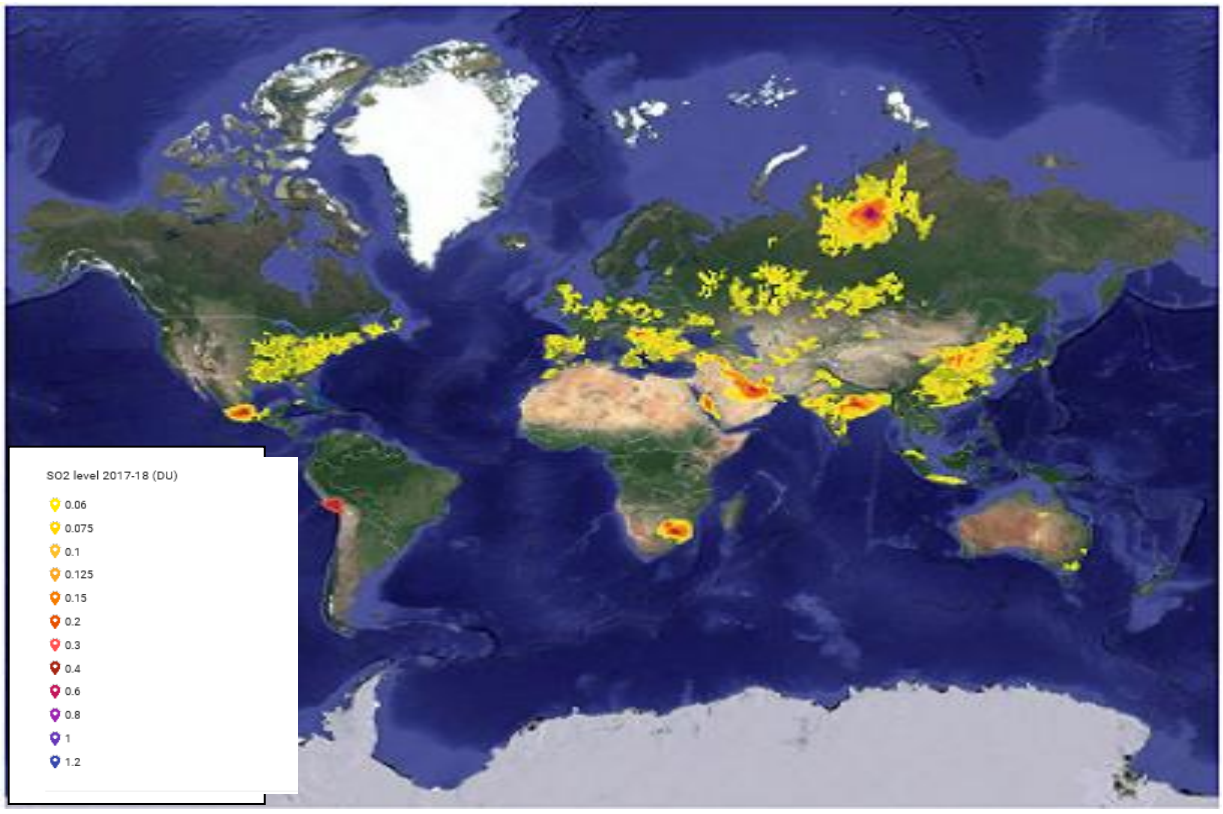

Figure 1.1: Highest SO_2 emissions hotspot in the world (Dahiya and Myllyvirta, 2019)

Combustion accounts for 42% while gasification emits 11% of South Africa's total SO_2 emitted. Governments of many developed and developing nations that put power producers under increasing pressure to reduce high SO_2 emissions in their operations have recommended the minimum emissions standards. In South Africa, minimum emissions standards for environmental protection are providing a need to comply with SO_2 emissions of 3500 mg/Nm^3 and 500 mg/Nm^3 by 2020 and 2025 respectively (Government Notice No. 248, 2010). There are heavy financial penalties associated with exceeding regulatory limits for minimum emissions standards for SO_2 emissions. According to Liu et al. (2016), it is estimated that SO_2 emission from the coal-fired power plant is charged at 0.63 Yuan per ton in China. In South Africa, violations of air quality licenses are criminal offences under Air Quality Act and on conviction, the company including its directors, could be liable for a USD 264 000 fine and/or 5 years' imprisonment, per offence.

For this purpose, South African electricity public utility, Eskom resolved to install flue gas desulphurization (FGD) technology for new boilers and wherever necessary to retrofit on the existing boilers. Globally, retrofit investments of the FGD units are incredibly high (Kılıç *et al.*, 2013). The primary reason is the time elapse of the contract and construction time shift. Furthermore, the difference in the exchange rate and escalated investment budgets throughout construction time also play a vital role. Therefore, adding an FGD installation typically increases the total costs of a power plant by one-third (Qian and Zhang, 1998). This is excessively expensive to the South African power utility, as electricity is sold at state – regulated low prices. Despite the good performance of the FGD system so far, the technology still greatly suffered from gypsum waste disposal, high volume of effluent (Liu et al., 2017), chemicals used can harm humans (Saikia et al., 2014a), high chemicals consumption (Mketo et al., 2016), being expensive regarding capital and operating cost as well as technically difficult to retrofit on existing plants. Additionally, the FGD process brings about effluent with high concentrations of the cationic and anionic impurities as well as heavy metals. Furthermore, using FGD requires that limestone be brought in from Northern Cape mines that are situated about a thousand kilometers away from Eskom's power plants. In addition, most of the coal-fired power plants have already passed their design half–life of 50 years while many will reach their end of life between now and the year 2045. Table 1.1 shows installed capacity and the age of coal-fired power plants for Eskom. Therefore, the strongest drive for the reduction of sulphur in coals is owing to the environmental guidelines hence sulphur reduction technologies have to be implemented in order for these plants to remain in operation for the remaining of their life. After taking all of these points into consideration, an economically viable pre-combustion desulphurization technique is required, by which the original properties of the parent coal are retained.

Table1.1: Installed capacity and the age of power station (Eskom, 2015)

Power Station	Years commissioned First to the last unit	Years in operation	Installed capacity of generator sets (MW)
Arnot	Sep 1971 to Aug 1975	44	1 × 370; 1 × 390; 4 × 400
*Camden	Aug 1967 to Sep 1969	50	3 × 200; 4 × 195; 1 × 185
Duvha	Aug 1980 to Feb 1984	35	6 × 600
Grootvlei	Jun 1969 to Nov 1977	42	4 × 200; 2 × 190
Hendrina	May 1970 to Dec 1976	43	5 × 200; 2 × 195; 3 × 170
Kendal	Oct 1988 to Dec 1992	27	6 × 686
*Komati	Nov 1961 to Mar 1966	54	4 × 100; 4 × 125; 1 × 90
Kriel	May 1976 to Mar 1979	40	6 × 500
Kusile	Under construction	0	6 × 800
Lethabo	Dec 1985 to Dec 1990	29	6 × 618
Majuba	Apr 1996 to Apr 2001	18	3 × 657; 3 × 713
Matimba	Dec 1987 to Oct 1991	28	6 × 665
Matla	Sep 1979 to Jul 1983	36	6 × 600
Medupi	Under construction	0	6 × 794
Tutuka	Jun 1985 to Jun 1990	29	6 × 609

* Moth-balled power stations that have been returned to service

1.3 Scope of the Study

In this study, the sulphur content in the thermal coal is reduced through microbial pre-combustion technique and coke production is extended through the addition of carbonization tar in the coal blend. Therefore, microbial desulphurization of the thermal coal and the effect

of carbonization tar addition on coking coal blend experiments were conducted. The study is composed of five parts:

- Waterberg thermal coal characterization with regard to SO_2 minimum emissions standards.
- Isolation of sulphur reducing bacterial strain, thermal coal desulphurization laboratory – scale performance evaluation experiments and optimization.
- Biodesulphurized Waterberg thermal coal characterization.
- Simulation of microbial desulphurization performance evaluation and key kinetics parameters estimation.
- Developing an effective coal fines reduction and carbonization tar disposal strategy through recycling in coking coal blends (Pilot plant and full-plant scale trials).

1.4 Research Hypothesis

In the current study, it is hypothesized that (a) reducing coal particle size exposes sulphur forms in the coal for effective use of microbial desulphurization, (b) simultaneous de-ashing and microbial desulphurization of power station coal with improved calorific value (CV) is possible and is a function of coal particle size, and (c) Recycling carbonization tar back in the process will improve coke quality, preserve coking coals and protect the environment.

1.5 The Objectives of the Current Study

1.5.1 General Objectives

The study consists of two parts. In the first part, the aim of the research is to investigate the feasibility using microorganisms desulphurization of coal as a pre-combustion technique such that flue gas desulphurization requirement is no longer an option for the power generation industry. In the second part, special emphasis was placed on carbonization tar recycling, coal fines reduction, coal blend cost analysis, extended coke production and improved coke quality as well as economic assessment studies. In order to achieve this objective, the following tasks must be met:

1.5.2 Specific Objectives

Part One:

- Characterize the dominant types of sulphur in the coal.
- The particle size distribution of as – received coal should be completed.
- The effect of coal biodesulphurization treatment on SO_2 emissions.

- Biological desulphurization experiments of incoming coal from the mine must be completed. The experiments should cover the following:
  - Effect of particle size on desulphurization treatment
  - The effect of coal biodesulphurization treatment on sulphur forms and their transformation
  - The effect of biodesulphurization treatment on coal sulphur content
  - The effect of biodesulphurization treatment on CV
  - The effect of biodesulphurization treatment on coal ash content
  - Effect of initial pH on desulphurization
  - The effect of biodesulphurization treatment on redox potential
  - Bacterial identification of microbes responsible for microbial desulphurization
  - The effect of biodesulphurization treatment on coal macerals
  - The effect of biodesulphurization treatment on macerals distribution
  - The effect of biodesulphurization treatment on proximate and ultimate analysis results
- Biological desulphurization mechanisms
- Processing plant sizing and operating challenges
- Overall process efficiencies
- Evaluate the kinetic parameters using established mathematical models for the microbial desulphurization technology employed.
- Conduct a preliminary economic assessment of cost-benefits analysis of the microbial desulphurization technology versus other commercial technologies
- Sulphur component analysis of received coal must be completed in order to
- Evaluate the kinetic parameters using established mathematical models for the pre-utilization technique employed.

Part Two:

- To determine the effect of recycling carbonization tar on coking coal blends and determine the quality of the metallurgical coke produced. The experiments should cover the following:
  - The characterization of blend coking coals
  - The effect of carbonization tar addition on coal proximate and ultimate analyses
  - The effect of carbonization tar addition on coal Roga
  - The effect of carbonization tar addition on basicity and catalytic index

  - The effect of carbonization tar addition on Free Swelling Index (FSI) and G-values
  - The effect of carbonization tar addition on Maximum contraction and dilatation
  - The effect of carbonization tar addition on plasticity and fluidity
  - The effect of carbonization tar addition on coal fines
- Propose a new design for incorporating carbonization tar addition into full-scale plant operation.
- Conduct economic assessment of carbonization tar addition process.

1.6 Thesis Outline

This thesis is a compilation of ten (10) peer-reviewed international journals manuscripts. Chapters four (4), five (5), six (6) and seven (7) have been published in nine (9) peer-reviewed international journals. In addition, Chapters five (5) is under Revision Review in a peer-reviewed international journal.

- **Chapter 1:** The first chapter contains the introduction, the statement of the problem, the objectives of this research, the scope of the research and the thesis layout.
- **Chapter 2:** The literature survey reviews previous work and developments in the area of steam coal, distribution of sulphur forms, petrography, attempted desulphurization's techniques for each sulphur form and microorganisms capable of utilizing sulphur as a source of energy.
- **Chapter 3:** Materials and Methods include details of the chemicals and reagents used, isolation and culturing of microorganisms, experimental set-up and analytical equipment used as per applicable ASTM and ISO standard procedures.
- **Chapter 4, 5, 6 and 7:** Results and Discussions present the experimental results, data analysis and discussions. Finally,
- **Chapter 8**: The conclusions and recommendations from this study are presented.

CHAPTER 2
LITERATURE REVIEW

2.1 Introduction

Coal plays an important role in the energy supply and is used as an input to most cement units, gasification, iron and steel industries (Meshram *et al.*, 2015). It contains a range of functional groups containing carbon (C), oxygen (O), nitrogen (N) and sulphur (S) as shown in Fig.1. The sulphur content in coals varies significantly from about 0.5% to 2% total sulphur (Chou, 2012), but can mount up to and above 10% (Maffei *et al.*, 2012). According to Saikia et al. (2014a), A review of the coal classification closely related to sulphur content suggests that coals are mostly characterized as low sulphur (<1% sulphur content), medium sulphur (1 to <3% sulphur content) and high sulphur coals (>3% sulphur content). In most cases, the sulphur in low – sulphur coals is derived primarily from the parent plant material making up the original peat, and is formed in a fluvial environment while seawater is the primary source of sulphur in high – sulphur coals and were deposited in coastal environments (Li *et al.*, 2014). Therefore, a better understanding of the physical and chemical transformation of coal sulphur during the combustion process is crucial for the balanced utilization of coal as well as for environmental protection (Gryglewicz *et al.*, 1995).

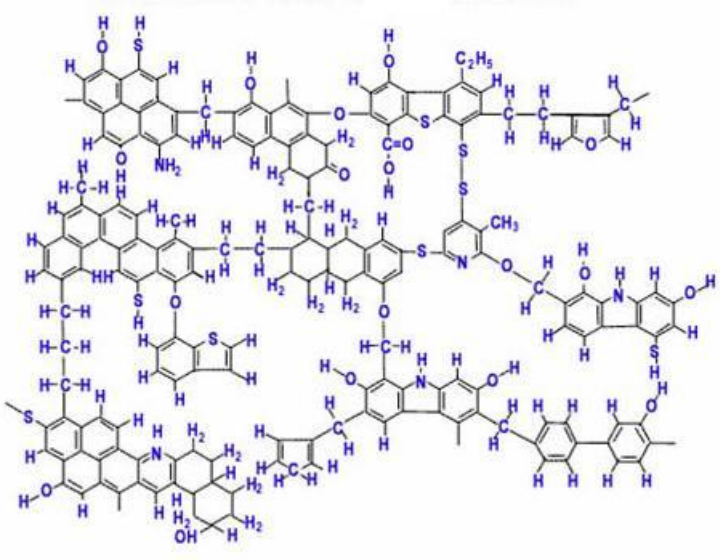

Figure 2.1: Typical coal structure (Cortés *et al.*, 2009)

Sulphur is an abundant element on the earth and it is found as elemental sulphur, mineral sulphur, sulphates, H_2S in natural gas and organic sulphur in combustible oils and coal. On the other hand, sulphur is a secondary nutrient required by vegetables and animals for some

biologic activities therefore sulphur is an essential element for all live beings. Some sulphur components are been carried out to rivers and sea and subsequently transformed into gaseous compounds such as H_2S and SO_2. In general, it is washed out by the water rain and plants in the atmosphere absorb a part of this concentration. The biogeochemical cycle of sulphur is very complex due to the different oxidation states presented by this element and because of some sulphur transformations are done by biotic and non-biotic pathways. Then, the role of bacteria is very important since they are involved in several oxidizing process all along the sulphur cycle.

The sulphur from the fuel is oxidized almost completely, mainly to SO_2 following Equation 2.1:

$$S + O_2 \rightarrow SO_2 \qquad (2.1)$$

Equation 2.1 shows that since SO_2 is formed by combustion of coal-sulphur, the concentration of the SO_2 rises with the sulphur content of the coal (Spörl *et al.*, 2013). In addition, the O_2 concentration also has a direct influence on the SO_2 formation rate, which increases with increasing oxygen content. According to Spörl *et al*. (2013), five principal parameters influencing the concentration of SO_2 formation in the flue gas include stoichiometric ratio/oxygen partial pressure, the sulphur content of coal, alkaline/earth-alkaline content of the ash, temperature and residence time. Moreover, combustion-operating conditions also have important influences on the formations of both NO_x and SO_x (Li *et al.*, 2008). The influence of the combustion temperature was studied in the range of 700 °C and 950 °C by Mastral *et al.* (2000). Mastral *et al*. (2000)'s findings indicate that the maximum emissions are emitted between combustion temperature of 750 °C and 850 °C.

2.2 Geological Setting

The Waterberg coalfield is the largest opencast coal mine in the world and operates the world's largest coal beneficiation complex producing various coal products from 38 Mtpa run of mine (RoM) using a conventional truck and shovel operation (Hancox and Götz, 2014). Apparently, the coalfield strikes approximately 90 km East–west and 40 km North–south, and covers an area of some 360,000 ha (Cairncross, 1990). The Waterberg coalfield is situated in some 17 km west of the town of Lephalale that is 300 km northwest of the capital Pretoria and occurs in the fault-bounded Permian, Karoo-age Ellisras sub-basin in the Limpopo

Province of South Africa (Fig. 2.2). Although Waterberg coalfield covers a relatively small area in relation to the other coalfields of South Africa, it contains a significant portion of the remaining large resources of the country's remaining coal reserves (Cairncross, 2001). According to Dreyer (2006), Waterberg coalfield contains between 40 – 50% of South Africa's remaining resources of bituminous coal and is considered the major energy hub in the country. Hence, the basis of the republic's power generation industries' long-term future focuses.

The coal – bearing sequence in the Waterberg coalfield is divided into 11 coal-bearing zones, locally referred to as benches (equivalent to coal seams). Benches 1 to 5 belong to the upper zone (Grootegeluk Formation), and Benches 6 to 11 to the poorer quality lower zone (Vryheid Formation). The benches in the Grootegeluk Formation typically contain bright coals at the base and grade upwards into shale. At the Waterberg coalfield, Benches 2, 3, and 4 yields coking coal on beneficiation, along with a thermal (steam) and an export product. Bench 5 is a thermal grade coal (with a high phosphorous content), and Benches 6 to 11 are dull coals, highly interbedded with mudstone and carbonaceous mudstone. Due to the fine mudstone intercalations in the Waterberg coalfield, the coals require extensive beneficiation, and the yield of saleable coal is typically less than 50% (Jeffrey, 2005). The coalfield is currently home to Eskom's Medupi and Matimba power stations as well as other power stations in Mpumalanga. According to Hancox and Götz (2014), of the 18.8 Mtpa production from the coalfield, significant 14.8 Mt is thermal or steam coal which is transported directly to Eskom's Matimba and Medupi power stations via a 7 km conveyor belt while an additional 1.5 Mtpa of metallurgical coal is sold domestically to the metals and other industries. For example, Grootegeluk produces 2.5 Mtpa of semi-soft coking coal, the bulk of which is railed directly to ArcelorMittal SA under a long-term supply agreement.

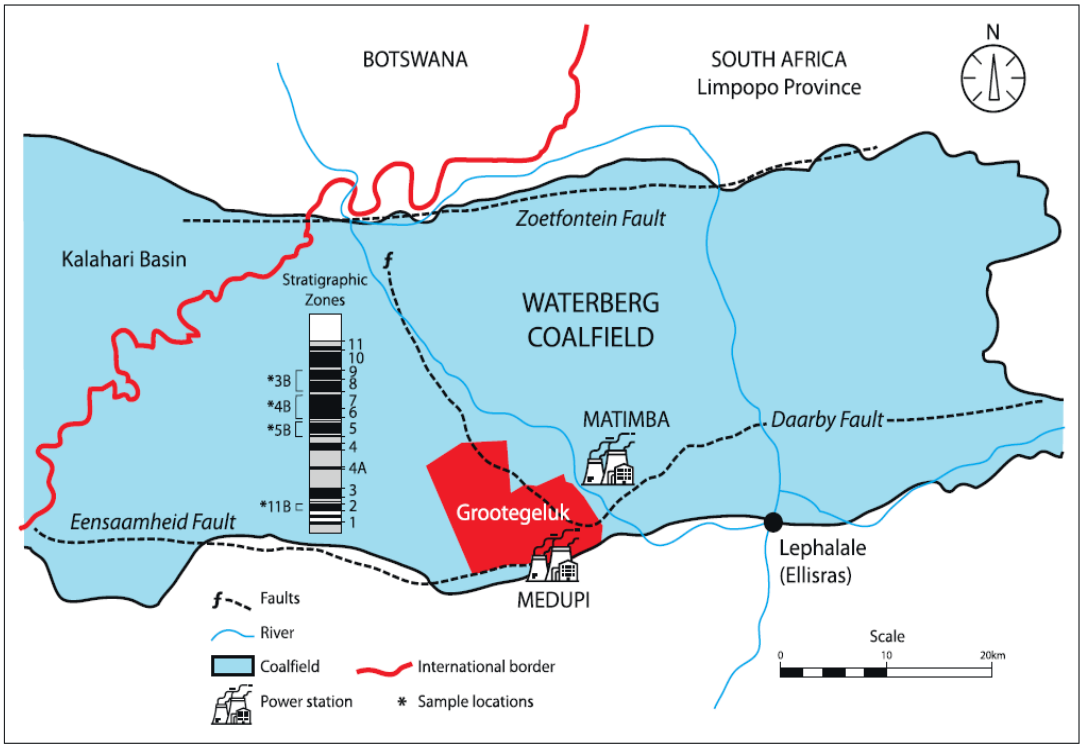

Figure 2.2: The Waterberg coalfield, including the location of the major faults and bar code like stratigraphy; the sample localities are indicated in the stratigraphic column (Hancox and Götz, 2014).

The coal deposit has been extensively drilled and is currently being mined at the Grootegeluk Colliery, so there are several sources of information on the geology, sedimentology and characteristics of the coals and associated strata (Cairncross, 2001). The coalfield is structurally deformed, being dissected by numerous east west and northwest–southeast trending faults. These have produced a series of horsts and grabens, which, in some areas, allow shallow coal to be mined, but in other areas, coal is too deeply buried to be economically mined. However, these inaccessible coals have been tested for coalbed methane potential. There are two main coal-bearing formations, with the upper formation referred to as the Grootegeluk (previously the Volksrust Formation), which is 60 m thick, up to 110 m thick in the south, and the lower, more carbonaceous and interbedded sequence referred to as the Vryheid Formation (55 m thick)(Jeffrey, 2005). Faure *et al.* (1996) provided a detailed discussion on the palaoenvironment of the Grootegeluk Formation and concluded that the coals are humic in origin. The base of the formation was interpreted to be distal, and the upper parts to have a more proximal setting. The coal seams are contained within the Ecca Group, specifically within the Vryheid Formation and the Volksrust Formation, which in the

Waterberg area is named the Grootegeluk Formation (Cairncross, 2001). The latter contains the main coal reserves and consists of a finely interlayered coal-mudstone sequence. The entire coal sequence attains thicknesses of up to 115 m. The underlying Vryheid Formation coal seams (numbered 1, 2, 3 and 4) are interbedded with sandstone and shale. Metallurgical coking coal used in ArcelorMittal may be produced from these lower seams by beneficiation.

The post-Karoo Daarby Fault, with a displacement of 200 to 400 m, divides the coalfield into a shallower western area and a deeper north eastern area. Smaller faults, mostly unmapped, subdivide the coalfield into blocks (Jeffrey, 2005). The general lack of data pertaining to these faults impacts on the uncertainty around the coal resource estimates (Fourie and Henry, 2009), although the Council for Scientific and Industrial Research (CSIR), South Africa) is conducting a detailed geophysical survey to remove some of the uncertainties and enhance the structural understanding of the basin (Fourie and Henry, 2009). The geochemistry of sulphur in coal is largely controlled by sedimentary environments during peat accumulation, as well as by the geologic conditions during diagenesis following peat formation.

2.3 Sulphur Dioxide Minimum Emissions Standards

More than 95% of sulphur content in coal is converted to sulphur dioxide from coal combustion (Franco and Diaz, 2009). The serious negative effects of sulphur from coal use are well known. The SO_X species such as SO_2 readily react with H_2O in the atmosphere to form acid rain that is detrimental to plant, animal life (Ozonoh et al., 2018) and water pollution (Hu et al., 2018). According to Barooah and Baruah (1996), sulphur dioxide is subsequently converted to SO_3 which in contact with water, forms sulphuric acid and acid rain. According to many authors (Chou, 2012; Saikia *et al.*, 2014a), sulphur dioxide emitted during coal combustion is a principal source of acid precipitation (acid rain). Acid rains resulting from the interaction of SO_2 with moisture in the air can cause acid rain incidence such as damages on materials (i.e. historical buildings), depletion of the earth's ozone layer, agriculture and natural ecosystems, Taking the case of Zhao *et al.*, (2008), the sulphur compounds in coal lead directly to the emission of SO_2 and SO_3 forming sulphate aerosols and corrode the boiler tubes during operation. Furthermore, sulphur generally reduces the heating value of coal and SOx reduce the adiabatic flame temperature (Gonsalvesh *et al.*, 2012). Furthermore, the SO_2 emissions are toxic and corrosive (Barooah and Baruah, 1996) can be the reason for sulphate aerosol formation (Gonsalvesh *et al.*, 2012) and chronic respiratory diseases (Mketo et al., 2016). Air pollution caused by SO_2 from coal burning is a

global issue and thus receives more and more attention (Gao et al., 2011). The emissions from coal burning not only affect local air quality but also transport over long distance and cause regional/global environmental issues. According to Gryglewicz *et al.* (1995), the high sulphur content in the coal is considered undesirable and detrimental to the utilization of this important natural resource. Therefore, governments throughout the world have recognized the problems and moved to reduce the amount of SO_2 emission through legislation (Prayuenyong, 2002).

The date, 1 April 2010 was very important in the South African coal-fired power sector, because the new minimum emissions standard were introduced and adopted. New minimum emissions standard limit the permissible levels of sulphur dioxide (SO_2) from coal boilers of 3500 mg/Nm^3 and 500 mg/Nm^3 by 2020 and 2025 as well as particulate matter and oxides of nitrogen as shown in Table 2.1. Stringent environmental legislation and potentially heavy financial penalties associated with exceeding regulatory limits will force coal utilization facilities to reduce their environmental footprint for the benefit of human health and the environment (Wagner and Tlotleng, 2012). It is unquestionable that the tightened emissions standards, mainly for SO_2, will strongly affect the demand for low-sulphur coal. It is expected to be so for combustion plants not equipped with FGD or fluidized-bed combustion boilers.

Table 2.1: New Emissions standards for Solid fuel combustion installations (Government Notice, 2010)

Common name	Chemicals	Plant Status	mg/Nm^3 under normal conditions of 10% O_2, 273 Kelvin and 101.3 Kpa
Particulate matter	N/A	New	50
		Existing	100
Sulphur dioxide	SO_2	New	500
		Existing	3500
Oxides of nitrogen	NO_2	New	750
		Existing	1100

2.4 Coal Macerals

Coal is a heterogeneous material that consists of mineral matter and distinct macerals derived from different components of the plant materials that went into forming the coal. The word maceral is derived from the Latin word to ‘‘macerate’’ implying that whatever the original nature of the coals was, they now consist of the macerated fragments of vegetation, accumulated under water (Scott, 2002). According to Rossi (2014), coal macerals is the name commonly given by petrographers to the complex organic materials occurring in coal in various petrographic types. Scott (2002) further explains the concept behind the word macerals with the emphasis that macerals are organic substance, or optically homogenous aggregates of organic substances, possessing distinctive physical and chemical properties, and occurring naturally in the sedimentary, metamorphic, and igneous materials of the earth. Therefore, maceral composition is controlled by peat-forming vegetation type, as well as by the Eh and the pH conditions, and the microflora of the peat, which all are, in part, controlled by the climatic conditions and sedimentary substrate upon which the peat develops, as well as the sedimentary influx into the peat. All these later factors are interrelated rather than independent of each other (O'Keefe *et al.,* 2013). Characterization of the coal macerals by petrographic methods originated in the steel industry where knowledge of the physical and chemical properties of coking coal macerals pertaining to carbonization processes has led to

the development of cost-effective coke production techniques. The role of different petrographic components on the combustion behavior has been long acknowledged and numerous research efforts have been made in this direction. According to Choudhury et al. (2008), it is established that the behavior of these macerals towards combustion is more affected by the rank than their types. However, there is very little data available to expand the use of similar coal characterization to other areas of coal processing such as chemical desulphurization (Hippo and Crelling, 1991).

Previous work is undertaken by O'Keefe *et al.* (2013) distinguished between coal grade and coal type as follows: coal grade reflects the extent to which the accumulation of plant debris has been kept free of contamination by inorganic material (mineral matter), including during peat accumulation (syngenetically) and after burial (epigenetically) as well as during rank advance. On the other hand, coal type reflects the amount of biogeochemical degradation experienced by organic components prior to burial, the nature of the plant debris from which the original organic matter was derived including the mixture of plant and non-plant components involved such as wood, leaves, algae, fungi, etc. and the depositional environments at the time of peat accumulation. In other words, coal rank is the extent of diagenetic/metamorphic transformation in the macerals and minerals, reflecting the maximum temperature to which the coal has been exposed and the time it was held at that temperature and, to a lesser degree, the pressure regime through the latter time and temperature. Therefore, coal type is expressed as the maceral composition of the coal and is independent of coal rank. According to O'Keefe *et al.* (2013), coal rank progresses regardless of coal type and grade. Target macerals including liptinite, vitrinite, semifusinite and fusinite were identified, as these maceral groups are common in most coals in general (Hippo and Crelling, 1991). According to Faure *et al* (1996), the maceral groups identified in Waterberg coalfield were vitrinite, liptinite, reactive semifusinite (RSF) and inertinite.

2.4.1 Liptinite

The liptinite macerals occur in minor proportions, are highly variable and have different trends in the coal and mudstone groups (Faure *et al.,* 1996). Liptinite group was mainly formed by microsporinite that was substantially more represented then macrosporinite (Fecko *et al.,* 2006). Scott (2002) indicated that liptinites were not only derived from hydrogen-rich plant organs and algal materials but also from decomposition products. Therefore, the chemistry of these macerals is important to their understanding and interpretation. It has

always been clear that many plant tissue types may be found as liptinites: cuticle–cutinite and pollen or spore walls–sporinite. However, the incorporation of these macerals into a single group masks their real diversity. According to O'Keefe *et al.* (2013), liptinite macerals include sporinite, composed of plant spores and pollen, cutinite, composed of plant cuticles and cuticular layers, resinite, composed primarily of resin but also of waxes, balsam, latex, oil, etc.; alginite, derived from algae; suberinite, formed from cornified cell walls found primarily in bark; bituminite, a decay product of algae and plankton, chlorophyllinite, a rare maceral composed of chlorophyll that is preserved only under the most anaerobic conditions, liptodetrinite, or detrital bits of liptinite, and exsudatinite, a secondary maceral that forms from other liptinite macerals and perhydrous vitrinite during coalification and flows to fill voids

2.4.2 Inertinite

According to Scott (2002), the term inertinite was originally claimed to refer to its behavior in coals of coking rank in which the maceral was not thought to soften during carbonization. The origin of inertinite is rather controversial with four pathways possible found in the literature: Hower *et al.* (2012) categorized inertinite pathway as follows: (I) a fire origin for fusinite and possibly some occurrences of semifusinite, secretinite and inertodetrinite; ii) a biochemical and/or microbial origin for funginite, macrinite, secretinite, and micrinite; iii) an oxidation and/or biochemical origin for semifusinite, secretinite, and inertodetrinite; and iv) an allochthonous environment for inertodetrinite and micrinite following the break-up of partially coalified matter due to water movement. Inertinite rich bands in coal seams have been ascribed to water table fluctuations that cause variable redox potentials in peat forming environments (Roberts, 1988). Therefore, inertinites are a diverse group, although they are classified together. The inertinite maceral group includes semifusinite, fusinite (pyrofusinite, degradofusinite, rank, and primary fusinite), funginite (including hyphae and mycelia; part of what was previously named sclerotinite), secretinite (part of what was previously named sclerotinite), macrinite, micrinite, and inertodetrinite.

The inertinites, once considered less reactive, have also shown good burning characteristics, particularly for the high inertinite Gondwana coals (Choudhury *et al.*, 2008). Hence, inertinite macerals have often been associated with burnout problems (Cloke *et al.*, 2002). For example, low-rank inertinites can have better burning characteristics than high-rank vitrinites (Choudhury et al., 2008). The other characteristic properties of inertinites include high

reflectance, little or no fluorescence, high carbon and low hydrogen contents, and strong aromatization (Scott, 2002). Therefore, abundant inertinite increases carbon emissions and then inertinite abundance should positively correlate with carbon emission factors determined for whole coals (Quick and Brill, 2002).

2.4.3 Vitrinite

Vitrinite is by far the most abundant of the coal maceral groups (Scott, 2002). The vitrinite group of macerals derives from organic precursors formed at relatively low redox potentials under more aerobic conditions and oxidative biodegradation (Roberts, 1988). Not only does this group contain true plant cell walls, but also detrital material and chemical precipitates. In many summaries of coal petrography, vitrinite is equated to woody cell walls, leading to the view that this implies forested peats (Scott, 2002). In an excellent review, Scott (2002) traced the original plant tissues through organic geochemistry of the coal and their incorporation into peat. The increase in vitrinite reflectance with increasing metamorphic grade is a function of the increasing aromatization of vitrinite molecules with progressive metamorphism (O'Keefe *et al.*, 2013). Vitrinite has been shown to burn readily although the rate of burnout will normally decrease as its reflectance increases (Cloke *et al.*, 2002). In general, vitrinite macerals become increasingly reflective as rank increases (O'Keefe *et al.*, 2013). The targeted coals of the Grootegeluk Formation have been reported by Faure et al. (1996) to be higher in vitrinite (especially near the top of the sequence) and are very high in mineral matter. The vitrinite reflectance of the Grootegeluk Formation is 0.72% (mean random) (Dreyer, 2006), corresponding to Medium Rank C bituminous coal (Following the ECE-UN in seam coal classification system). This Permian coalfield typically contains high vitrinite, high ash coals in the Kungurian Grootegeluk Formation and high inertinite as opposed to low ash coals in the Artinskian Vryheid Formation.

Roberts (1988) discussed the relationship between macerals and sulphur content of some South African Permian coals and showed that since pyritic and organic sulphur is associated with vitrinite in coals, sulphur content mirrors the trend of this maceral group. For example, increasing from west to east. Besides inertinite, the relative amounts of vitrinite and liptinite also influence whole-coal carbon emissions (Quick and Brill, 2002). Vitrinite macerals contain most of the organic sulphur in coal, therefore are more reactive toward desulphurization processes than any of the other maceral group.

2.4.4 Fusinites and semifusinites

Fusinite is accepted to be a brightly reflecting fire-derived maceral (O'Keefe *et al.,* 2013). According to O'Keefe *et al*. (2013), fusinite appears white under reflected light and generally has reflectance values higher than 6% Rr. Fusinite displays well preserved cellular structures, reflective of its rapid origin during combustion events. According to Scott (2002), fusinites and semifusinites are distinguished primarily by their degree of fusinitization. However, they are characterized by their high reflectance and their open cellular structure. These macerals were subdivided with regard to their presumed process of origin into: pyrofusinite, degradofusinite, rank fusinite, and primary fusinite (Scott, 2002). Semifusinite, an intermediate maceral between huminite/vitrinite and fusinite, having formed in the peat by weak humification, dehydration, and redox processes, may show vague or partially visible cell lumens derived from parenchymatous and xylem tissues of stems, herbaceous plants, and leaves (O'Keefe *et al.,* 2013). The semifusinite with reflectance value of 0.3% R_0V or less above the mean maximum reflectance of the associated vitrinite is regarded as reactive semifusinite, in the sense that it behaves more like vitrinite than inertinite during carbonization. Semifusinite contains significantly smaller amounts of organic sulphur than the vitrinites. According to O'Keefe *et al.* (2013), Gondwana semifusinite is leaf-derived and Carboniferous semifusinite is wood – derived. Fusinite and semifusinite are the most abundant macerals in most of the coals with semifusinite exceeding 60 vol. % (mineral included basis) in several Botswana and Zambia coals (Hower *et al,* 2012). While some of the fusinite and semifusinite might be considered to be inertodetrinite (Hower *et al.,* 2012).

2.5 Sulphur Forms in the South African Coals

Coal contains a variety of functional groups involving carbon, oxygen, nitrogen and sulphur (de Korte, 2001). The sulphur content in coals varies widely within the range of 0.5% to 2% total sulphur (Chou, 2012), but can go up to and above 10% (Maffei *et al.,* 2012). According to Saikia *et al.* (2014b), the coals are generally termed as low sulphur (<1% sulphur content), medium sulphur (1 to <3% sulphur content) and high sulphur coals (>3% sulphur content) based on their sulphur contents. In most cases, the sulphur in low – sulphur coals is derived primarily from the parent plant material and is formed in a fluvial environment while seawater is the primary source of sulphur in high – sulphur coals and were deposited in coastal environments (Li and Tang, 2014). According to Calkins (1994), much of the sulphur

in low sulphur coal derived from the sulphur content of the plant material making up the original peat.

Various authors have note that sulphur is the most notorious environmental contaminant, which produces sulphur dioxide during combustion (Chou, 2012; Saikia *et al.* 2014a; Cheng *et al.*, 2003). According to Hancox and Götz (2014), environmental pollutants such as sulphur dioxide, sulphuric acid and hydrogen sulphide have been linked to the presence of sulphur in coal and as such, an understanding of the nature of the sulphur and its distribution in the coal is of paramount importance. Therefore, removal of sulphur content from coal is necessary and requires prior knowledge of the sulphur forms distribution. For example, the physical processes for reducing sulphur content such as gravity separation, froth flotation, oil agglomeration and magnetic separation are only applicable for the removal of inorganic sulphur forms. A considerable amount of study has been conducted to determine the forms of sulphur in the coal. There are limited published studies on the investigation of sulphur forms in the coal compounds, especially organic sulphur compounds in South African coal. To partially rectify this situation, Kalenga (2011) undertook work into the characterization and distribution of the sulphur components in South African coals. Sulphur in coal is present in both inorganic and organic forms as depicted in Fig. 2.3. The inorganic sulphur occurs in South African coals in two forms, these being sulphide and sulphate. The inorganic forms are typically elemental (Borah and Baruah, 1999) while sulphide minerals are mainly pyrite, marcasite and siderite with pyrite being the major dominant inorganic sulphur host in most coals (Li and Tang, 2014). The earlier form, pyrite has the same composition, FeS_2, as marcasite that differs in crystalline structures. Primary (or organic) forms of sulphur are trapped in the organic matrix at the time of peat formation. Secondary (or inorganic) sulphur occurs along with cleats and fractures. The type and nature of the sulphur are important in terms of the degree of liberation during beneficiation.

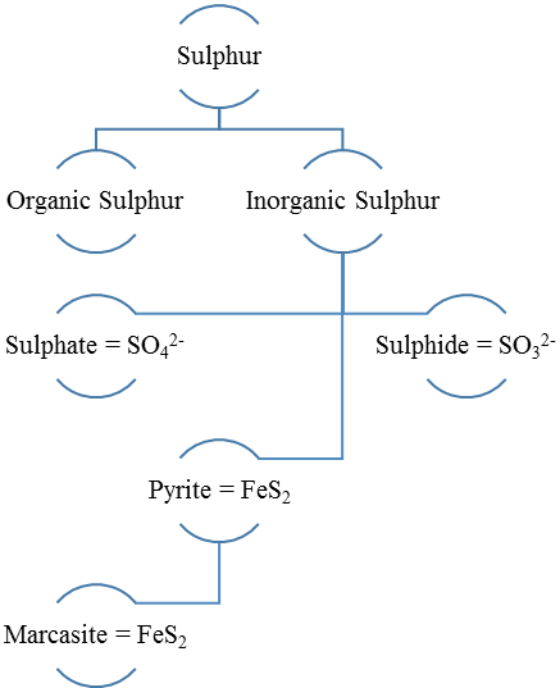

Figure 2.3: Sulphur forms in coal

2.5.1 Pyritic sulphur

Pyrite is held together in coal by mechanical incorporation, is cubic with the octahedrally coordinated metal atoms at the corner and is nodular nature (Pandey *et al.*, 2005). Coal pyrite differs from the ore pyrite in several properties (viz. surface area, semiconducting properties, morphology and reactivity toward ferric ions and oxygen) and coal pyrite varies significantly depending on the rank of the coal (Olson and Kelly, 1991). Therefore, the differences in the rate of microbial attack of coal pyrite compared to ore pyrite could also be attributed to differences in semiconducting properties between ore pyrite (n-type) and coal pyrite (p-type). Either pyritic or organic sulphur predominates over other forms of sulphur in most of the coals (Borah and Baruah, 1999). According to Faure *et al.* (1996), pyritic sulphur is the dominant sulphur form - containing mineral in the Waterberg coals. Pyrite occurs in several forms, most commonly as (a) disseminated pyrite, having particle sizes ranging from a few millimeters to less than one micrometer, (b) thin, platy pyrite in cleats, (c) as cell fillings, especially in fusinites, (d) pyritic nodules and partings, (e) pyrite veins, and (f) pyrite in permineralized peat or coal balls (Chou, 2012). Sulphur. A hypothesis for the formation of pyrite has been proposed, according to which iron and sulphate combine to yield ferric sulphate and the resultant product of the reaction of this ferric sulphate and hydrogen sulphide is pyrite (Barooah and Baruah, 1996). According to Kargi (1982), the pyrites in coal can occur in balls or nodules, lenses and bands, or as finely disseminated particles. In another

case, Fecko *et al.* (2006) mentioned that pyrite is presented in the epigenetic and syngenetic forms. Syngenetic pyrite was formed during the first phase of the coal forming process and that is, why it is interspersed within the coal substance. Epigenetic pyrite is geologically younger, therefore it acts as a filling material in the joints and fissures (Fecko *et al.*, 2006). Pyrite is a semiconducting sulfide mineral that may have both n- and p-type conductivity. Its valence band is narrow and non-bonding, hence electron transfer within this band (hole injection) will not affect the structure and bonding of the solid, and no corrosion will occur (Orsi *et al.*, 1991). Baruah (1992) agrees that the constituents of pyrite formation were accumulated at an early stage of a coal formation with the fresh water being the main supplier of iron while seawater supplied sulphur in the form of sulphate. According to Hancox and Götz (2014), pyrite in the coal is also one of the main components responsible for the wear and abrasion and high level of coal abrasiveness index in South African coals. Therefore, the size and distribution of pyrite particles in coal influence the effectiveness of pyritic sulphur removal processes. Pyritic sulphur can be removed by conventional mineral processing methods, grinding the coal to liberate the pyrite grains, high-density washing, usually gravity separation or flotation methods (Eligwe, 1988), although Rossi (2014) claimed to have successfully applied macroscopic and magnetic separation. According to Eligwe (1988), when pyrite is exposed to oxygen and water, the pyrite dissolves as per Eq. (2.2):

$$FeS_2 + 7/2O_2 + H_2O \rightarrow Fe^{2+} + 2SO_4^{2-} + 2H^+ \quad (2.2)$$

The ferrous ion produced can be oxidized further by dissolved oxygen to ferric ion (Fe^{3+}) as shown in reactions (2.2) and (2.3):

$$2Fe^{2+} + ½O_2 + 2H^+ \rightarrow 2Fe^{3+} + H_2O \quad (2.2)$$

$$2FeS_2 + 7O_2 + 2H_2O \rightarrow 2FeSO_4 + 2H_2SO_4 \quad (2.3)$$

The released ferrous iron is stable under aerobic, acidic conditions. Ferric ion is a good oxidant of pyritic sulphur, producing sulphate (reaction 2.4) or elemental sulphur (reaction 2.5):

$$FeS_2 + 14Fe^{3+} + 8H_2O \rightarrow 15Fe^{2+} + 2SO_4^{2-} + 16H^+ \quad (2.4)$$

$$FeS_2 + 2Fe^{3+} \rightarrow 3Fe^{2+} + 2S \quad (2.5)$$

Since pyritic sulphur oxidizing microorganisms are autotrophy, the microbial pyritic sulphur removal from coal provides a useful means for the utilization of carbon dioxide released from coal combustion processes (i.e. the stack gas) (Kargi, 1982). Some microorganisms have been shown to solubilize pyrite and marcasite. It has been suggested that these organisms may be useful in a biological treatment process for the reduction of sulphur content from coal. Most of the literature on microbial coal processing concerns the use of bacteria as agents for pre-combustion removal of pyritic sulphur (Olson and Brinckman, 1986). Microbial removal of pyritic sulphur has been extensively investigated over the last 50 years. The microbial oxidation of pyrite in acidic environments results in the formation of ferric sulphate [$Fe_2(SO_4)_{2.}$]. The ferric ion itself can also further oxidize pyrite and other metal sulphides that may be associated with coal as per reaction 2.6:

$$Fe^{3+} + \text{pyrite} \rightarrow Fe^{2+} + \text{elemental sulphur} \qquad (2.6)$$

The microbial desulphurization of coal is usually carried out with pyrite-oxidizing microorganisms such as *Thiobacillus ferrooxidans' Leptospirillum sp.* and *Sulpholobus sp*. to provide partially cleaned coal before combustion (Beyer *et al.,* 1987).

Microbiological removal of pyritic sulphur from coals has been a topic of many investigations by numerous authors. A mixed culture of T. ferrooxidans and *T. thiooxidans* was reported to be more effective than a pure culture of *T. ferrooxidans* in removing pyritic sulphur from coal. An example of this is a mixed culture of *Leptospirillum ferrooxidans* and *Thiobacillus thiooxidans.* L. *ferrooxidans* can only oxidize ferrous iron but cannot grow on sulphur or sulphide compounds. In addition, *T. Thiooxidans* can grow on elemental sulphur but cannot oxidize ferrous iron. There are several reports on the removal of pyritic sulphur from coal by bacterial means using *Thiobacillus ferrooxidans* and certain microorganisms present in coal (Kargi and Robinson, 1986; Chandra *et al.,* 1979). A mixed culture of microorganisms present in acidic coal mine waters was also used for pyritic sulphur removal from a pulverized coal blend (Kargi, 1982). Pandey *et al.* (2005) investigated the bioleaching of high pyritic coal and managed to remove 79% of pyrite and 75% of ash contained in the coal. For the removal of pyrite sulphur, leaching processes using e.g. autotrophic *Thiobacillus* species were developed and already scaled up into pilot plants (Klein *et al.,* 1994). In another case, Kargi and Robinson (1986) used the thermophilic organism *Sulfolobus acidocaldarius* for the removal of > 90% of pyritic sulphur from bituminous coal. Gonsalvesh et al. (2012)

also reported another case where the microbial culture demonstrated effectiveness in the pyritic sulphur removal. According to Gonsalvesh *et al.* (2012), 40 – 90% of pyritic sulphur desulphurization effects have been achieved. However, acidophilic iron – oxidizing bacteria such as *Thiobacillus ferrooxidans* and *Leptospirillum ferrooxidans* rapidly oxidize the ferrous iron to ferric iron and gain metabolic energy in the process (Olson, 1994). In a separate case, a mixed culture of acidophilic iron and sulphur-oxidizing mesophilic microorganisms including *Acidithiobacillus ferrooxidans*, *Acidithiobacillus thiooxidans* and *Leptospirillum ferrooxidans* was used to remove pyritic sulphur from the high sulphur coal of Mehr Azin, Tabas, Iran (Kiani *et al.*, 2014).

Biodesulphurization of coal could be especially promising where coal contains very finely disseminated pyrite that is generally not removable by mechanical techniques (Olson and Brinckman, 1986). However, some challenges related to microbial coal desulphurization include relatively long bioprocessing times (days to weeks), the production of acidic and corrosive leaching solutions. These challenges have hindered microbial desulphurization of pyritic sulphur processes moving toward scale – up designs and cost estimates for heap leaching and slurry reactors (Olson, 1994).

2.5.2 Sulphate sulphur

Generally, the occurrence of sulphate sulphur is very low in comparison to other sulphur forms (Barooah and Baruah, 1996). According to Chou (2012), coals contain trace to minor amounts of sulphate sulphur and the amount of sulphate sulphur in freshly mined coal is usually less than 0.1 wt.%. The sulphate content of coal gradually increases after mining due to the oxidation (biological and chemical) of pyrites in the presence of air (Kargi, 1982). Sulphate sulphur usually occurs in smaller amounts often as ferrous sulphate that formed by the oxidation of pyrite (Chou, 2012) or sulphate minerals (Mishra *et al.*, 2014). Sulphate minerals found in some fresh coals mainly as gypsum [$CaSO_4 \cdot 2H_2O$] and barite [$BaSO_4$] originated primarily during the carbonization process and secondarily during the weathering of pyrites (Fecko *et al.*, 2006). Sulphate sulphur has been removed with the use of *Thiobacillus ferrooxidans* and certain microorganisms present in the coal (Chandra *et al.*, 1979). Sulphate reduction is rather complicated process made up of eight steps as depicted in Fig. 2.4. According to Cypionka (2006), first the double-charged anion has to be taken up by specific transport systems. Cypionka (2006) summarized the reduction process as follows: (1)

Uptake by symport with protons, (2) ATP sulfurylase, (3) pyrophosphatase, (4) APS reductase, (5) sulfite reductase, (6) hydrogenase, (7) cytochrome, (8) ATP synthase

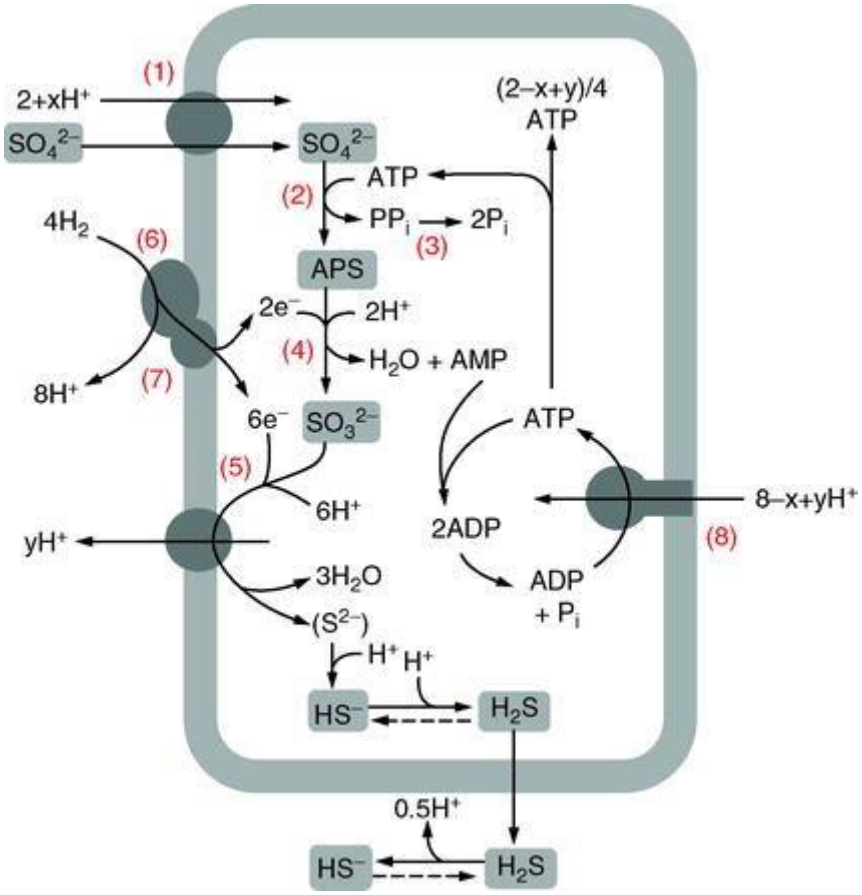

Figure 2.4: Pathway of Sulphate-Reducing Bacteria using Hydrogen as an electron donor

2.5.3 Sulphide sulphur

Limited information is available on the sulphide form in coals. Sulphide minerals found in the coal include marcasite, pyrrhotite, sphalerite, galena and chalcopyrite as well as rare occurrences of getchellite and alabandite (Chou, 2012).

2.5.4 Organic sulphur

The organic sulphur in coal is covalently bound into its large complex structure. Therefore, organic sulphur is characterized by covalent C – S bonds and can be regarded as an element that is an integral part of the molecular coal matrix (Klein *et al.,* 1994). Organic sulphur atoms are chemically bonded to the other atoms in coal and exists in various types such as aliphatic, aromatic, thioether or heterocyclic sulphur structures (Ye *et al.,* 2018); thioether, thiophenol (Borah and Baruah, 1999); thiols, sulphides (Karavaiko and Lobyreva, 1994); disulphides, and complex thiophenic ring systems (Rossi, 2014). Organic sulphur is mainly

bound to the structures of dibenzenethiophene, benzenethiophene and thiols, Fecko *et al.* (2006). According to Klein *et al.* (1994), the organic sulphur compounds in coal can be described by the following classification: (i) Aliphatic or aromatic thiols (mercaptans, thiophenols), (ii) Aliphatic, aromatic, or mixed sulfides (thioethers), (iii) Aliphatic or mixed disulphides (dithioethers), (iv) Heterocyclic compounds of the thiophene type (dibenzothiophene). Amount of each type depends on the environmental conditions of an early stage of coal formation, i.e., peat bog, the progress of biochemical reactions at that stage, and the degree of metamorphism. According to Mukherjee and Borthakur (2003), about 95% of the organic sulphur in the coal was in the form of complex thiophenes. According to Alson and Kelly (1991), about 40 – 60% of the organic sulphur in bituminous coals was estimated to be thiophenic. Separately, according to Kargi and Robinson (1986), the organisms capable of oxidizing dibenzothiophene (DBT) removed organic sulphur from coal. Given that organic sulphur occurs in various forms, then which type of organic sulphur compound does the desulphurization process attack? Therefore, it is important to identify which organic sulphur species are associated with the Waterberg coal.

Some workers reported that organic sulphur in Waterberg coal occurs as mercaptan and disulphide whereas others believed that thiol, sulphide, disulphide and ring compounds are the types of organic sulphur in these coals. However, these researchers could not show any precise experimental pieces of evidence of the nature of organic sulphur in Waterberg coals. Organic sulphur compounds were characterized for South African coal samples in order to determine the dominant forms (Kalenga, 2011). Kalenga (2011) identified and quantified different organic sulphur species in the coal and found mainly in the form of 2-methyl thiophene, 3-methyl thiophene, 2-ethyl thiophene and dibenzothiophene. The nature of organic sulphur in Waterberg coals has been precisely determined and the literature on this is sufficient. Our knowledge about the molecular structure of organic sulphur compounds has been keeping pace with the development of new analytical instrumentation and methods (Chou, 2012). The research on the microbial removal of organic sulphur from the coal has been focused on the development and characterization of microorganisms that display a preference/specificity for the cleavage of carbon-sulphur bonds. Although the development of techniques to remove organic sulphur is being investigated in laboratories around the world, so far none of these techniques has proved to be inexpensive enough to be commercially successful.

Kargi (1982) earlier on claimed that organic sulphur compounds present in coal cannot be removed by conventional physical cleaning processes but require chemical treatment. However, organic sulphur is hard to be removed by chemical treatment like hydrogenation as its removal must involve splitting a covalent C – S bond, which is resistant to chemical treatment. According to Prayuenyong (2002), the organic sulphur in coal is covalently bound into its large complex structure and is difficult to remove physically by mechanical separation methods (Olson and Brinckman, 1986), in contrast to pyritic or inorganic sulphur. Other forms of organic sulphur can be removed when coal is coked or hydrodesulphurized (Kargi, 1982). In general, some authors have observed the microbiological removal of organic sulphur compounds from coals. There has been a great increase in the number of published papers in this area over the past 20 years. Therefore, the application of biodesulphurization processes using microorganisms has attracted attention as a new eco-technology or a clean alternative method to remove organic sulphur from coals in order to achieve more efficient desulphurization as well as to minimize the environmental problems associated with the combustion of high sulphur coals (Handayani *et al.*, 2017).

Most of the literature is confined to removal of pyritic sulphur and total sulphur while very few studies have been reported on organic sulphur removal from coal by microbial catalysis. While most of the inorganic sulphur in coal can be removed by physical methods such as heavy media cycloning techniques, centrifugation, and froth flotation, the organic sulphur does not lend itself to removal by these techniques (Hippo and Crelling, 1991). Chandra *et a1*. (1979) used a mixed heterotrophic culture isolated from soil and enriched on dibenzothiophene to remove organic sulphur from coal. Nearly 20% of organic sulphur removal from bituminous coal was reported. Gökcay and Yurteri (1983) used a thermophilic (50°C) *Thiobacillus* type organism for the removal of organic sulphur from Turkish lignite. About 50% of organic sulphur removal was reported in 25 days of incubation. In another case, the thermophilic, sulphur-oxidizing organism *Sulfolobus acidocaldarius* was used in the study to remove organic sulphur from inorganic sulphur – free coal samples. The organisms were first adapted to dibenzothiophene in a sulphate – free mineral salts medium. Nearly 44% of initial organic sulphur was removed from coal slurries at 70°C in about four weeks (Kargi and Robinson, 1986). Perhaps the most interesting recent development in the microbial removal of organic sulphur from coal is that *IGTS7* can remove up to 91% of the organic sulphur from coal (Kilbane, 1989). If organic desulphurization involved the carbon-

destructive pathway, it could be argued that the fuel value of coal would be virtually destroyed by the removal of this much sulphur. The validity of the analytical methods is thereby called into question.

Although extensive studies have been done on the bioremoval of organic sulphur, there remains some disagreement and incomplete understanding of this matter. Most of these studies were carried out using model compounds that are recognized to behave differently to sulphur in coal. Experimentation using specific coal types is undoubtedly a requirement to enable an assessment of this technology (Prayuenyong, 2002). Therefore, it has generally been impossible to fully evaluate the validity of these reports because insufficient data is presented in support of the findings. Where sufficient detail has been provided, data reproducibility and biomass contamination of the coal has left doubts as to the results (Olson, 1994). Other deficiencies include the difficulties associated with direct measurements of organic sulphur (Olson and Kelly, 1991), and lack of appropriate experimental controls and the absence of data on coal recovery and associated elemental analyses (Olson, 1994). Unfortunately, organic sulphur in the coal is generally measured by difference (total sulphur minus pyritic sulphur), potentially leading to large analytical errors (Olson and Brinckman, 1986) and organic sulphur value may also include sulphur which is not organic at all. For example, this might include elemental sulphur and non-pyritic sulphide mineral sulphur (especially from ZnS) (Davidson, 1994).

A thorough making interpretation of biological removal of organic sulphur is difficult. The most common measurement method in the analysis of organic Sulphur is the American Society of Testing Materials (ASTM) Method. This analytical technique is not very consistent since replicating analyses performed by the same laboratory differed by 10% and replicating analyses performed by different laboratories by 20% (Kilbane, 1989). Furthermore, almost every research group involved reports problems with stability or reproducibility. Conventional coal beneficiation processes do not affect the removal of the organic sulphur, which is an inherent part of the coal structure (Eligwe, 1988). The research on the microbial removal of organic sulphur from the coal has been focused on the development and characterization of microorganisms that display a preference/specificity for the cleavage of carbon-sulphur bonds (Kilbane, 1990). Several microorganisms including bacteria and fungus have been reported by various authors (Chandra *et al.*, 1979; Karavaiko and Lobyreva, 1994; Mishra *et al.*, 2014) and the detailed summary is provided in Table 2.2.

Table 2.2: Summary of organic sulphur bioremoval (Rossi, 2014)

Number	Result	Organic sulphur removal (%)	Substrate for adaptation	References
1	*Pseudomonas janji*	> 95	DBT	Kodama (1970)
2	*Bacterial mixed culture*	30	DBT	Chandra *et al.* (1979)
3	*Acidithiobacillus ferrooxidans*	56	-	Göckay and Yurteri (1983)
4	*Pseudomonas sp.*	47	DBT	Isbister (1985)
5	*Sulfolobus acidocaldarius*	10	DBT	Kargi and Robinson (1986)
6	*Defined bacterial species*	< 7	Thiophene, cysteine, benzene, sulphonic acid	Klubek *et al.* (1988)
7	*Bacillus sp.*	36	DBT	Chandra and Mishra (1988)
8	*Pseudomonas putida*	37	DBT	Rai and Reyniers (1988)
9	*Hansenula sp.*	< 46	Cysteine, methione	Stevens and Burgess (1989)
10	*Bacterial mixed culture*	33	DBT	Runnion and Combi (1990)
11	*Brevibacterium sp.*	> 95	DBT and thiamine	Van Afferden *et al.* (1990)
12	*Fungus*	< 20	Not specified	

2.6 Desulphurization Techniques

The research on desulphurization techniques dates back to the late 1979s when the major driving force was to reduce high sulphur content in coking coals. Later on, with SO_2 minimum emissions concern, this has since shifted to the power stations and gasification space. A number of desulphurization processes have been developed for the removal of sulphur compounds from coal. These processes can be classified into pre-combustion desulphurization processes and post-combustion desulphurization process such as flue gas desulphurization (FGD). Several pre-combustion desulphurization techniques have been developed for high sulphur content coals and reported by several authors (Olson and Brinckman, 1986; Cara *et al.,* 2006; Saikia *et al.,* 2016). The effectiveness of different methods (viz. physical, chemical, thermal, radiolytic or biological methods) depends on the structure and composition of the minerals and their association in the coal (Mukherjee and Borthakur, 2003). Fig. 2.5 shows various technologies for roadmap to clean coal technology. The following sections deal with various technologies for pre-combustion processes and post – combustion processes to meet both economic and environmental emissions limits.

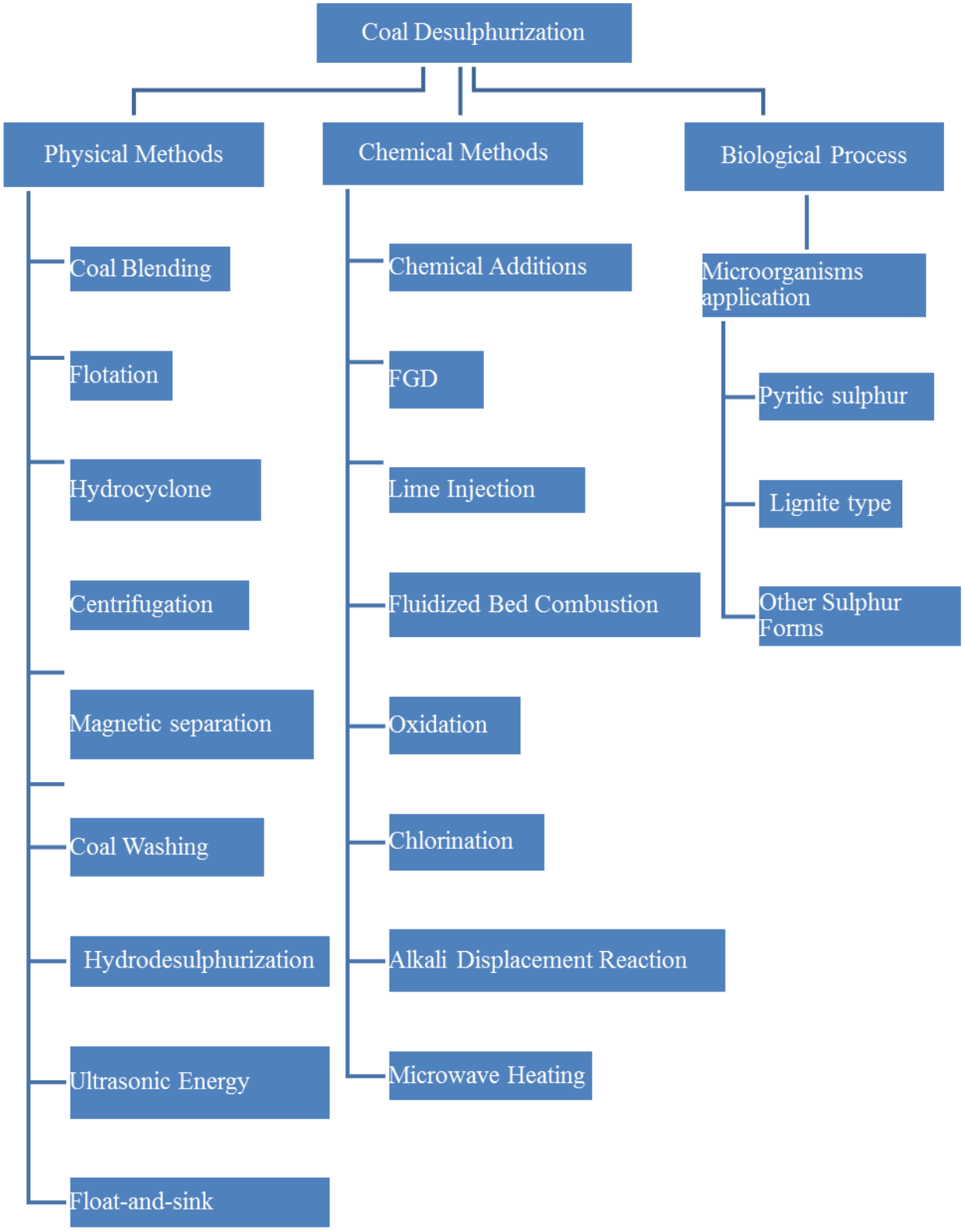

Figure 2.5: Various technologies for roadmap to clean coal technology

2.6.1 Coal blending

Global society is moving towards zero-sulphur content coal because of a negative influence that the combustion of Sulphur – containing coals cause to the environment (Martínez *et al.*, 2017). Among various methods for controlling the aforementioned pollutants in coal-based power generation is coal blending and oxy-combustion of coal (Rokni *et al.*, 2016). Coal blending is designed to meet technical, environmental and economic objectives. Coal blending has been widely utilized by other coal-based industries particularly with metallurgical coals to produce different types of cokes. There is evidence that the thermoplastic properties of blends are modified by interactions between the component coals. Similarly, coal blends can be utilized at power plants with the aim to produce energy at the lowest cost without breaking environmental regulations. Rokni et al. (2016) who mentioned that coal blending has been shown to reduce SO2 emissions support the latter. Moreover, coal blending also has a positive effect in reducing the NO_x emissions, depending on the combustion characteristics of the blends in particular boilers (Rokni *et al.*, 2016). As sulphur contents are directly proportional in blending, therefore according to Cheng *et al.* (2003), the blend ratio of component coals can be determined based on sulphur content to meet emission levels. Furthermore, combustion – related properties of coal blends may not be proportional to the weighted average values of individual coals. Helle *et al.* (2003) conducted a similar type of study on blends combustion and experience with blends combustion has shown that several of the relevant operational variables do not agree with the expected behavior of the expected weighted average value of parameters as determined from the coals used in the blend. The main reason behind the observed deviations from such averaged behavior is suspected to be the interaction among the coals of the blend (Helle *et al.*, 2003). Furthermore, this is due to the non-linear nature of the combustion process and due to the interaction between some of the combustible constituents in coal (Santhosh Raaj *et al.*, 2016). Therefore, more evidence of interaction among the coals requires the study of some parameters that affect combustion efficiency and related emissions (Helle *et al.*, 2003). Unburnt carbon in fly ash is the major determinant of combustion efficiency in coal-fired boilers and appears as a good sensor of the efficiency in the coal combustion of blends.

2.6.2 Flue gas desulphurization

Effective technologies are well documented in the literature to remove sulphur after or during combustion. Several schemes, such as fuel pre-treatment, concurrent burning and adsorption,

and flue gas post – treatment have been proposed (Gao *et al.*, 2011). Wet and dry FGD processes represent the major industrial routes used to control SO_2 emissions in the atmosphere (Efthimiadou *et al.*, 2015). The FGD scrubbers are estimated to remove approximately 90% of the SO_2 and a significant portion of gaseous chlorides and fluorides that may be present in the flue gases (Srivastava and Jozewicz, 2001). Xiong et al. (2016), whose findings demonstrated SO_2 removal efficiency of 92.50%, 82.50% and 50.0% using Wet-FGD, Dry-FGD and Semi-dry FGD, respectively, also assessed the effectiveness of the FGD technology. In addition, Benko et al. (2007) investigated the effect of installed FGD units at high capacity power plants on regional air pollution in the Carpathian Basin. Based on the simulation results, FGD units with 90% SO_2 removal efficiency reduce the horizontal distribution by 79%, and the vertical distribution by 66% for the yearly average (Benko *et al.*, 2007). In spite of the good performance of the FGD technology thus far, the process produces an effluent with high concentrations of the cationic and anionic impurities – Ca, Mg, Cl and heavy metals. According to Hao *et al.* (2016), a large amount of FGD gypsum ends up in landfills or outdoor storage that may result in environmental pollution. Consequently, the effluent generated cannot be re-used anywhere else in the power station without intensive treatment (Singleton, 2010). In addition, the problems with the existing FGD technology concerning costs, efficiency, applicability, and waste disposal cannot be under estimated (Klein *et al.*, 1994). Microbial processes have the potential to overcome some of these problems. Therefore, rigorous FGD (that is wet of semi – dry FGD technology and fluidized bed combustion) is not economically feasible for plants with limited service life (less than 20 years).

The limestone addition is a recognized successful practice used to capture the SO_2 during coal combustion. However, the efficiency of SO_2 removal by limestone is influenced by the operational conditions (Efthimiadou *et al.*, 2015). Fluidized bed combustion (FBC) has been used in another instance. This technology cleans coal inside the furnace where the coal is actually burned. In summary, coal is ground into small particles, mixed with limestone and injected with hot air into the boiler. This mixture, a bed of coal and limestone, is suspended on jets of air and resembles a boiling liquid. As the coal burns, the limestone acts as a sponge and captures the sulphur. A dry desulphurization process, such as an induct sorbent injection process, causes reactions by dispersing free gas with a solid sorbent powder sprayed into it was investigated by Kang *et al.* (2015). Among the SO_2 control technologies available, direct

injection of sorbent in the furnace is an interesting candidate, as it combines low cost, the ease with which it can be implemented to existing boilers, the attractiveness of a dry product and reduced space requirements (Vekemans *et al.*, 2016). However, its disadvantages are that because of the high temperature and low residence time characteristic of pulverized coal boiler, SO_2 reduction efficiencies only up to 25 – 50% can be achieved, and those risks of slagging and fouling on the boilers surfaces are increased (Vekemans *et al.*, 2016).

2.6.3 Physical method

Physical methods are based on the differences in the physical properties of the minerals and the carbonaceous part of the coal, Mukherjee and Borthakur (2003). Effective sulphur reduction by physical coal cleaning processes can only be achieved provided the sulphur to be removed is well-liberated (Shu *et al.*, 2002). Therefore, in physical processes coal is crushed, ground and washed. Such processes remove 30 – 90% of the pyritic sulphur associated with the mineral matter in coal (Gryglewicz, *et al.*, 1995). This allows for up to 90% of pyrite (the predominant form of inorganic sulphur in coal) to be removed (Prayuenyong, 2002). Coal washing is known to have a beneficial effect on sulphur emissions values (Shah et al., 2002). In the United Kingdom (UK), it has been estimated that conventional coal washing for ash reduction also reduced sulphur emissions by 20 – 30 wt.% (Shah *et al.*, 2002). On another case, the two physical methods used together, hydrocyclone and flotation equipment bring about a reduction of 20.8% in the sulphur content and 41.1% in the ash content (Martínez et al., 2003). However, physical methods (flotation, magnetic separation) result in large energetic losses by removing pyrite containing coal particles (Kargi, 1988). The physical methods do separate much of the mineral material but their yield decreases considerably when the mineral matter in the carbon matrix is more disperse. While most of the inorganic sulphur in coal can be removed by physical methods such as heavy media cycloning techniques, centrifugation, and froth flotation, the organic sulphur does not lend itself to removal by these techniques (Hippo and Crelling, 1991). Cara et al. (2006) who mentioned that physical methods have no effect on organic sulphur support the latter.

Yingzhong et al. (2010) reported the feasibility of the desulphurization of high sulphur coal through float-and-sink test. Washability study results showed that when using the media density below 1.5 g/cm^3 to float the coal, the total sulphur could be reduced to 1.53%, with coal recovery of 83.80%. Using the floatation media with a density of 1.40g/cm^3～1.50 g/cm^3, most of the sulphur can be removed from the lightest coal portion (density <1.4). The

ash content of the coal portion with a density below 1.5 g/cm^3 is fairly low and decreasing more significantly with the coal density. Both sulphur and ash content gradually increase in the coal with a density of above 1.6 g/cm^3 (Yingzhong *et al.,* 2010). On the other hand, ultrasonic coal-wash is a method in which ultrasound power can be used for the beneficiation of coal by removing the unwanted mineral matters (ash) and sulphur prior to combustion. Ultrasonic method of coal wash is followed elsewhere (Saikia *et al.,* 2013). However, the coal washing by this method is not practiced so far commercially in India. In a separate case, Saikia *et al.,* (2014) paper reported an attempt of using low ultrasonic energy (20 kHz) to clean some low - rank medium to high sulphur coal samples from northeast India in the presence of H_2O_2 solutions. The study showed satisfactory removal of all the forms of sulphur and mineral matters (ash) from the coal samples (Saikia *et al.,* 2014a). The desulphurization reaction accomplished by electron transfer process involving Co^{2+} ion is an effective method of removing organic sulphur from coal (Borah, 2006). According to Borah (2006), the method has succeeded in removing as much as 28.5 wt.% organic sulphur from coal in the presence of naphthalene in comparison to its absence (24.6 wt.%) at 4 h and 5 °C.

Hydrodesulphurization, a physicochemical technique, has been applied as a conventional method for sulphur removal worldwide. It is a high-pressure (10 – 17 bar) and high temperature (200 – 425 °C) process in which sulphur is converted to H_2S (Prayuenyong, 2002). Although high reaction rates are given when chemical or hydrodesulphurization processes are used, they are costly, producing hazardous products and the structural integrity of the coal is affected (Prayuenyong, 2002). However, hydrodesulphurization suffers many limitations, e.g., it works under severe and hazardous operation conditions, it is not efficient in desulphurization of some refractory sulphur – containing compounds, it needs high capital and operating costs and it generates the hazardous H_2S product, among others (Martínez *et al.,* 2017). Although these techniques are efficient, they are rather expensive and prevent coal prices from competing with other energy sources (Gómez *et al.,* 1997). Applications of ultrasonic energy in aqueous H_2O_2 medium was reported by Saikia *et al.* (2016) as suitable for removing sulphur and ash from Brazil power coal. It has the potential to replace other conventional coal cleaning methods in terms of less energy, less treatment time, less reagent volume, and low reagent concentrations and may be used for larger-scale trial with the high-sulphur and high-ash coals in the world. Physical desulphurization methods, like flotation, are

more cost – effective than chemical methods but have the disadvantage of resulting in energy loss by removing coal particles containing finely disseminated pyrite (Kargi, 1982).

2.6.4 Chemical method

The chemical methods that involve treatment with different chemicals are effective for removing mineral matter, which is finely distributed and bound strongly to the coal (Mukherjee and Borthakur, 2003). A number of chemical methods for the removal of both pyritic and organic sulphur from coal have been advocated (Eligwe, 1988). According to Cara *et al.* (2006), chemical methods rely on oxidizing agents, reduction with chemicals, and alkaline and acidic solutions to separate mineral matter from coal, and although yields are good (about 90% inorganic and 10% organic sulphur are removed), part of the combustible matter of the coal is lost. A wide variety of chemical methods has been used for reducing the sulphur content from coal combustion. Mukherjee and Borthakur (2003) reported removal of 80 – 90% of ash and 70 – 80% of total sulphur present in several bituminous coals with 80 – 90% recovery by treating with molten mixtures of NaO and KOH at 350 – 370 °C. KOH solution of 2% at 95.8 °C removes around 94% pyritic sulphur and 94 – 95% sulphate sulphur from the coal samples against the removal of 84 – 90% pyritic sulphur and 90 – 92% sulphate sulphur by sodium hydroxide solution under similar conditions. The entire sulphate sulphur and over 98% pyritic sulphur from the coal samples may be removed by leaching with 8% KOH solution at 95. 8 °C. KOH of 16% solution removes 11–15% organic sulphur against 9 – 11% as found with sodium hydroxide solution at 95. 8 °C (Mukherjee and Borthakur, 2003). On another case, Mukherjee and Borthakur (2003) investigated Assam coal treatment with an aqueous solution of KOH alone or followed by mild hydrochloric acid. KOH alone removes 2 – 19% ash and 16 – 30% of the total sulphur from Boragolai and Ledo coal which increases, respectively, to 28 – 45% and 22 – 35% by the two – step process (Mukherjee and Borthakur, 2003). Sulphur and ash removal was found to increase with the increase of reaction time and temperature. In another case, Vasilakos and Clinton (1984) studied the removal of sulphur and ash from coal treated with aqueous hydrogen peroxide sulphuric acid solutions at ambient temperature, under a variety of experimental conditions. Almost complete elimination of the sulphate and the pyritic sulphur was observed in most cases, as well as a substantial reduction in the ash content. The other components of the organic coal matrix were not affected to a significant extent, indicating high selectivity of the H_2O_2/H_2SO_4 system towards sulphur oxidation. An optimal H_2SO_4 concentration was

established, above which the acid was found to have an adverse effect on the oxidation of pyrite by hydrogen peroxide (Vasilakos and Clinton, 1984). Table 2.3 shows chemical additives and their corresponding sulphur form. The focus was on the dominant form of sulphur as opposed to the total forms.

It is suggested that coal of high organic sulphur content, must be treated chemically to achieve an acceptable level of sulphur content. However, there are problems associated with the method including cost, efficiency, reliability and waste disposal (Olson and Brinckman, 1986). According to Eligwe (1988), the chemical desulphurization methods have drawbacks such as (i), they are often expensive and (ii) they destroy the caking properties of coal. On another hand, chemicals employed for desulphurization may sometimes hazardous to the environment and lethal to the humans for their explosive and toxic nature (Saikia *et al.*, 2016). Furthermore, although chemical methods techniques are efficient, they are rather expensive and prevent coal prices from competing with other energy sources (Gómez *et al.*, 1997). Lastly, chemical desulphurization processes operate at high temperatures (100 – 400°C) and therefore are energy – intensive (Kargi, 1982). Therefore, no such process is, as yet, commercially available, although several processes are under active development (Gryglewicz *et al.*, 1995).

Table 2.3: Chemical additives and sulphur form removal

Coal Type	Additives	S_{PYR}	S_{ORG}	S_{IN}	S_S	S_{TOT}	Ash	References
Makum coalfield	NaOH and Acid Solution	-	10%	100%	-	-	50%	Mukherjee and Borthakur (2001)
-	NaOH	100%	40%	-	-	-	-	Warzinski and Friedman (1977)
Subbituminous coal	NaOH	-	-	-	-	30%	29%	Araya *et al.* (1981)
Turkish lignites	NaOH	-	-	-	-	65%	60%	Karaca and Ceylan (1997)

- = Not reported, S_{PYR} = Pyritic sulphur (wt.%, db), S_{S} = Sulphate sulphur (wt.%, db), S_{ORG} = Organic sulphur (wt.%, db), S_{T} = Total sulphur (wt.%, db)

2.6.5 Biological method

Microbial desulphurization has emerged as a potential alternative to meet the challenge of high sulphur content in power station coals. Microbial desulphurization involves the oxidation of sulphur compounds by microorganisms on the surfaces of coal particles. Therefore, the available particle surface area is one of the critical factors that determine the rate of sulphur removal from coal (Kargi, 1980). According to Kargi (1982), the process involves microbial growth on the surfaces of coal particles with the diffusion of dissolved nutrients (including oxygen and carbon dioxide) through the product layer surrounding the coal particles. The principle underlying microbial desulphurization, with special emphasis on inorganic sulphur removal, is based on a complex combination of spontaneous (non-biological) and microbiologically catalyzed oxidations of inorganic sulphide mineral present in the coal. Therefore, the C – S bond cleavage can be regarded as an important precondition for the desulphurization of coals.

Some *fungi* are also tested for coal biodesulphurization since they are able to metabolize a broad range of anthropogenic chemicals and hydrocarbons, including polycyclic aromatic hydrocarbons and organosulphur compounds through the action of cytochrome P-450 and extracellular enzymes (Gonsalvesh *et al.*, 2012). By applying white – rot fungi *Trametes versicolor*, the maximum total sulphur desulphurization of 40% is recorded for Tunçbilek lignite without a change in calorific value (Gonsalvesh *et al.*, 2012). *Aspergillus-like fungi* are reported as capable of removing about 70 – 80% of total sulphur from Assam coal in 10 days (Gonsalvesh *et al.*, 2012). The authors especially underline that the results indicate a microbial attack on organic sulphur since sulphur presence in Assam coal is mainly in organic form.

During the last four decades, researchers focused on sulphur removal from different kinds of coal through mesophilic and acidophil microbes. According to Ye *et al.* (2018), *A. ferrooxidans, A. thiooxidans* and *Leptospirillum ferrooxidans* have been applied and removed 91.81%, 63.17% and 9.41% of sulphur content from Rajasthan lignite, Polish bituminous coal and Assam coal respectively. Kilbane (1990) who concluded that the microbiological process could remove up to 90% or more of the inorganic sulphur within a few days supports the latter statement. In a follow-up study, Kargi and Robinson (1986) used *Sulfolobus acidocaldarious* to remove organic sulphur from inorganic-sulphur-free bituminous coals and organic sulphur decrease of about 44% is achieved. Separately, *Pseudomonas putida* is

claimed to have reduced pyritic sulphur by 75% and organic sulphur by 37.4% from Texas lignites in 5 –7 days for particle sizes varying from 74 μm to 295 μm (Gonsalvesh *et al.*, 2012). In one case, they reported a case where a mixed heterotrophic culture isolated from soil and enriched on dibenzothiophene was used to remove organic sulphur from coal. Nearly 20% of organic sulphur removal from bituminous coal was reported. In another case, a thermophilic (50°C) *Thiobacillus* type organism (the strain THl, originally isolated by C. L. Brierley) was used for the removal of organic sulphur from Turkish lignite. About 50% of organic sulphur removal was reported in 25 days of incubation. The thermophilic, sulphur-oxidizing organism *Sulfolobus acidocaldarius* was used to remove organic sulphur from inorganic sulphur – free coal samples. The organisms were first adapted to DBT in a sulphate-free mineral salts medium. Nearly 44% of initial organic sulphur was removed from 10% coal slurries at 70°C in about four weeks. The most studied microorganism for coal desulphurization and sulphide ore leaching is the chemoautotroph *Thiobacillus ferrooxidans* (Gonsalvesh *et al.*, 2012). According to Gonsalvesh *et al*. (2012), this microbial culture has demonstrated effectiveness in pyritic sulphur removal. Depending on coal quality and experimental conditions, 40 – 90% of pyritic sulphur desulphurization effects have been achieved. Lastly, microbiological chemical leaching (MBCL) methods are also reported in the literature and are promising in terms of coal purification from an environmental point of view (Mketo *et al.*, 2016). However, MBCL methods are tedious and not so feasible for an industrial large-scale purpose.

Biological desulphurization of coal has been given increasing attention over the years. The research on microbial desulphurization of coal has concentrated on the removal of pyritic sulphur using *Thiobacillus ferrooxidans* or a mixed culture of *T. ferrooxidans and T. thiooxidans* (Kargi and Robinson, 1986). Most of the reported studies on microbial coal desulphurization using *T. ferrooxidans* have been concerned with the influence of particle size on the pyritic sulphur removal rate (Kargi, 1982). Biological processes technique offer many advantages over conventional physical and chemical processes. Biological desulphurization is performed under mild conditions (Gonsalvesh *et al.*, 2012); and the value of coal is not affected (Prayuenyong, 2002). Biological desulphurization is generally a low energy process even with the energy cost of stirring (Cara *et al.*, 2005). It has low operating and capital costs. According to Olson and Brinckman (1986), some problems that are anticipated with microbial coal desulphurization are relatively long bioprocessing times (days

to weeks) and the production of acidic, corrosive leaching solutions. However, the technique of biodesulphurization suffers from the limitation of slow kinetics (Agarwal *et al.*, 2016). According to Orsi *et al.* (1991), the use of heterotrophs such as *Pseudomonas* genus will require much more care in the design and operation of the bioreactors and circuits owing to the much greater risks of contamination and disastrous consequences deriving from the neutral pH environment suitable for these microbial strains. On the other hand, microbiological processes must be competitive with more conventional technologies such as flue gas desulphurization in order to achieve commercial application (Olson, 1994). The main impediment in the commercial application of a microbiological process for the removal of sulphur from coal, three, in particular, can be identified including the need for more and better bacterial cultures, the lack of stability of desulphurization abilities in microbial cultures and the lack of convenient as well as accurate analytical techniques for measuring organic sulphur. What is needed is to achieve these levels of sulphur removal for forms of sulphur in a single cost-effective culture or process in order to mitigate the high level of SO_2 emissions resulting from high sulphur content.

2.7 Desulphurization Mechanisms

In the periodic table, sulphur is a second-row constituent of the oxygen (O) or chalcogen group (Group 16) of non-metal elements. Therefore, sulphur displays chemical and physical similar to oxygen, which is appreciated for its role on the biology. Thus far, sulphur possesses unique characteristics that are different from oxygen and facilitate distinct biochemistry fundamental to life. These differences are attributed predominantly to a function of atomic size since sulphur is larger than oxygen. This increased atomic radius also causes sulphur to be less electronegative, with greater charge separation than oxygen. This leads to bond formation that is less ionic and weaker as is seen in bonds between carbon and sulphur. The larger radius of sulphur also lends it greater reactivity than oxygen, as electrons are more easily stripped away. Unlike oxygen, sulphur atom contains available *d* orbitals for bond formation that confer stability to species of varied oxidation states ranging from – 2 to +6 (Greenwood and Earnshaw, 1997). Furthermore, sulphur atoms are more hydrophobic such that they are unable to readily form hydrogen bonds like oxygen. However, bonds between two sulphur atoms (disulphide; R-S-S-R) are more stable than those between two oxygen atoms (peroxide; R-O-O-R), which is a critical feature of sulphur biochemistry. This is

particularly important to the redox chemistry mediated by sulphur containing functional groups as shown in Table 2.4.

Table 2.4: Important forms of sulphur and their oxidation states (Huxtable and Lafranconi, 1986)

Compound	Formula	Oxidation state (s) of sulphur
Sulphide	S^{2-}	–2
Sulphur[a]	S_8^0	0
Hyposulphite (dithionite)	$S_2O_4^{2-}$	+2
Sulphite	SO_3^{2-}	+4
Thiosulphate[b]	$S_2O_3^{2-}$	0, +4
Dithionate	$S_2O_6^{2-}$	+4
Trithionate	$S_3O_6^{2-}$	0, +4
Tetrathionate	$S_4O_6^{2-}$	0, +4
Petrathionite	S_5O_6	0, +4
Sulphate	SO_4^{2-}	+6

[a] Occurs in an oactagonal ring in crystalline form

[b] Outer S has a valence of 0, Inner S has a valence of +4

The important reactions involved in chemolithotrophic oxidation of sulphur forms can be observed in Fig. 2.6:

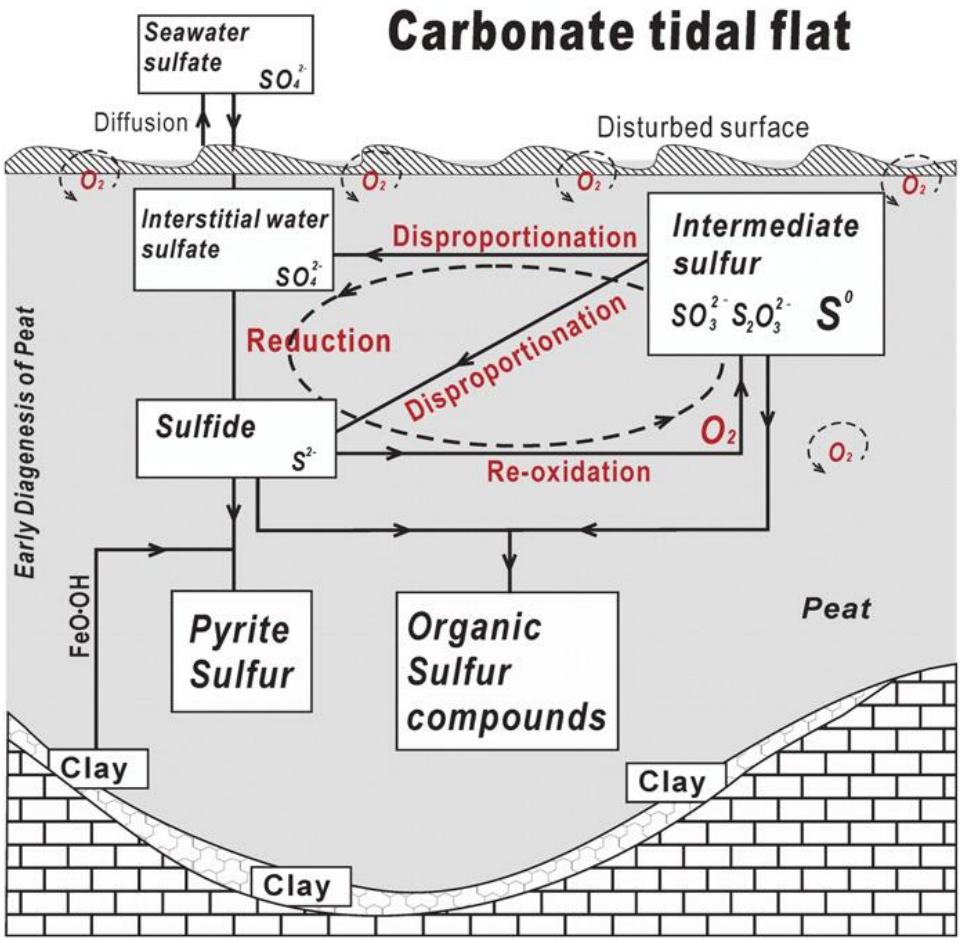

Figure 2.6: A cycle model of sulphur reduction, reoxidation, and disproportionation (Li and Tang, 2014)

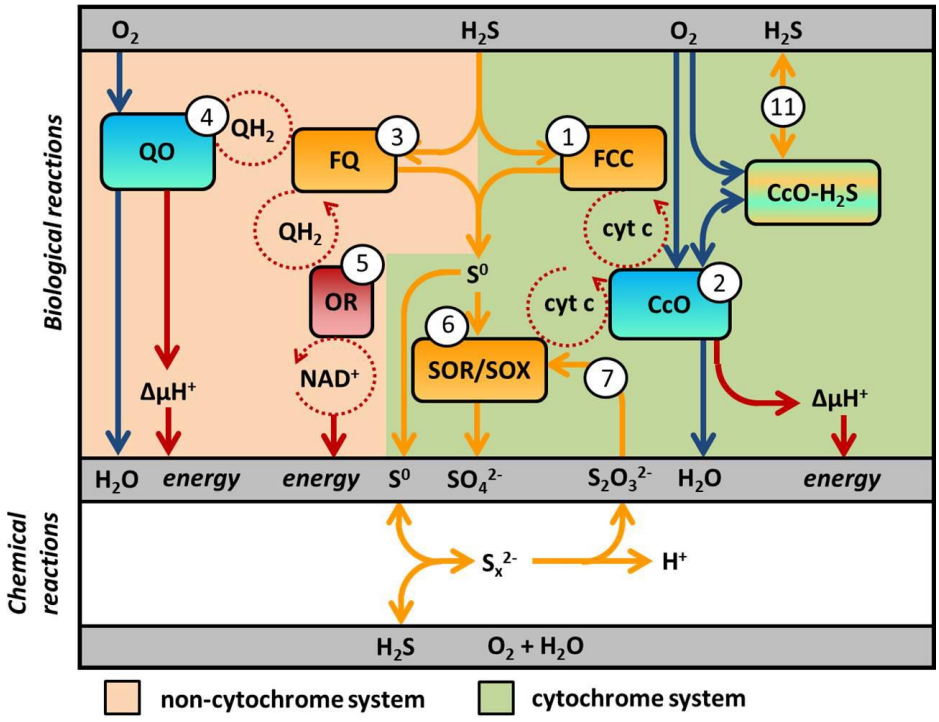

Figure 2.7: Reaction pathways that lead to the (biological and chemical) formation of S^0, $S_2O_3^{2-}$ and SO_4^{2-} from the oxidation of hydrogen sulphide (Cara *et al.*, 2006). Numbers inside circles refer to reaction equation numbers mentioned in the text.

A schematic overview of the modeled bacterial catalysis processes is shown in Fig. 2.7. Bacterial catalysis process is characterized by a double mechanism, direct and indirect (Cara *et al.*, 2006). In the direct mechanism, the oxidation of sulphur to sulphate depends on a close contact between the bacteria and the surface of the pyrite in aerobic conditions, on the other hand, by the indirect mechanism, the bacteria oxidize ferrous iron to ferric, and the ferric ions, in turn, oxidize pyrite (ferric-induced oxidation) while being reduced to ferrous iron.

Cara *et al.* (2006) summarized the reduction process according to the following processes: (1) FCC, (2) Cco, (3) FQ, (4) Qo, (5) OR, (6) SOR/SOx, (7) SOR/SOx, (11) Reversible H_2S - Cco-H_2S formation. According to Kargi (1982), the major role of bacteria in the indirect mechanism is to regenerate the ferric iron for chemical oxidation of pyrite. Karavaiko and Lobyreva (1994) explain the summary of the mechanisms of oxidation of complex sulphur organic compounds. According to Karavaiko and Lobyreva (1994), since heterocyclic sulphur organic compounds are not water-soluble, two different pathways of primary reactions occurring on the cell surface are possible: (a) homogenization and subsequent

transfer of aromatic compounds into cells; (b) cleavage of the aromatic ring outside the cell and the transfer of soluble products into the cell. The first mechanism of microbial cell interaction with an insoluble substrate could be illustrated by oxidation of benzpyrene. Borah and Baruah (1999) reported the cleavage of the C – S bond by radical ion electron transfer reactions. Therefore, C – S bond cleavage can be regarded as an important precondition for the desulphurization of the coal (Klein *et al.,* 1994). In general, for a successful application of bacterial strains several preconditions must be fulfilled: (a) the biocatalyst has to survive under process conditions; (b) the organic sulphur has to be available for a biological attack; (c) the desulphurizing enzymes have to recognize the sulphur-containing region for a catalytic action.

This mechanism requires physical contact between bacteria and sulphur forms of particle sizes. Therefore, the bacteria are initially attached to the coal particles, which in turn solubilize the minerals. This attachment, which is part of the overall process, is known to be fast compared to the rest of the procedure (Weerasekara *et al.,* 2008). The attachment normally takes place in specific locations in the particle or mineral, such as cracks, voids, defects, etc. Following the attachment, the leaching reaction can be assumed to take place (Weerasekara *et al.,* 2008). This is shown by reaction 2.7:

$$\text{Pyrite} + \text{Attached cell} \rightarrow \text{cells in liquid} + 15Fe^{2+} + H_2SO_4 \qquad (2.7)$$

It needs to be mentioned that the cellular location of the biodesulphurization metabolism has been a debated issue. Agarwal *et al.* (2016) have proposed that biodesulphurization reaction occurs inside the microbial cells. Although there is no evidence that enzymes responsible for first two oxidations of the sulphur compound are secreted into the medium (Agarwal *et al.,* 2016); the size of the substrate metabolized and utilization of the liberated sulphur by other bacteria make it more likely that desulphurization occurs in association with external surface of the cells (Agarwal *et al.,* 2016). In *Rhodococcus strains*, substantial desulphurization activity was found in the cell debris fraction that contained external cell membrane cell wall fragments (Agarwal *et al.,* 2016). However, some papers have also conjectured that desulphurization occurs in association with an external surface of the cells or the cell membrane, which is a location at which both extracellular substrates and intracellular cofactors can be, accessed (Agarwal *et al.,* 2016). Therefore, sulphur forms in the coal follow one of the following pathways in order to carry out the desulphurization process: sulphur

oxidation, C – C bond cleavage or C – S bond cleavage. The organic aromatic sulphur containing compounds such as DBT, require special desulphurization methods to break the C – S bond and release the sulphur atom present in the aromatic ring (Mishra *et al.*, 2014). Figure 2.8 depicts the metabolic pathway of biodesulphurization of DBT by '4S' mechanism.

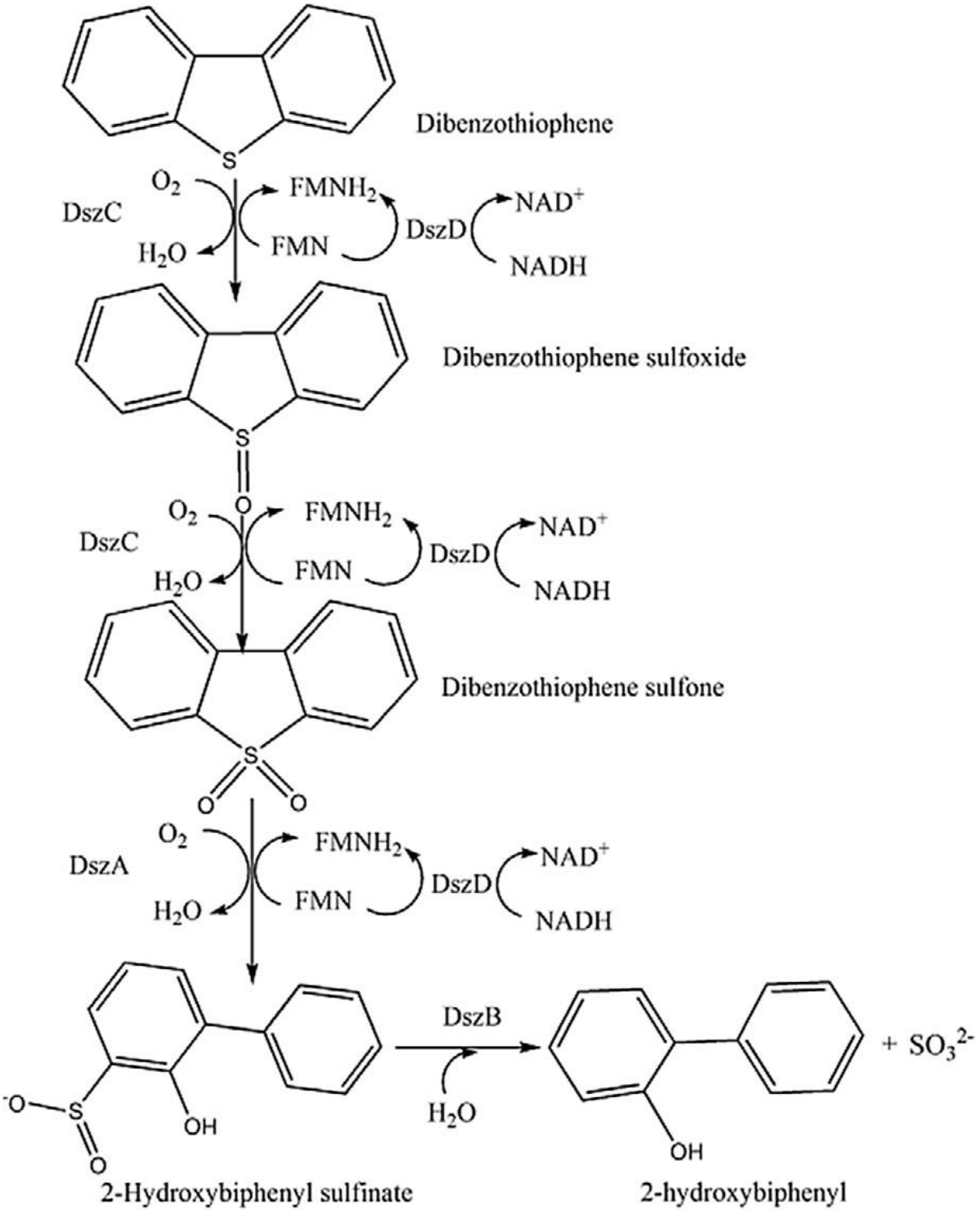

Figure 2.8: Metabolic pathway of biodesulphurization of DBT by '4S' mechanism (Agarwal et al., 2016).

The *Rhodococcus* and *Pseudomonas* species carry out desulphurization through oxidative and non-destructive 4S pathway, which converts the dibenzothiophene into sulphur – free 2-hydroxy biphenyl (Agarwal et al., 2016). The 4S pathway, as shown in Fig. 2.5 of desulphurization involves 3 intermediates, viz. DBT sulphoxide, DBT sulphone, and hydroxyl biphenyl. The enzymes involved in the pathway are two monooxygenases and one desulphinase. A distinct merit of 4S metabolic pathway (over the alternate Kodama pathway) is that it involves breakage of C – S bond (and not C – C bond as in Kodama pathway), which also results in conversion of the fuel value.

2.8 Bacteria in Coal and Microorganisms for Sulphur Removal

It was shown as early as in the year 1962 that coals contain bacteria (Lin *et al.,* 1993). However, the bacteria found in the coal could be indigenous in origin or be contaminated from coal processing plants. Sulphur is frequently present in microorganisms and occurs in organic compounds such as amino acids, proteins, enzymes, antibiotics and fats. Either these compounds serve as a source of sulphur for assimilation and synthesis of organic compounds or they are used as electron acceptors or donors in dissimilation processes (Pokorna and Zabranska, 2015).

Therefore, biodesulphurization of coal can be obtained in inexpensive conditions by using bacteria inherent in the coal itself. The advantages of using bacteria inherent in the coal over using the pure isolated bacterium are the immediate adaptation of the microorganisms to the coal and the reduced adaptation period. Furthermore, the complication in controlling pure microorganism will not be a factor in cases where bacteria inherent in the coal itself is used (Prayuenyong, 2002). Table 2.5 shows a list of bacteria identified in the different coal samples.

Table 2.5: Bacteria identified in the different coal samples (Gómez *et al.*, 1997)

Number	Result
1	*Chryseomonas luteola*
2	*Xanthomonas maltophilia*
3	*Pseudomonas cepacia*
4	*Pseudomonas pseudomallei*
5	*Pseudomonas putrefaciens*
6	*Pseudomonas mesophilica*
7	*Pseudomonas vesicularis*
8	*Pseudomonas chlororaphis*
9	*Pseudomonas aerofaciens*
10	*Pseudomonas Juorescens*
11	*Pseudomonas oaucimobilis*
12	*Moraxella phenilpyruuica*

2.9 Factors Affecting Desulphurization

The efficiency of microbial oxidation of sulphur forms depends on a number of factors such as the coal particle size, the sulphur form content and their distribution in the coal, the type of inoculum of micro-organisms to be used, iron concentration in the leachate, nutrient media composition, pH, temperature, aeration and reactor design (Cara *et al.*, 2005). In addition, the sulphur removal depends on the nature of the organic sulphur matrix, conditions of treatment, diffusion phenomena and chemical reaction characteristics (Kolja, 1995). Below is a summary of key factors affecting the desulphurization process:

(a) Particle size and coal concentration (pulp density)

Particle size is a major factor affecting the rate of sulphur reduction. The particle surface area is one of the critical factors that determine the rate of sulphur removal

from coal, Kargi (1982). The size of the coal particle is an important factor in the microorganism's ability to desulphurize the coal. It determines the accessibility of the sulphur form and exerts a considerable influence on the rate of oxidation of sulphur form thereby, total sulphur removal. The early work of Olson and Brinckman (1986) and later on Acharya *et al.* (2001) showed that the best removal of sulphur was achieved with small particle sizes. According to Eligwe (1988), the rate of metal extraction from ores as well as metal recoveries increases with increasing specific surface area (i.e., reduction in the particle size). This is supported by another case reported by Shen et al. (2012) who mentioned that desulphurization efficiency increase with the decrease of coal particle size. The reason is that small particle size has higher mass transfer efficiency in favorable of spreading. Therefore, the best removal of sulphur could be achieved with the finest size fraction in all the coals. One other important parameter from the viewpoint of plant design and operation is the solids concentration in the pulp. Early biohydrometallurgical investigations by Kargi (1982) pointed to a 20% solids concentration as the threshold beyond which bioleaching rates start declining. Therefore, the microbial cell concentration has to be large at high concentrations of coal (i.e. high pulp density) for the effective removal of sulphur from coal (Kargi, 1982).

(b) Eh, EP and conductivity of sulphide minerals

The redox potential (Eh) of a bacterial leaching medium affects the rate of metal sulphide oxidation by microbial means. The chemoautotrophic bacteria thrive in limited intermediate redox potentials and to avoid the precipitation of iron as jarosite during leaching an Eh range of + 400 to + 500 mV is generally recommended. Eligwe (1988) published accounts on the effect of Eh on bacterial leaching which indicated that Eh values between + 220 and + 600mV have been observed during the oxidation of metal sulphides by *T. thiooxidans*. Notwithstanding that the redox potential varies from + 190 to about + 555 mV during the oxidation of ferrous ion to ferric ion by *T. ferrooxidans*, (Eligwe, 1988). The electrode potential (EP) of sulphide minerals as well as their conductivities and crystal structures also influence their microbial leaching rates.

(c) pH

PH control is an important coal desulphurization parameter. The value of the pH variations during the microorganisms driven desulphurization process are known to have a great effect on the rate of the reactions (Weerasekara *et al.*, 2008). Bioleaching microorganisms are generally acidophile and grow in the pH range of 1 – 2.5 (Kiani *et al.*, 2014). Kiani *et al.* (2014) observed that by decreasing pH from 2 to 1, both total sulphur and ash content of the coal was decreased. These results may be due to the formation of sulphate and jarosite precipitates at higher pH values (Kiani *et al.* 2014). It should be noted that the pH of a desulphurization system significantly affects the growth and activity of acidophilic microorganisms, the precipitation of jarosite and the dissolution rate of acid-soluble minerals. The optimum pH for bacterial leaching of metal sulphides varies with the nature of the substrate and it is within the range of 2 to 3.5 (Eligwe, 1988). The optimum pH for pyrite removal from coal lies within the range 2 to 2.5 (Eligwe, 1988).

(d) Dissolved gases

Oxygen is the primary terminal electron acceptor for iron and sulphur oxidation by species of microorganisms and must be made available to the organisms for oxidation.

(e) Temperature

Optimum growth at moderate temperatures of 28 – 35°C and optimum temperatures for desulphurization of coal by microorganism are within the same range (Olson and Brinckman, 1986). It is well established that bacteria can grow between the temperature ranges of 18 to 105 °C (Eligwe, 1988). According to Eligwe (1988), the optimum temperature of oxidizing Fe^{2+}, S(0) and metal sulphides by mesophilic bacteria lie within 30 – 45°C temperature variations.

(f) Other factors

Coal porosity plays a major role in the process kinetics in that the higher the porosity, the greater the exposed surface and the smaller the particle size the greater the surface area-to-volume ratio. In some cases, acidic prewash of coal has improved biodesulphurization, possibly attributable to the removal of acid-consuming materials or toxic elements. Furthermore, the presence of toxic metals in coal (Ag, Hg, Cd, and MO) also has an impact on the rate of desulphurization.

Table 2.6 shows key variables factors in the various sulphur removal techniques. For example, there are those factors such as coal particle size that are applicable across all techniques.

Table 2.6: Variables in the sulphur removal process (Olson and Brinckman, 1986; Orsi *et al.*, 1991)

Physical Method	Chemical Method	Biological Method
Temperature	Rank of coal	Microbial strain
Coal particle size	Dissolved gases	Microbial interactions
Coal porosity	Metal resistance	Inoculum size
Pressure	Composition of culture medium	Resistance to metal ions
Solid Concentration	pH	Cell concentration

2.10 Desulphurization Reaction Kinetics

There is limited kinetics data for sulphur transformation during the desulphurization of coal in the literature. The degree of sulphur conversion can be calculated by Equation (2.8):

$$X_0 = 1 - \eta \frac{S}{S_0} \quad (2.8)$$

where: η = efficiency, S = sulphur content after treatment (wt.%, db), S_0 = Initial sulphur content before treatment (wt.%, db)

Thus, a pseudo first-order rate equation can be assumed for the removal of sulphur from coal during biodesulphurization. The relation was described theoretically in terms of total sulphur content:

$$-\frac{dS}{dt} = k_s S \quad (2.9)$$

$$S(0) = S_0 \quad (2.10)$$

$$X_0 = 1 - \eta \frac{S}{S_0} \quad (2.11)$$

The solution of the system of Equations (2.8) – (2.11) gave

$$X_S = 1 - \exp(-k_s t) \quad (2.12)$$

where: k_s = the first-order rate constant, t = time in hours

To calculate the reaction rate constants for the reaction, measured kinetic parameters from a lab-scale apparatus can be employed. According to Acharya *et al.* (2005), the reaction rate can be modelled by an Arrhenius type equation, which is expressed as Equation (2.12).

The general conclusions about biodesulphurization reaction kinetic system that can be drawn from the previous literature are as follows: (i) kinetics of biodesulphurization is best described by competitive substrate inhibition model; (ii) the rate of biodesulphurization reduces with number of substituent of DBT as indicated by rise in Michaelis constant and reduction in inhibition constant; (iii) rate of biodesulphurization is not affected by transport of the substrate and intermediates of 4S pathway across cell membrane, concentration of the reduced cofactors and activity of enzymes of 4S pathway (Agarwal *et al.*, 2016). According to Eligwe (1988), the inhibitory effect of organics in coal desulphurization can be remedied by the use of activated carbon that can adsorb the organics. It has been suggested that the problem may also be remedied by the use of heterotrophic microbes such as *T. acidophilus*, *T. novellus* and *T. perometabolis*, which metabolize organic compounds such as alcohols, organic acids and amino acids in a symbiotic culture with *T. ferrooxidans*.

2.11 Microorganism and Desulphurization Efficiency

Microbial cultures can remove either organic or inorganic sulphur from the coal. Several bacterial cultures have been claimed over the years to be capable of breaking the C – S bonds in the coal. These microorganisms convert the inorganic sulphur to sulphate, which is soluble in water (Acharya *et al.*, 2001). After the completion of the cleaning process, the coal is separated from the liquid phase containing sulphate and washed with water to obtain coal with lower sulphur content. Example of the microorganisms capable of removing sulphur forms from coal include *Pseudomonas spec (*Klein *et al.*, 1994); *Bacillus spec* (Klein *et al.*, 1994)*; Pseudomonas putida* (Klein et al., 1994)*; Beijerinckia*, *Acinetobacter*, *Desulfovibrio desulphuricans*, *Rhodococcus rhodochrous*, *Sulfolobus*, *Sulfolobus* acidocaldarious (Kargi and Robinson, 1986); *Brevibacterium*, *Cunninghamella elegans*, *Escherichia coli* and *Rhizobium* (Rossi, 2014). Table 2.7 shows coal type, microorganisms and various sulphur distribution as well as total sulphur removal efficiency. The impact of other forms of sulphur was not determined other than the focus on the organic sulphur form. It is now clear that for sulphur content to comply with the new minimum emissions standards.

Table 2.7: Coal type, microorganisms and various sulphur distributions

Coal Type	Organisms	S_{PYR}	S_{ORG}	S_{IN}	S_S	S_{TOT}	Duration	References
Bituminous coals	*Sulfolobus acidocaldarious*	-	44%↓	-	-	-	-	Kargi and Robinson (1986)
Texas lignites	*Pseudomonas putida*	75%↓	37.4%↓	-	-	-	5 – 7 Days	Rai and Reyniers (1988)
Illinois Basin Coal	*Rhodococcus rhodochrous* IGTS8	-	35%↓	-	-	-	3 Weeks	Gonsalvesh *et al.* (2012)
		-	27.1%↓	-	-	-	-	Özbas *et al.* (1996)
Turkish lignites	*R. rhodochrous*	71.4%↓	47.8%↓	-	97.7%↓	57.8%↓	-	Özbas *et al.* (1993)
Turkish lignites	*Sulfolobus solfataricus*							
Tunçbilek lignite	white rot fungi *Trametes versicolor*	-	-	-	-	40%↓	-	Aytar *et al.* (2008)
Assam coal	*Aspergillus-like* fungi	-	-	-	-	80%↓	10 Days	

- = Not reported

2.12 Summary

The sulphur in the coal occurs as both inorganic and organic form. The inorganic forms are typically elemental, metallic sulphides and sulphates, with pyrite being the major dominant inorganic sulphur host in most coals. Many authors have provided the atlas on Waterberg coalfield geological setting. From the literature survey, it can be summarized that the nature of the sulphur forms and their distribution in the Waterberg coalfield has not yet been precisely determined and the literature on this is insufficient. Coal maceral analyses coal showed that inertinite, vitrinite and liptinite are the main maceral groups' occurring in most coals. However, there are contradicting statements in the literature with regard to the dominant macerals in the Waterberg coals. Some authors believe that the Grootegeluk Formation is higher in vitrinite while others reported that the coalfield is enriched in inertinite compared to the other coal macerals. The difference in the information shared in the literature is attributed to different coal products produced from Waterberg coals beneficiation process.

Wide varieties of processes (viz. microbial, chemical and physical methods) that have been known to desulphurize coal are documented in the scientific literature. Various technologies for roadmap to clean coal technology have since been proposed. Among all the processes mentioned, microbial treatment arises as a clean, efficient and environmentally reasonable technique that is having low capital and operating costs as well as being less energy – intensive. Microbial desulphurization of coal has been given increasing attention over the years. However, the vast majority of the literature on coal desulphurization has centered mostly on pyritic sulphur removal, which represents one of the forms total sulphur content in coal. There is no published information on microbial desulphurization on various forms of sulphur content in the Waterberg steam coal.

Important forms of sulphur and their oxidation states that is the basis for desulphurization mechanisms have been provided. Therefore, the efficiency of microbial oxidation of sulphur forms depends on a number of factors such as the coal particle size, the sulphur form content, the type of inoculum of microorganisms to be used, iron concentration in the leachate, nutrient media composition and pH. However, process variables, such as the availability of CO_2 for microbial use or the coal particle concentration in the reaction medium were not considered in the reported studies. It can also be concluded that the removal of pyritic sulphur form from coal by pure cultures including *Rhodococcus rhodochrous, Sulfolobus acidocaldarius, Acidithiobacillus ferrooxidans, Acidithiobacillus caldus, T. ferrooxidans, T.*

thiooxidans, Leptospirillum ferrooxidans, Bacillus subtilis, Paenibacillus polymyxa, Pseudomonas aeruginosa and fungi (the genus Aspergillus, Pseudomonas putida and other microorganisms have been reported by various authors. The intensity of research in both range and depth shows deepening concern over the interest in developing various desulphurization techniques to reduce the amount of sulphur content in the coal to an acceptable level. Although extensive studies have been done on bioremoval of pyritic with a few attempt on organic sulphur forms, most of organic sulphur forms studies were carried out using model compounds that are recognized to behave differently to the actual sulphur content in the coal.

CHAPTER 3
MATERIALS AND METHODS

3.1 Basal Mineral Medium

Basal mineral medium (BMM) was prepared by dissolving (in 1 L distilled water): 1.013 g/L NH_4Cl; 0.620 g/L $NaH_2PO_4 \cdot 2H_2O$; 2.5 g/L K_2HPO_4; 0.0103 g/L $MgSO_4 \cdot 7H_2O$; 0.00425 g/L $CaCl_2 \cdot 2H_2O$; and 0.00085 g/L $FeCl_3 \cdot 3H_2O$ (Roslev et al., 1998). The BMM was adjusted by adding 1 mL of trace metals prepared by dissolving (in 1 L distilled water): 0.243 g/L $FeCl_3 \cdot 6H_2O$; 0.060 g/L $MnCl_2 \cdot 2H_2O$; 0.041 g/L $ZnCl_2$; 0.026 g/L $CuCl_2 \cdot 2H_2O$; 0.036 g/L $CoCl_2 \cdot 2H_2O$; 0.015 g/L $Na_2B_4O_7 \cdot 10H_2O$; 2.205 g/L $Na_3C_6H_5O_7$; 0.026 g/L $(NH_4)_6Mo_7O_{27} \cdot 4H_2O$; 5.104 g/L KH_2PO_4; 3.105 g/L $NaH_2PO_4 \cdot H_2O$; 1.980 g/L $(NH_4)_2SO_4$; 18.450 g/L NH_4Cl; 2.205 g/L $CaCl_2 \cdot 2H_2O$; 3.049 g/L $MgCl_2 \cdot 6H_2O$; and 0.025 g/L $NiCl_2 \cdot 6H_2O$), and 5 mL of a trace vitamin stock solution (g/L): 0.004 biotin; 0.004 folic acid; 0.02 pyridoxine hydrochloride; 0.01 riboflavin; 0.01 thiamin; 0.01 nicotinic acid; 0.0002 B_{12}; 0.01 p-aminobenzoic acid; and 0.01 thiotic acid). All chemicals used in the preparation of BMM were obtained at purities higher than 99% from MERCK Chemicals (Sandton, South Africa).

3.2 Culture Conditions and Chemicals

A mixed – culture of sulphur reducing bacteria was obtained from collected coal samples used in power generation. Coal samples were obtained from the coal feed into the power plant mills, by auto sampling equipment. The start-up culture was prepared by overnight cultivation in Luria-Bettani (LB) broth at 32 °C. The bacterial culture was incubated in an incubator shaker at 30 °C and 125 rpm. After 24 hours, the bacterial culture was filtered through a weighed glass – fibre filter (Whatman, GF/A, 90 mm of diameter, 1.2 µm pore size), and the isolated cultures were used to inoculate the reactor during biodesulphurization experiments. LB broth for culture cultivation and LB agar for colony development was obtained from Biolab (Midrand, South Africa).

3.3 Coal Samples Source

The coal samples were obtained from the supply stream of the newly commissioned Medupi Power Station situated some 17 km west of the town of Lephalale, Limpopo Province, South Africa. Waterberg coalfield supplies Eskom's coal-fired Medupi and Matimba power stations.

3.4 Steam Coal Samples Preparation

Coal samples were riffled to ensure a well-mixed and representative coal sample. Approximately 2 kg of riffled coal was loaded into the top sieve in the sieving pot and the cover replaced to ensure no particle leakage. The coal samples were crushed and screened for 5 min in the Ro-Tap® Testing Sieve Shaker using five different size fractions (+4.60 mm, −4.60 + 2.30 mm, −2.30 + 1.00 mm, −1.00 + 0.85 mm and −0.85 mm). The estimated error on particle size measurement itself is less than 3%. The precision (repeatability) of the measurements was assessed on a test bench, by quantifying the standard deviation of a series of measurements. The standard deviation was lower than 1.5%. Finer coal particles below – 0.85 mm was not considered, as fine coal particles are difficult to settle and good mixing environment is required for creating enough contact of coal particles and bacterial consortium for effective biodesulphurization. On the other hand, coarse particle greater than +4.60 mm particle sizes were also not considered due to stirring difficulties associated with coarse particles sizes.

3.5 Coking Coals Blend Preparation

Coal blending involved mixing four coking coals with different properties with respect to volatiles, ash, sulphur content and geographical origins.

3.6 Biodesulphurization Experiments

The desulphurization experiments were conducted in 500 mL continuously stirred Erlenmeyer flask. The reactor was inoculated with 250 mL of bacterial consortium from primary enrichment batch reactors and 200 g of the coal sample. A magnetic stirrer operating at a rate of 200 rpm in order to maintain a completely stirred tank reactor (CSTR) conditions homogenized the medium. Four different size fractions (+4.60 mm, −4.60 +2.30 mm, −2.30 +1.00 mm and − 0.85 mm) were considered to ensure an adequate representation. The particle size fraction of −1.00 +0.85 mm was not considered mainly because their proximate and ultimate analyses were found to be within the error of repeatability for – 0.85 mm. The reactor was operated at three different conditions as follow: inoculated (23 ± 3 °C), uninoculated (23 ± 3 °C) and uninoculated (30 ± 2 °C). The 20 g of coal samples obtained from biodesulphurization experiments were withdrawn at regular time intervals. For experiments with sterilized coal (to remove inherent bacteria), sterilization was done by autoclaving at 103 Pa (gauge) for 15 min.

At the end of biodesulphurization experiments, peristaltic pump was used to introduce the treated coal samples to vacuum filtration followed by vigorous wash to dissociate bacteria that may be attached to coal particles. Treated coal samples were dried overnight in a Protea Drying Oven at 30 ± 2 °C and analyzed as depicted in Figure. 3.1.

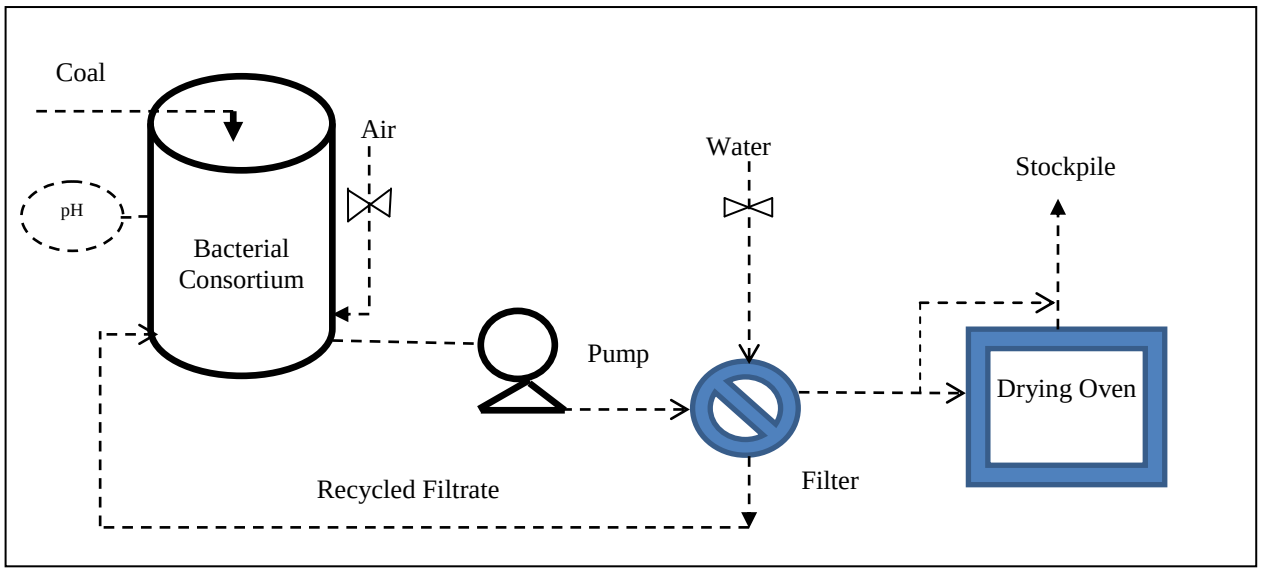

Figure 3.1: Schematic representation of the Biodesulphurization process

3.7 Determination of Carbonates, Ash Oxides and Trace Elements

Ultimate analyses such as Carbon (C), Hydrogen (H) and Nitrogen (N) were determined using LECO-932 CHNS Analyzer following ISO 12902:2001 standard procedure. Reproducibility for C, H and N were ±0.5%, ±0.25% and ±0.10% respectively (ISO 12902, 2001). Carbonate in coal samples was measured following ASTM D6316 method. For trace element determination, the coal samples were first subjected to microwave digestion using a Milestone Ethos Microwave High – Pressure Lab station. NIST traceable multi-element standards and SARM 18, 19, and 20 were used for calibration of trace element concentrations. The trace elements analyses in the coal ash sample were performed as per ISO 23380 (2008) standard procedure. X-ray Fluorescence (XRF) was used to determine the elemental composition of coal ash (ash analysis) following ASTM D3682-13 method. Coal samples were burnt in a bomb calorimeter and CV is measured following ISO 1928 (2009) method.

3.8 Proximate and Ultimate Analyses

The proximate analyses involve the determination of parameters namely; moisture, volatile matter, ash, and fixed carbon (by difference). The solids remaining after the determination of the volatile matter are the whole of the mineral matter and the non-volatile matter in the coal. The non-volatile organic matter is termed "fixed carbon". In the proximate analysis, the fixed carbon is determined by subtracting the total of the percentage moisture, volatile matter and ash from a hundred. As a result, fixed carbon gathers all errors from other variables tests (ash, moisture and volatile matter). Moisture content in the coal was determined by establishing the mass loss of a coal sample after drying it in an oven with a set temperature of 150 ± 5 °C and forced air circulation following the ISO 11722 (2013) standard procedure. Ash is the residue that remains after all the organic matter has been driven off during combustion Ash is determined in a furnace maintaining at a temperature of 815 °C ± 10 °C using ISO 1171 (2010) standard procedure. Volatile matter is determined in a carbolite furnace at a temperature of 1000 °C following the ISO 562 (2010) standard procedure.

3.9 Forms of Sulphur Analyses

Microwave assisted extraction (MAE) followed by Inductively Coupled Plasma–Optical Emission Spectrometry (ICP-OES) was used for extraction, identification and quantification of forms of sulphur in coal samples following ISO 157 (1996) standard and the organic sulphur was calculated by difference from the total sulphur obtained earlier by ASTM D4239-14 standard and forms of sulphur measurement.

3.10 Petrographic Analyses Sample Preparation

The samples were received crushed to -1 mm. The particles were set in epoxy resin under vacuum (24 hours) and the block was subsequently ground to achieve a polished surface, as per ISO 7404 part 2, using a Struers Tegraforce polisher.

3.11 Maceral Group and Vitrinite Reflectance Measurements Analyses

A petrographic block of coal was prepared from particles sized between 300 and 1000 µm and examined under a petrographic microscope. A total maceral reflectance scan, in which 250 reflectance readings were taken on all macerals over the polished surface of the petrographic block, was also undertaken on the coal samples. The polished blocks were assessed using a Zeiss AxioImager M2M petrographic microscope fitted with a Fossil Hilgers system for with a semi-automated point counting stage for maceral analysis, at a

magnification of × 500 under oil immersion following the Standard ISO 7404-3 (1994) method. Vitrinite reflectance is measured as the amount of reflected light from coal particles viewed under the microscope on prepared tablets composition. Photomicrographs were taken on a Zeiss Universal petrographic microscope with Axio vision software. Vitrinite reflectance was measured on 100 counts on vitrinite particles. Petroglite software and an automated stage were used for point counting. Vitrinite reflectance measurements establishing the coal rank were carried out in accordance with ISO 7404-5 (1994) standard procedure.

3.12 Carbonization Experimental Procedure

Carbonization tests were carried out in one of the coke making battery consisting of 50 slot ovens. The oven dimensions are 450 mm width × 1385 mm length × 620 mm height. The coal blend was prepared by mixing four coking coals covering a wide range of rank and coal measures such as volatile matter content, ash content, sulphur content, geographical origin and thermoplastic properties. The carbonization tar was produced from the base blend that was collected from tar decanters of the coking making plant by-products and stored in a tar storage tank at 55 ± 2 °C. Up to 2 – 8 wt.% of carbonization tar collected from the tar decanters arising as by-products from the coking plant was mixed with prepared coal blend through 8 nozzles of 8 mm diameter fitted in three rows on a single horizontal header pipe. Given that getting carbonization tar to get uniformly mixed in the coal blend has always been a challenge, this challenge was overcome by spraying carbonization tar in the conveyor belt feeding the crusher in order to increase contact period as the liquid infiltrated the porous nature of the coal on its way to the crusher and resulted in a better coal blend – carbonization tar mix. Coal blend was charged under gravity through charging holes into the coke oven that had reached 1200 °C. A programmable controller was used to keep the oven temperature constant. The temperature at the center of the coal charge was monitored by means of a thermocouple connected to a computer. The temperature of the wall was kept constant and the coking time was fixed at around 19 h throughout. Schematic layout of coke oven tar addition plant used for the experiments is depicted in Fig. 3.2 and the details of the associated equipment are shown in Table 3.2.

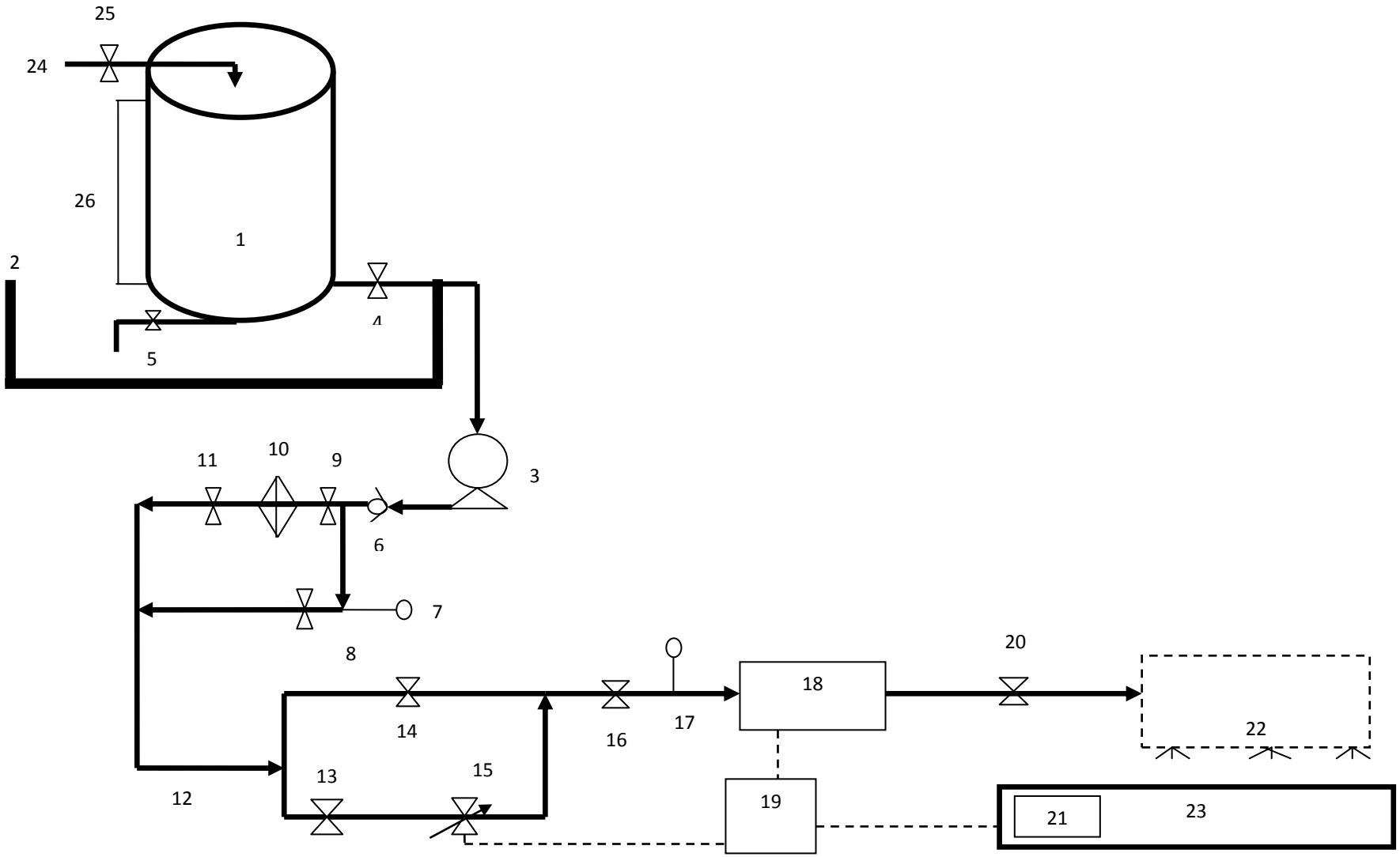

Figure 3.2: Schematic layout for coke oven tar addition plant

Table 3.1: Equipment for coke oven tar addition plant set-up

No	Item Description
1.	Coke oven tar Tank
2.	Bund Wall
3.	Motor-pump unit
4.	Hand Shut-off valve
5.	Drain valve
6.	Non-return valve
7.	Pressure gauge
8.	By-pass valve
9.	Hand valve
10.	Filters
11.	Hand valve
12.	32 mm pipe
13.	Auto-shut off valve
14.	By-pass valve
15.	Flow control valve
16	Manual control valve
17.	Pressure gauge
18.	Flow meter
19.	Programmable Logistic Controller
20.	Manual shut off valve
21.	Weighing scale
22.	Canopy with nozzles
23.	Tar resistant Conveyor Belt
24.	From Coke oven tar Storage
25.	Hand valve
26.	Level Indicator

3.13 Coking Coal Blends and Coke Analyses

Thermoplastic properties of the coal blends were carried out using Gieseler Plastometer (Preiser Scientific, China) following the ISO 10329 (2009) standard procedure. Total dilatation for coal blends was measured using a Rühr dilatometer (Netzsch, Germany) as per ISO 349 (1975) standard procedure. Coke samples produced were prepared and tested for Coke Strength after Reaction (CSR) and Coke Reactivity Index (CRI) measurement as per specification in the ASTM D5341 – 99 (2004) standard procedure. The Coke Micum indices measurements and coke cold strength were evaluated as per ISO 556 (1980) standard procedure. Stability factor reflecting the load carrying strength or impact resistance of the coke was determined following the ISO 501 (2012) standard procedure.

3.14 GC/MS Analyses of Carbonization Tar

Carbonization tar compounds were identified by Gas Chromatograph coupled with Mass Spectroscopy (GC/MS). Carbonization tar analysis was carried out using an Agilent 6890N GC-MS equipped with a HP – 5 capillary columns and a flame ionization detector (FID). Helium was used as carrier gas at a flow rate of 1.2 mL/min. The detector and injector temperatures were set at 280 °C and the column initial temperature was kept at 60 °C for 5 min, and then heated to 280 °C at a heating rate of 4 °C/min and held at the temperature for 10 min.

3.15 Viable Biomass Characterization

For this study, 0.1 mL of the bacterial sample was withdrawn in order to measure the bacterial cell count. Samples were serially diluted in 0.9 mL sterile 0.85% NaCl solution. Each diluted was then added to agar plates (100 cm × 15 cm size) followed by through mixing with approximately 10 mL of liquid agar at 46°C. Colonies were counted after 24 h incubation and the bacterial count was reported as colony forming units (CFU) per mL of sample. The dry weight of cell with known CFU count was converted to mass concentration. A conversion factor of 1.833×10^{-10} mg/cell was determined and used to convert CFU to the mass concentration.

A phylogenetic characterization of viable cells was performed on individual colonies of bacteria from the 8^{th} – 10^{th} tube in the serial dilution preparation. A 16S rRNA fingerprinting method was used to obtain DNA sequences of pure isolates. In preparation for the 16S rRNA sequence identification, the colonies were first classified based on morphology. Genomic DNA was extracted from the pure cultures using a DN-easy tissue kit (QIAGEN Ltd, West Sussex, UK) as per manufacturer's instruction. Reverse transcriptase-polymerase chain reaction (RT-PCR) using primers pA and pH1 then amplified 16S rRNA genes of the isolates. The primer pA corresponds to position 8 – 27 and primer pH1 corresponds to position 1541 – 1522 of the 16S gene (Coenye et al., 1999). The PCR products were then sent to Inqaba Biotech facility (Pretoria, South Africa) for sequencing where an internal primer pD was used. The sequence relationships to known bacteria were determined by searching known sequences in GenBank using a basic BLAST search of the National Centre for Biotechnology Information (NCBI, Bethesda, MD) gene library.

3.16 Phylogenetic Analyses

For phylogenetic analyses, 16S rRNA sequences were compared with available database sequence via NCBI-BLAST search and the related taxa were obtained from GenBank. The multiple alignments were performed with the CLUSTAL X program (Thompson et al., 1997). Sequences of 16S rRNA gene were edited with the BioEdit program (Hall, 1999). The phylogenetic trees were constructed via the neighboring –joining and the maximum – parsimony algorithms with the MEGA 3 program (Kumar et al., 2004). The similarity of the rRNA gene sequences of the clones were compared with those of other known sulphur reducing species.

3.17 Gravimetric Analysis of Biomass

2 mL of solution was drawn from the bioreactor and placed in pre-weighed centrifuge tube and centrifuge on Mini Spin (Eppendorf) for 10 min at 10,000 rpm. After decanting the supernatant, the wet centrifuge tube was weighed and placed into an oven at 50°C for 24 h. The resulting change in weight from dried centrifuge tube with biomass and without was used to determine the cell weight. The mass and the volume filtered were used to calculate suspended cells concentration in mgL^{-1}.

3.18 Parameters Estimation using AQUASIM 2.0 Software

Parameters estimation for microbial desulphurization of steam cola were evaluated under transient state using the AQUASIM 2.0 software. In AQUASIM 2.0, the mass balance equations were evaluated numerically by the forth order Runge-Kutta method (RK-4). The parameters were obtained by minimizing the Chi-square (χ^2) values between the model data and the actual data using a simplex method built within AQUASIM (Reichert, 1998). Using Monod's theory for batch cultures and taking account of the exponential microbial growth (Panikov, 1995), the bacteria concentration (X_0) can be estimated using the Eq. (3.1):

$$\frac{dx}{dt} = \mu \frac{Z}{K_S + Z} x \qquad (3.1)$$

where: K_s =Substrate saturation constant ($\mu g\ L^{-1)}$, z = Steady-state substrate concentration ($\mu g\ L^{-1}$), μ = Maximum specific growth rate (h^{-1}), x = denotes microbial biomass (gm^{-3})

CHAPTER 4
COAL CHARACTERISTICS AND SO_2 MINIMUM EMISSIONS STANDARDS

4.1. Introduction

Coal remains the backbone of the economy in many successful industrial nations like United States, Japan, China, India, Australia, and South Africa, with coal power plants contributing over 50% to the energy needs of some of these countries (IEA, 2008). Ninety-one percent (91%) of the electricity generated in South Africa is based on coal combustion in steam-turbine driven power plants (IEA, 2014). The dependence of coal for the national energy stock strategy will probably not change for the next 50 years unless other low carbon footprint energy sources are developed to replace coal as the main energy source in the coming decade (Charleson and Juerg Weber, 1993; Chikkatur *et al.*, 2009). The pace at which other forms of energy are being developed is slow, which reinforces the probability of continued dependence on coal for the next 50 or more years. The Waterberg coalfield in Limpopo Province of South Africa is one of the remaining large resources – it contains about 50% of South Africa's remaining coal reserves and contributes 40% of the national output of coal for electricity generation (Eberhard, 2011). The geological setting of the Waterberg coalfield is well documented in the literature by numerous researchers (Faure et al., 1996; Wagner and Tlotleng, 2012). The depletion and coal reserves decline of the Witbank, Springbok Flats and Highveld coalfields as well as the coal quality changes in the other coalfields in Mpumalanga and Free State Provinces puts pressure on the Waterberg coalfield where coal quality is still good (Jeffrey, 2005). The latter point is critical in placing Waterberg coalfield as the basis of South Africa's power generation industry coal supply in the long-term.

Historically, the power plants operated by South African National Power Utility (Eskom) have not been designed with sulphur dioxide (SO_2) reduction in mind since SO_2 emission limits were not legislated at the time these plants were designed and built. However, Eskom has made the decision to employ flue gas desulphurization (FGD) technology for power stations being constructed (Singleton, 2010). Power stations that have already passed their half-life need serious review in light of what the country can afford. The FGD technology is used to reduce sulphur emissions in coal-fired power utilities by using pulverized limestone

in a spray tower to react with SO_2 in the flue gas and remove sulphur as a solid product (gypsum). It is of continued necessity to reduce or eliminate SO_2 and NO_2 in the atmospheric discharges from coal combustion in order to avoid the formation of H_2SO_4 and HNO_3 acid rain, which is detrimental of forest areas and sensitive aquatic ecosystems (Zhao *et al.*, 2008).

The FGD scrubbers are estimated to remove approximately 90% of the SO_2 and a significant portion of gaseous chlorides and fluorides that may be present in the flue gases (Srivastava and Jozewicz, 2001). Xiong et al. (2016) whose findings demonstrated SO2 removal efficiency of 92.50%, 82.50% and 50.0% using Wet-FGD, Dry-FGD and Semi-dry FGD, respectively also assessed the effectiveness of the FGD technology. In spite of the good performance of the FGD technology thus far, the process produces an effluent with high concentrations of the cationic and anionic impurities – Ca, Mg, Cl, and heavy metals. According to Hao *et al.* (2016), a large amount of FGD gypsum ends up in landfills or outdoor storage that may result in environmental pollution. Consequently, the effluent generated cannot be re-used anywhere in the power station without intensive treatment due to the high sulphur content (Singleton, 2010). Hence, FGD must be supplemented with other technologies in order to achieve full environmental compliance in modern power plants to consistently meet the SO_2 emission standards and increase power station availability.

The characteristics of coal used by power stations in the Waterberg region of South Africa have not yet been precisely evaluated regarding SO_2 emissions. Therefore, it is not possible to predict the full impact of SO_2 emissions resulting from its long-term usage. The current study provides precise information on the pollution potential of the coal originating from Waterberg coalfield. An impact analysis is proposed for possible SO_x emissions for generation plants relying on this source.

4.2. Results and Discussion

4.2.1 Particle size distribution analyses

Particle size is one of the important factors in coal desulphurization. The particle size distribution (PSD) of the two selected coals samples were determined to establish the range of coal particle size fractions in the feed and subsequent sulphur content with particle size. As shown in Fig. 4.1, the PSD yield results observed indicated that as the particle size decrease from +4.60 mm to – 0.85 mm, the yield distribution indicated a corresponding linear increase from 6% to 47% respectively, demonstrating that the dominant size fraction of the raw coal

was – 0.85 mm with a yield of 47%. In addition, the effects of particle size distribution on the sulphur content were also investigated. The sulphur content of the coal samples increased with decreasing particle size with the exception of −1.00 + 0.85 mm. This aspect indicated that the total sulphur present in the – 0.85 mm size attained maximum liberation through milling and thus indicated the possibility of responding better during desulphurization treatmernt to microbial attack. However, for a better PSD representation, all particle sizes range was thus considered for all biodesulphurization experiments.

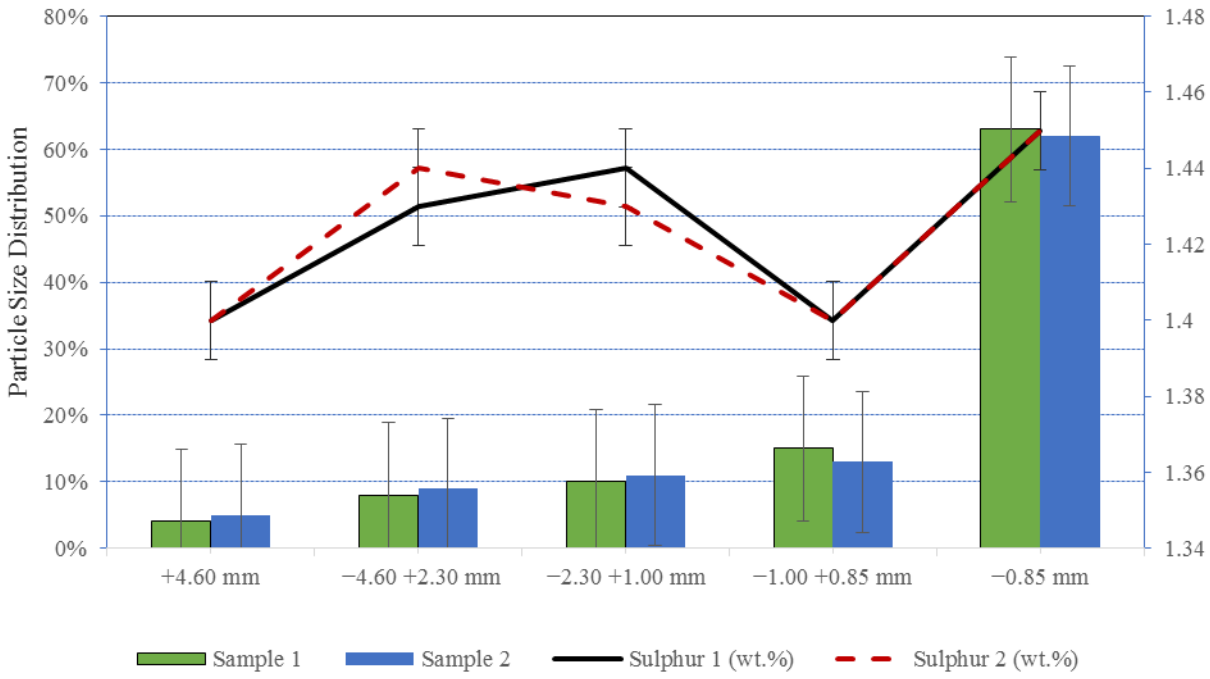

Figure 4.1: Particle size distribution for selected coal samples

4.2.2 Ultimate, ash and calorific value analyses

The classification of coal is generally performed with reference to the elemental composition of coal such as carbon, oxygen, nitrogen, hydrogen and sulphur. In this study, the carbon, hydrogen, Sulphur and oxygen elemental composition analyses was conducted and the results reported as the mean of duplicated determination as shown in Table 4.1. In these results, it was considered that carbon, hydrogen and oxygen average values of 51.2 wt.%, 3.02 wt.% and 5.75 wt.%, respectively to be predominant compared to other elements such as N (1.20 wt.%) and sulphur (1.33 wt.%) which were very low. Oxygen is determined by subtracting the total of the percentage carbon, hydrogen, nitrogen, sulphur, carbonate, ash and moisture

content from a hundred. Just like fixed carbon, oxygen gathers all errors from other variables tests. The oxygen content helps with the ignition of coal samples during combustion and it is generally inversely proportional to the carbon content. Hence, coal samples containing higher oxygen content of 5.75 wt.% are more prone to spontaneous combustion. Furthermore, the nitrogen content of 1.20 wt.% does not relate to the rank of coal, and therefore it would not have any effect on spontaneous combustion, unlike oxygen. During coal combustion, nitrogen in combustion air and coal is converted to NO_2 and NO, commonly referred to as NOx. These N-oxides are relevant as they contribute to the formation of acid rain with similar impact as SOx impact.

Sulphur content of 1.15 – 1.49 wt.% range is observed indicating that the coal is a medium sulphur coal type as per classification of coal as proposed by Chou (2012), where coal is generally termed as low sulphur (≤1 wt.% sulphur content), medium sulphur (≥1 to ≤3 wt.% sulphur content) and high sulphur coal (≥3 wt.% sulphur content) based on their sulphur content. The sulphur content in medium sulphur coal type derives from the sulphur content of the original plant material incorporated at the time of peat accumulation and sulphate in seawater that flooded peat swamps (Chou, 2012).

Ash ranged between 29.0 – 34.8 wt.% in our current study which classified coal as high ash. The ash remaining after the coal has been incinerated in the air is derived from inorganic complexes present in the original coal substance and the associated mineral matter (ISO 1171, 2010). Ash generally affects the sizing of the boiler and its performance. This is supported in another case reported by other researchers (Saikia *et al.*, 2013; Santhosh Raaj *et al.*, 2016) who indicated that high ash in the coal leads to the requirement of a higher number of mills and influences boiler performance. Other effects include the sizing of primary air fans, air pre-heaters, particulate matter, electro static precipitators as well as coal and ash handling systems.

Table 4.1 Proximate analysis and ultimate analyses results (wt.%. db)

PSD (mm)	C	CO_3^{2-}	H	N	O	S	A	H_2O	VM	FC
− 0.85	52.7	2.90	3.20	1.10	5.63	1.45	31.0	2.70	21.4	44.9
	52.2	2.90	2.75	1.22	6.04	1.45	31.3	2.50	24.0	42.2
−2.30 +1.00	48.7	1.20	2.98	1.12	6.65	1.41	34.5	2.20	24.9	38.4
	50.8	1.20	3.18	1.14	6.66	1.40	31.8	2.50	24.8	40.9
−4.60 +2.30	49.5	1.40	3.13	1.14	6.15	1.44	34.2	2.50	25.7	37.6
	51.5	1.40	2.79	1.58	4.27	1.43	34.0	1.80	25.6	38.6
+4.60	51.2	2.60	3.07	1.18	5.15	1.44	33.4	2.10	24.6	39.9
	53.2	2.60	3.07	1.11	5.41	1.43	31.0	2.20	26.2	40.6

A: ash; C: carbon; CO_3^{2-}: carbonate; H: hydrogen; H_2O: moisture; N: nitrogen; O: oxygen (By Difference); VM: volatile matter; S: sulphur; CV: calorific value; FC: fixed carbon (By difference)

The CV of coal samples used ranged from 19.0 – 21.0 MJ/kg indicating heat liberated when these coal samples undergo complete combustion. The results of duplicate determinations of these CV values do not differ by more than 0.12 MJ/kg indicating the extent of repeatability. These values are well within the degree of reproducibility (0.3 MJ/kg) for eight samples analyzed. The CV of coal samples studied can be calculated based on its C, H, S, and Ash as per Eq. (4.1):

$$CV = 0.47C + 1.30H + 0.190S + 0.107A - 12.12 \quad (4.1)$$

where: C = Carbon, H = Hydrogen, S = Total Sulphur, and A = Ash

Using corresponding measured values for elemental composition of eight coal samples on Eq. 4.1, calculated CV values and coefficient of variation (σ) values with measured CV values were obtained as reported in Table 4.2. σ values are quite acceptable in the range of 0.00 to 1.6 that indicates that Eq. (4.1) hold for Waterberg coalfield.

Table 4.2: Calorific Value Analyses

PSD (mm)	Measured CV(MJ/kg)	Calculated CV (MJ/kg)	σ (MJ/kg)
− 0.85	20.4	20.4	0.0
	21.0	19.6	1.4
−2.30 +1.00	20.2	18.6	1.6
	20.1	19.6	0.5
−4.60 +2.30	20.3	19.1	1.2
	20.3	19.6	0.7
+4.60	20.4	19.8	0.6
	20.8	20.5	0.3

4.2.3 Ash composition analyses

Table 4.3 shows ash analysis constituents found in coal samples. The results are presented as oxide basis of which the sum approximates to 100%. The ash chemistry is dominated by SiO_2 and Al_2O_3 (57.3 – 58.8 wt.%, and 25.8 – 27.9 wt.% respectively). The phosphorous average of 0.28 wt.% as apatite is mainly attributed to the breakdown of organic material. The results correlate well with the previous studies reported by Wagner and Tlotleng (2012).

Table 4.3: Ash oxide analyses (wt.%. db)

PSD (mm)	SiO_2	Al_2O_3	Fe_2O_3	TiO_2	P_2O_5	CaO	MgO	Na_2O	K_2O	SO_3	MnO
− 0.85	58.5	27.6	4.00	1.20	0.40	3.80	2.60	0.20	0.90	1.30	0.03
	57.6	27.7	4.00	1.30	0.28	5.40	1.10	0.50	1.10	1.80	0.02
−2.30 +1.00	57.3	27.4	4.80	1.10	0.67	5.60	0.50	0.60	0.40	1.70	0.07
	58.0	27.7	5.70	1.30	0.50	3.20	0.90	0.10	0.80	2.10	0.02
−4.60 +2.30	58.0	25.8	4.10	1.30	0.42	5.40	1.10	0.10	0.80	2.80	0.03
	58.2	27.9	4.90	1.40	0.66	5.40	1.00	0.20	0.40	2.10	0.05
+4.60	58.1	27.4	5.20	1.30	0.65	10.1	0.50	0.60	0.40	1.40	0.04
	58.8	27.3	4.10	1.30	0.68	9.70	0.50	0.60	0.40	1.90	0.08

4.2.4 Trace elements analyses

Understanding the quantities and distribution of minor and trace elements bonded to the coal matrix is very significant as this has implications for their availability to the environment during coal preparation and use. The latter statement is supported by another case reported by Duan et al. (2016) who mentioned that trace elements are receiving increasing attention lately due to their potentially toxic nature on human health and ecosystem. As a result, duplicated trace elements concentrations in coal sample ash were analyzed in the current study and the results are reported as depicted in Fig. 4.2. The elements with the highest concentration are Sr (72.10 ppm), followed by V (65.13 ppm), whereas Cd (0.19 ppm) followed by Te (0.06 ppm) have the lowest concentrations. The concentration of all other trace elements (Zn, Cr, Rb, Cu, Pb, Ga, Li, Ni, Co, U, Be, Mo, Ag, Bi, Ti) lies in between. Concentration of trace elements in both coal samples were found to be in the order Sr > V > Zn> Cr > Rb > Cu > Pb > Ga > Li > Ni > Co > U > Be > Mo > Ag > Bi > Ti > Cd> Te. According to Faure *et al.* (1996), geochemical factors such as volcanic ash and hydrothermal fluids are responsible for the enrichment of these trace elements.

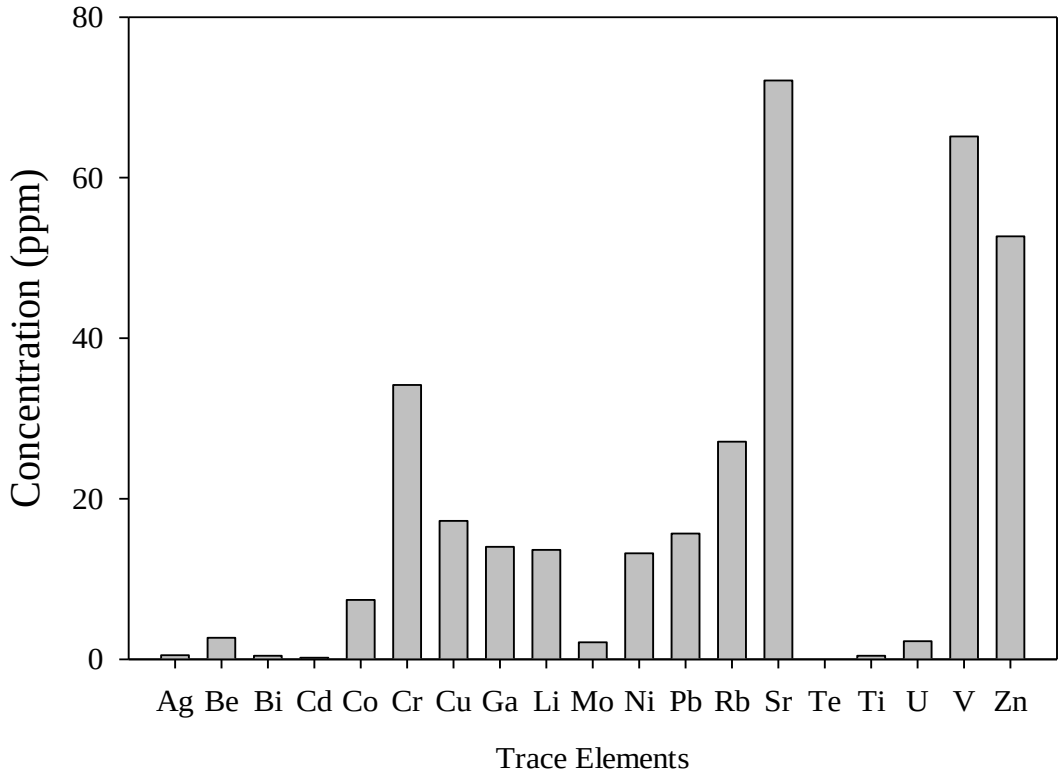

Figure 4.2: Trace elements concentration (in ppm) in coal ash samples

4.2.5 Petrographic study

Scott (2002) defined macerals, the microscopic constituents of coal, as an organic substance, or optically homogenous aggregates of organic substances, possessing distinctive physical and chemical properties, and occurring naturally in the sedimentary, metamorphic, and igneous materials of the earth. Scott (2002) documented coal petrology and the origin of coal macerals. In the current study, coal macerals found included vitrinite, liptinite, reactive semifusinite, inertinite and visible mineral as shown in Table 4.4. Vitrinite is the dominant maceral (up to 51.8 vol.%), whereas inertinite, liptinite and reactive semifusinite occurred in minor proportions as 22.6 vol.%, 2.9 vol.% and 5.3 vol.% respectively. Because the volume percentage of vitrinite in a sample is 51.8%, then the operator can expect to get two results differing by less than 6.4% points as per repeatability limit for maceral group composition. Visible minerals include materials intimately admixed within the macerals as well as discrete minerals in coal samples. Visible minerals consisted of 17.5 vol.%.

Table 4.4: Maceral analyses of coal

Maceral	Sample 1	Sample 2
Vitrinite [vol.%]	51.8	50.8
Liptinite/Exinite[vol.%]	2.9	2.5
Reactive Semifusinite [vol.%]	5.3	5.2
Total Inertinite [vol.%]	22.6	24.6
Visible Minerals [vol.%]	17.5	18.2
Maximum Reflectance%Rr,	0.76	0.76
Random Reflectance%	0.71	0.72

Vitrinite has been shown to burn readily, although the rate of burnout will normally decrease as its reflectance increases (Cloke *et al.,* 2002). According to Cloke *et al.* (2002), inertinite once considered being less reactive maceral group often having been associated with burnout problems. Inertinite is believed to be the product of the fungal activity, cold climatic conditions and atmospheric exposure of peat resulting in oxidation (Van Niekerk *et al.,* 2008). Liptinite macerals were formed mostly from various protective waxy coatings of plants (Siddhartha, 2013). The liptinite maceral group includes the optically distinct parts of plants such as spores, cuticles, suberine, etc., some degradation products, and those generated during the coalification/maturation process.

Examples of the forms of macerals such as vitrinite, liptinite and fusinite are shown in Fig. 4.3. Vitrinite is well known from other maceral groups primarily based on its morphology. Van Niekerk *et al.* (2008) reported vitrinite up to 90 vol.% in the Waterberg coals as opposed to 51.8% found on the current study which then supports Faure *et al.* (1996)'s findings. It is believed that macerals have decreased with the depth of Waterberg Formation (Faure *et al.,* 1996). The variation of the maceral concentrations is consistent with the evidence from the mineralogy of the mudstones and carbonaceous mudstone layers which report that the base of the formation was deposited in the distal part of the basin and the upper parts were deposited in a relatively more proximal setting (Faure *et al.,* 1996; Van Niekerk *et*

al., 2008). Reactive semifusinite is a term used in the coal industry for macerals in the inertinite group that are partially degraded vitrinite (Faure *et al.*, 1996). The following Eq. (4.2) proposes the positive correlation between the percentages of vitrinite and reactive semifusinite for Waterberg Formation:

$$RSF = 0.0026V^2 - 0.6676V + 32.91 \quad (4.2)$$

where, RSF= Reactive Semifusinite (vol.%) and V= Vitrinite (vol.%).

Reactive semifusinite is distinguished under the microscope by being somewhat lighter in color than vitrinite and liptinite (Fig. 4.3 and Fig. 4.4). Waterberg coalfield contains considerable amounts of low reflecting semifusinite, called 'reactive semifusinite'. Reactive semifusinites and inert semifusinites (Fig. 4.4) are distinguished primarily by their degree of fusinitization (Scott, 2002). Semifusinite, an intermediate maceral between huminite/vitrinite and fusinite, having formed in the peat by weak humification, dehydration, and redox processes may show vague or partially visible cell lumens derived from parenchymatous and xylem tissues of stems, herbaceous plants, and leaves (O'Keefe *et al.*, 2013).

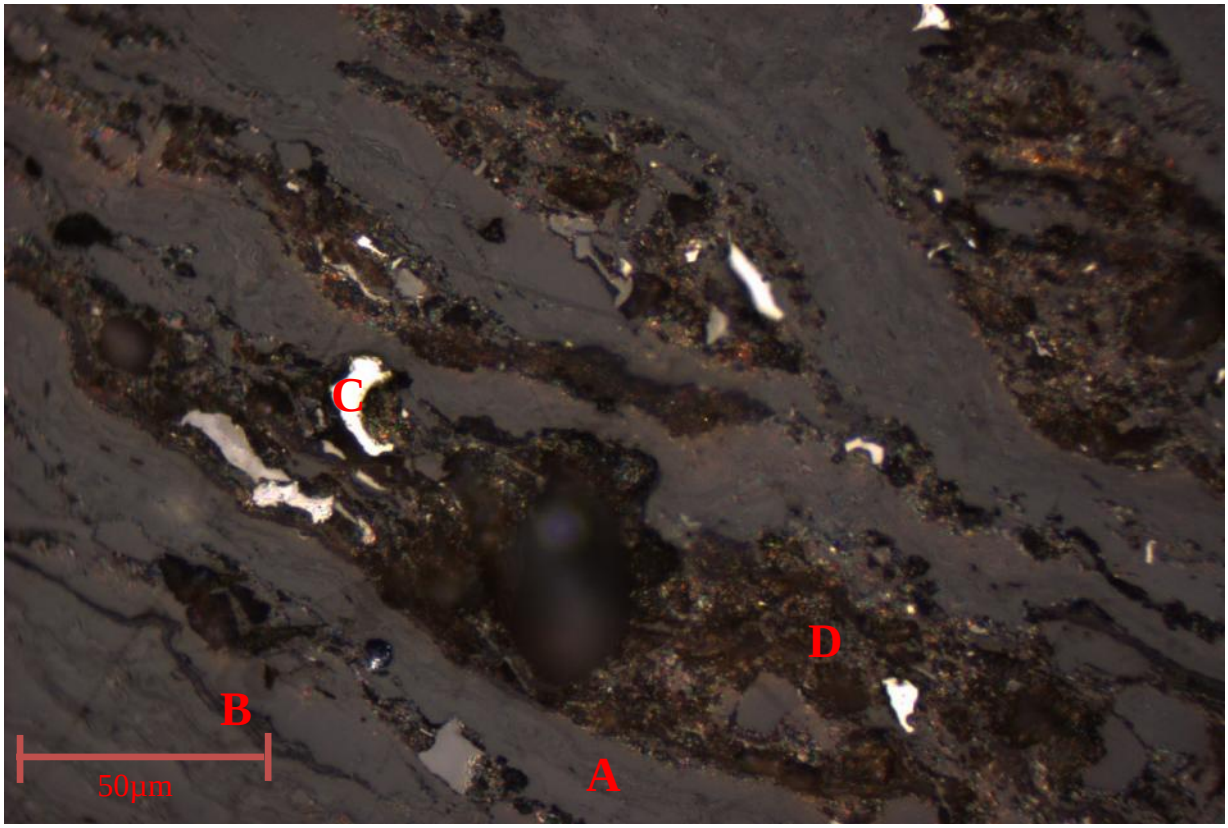

Figure 4.3: A: Vitrinite, B: Liptinite, C: Fusinite and D: Visible Minerals (Scale – 50 µm)

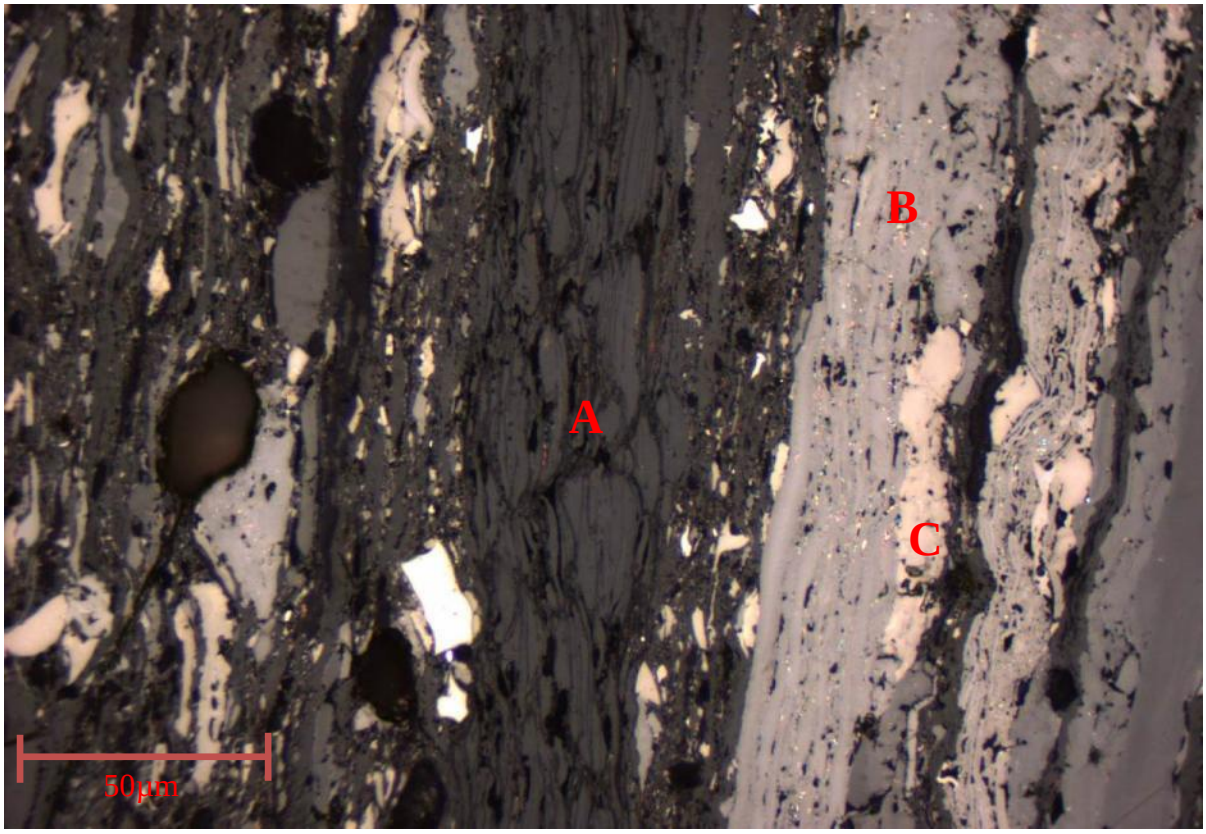

Figure 4.4: A: Vitrinite, B: Reactive Semifusinite and C: Inert Semifusinite (Scale – 50 µm)

Earlier studies by Roberts (1988) established that there is a positive correlation between vitrinite and sulphur content in the coal. According to Roberts (1988), vitrinite contains most of the organic sulphur in the coal and semifusinite contains significantly smaller amounts of organic sulphur. Hoppo and Crelling (1991) investigate the desulphurization behavior of individual coal macerals. It was found that the vitrinite maceral contained most of the organic sulphur in coal is more reactive toward desulphurization processes than any of the other macerals. In a separate case, Roberts (1988) established that within the Permian coal of Vryheid Formation, South Africa, sulphur and vitrinite contents are positively correlated, indicating that vitrinite has higher sulphur content than inertinite. According to the international codification system for medium and high rank, vitrinite reflectance analysis, R_m of 0.76% places coal in the medium-rank bituminous C category in accordance with ISO standard 11760 (2005), which is in good agreement with other petrographic assessments completed by other researchers (Snyman, 1989; Faure *et al.*, 1996; Jeffrey, 2005).

4.2.6 Random reflectance measurement

The reflectance distribution provides valuable information about the rank of the coal and this method can be used to explain thermal coal maturity. Random reflectance measurement was

conventionally taken on the vitrinite maceral and the results are expressed as a reflectogram (Fig. 4.5) which shows the vitrinite-class distribution. Reflectance ranges of V05 (0.50 – 0.59), V06 (0.60 – 0.69), V07 (0.70 – 0.79), V08 (0.80 – 0.89) and V09 (0.90 – 0.99) resulted in count values of 2, 41, 47, 9 and 1 respectively. Therefore reflectance range is dominated by V07 (0.70 – 0.79) and V06 (0.60 – 0.69) respectively.

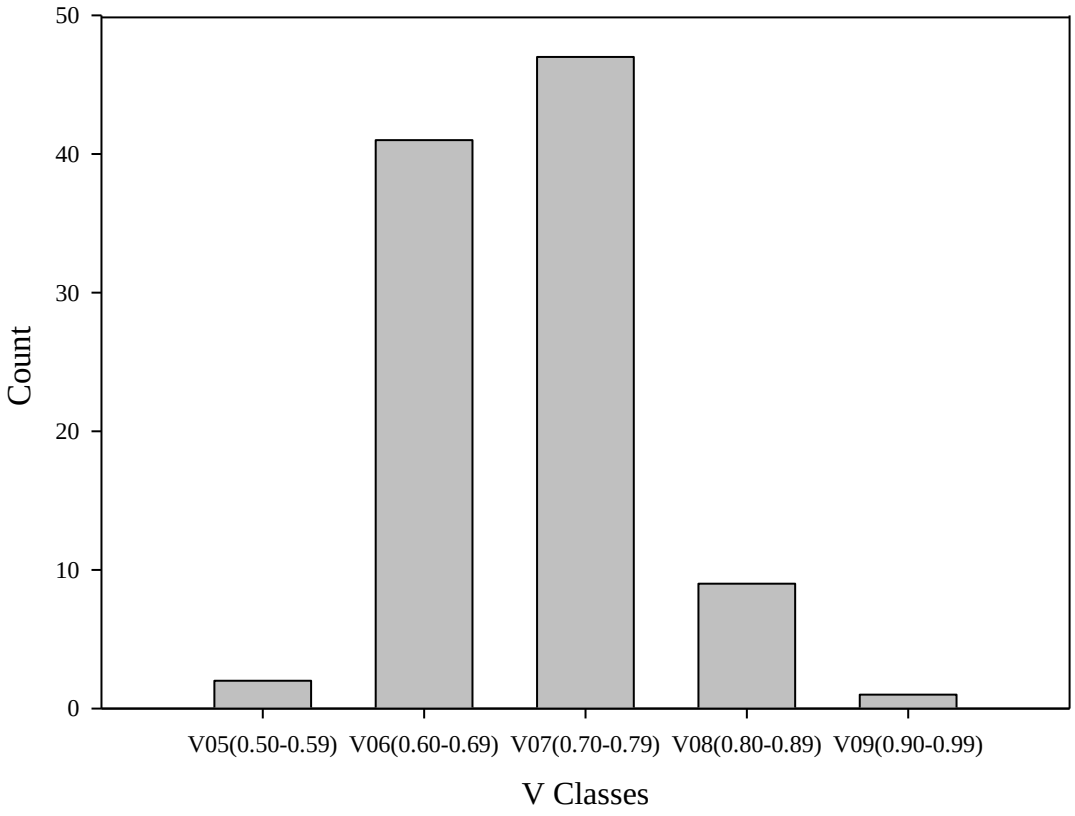

Figure 4.5: V classes on the vitrinite maceral and count

4.2.7 Analyses of sulphur forms in coal and distribution of sulphur forms in coal

Coal samples were analyzed for forms of sulphur in coal and the results are recorded in Table 4.5. Table 4.5 shows that sulphur in coal occurs in various forms such as pyrite, mineral/sulphide sulphur, inorganic sulphates and organic sulphur. Pyritic sulphur (FeS_2) (0.64 wt.%), is the dominant sulphide mineral in the coal, followed by organic sulphur (0.56 wt.%) then sulphide sulphur (0.14 wt.%) and trace to minor amounts of sulphate sulphur (0.03 wt.%). These pyritic sulphur results are in good agreement with the earlier finding by Kargi (1986) who suggested that bituminous coal contains high levels of pyritic sulphur varying between 0.5% and 6% depending on the coal. According to Li and Tang (2014), the

pyritic sulphur content is usually similar in amount to the organic sulphur content. The difference in the current study with Li and Tang (2014)'s findings could be attributed to errors accumulation in calculating organic sulphur content. Because the sulphur is generally pyritic and nodular, physical separation technique such as high-density washing could be utilized to reduce much of the sulphur content (Gryglewicz et al., 1995).

Organic sulphur found in coal consists primarily of sulphur atoms covalently bonded to aliphatic or aromatic carbon atoms contained in the backbone of the coal macromolecule. According to Saikia et al. (2014a), organic sulphur is integrated into the structural matrix in the form of thiols, sulphides and disulphides, and thiophene and its derivatives. The ratio of pyritic sulphur to organic sulphur as a function of the total sulphur content was found to be 1.03 on average.

The relationship between distributions of sulphur forms in coal was completed for all eight-coal samples studied. The relationship is based on the characterization of total sulphur content in terms of the main coal structure. Therefore, the following general linear relation for the total sulphur is given by Eq. (4.3):

$$Y = m \times S_{TOT} \tag{4.3}$$

where Y is the form of sulphur [e.g. total inorganic sulphur, sulphide/mineral sulphur (S_{IN}), pyritic (S_{PYR}), sulphate sulphur (S_S) and organic sulphur (S_{ORG})]; S_{TOT} is Total sulphur; m is the distribution factor constant.

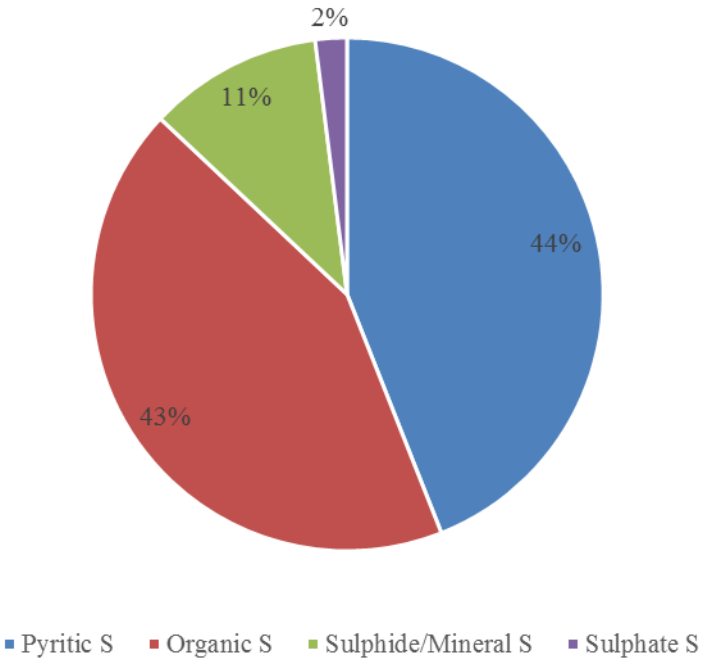

Figure 4.6: Distribution summary of sulphur forms in Waterberg coals

Using Fig. 4.6 and Eq.4.3, the following gradient or distribution factor (*m*) relationship is established for the current study:

$$Y = m \times S_{TOT} \tag{4.4}$$

$$S_{IN} = 0.11 \times S_{TOT} \tag{4.5}$$

$$S_{PYR} = 0.44 \times S_{TOT} \tag{4.6}$$

$$S_{S} = 0.02 \times S_{TOT} \tag{4.7}$$

$$S_{ORG} = 0.43 \times S_{TOT} \tag{4.8}$$

The linear relationship between pyrite, sulphate, mineral/sulphide sulphur and organic sulphur has been established for Waterberg coalfield using Eqs. 4.4 – 4.8 and the results are reported in Table 4.5. This information on the distribution of sulphur forms in coal is crucial in determining further processing techniques requirements.

Table 4.5: Analysis of sulphur forms in coal samples (wt.%)

PSD (mm)	Sulphide Sulphur	Organic Sulphur	Pyritic Sulphur	Sulphate Sulphur	Total Sulphur
− 0.85	0.14	0.56	0.64	0.03	1.37
	0.16	0.64	0.66	0.03	1.49
−2.30 +1.00	0.15	0.58	0.59	0.03	1.35
	0.13	0.49	0.51	0.02	1.15
−4.60 +2.30	0.13	0.52	0.53	0.02	1.20
	0.16	0.64	0.65	0.03	1.48
+4.60	0.15	0.58	0.59	0.03	1.34
	0.15	0.57	0.58	0.03	1.32

4.2.8 Sulphur content in coal and SO_2 emissions

Coal contains the most notorious environmental pollutant, sulphur, which produce SO_2 during combustion (Cheng *et al.*, 2003; Chou, 2012; Saikia *et al.*, 2014b). The SO_2 emitted during coal combustion is a principal source of acid rain which poses a health issue and has harmful effects on the natural environment (e.g. lakes, rivers, soils, fauna and flora) and building structures such as cultural heritage (Benko *et al.*, 2007). In the light of impending greenhouse gas emissions reduction programmes, environmentally conscious society have introduced emissions legislative requirements for SO_2 emissions and this has been adopted by numerous countries including South Africa. Minimum Emission Standards for SO_2 emission limits is explicit for existing plants and the limit has been set as 3500 mg/Nm^3 at 10% O_2 which came into effect in April 2015, and more stringent target for new plants has been set as 500 mg/Nm^3 at 10% O_2 which shall come into effect in April 2020 (Government Notice No.248, 2010). Earlier sections of the chapter dealt with the nature and type of sulphur content in the Waterberg coal. This section deals with the implications on the compliance of SO_2 emissions requirements in the power plant using coal from Waterberg coalfield.

Because SO_2 emissions from power generation depend largely on the sulphur content in the coal and mass of coal burnt, Eq. (4.9) is used to develop estimates of sulphur emissions from

an operating unit with coal burnt of 343 tons/hr for various range of sulphur content in coal samples generating 800 MWh.

$$SO_{2\ Formed} = \left(\frac{\mu \times \left(\frac{S_T}{100} \times \frac{1000}{32.064} \right)}{(1000 \times 64.0628)} \right) \text{Kg/Kg Coal}_{\text{dry}} \qquad (4.9)$$

where: μ = mass of coal burnt (Kg/h), S_T = Total Sulphur in coal (wt.%)

$$SO_{2\ Formed} = \left(\frac{\mu \times \left(\frac{S_T}{100} \times \frac{1000}{32.064} \right)}{(1000 \times 22.4)} \right) \text{Sm}^3/\text{h} \qquad 4.10)$$

$$SO_{2\ Emmision} = \left(\frac{\mu \times SO_{2\,Formed} \times 10^6}{(\sum F)} \right) \text{mg/Nm}^3 \qquad (4.11)$$

where $\sum F$ equals to the sum of Flue Gas products (in Sm^3/h)

$$SO_{2\ Emmision} = \left(\frac{\text{SO}_{2\,\text{Emmision}} \times (21-10)}{(21-6)} \right) \text{mg/Nm}^3 \text{ (At 10\% Oxygen)} \qquad (4.12)$$

Eq. 4.12 represents the maximum emission of sulphur in the form of SO_2 and has been used to calculate SO_2 emissions for coal samples studied and the results are depicted as shown in Fig. 4.7. The estimate for SO_2 emissions is not just a forecast but is based on observed data. It is evident from Fig. 4.7 that SO_2 concentration increases with increasing sulphur content of the coal samples. Therefore, the sulphur content in coal samples results in SO_2 emissions in a nearly linear way meaning volumes of emission of sulphur compounds are directly proportional to amounts of elemental sulphur present in the parent coal. As shown in Fig. 4.7, coal samples with sulphur content (in wt.%) of 1.37, 1.49, 1.35, 1.15, 1.20, 1.48, 1.34 and 1.32 resulted in SO_2 emissions (in mg/Nm^3) of 3511, 3815, 3456, 2944, 3072, 3789, 3431 and 3380 respectively against a target of 3500 mg/Nm^3. As a rule of thumb for a full load or 343 tons/hr of coal used, a slight increase in the sulphur content of 0.01 wt.% results in a corresponding increase of 25.60 mg/Nm^3 (including decimals) of SO_2 emissions. The latter point is confirmed by comparing coal sample 2 (with sulphur content of 1.49 wt.%) and sample 6 (with sulphur content of 1.48 wt.%) as well as coal sample 3 (with sulphur content

of 1.35 wt.%) and coal sample 7 (with sulphur content of 1.34 wt.%). Therefore, dividing the product of sulphur content in coal sample and 25.60 factors by 0.01 will give the resulting SO_2 emissions for Waterberg coal. Consequently, the sulphur content of ≥ 1.37 wt.% is not sufficient to comply with the minimum emission standards limit of 3500 mg/Nm^3. However, the sulphur content of ≤ 1.37 wt.% will act as a form of SO_2 mitigation for 3500 mg/Nm^3 target. Therefore, future coal supply contract should be negotiated with a limit of maximum sulphur content of ≥1.37 wt.% of which any sulphur content beyond that should be rejected. By comparison, Barooah and Baruah (1996) reported that some air pollution law stipulates the use of 1 wt.% or less sulphur content coals.

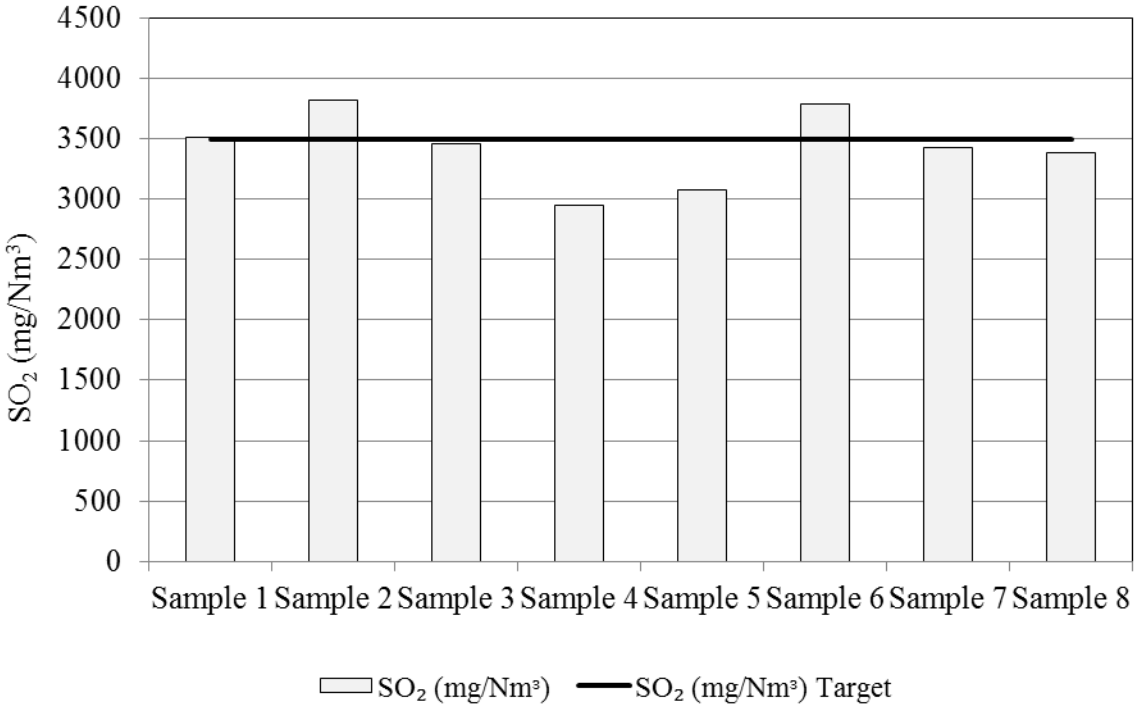

Figure 4.7: SO_2 emissions for 3500 mg/Nm^3 for a full load

Fig. 4.8 depicts SO_2 emissions for the reduced load. Coal samples with sulphur content (in wt.%) of 1.37, 1.49, 1.35, 1.15, 1.20, 1.48, 1.34 and 1.32 resulted in SO_2 emissions (in mg/Nm^3) of 2631, 2858, 2590, 2206, 2302, 2839, 2571 and 2532 respectively against a target of 3500 mg/Nm^3. Similar to a full load scenario, as a rule of thumb, the sulphur content of 0.01 wt.% results in 19.18 mg/Nm^3 (including decimals) of SO_2 emissions for a reduced load unlike 25.60 mg/Nm^3 obtained in full load case. Reducing the load to three mills instead of four mills (Fig. 4.7) which directly translate to reducing the load by decreasing coal burnt from 343 tons/hr to 257 tons/hr, reduce the volume of SO_2 emissions by 25% which complies

with the stringent minimum emissions standards. However, at reduced load, Verma *et al.* (2013) highlighted that lower combustion efficiency, very high CO and dust emissions are experienced by most boilers that is less desirable.

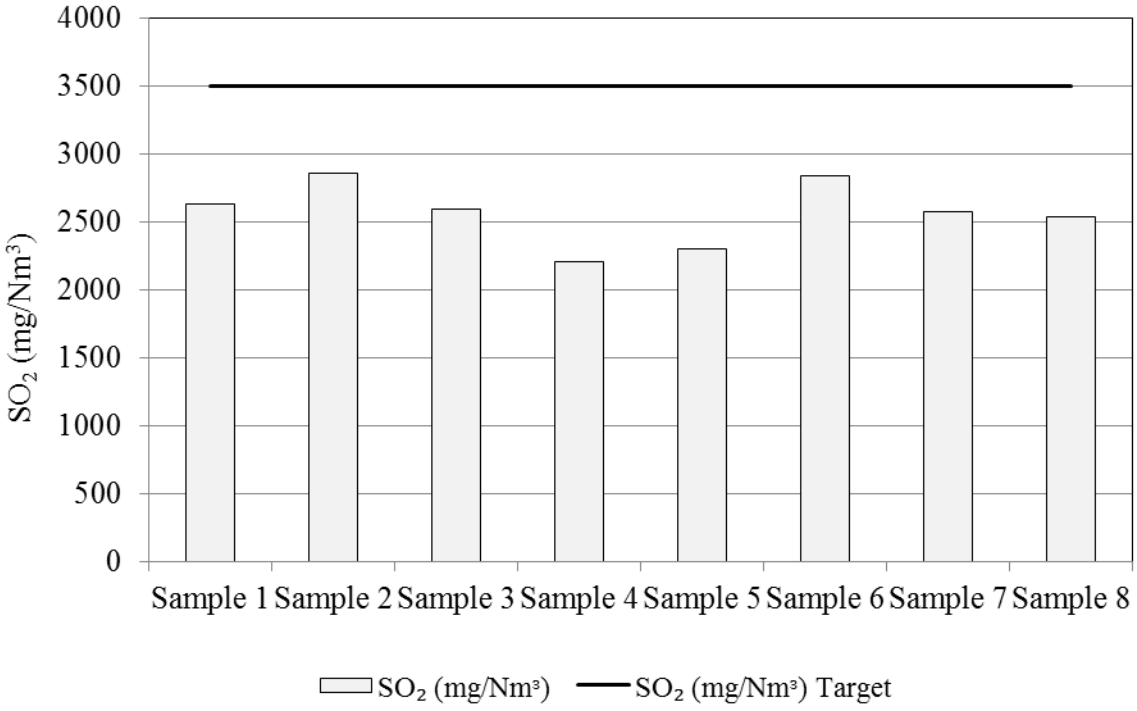

Figure 4.8: SO_2 emissions for 3500 mg/Nm^3 for reduced load

Sulphur content in coal varies from one seam to another. Sloss (2014) studied the behavior of coal blends in power generation and it is accepted that values for Fixed Carbon, H, C, O, S (proximate and ultimate contents) and CV value are additive – meaning the value of the blend will be the average value of the coals within the blend. Generally, coal blending such as the combination of high sulphur coals with low sulphur coals can be used as mitigation for SO_2 to ensure compliance with strict sulphur emission limits. Therefore, the blending of coal in order to reduce SO_2 emissions of the Waterberg coal is a mitigation option worth exploring. The foremost challenge to overcome includes excellent stacking and reclaiming philosophies in coal stockpiles for effective blending. In addition, the availability of low sulphur content coal to blend with. In case of only high sulphur content coal being available, the feasibility of pre-combustion technique(s) should be investigated as a pre-desulphurization option in order to reduce the sulphur content of $\geq$ 1.37 wt.% to an acceptable level.

4.2.9 Pre-combustion technology analysis competitive to FGD

Although Waterberg coal used for power generation is already beneficiated close to its economic limit but is not clean enough in terms of sulphur content to comply with the tightened minimum emission standards. The question is posed: can the medium sulphur coal be reprocessed such that the sulphur content can be further reduced to low sulphur coal without disturbing the properties of the parent coal? Moreover, what is the required sulphur content in the Waterberg coal in order to comply with the minimum emission standards of 500 mg/Nm^3 without employing post-combustion technology, FGD? Revisiting Eq.4.9 and doing reverse calculation clearly indicate that coal with a sulphur content of 0.20 wt.%, low sulphur coal type, is a requirement for compliance with minimum emission standards of 500 mg/Nm^3. Therefore, Eq. (4.13) is developed to establish each pre-combustion process efficiency, η required to reduce coal samples studied to 0.20 wt.%.

$$\eta = \frac{S_{Feed} - S_{Treated}}{S_{Feed}} \times 100 \qquad (4.13)$$

where S_{Feed} is total sulphur in the feed; $S_{Treated}$ is total sulphur the treated coal.

Overall pre-combustion process efficiency (η) of 81.0%, 82.6%, 80.7%, 77.4%, 78.3%, 82.4%, 80.6% and 80.3% is required to treat coal samples with sulphur content of 1.37 wt.%, 1.49 wt.%, 1.35 wt.%, 1.15 wt.%, 1.20 wt.%, 1.48 wt.%, 1.34 wt.% and 1.32 wt.% respectively. Sulphur content of ≤ 0.20 wt.% or competitive pre-combustion process with more conventional technology such as FGD will act as a form of SO_2 mitigation for 500 mg/Nm^3 target. Reducing load is not even an option in the case of 500 mg/Nm^3 target as one mill in operation results in high SO_2 emissions 898 mg/Nm^3 that is less desirable. Therefore, SO_2 current minimum emissions limit of 500 mg/Nm^3 is difficult to meet with the current medium sulphur coal samples studied. It is therefore undeniable that the stringent emissions standards will strongly affect the demand for low-sulphur coal in the near future. It is expected to be so for combustion plants not equipped with FGD or fluidized-bed combustion boilers (Kudelko, 2003). The last question then is which pre-combustion process can give an efficiency range of 77.4 – 82.6% required to treat coal samples with sulphur content discussed in the current study? There are several methods in literature such as biological, physical and chemical methods (Huifang and Yagin, 1993; Saikia *et al.*, 2013; Saikia *et al.*, 2014b; Meshram *et al.*, 2015) for the removal of different forms of sulphur in coal. The physical processes for reducing sulphur content such as gravity separation, heavy media

cycloning techniques, centrifugation, oil agglomeration magnetic separation and froth flotation are applicable only for the removal of inorganic sulphur (Gryglewicz *et al.*, 1995). According to Gryglewicz *et al.* (1995), such processes remove 30 – 90% of the pyritic sulphur associated with the mineral matter in coal. Gonsalvesh et al. (2012) have reported total sulphur desulphurization in the range of 25.3 – 54.2% after chemical treatments. Inorganic sulphur (pyritic and sulphatic) is mainly attacked. Several authors (Kilbane, 1990; Acharya et al., 2005; Cara et al., 2006) have evaluated microbial desulphurization of medium sulphur coal containing mostly pyritic sulphur. Kilbane (1990) performed biodesulphurization experiments using a strain of mixed bacterial culture, IGTS7 from Illinois Basin coal. Based on these mixed microbial cultures, up to 90% of organic sulphur was removed. In another case, Aller *et al.* (2001) reported that coal-derived inocula removed 90% of pyritic sulphur in bituminous coal from Spain. These techniques need to be evaluated individually as different techniques to reduce sulphur in Waterberg coal in order to establish their efficiencies in comparison with post combustion, FGD technique.

4.3 Summary

The study presents coal qualities data set (proximate and ultimate parameters, sulphur contents, trace elements and SO_2 emissions concentrations) for Waterberg coalfield eight samples. Four forms of sulphur - pyrite, mineral/sulphide sulphur, inorganic sulphates and organic sulphur are present in Waterberg coal. Sulphur content of 1.15 – 1.49 wt.% range classified coal as a medium sulphur coal type (≥ 1 wt.% ≤ 3 wt.%) with pyritic sulphur (≥ 0.51 wt.%) and organic sulphur (≥ 0.49 wt.%) accounted for the bulk of the total sulphur in coal. Maceral analyses of coal studied showed that vitrinite is the dominant maceral (up to 51.8 vol.%), whereas inertinite, liptinite and reactive semifusinite generally occur in minor proportions as 22.6 vol.%, 2.9 vol.% and 5.3 vol.% respectively. Theoretical calculations were developed, verified with the current plant data and used to predict SO_2 emissions using conditions typical to the power-generating unit. These results suggest that that coal with a sulphur content of ≥ 1.37 wt.% is not able to comply with the minimum emission standards limit of 3500 mg/Nm^3. In addition, coal with a sulphur content of ≤0.20 wt.% (translate to the efficiency of > 87%) is a requirement for compliance with minimum emission standards of 500 mg/Nm^3 which is competitive with FGD. Kilbane (1990) suggested that often as much as 90% of the sulphur in coal must be removed in order to meet the Clean Air Act standards for sulphur emissions that support the findings of the current study. However, further studies are

required to identify a pre-combustion technique that can enable the current Waterberg coal with sulphur content of ≥ 1.37 wt.% to be treated (i) in order to comply with 3500 mg/Nm^3, and to be treated successfully to ≤0.20 wt.% such there is no need for post-combustion technique, FGD employment.

CHAPTER 5
THE DESULPHURIZATION POTENTIAL OF WATERBERG STEAM COAL USING BACTERIA ISOLATED FROM COAL: THE SO_2 EMISSIONS CONTROL TECHNIQUE IN A POWER PLANTS

5.1 Introduction

The supply of energy in South Africa depends significantly on coal as the dominant primary energy source and will continue to do so for the near future. The deployment of renewables to replace coal is hindered by their unreliability and concerns over present power lines and infrastructure needed to move electricity to consumers. The current power lines and infrastructure were built to receive and transmit power generated in coal-fired mainly situated in the Highveld areas, Mpumalanga, Gauteng and the North West provinces. Since the early 1900's, coal has remained the driving force of the South African economy. According to Ozonoh et al. (2018), almost about 95% of electricity generation in South Africa is from coal-fired power plants. Coal use in electricity generation has attracted much attention recently mainly due to the sector been identified as the main source of Sulphur dioxide (SO_2) emissions globally (Barreira et al., 2017). During combustion, organic and pyrolytic sulphur compounds in coal are readily oxidized to SO_X species due to the presence of oxygen in the air and high temperatures. The SO_X species such as SO_2 readily react with H_2O in the atmosphere to form acid rain that is detrimental to plant, animal life (Ozonoh et al., 2018) and water pollution (Hu et al., 2018). Additional issues including human health such as chronic respiratory illnesses (Mketo et al., 2016), sulphate aerosols from S(0)/S(-2) oxidation causing corrosion (Zhao et al., 2008), abrasion, fouling and slagging of metal bodies (Mketo et al., 2016) as well as and boiler tubes leaks (Saikia et al., 2013) also add to the list of concerns.

Governments of many developed and developing nations that put power producers under increasing pressure to reduce high SO_2 emissions in their operations have recommended the minimum emissions standards. In South Africa, minimum emissions standards for environmental protection are providing a need to comply with SO_2 emissions of 3500 mg/Nm^3 and 500 mg/Nm^3 by 2020 and 2025 respectively (Government Notice No. 248, 2010). For this purpose, South African electricity public utility, Eskom resolved to install flue gas desulphurization (FGD) technology for new boilers and wherever necessary to retrofit on

the existing boilers. Despite the good performance of the FGD system so far, the technology still greatly suffered from gypsum waste disposal, high volume of effluent (Liu et al., 2017), chemicals used can harm humans (Saikia et al., 2014a), high chemicals consumption (Mketo et al., 2016), being expensive regarding capital and operating cost as well as technically difficult to retrofit on existing plants. Additionally, the FGD process brings about effluent with high concentrations of the cationic and anionic impurities as well as heavy metals. Furthermore, using FGD requires that limestone be brought in from Northern Cape mines that are situated about a thousand kilometers away from Eskom's power plants. Also, most of the coal-fired power plants have already passed their design half–life of 50 years while many will reach their end of life between now and the year 2045 (Eskom, 2015). With respect to the abovementioned limitations, retrofitting FGD technology on power plants with a limited service life of fewer than 20 years is not economically feasible.

The development of alternative technologies that can desulphurize coal has been a focused topic among the scientific community. Among the microbial, chemical and physical methods for coal desulphurization, microbial treatment emerges as a clean, less energy – intensive, efficient and environmentally reasonable technique with low capital and operating costs (Gonsalvesh et al., 2012). Microbial treatment is based on certain microorganism’s ability to metabolize some stable Sulphur – containing compounds or degradation of sulphur compounds by microorganisms. Therefore, it is noticeable that certain bacteria exist with demonstrated strong abilities to oxidation and metabolism of Sulphur content in the coal and to use the energy released to support their growth (Ghosh and Dam, 2009). Among all the reported work on coal desulphurization, only one microbial treatment of coal has been successful - the removal of pyritic sulphur. Various authors (Huifang and Yagin, 1993; Dong-chen et al., 2009; Mishra et al., 2014) have reported the reduction of pyritic Sulphur using several bacterial and fungal strains. Although pyritic sulphur is the dominant sulphide mineral in the Waterberg coals, organic sulphur also exist in a greater proportion (Wagner and Tlotleng, 2012).

Very few attempts were made on desulphurization of other forms of sulphur content like organic sulphur. Most of the organic sulphur reduction studies were carried out using a model compound such as dibenzothiophene (Gonsalvesh et al., 2012; Mishra et al., 2014; Han et al., 2018) which is recognized to behave differently to the actual sulphur in the coal. Of the little simultaneous microbial desulphurization of sulphur forms attempted, the application has been

on lignite type only (Aytar et al. 2011). The main difference between lignite and the Waterberg steam coal lies in the rank of the coal, with the Waterberg coal being a bituminous coal, higher in rank than the lignite. In addition, the Waterberg coal studied reported comparatively higher in calorific value (CV), ash, sulphur and nitrogen contents. Therefore, despite the plethora of desulphurization studies that have made epigrammatic progress, there is still limited information provided by the current literature for biodesulphurization application of all sulphur forms in coal studies. The novelty of the current study compared to the state of the art consists of bacteria isolated from coal been used for the first time towards simultaneous biodesulphurization of various forms of sulphur in the Waterberg steam coal. Waterberg steam coal is unique in various aspects on high sulphur Indian coals dominating the literature (Saikia et al., 2013, 2014a; 2014b). Furthermore, the Waterberg steam coal is one of the remaining large resources of South Africa's remaining coal reserves (Eberhard, 2011). Therefore, biodesulphurization of Waterberg steam coal is a new contribution to clean coal technologies research with the intention to reduce SO_2 emissions spikes from the power plant. The main objective is evaluating the feasibility of biodesulphurization treatment of Waterberg steam coal using a bacterial consortium isolated from coal as a pre-combustion technique to reduce SO_2 emissions spikes from the power plant.

5.2 Results and Discussions

5.2.1 The effect of microbial desulphurization treatment on coal sulphur content

The relationship between reductions of total sulphur in coal samples by biodesulphurization treatment against reaction time for − 0.85 mm, for −2.30 +1.00 mm, −4.60 +2.30 mm and +4.60 mm particle size fractions are presented in Figs. 5.1 – 5.4. As can be observed in Fig. 5.1 that for the finer particle size of – 0.85 mm, total sulphur showed a significant reduction from 1.45 wt% to 0.50 wt% within 18 Days. However, when the temperature was increased from 23 ± 3°C to 30 ± 2°C, further degree of desulphurization of total sulphur content of 0.40 wt.% was accomplished. This additional sulphur content reduction due to temperature rise is desirable and highly encouraging. The reason for increase in desulphurization with increasing temperature is mainly that this condition is culture rich in bacteria since 30 ± 2°C is a culturing temperature. In comparison, there was significantly lesser reduction of total sulphur content to 1.27 wt.% observed in the uninoculated 23 ± 3°C (control experiments), which minor desulphurization activity can be attributed to the action of microbes present in the coal. However, process difficulties were experienced when studying the effect of inoculation (30 ±

2 °C) on biodesulphurization. Precipitates were observed in the microbial solution due to high microbial concentration.

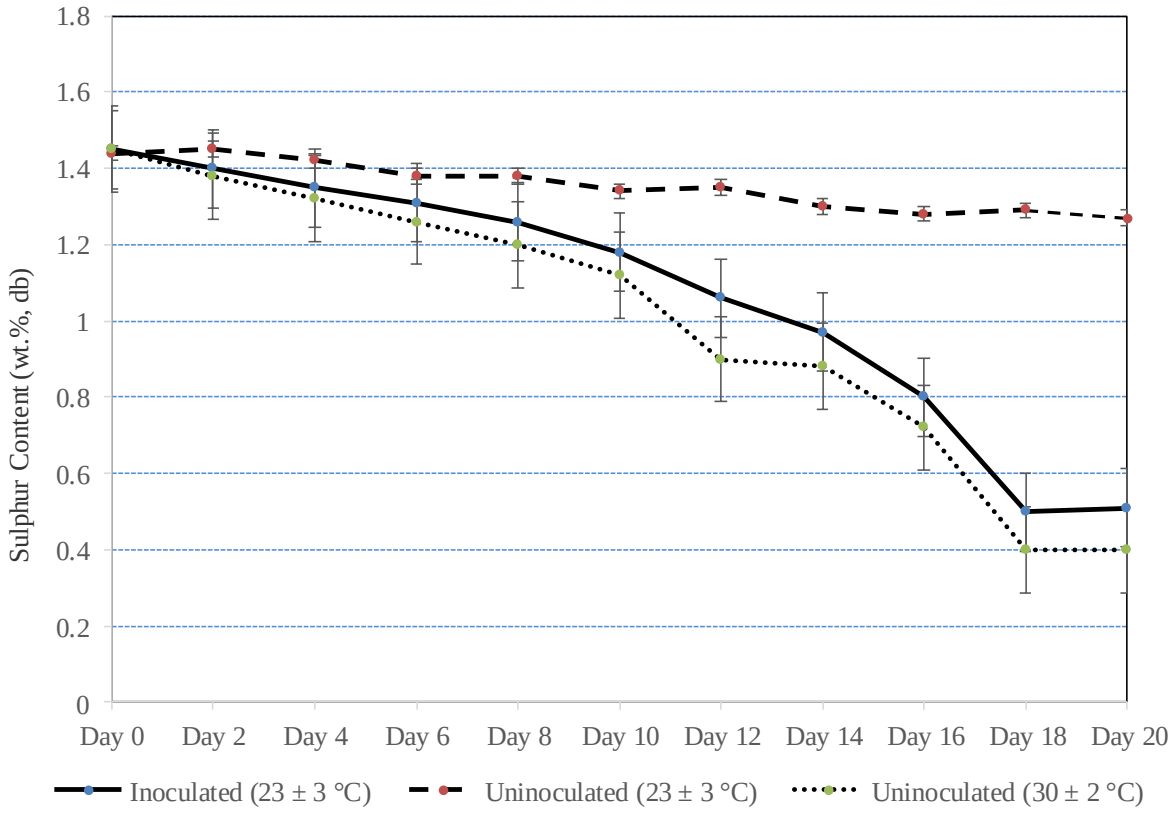

Figure 5.1: Variation of sulphur content with reaction time for − 0.85 mm particle size

In the case of – 2.30 + 1.00 mm particle size, total sulphur also showed a good reduction from 1.41 wt% to 0.65 wt% as depicted in Fig.5.2. When the temperature was increased from 23 ± 3°C to 30 ± 2°C, further sulphur content reduction of 0.60 wt.% was observed. In comparison, there was a significantly lesser reduction of total sulphur content to 1.29 wt.% observed in the uninoculated 23 ± 3°C (control experiments), which confirm the minor desulphurization activity of microbes present in the coal.

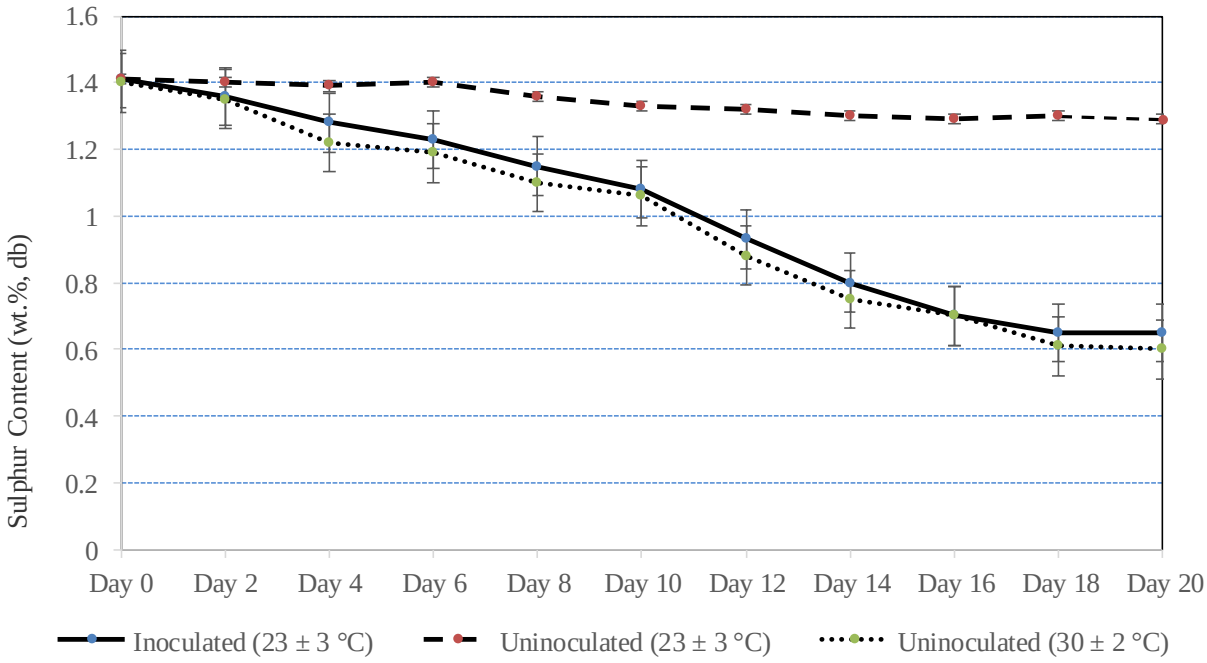

Figure 5.2: Variation of sulphur content with reaction time for −2.30 +1.00 mm particle size

Furthermore, −4.60 +2.30 mm particle size showed a good reduction of sulphur content from 1.44 wt.% to 0.73 wt.% as shown in Fig. 5.3. Nevertheless, when the temperature was increased from 23 ± 3°C to 30 ± 2°C, a further decrease in sulphur content reduction to 0.66 wt.% resulted. In evaluation, there was a minor reduction of total sulphur content to 1.29 wt.% observed in the uninoculated 23 ± 3°C (control experiments), which confirm the microbial action of microbes present in the coal.

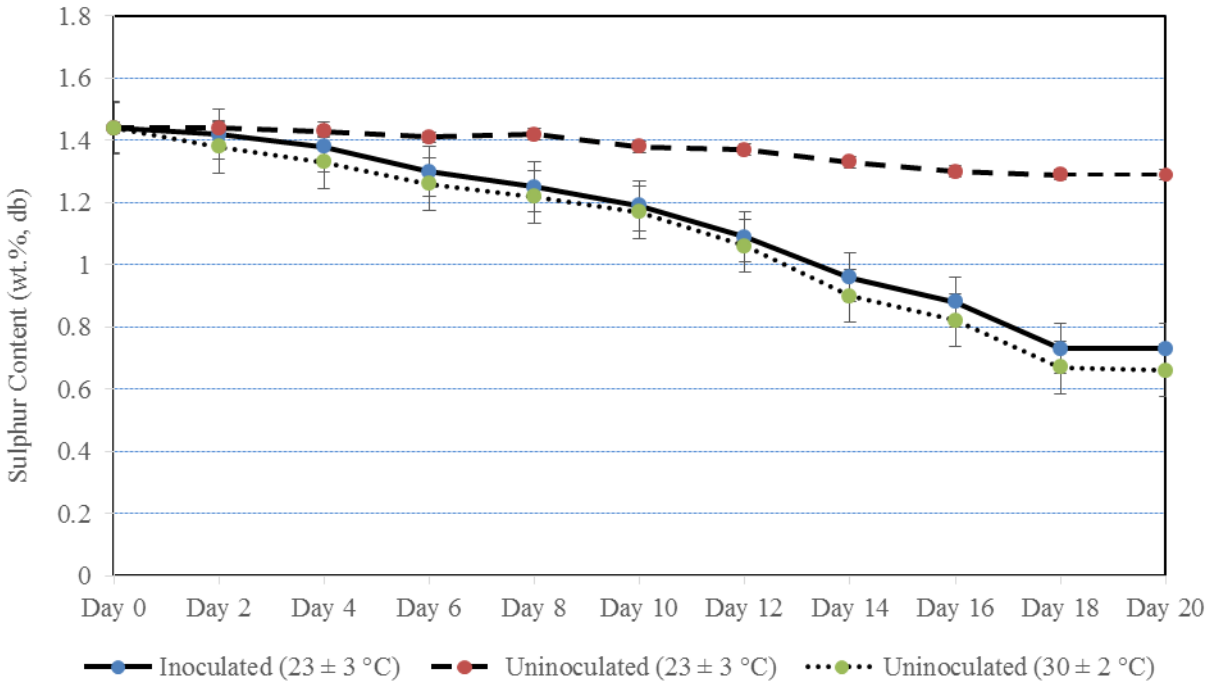

Figure 5.3: Variation of sulphur content with reaction time for −4.60 +2.30 mm particle size

In case of larger particles of + 4.60 mm, there was an insignificant reduction in total sulphur from 1.43 wt.% to 1.1 wt.% observed as shown in Fig. 5.4. All the same, when the temperature was increased from 23 ± 3°C to 30 ± 2°C, extra sulphur content reduction of 1.03 wt.% was observed. In comparison, there was significantly lesser reduction of total sulphur content to 1.35 wt.% observed in the uninoculated 23 ± 3°C (control experiments), which confirm minor microbial desulphurization activity of bacteria present in the coal. Lower sulphur content reduction observed on the coarse particle size fraction may be due to large particles size bringing about challenges of agitation, dissolving of coal particles and poor bacteria – coal surface area interaction due to less liberated sulphur content (Pandey et al., 2005). In addition, there is large mass transfer resistance throughout the microbial solution and coal particles. Fig. 5.4 clearly shows that for larger particle size effective stirring started on the 4th day after 40 g of coal samples were withdrawn through routine sampling, only then desulphurization activity started to happen. Therefore, coal particle sizes control the accessibility of the sulphur content and exert a significant influence on the rate of oxidation and metabolism of sulphur forms creating successful sulphur reduction.

The maximum sulphur reduction was obtained at the smallest particle size of – 0.85 mm (0.5 wt%) within 18 days which is desirable as according You and Xu (2010), the most economic means to reduce SOx emission now is to fire low-sulphur coal of <0.6 wt% which is in good

agreement with the current study. The reason is that small particle size fraction has higher mass transfer efficiency than bigger particle size attributed to the surface area (Saha et al., 2017). Further increase in the reaction time to day 20th did not result in any further improvements in the reduction efficiency of sulphur content. Since coal is a solid particle, the bacteria are unable to penetrate beyond a certain limit depending upon the porosity, cracks and surface area of the coal. Prayuenyong (2002), who mentioned that with certain coals, the direct mechanism for the oxidation of sulphur forms might be limited because the microorganisms are too large to enter most of the coal pores, better explains this. Secondly, the inhibition caused by the intermediates of the sulphur pathway is also an important bottleneck and are responsible of the major inhibitory effects on microbial cell growth. Hence, a further reduction in total sulphur is restricted beyond the 18th day. However, the 18 days duration for the successful microbial desulphurization process ties quite well with the fact that seasonal stockpile were built to last for around 20 days (Eberhard, 2011).

It is well known that fine coal dust is seen as a major hazard due to its tendency to ignite explosively causing coal losses, environmental pollution and plant equipment damages. Despite serious environmental challenges such as spontaneous coal combustion, air and water pollution, personnel exposure to excessive coal dust resulting from fine coal causes serious occupational lungs disease such as pneumoconiosis and other health – related conditions. These challenges will be managed by ensuring that coal particle size is reduced by milling coal from bunkers to the microbial reactor and the final product is stored at the silos with no personnel exposure to coal fine coal.

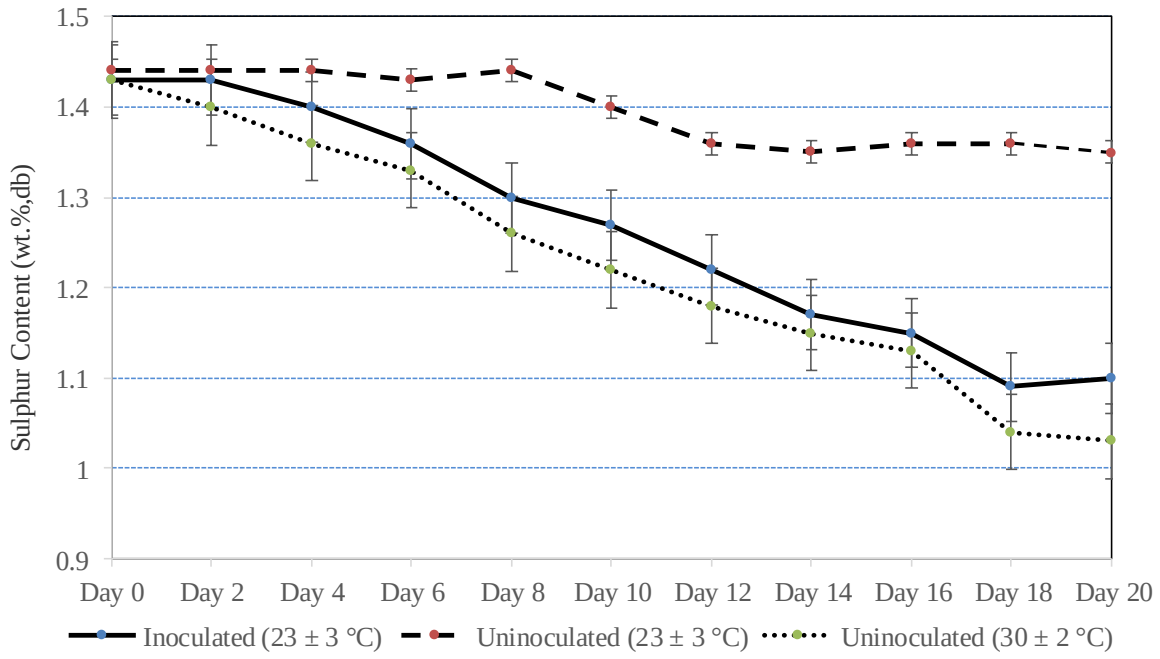

Figure 5.4: Variation of sulphur content with reaction time for +4.60 mm particle size

Eq. 5.1 can express the relationship between pre – treated total sulphur and post – treated total sulphur in the coal:

$$\text{Sulphur}_{\text{Treated coal, T,n}} = \text{Sulphur}_{\text{Untreated coal, T,0}} - \sum(a,T_1;b,T_2;c,T_3...k,T_{11}) \qquad (5.\ 1)$$

where T, n = Time in any day; $\sum(a,T_1;b,T_2;c,T_3...k,T_{11})$ = sum of daily sulphur decrease over the biodesulphurization period

The sulphur reduction rate is continuous from Day 0 to Day 18 as clear from Fig. 5.5. The most reduction rate of sulphur was found to be 0.30 wt.% at Day 18th for – 0.85 mm particle size. The high sulphur reduction rate by Day 18th for all coal particle sizes with the exception of +1.00 mm size could be explained by the fact that coal particle size has a great influence on its solubility that was crucial to sulphur nutrient transportation and its overall reduction in the biodesulphurization process. In case of both +1.00 mm and +2.30 particle sizes, the greatest reduction rate of sulphur was found to be 0.150 wt.% at Day 12th. The overall decrease in sulphur content is the sum of the individual sulphur content for each day. Therefore, the sulphur reduction rate was found to be a coal particle size – dependent. A first-order kinetic model has been used assuming that the desulphurization rate is a function of

total sulphur content in the coal. Therefore, the desulphurization rate can be expressed as Eq.5.2:

$$-\frac{dS}{dt} = kS_T \tag{5.2}$$

where S_T is total sulphur content, k is the first-order rate constant. The constant k and can be estimated using Eq.5.3:

$$\log\left(S_{T,i} - S_{T,0}\right) = \frac{kt}{2.303} + \log S_{T,i} \tag{5.3}$$

where $S_{T,i}$ is the initial amount of total sulphur in the coal and $S_{T,0}$ is the total sulphur amount lost at time t in days.

Therefore, Eq.5.3 has been adopted to calculate the activation and frequency factor of the desulphurization reaction just like in a typical Arrhenius equation. The suggestion is supported by earlier studies by Acharya *et al.* (2005), where simple first – order kinetics of coal desulphurization was used in the biological desulphurization.

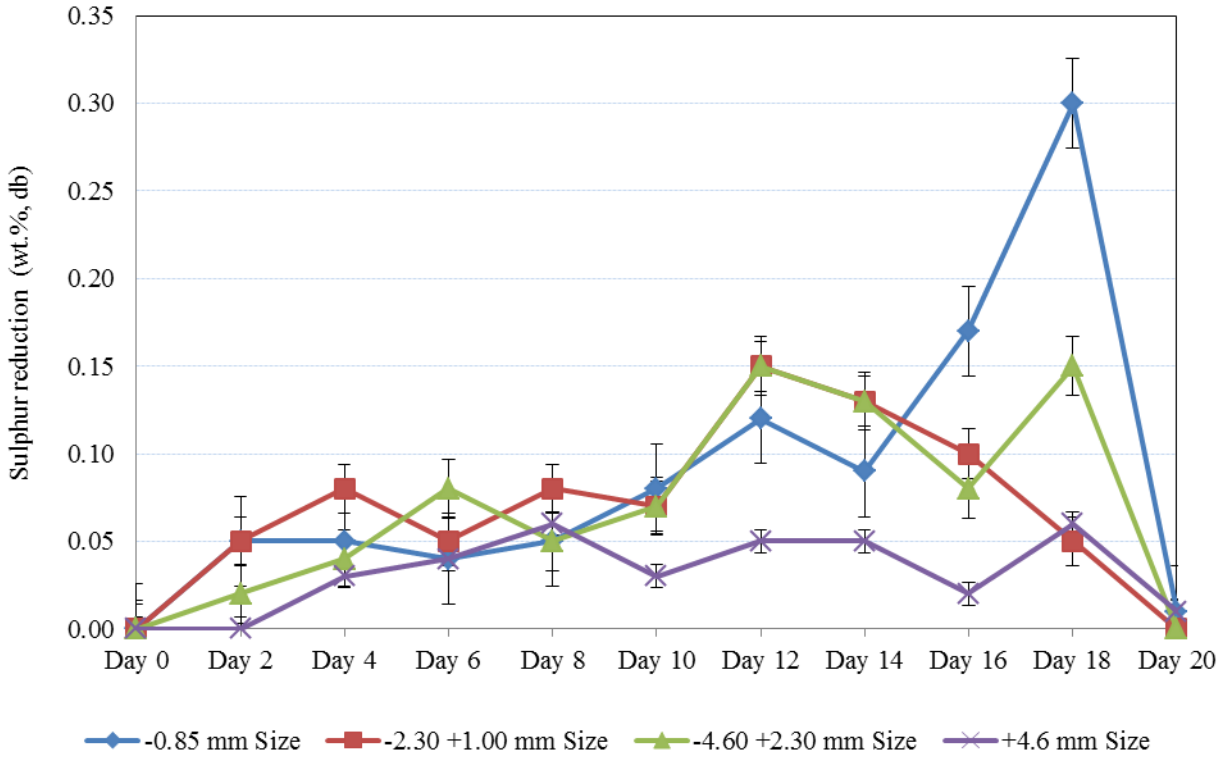

Figure 5.5: Biodesulphurization reduction rate for sulphur content over various particle sizes

5.2.2 The effect of microbial desulphurization treatment on calorific value

The CV, also called a heating value is defined as the amount of energy released upon complete combustion per unit mass. The CV is used as an indicator of the chemically stored energy in the coal (Matin and Chelgani, 2016). Therefore, a CV is a very important coal quality measure in the assessment of its value as a fuel for power generation and could be used as a coal key property for the purchase of coal. The changes in coal samples CV due to biodesulphurization treatment were evaluated and the results are as depicted in Fig. 5.6 and Fig.5.7. It is obvious from both figures that there was a progressive increase in CV from 20.3 MJ/Kg to 24.16 MJ/Kg on the 14th day translating to CV increase of 19% for – 0.85 mm particle size. However, in case of both +1.00 mm and +2.30 mm particle sizes, CV increased from 20.3 MJ/Kg to 23.4 MJ/Kg on the Day 14th and Day 18th respectively translating to CV increase of about 15%. Lastly, an increase in CV from 20.3 MJ/Kg to 21.6 MJ/Kg on the 14th day translating to CV increase of 6% for +4.60 mm particle size. When the temperature was increased from 23 ± 3°C to 30 ± 2°C, there was insignificant change on the CV values as depicted by both figures. After breakthrough (increase in CV values), desulphurized coal

produces more heat than the untreated one. This conclusion was consistent with the results of Liu *et al.* (2017) who also showed that a significant increase in the CV of the two-lignite coal samples from 26.03 MJ/Kg to 26.82 MJ/Kg and then 26.43 MJ/Kg respectively after biodesulphurization treatment. More importantly, the reason for the gain in CV has been ascribed to 33% decreased ash content, removal of non-combustible material and coal becoming more enriched in organic matter during the desulphurization process (Mishra *et al.* 2014).

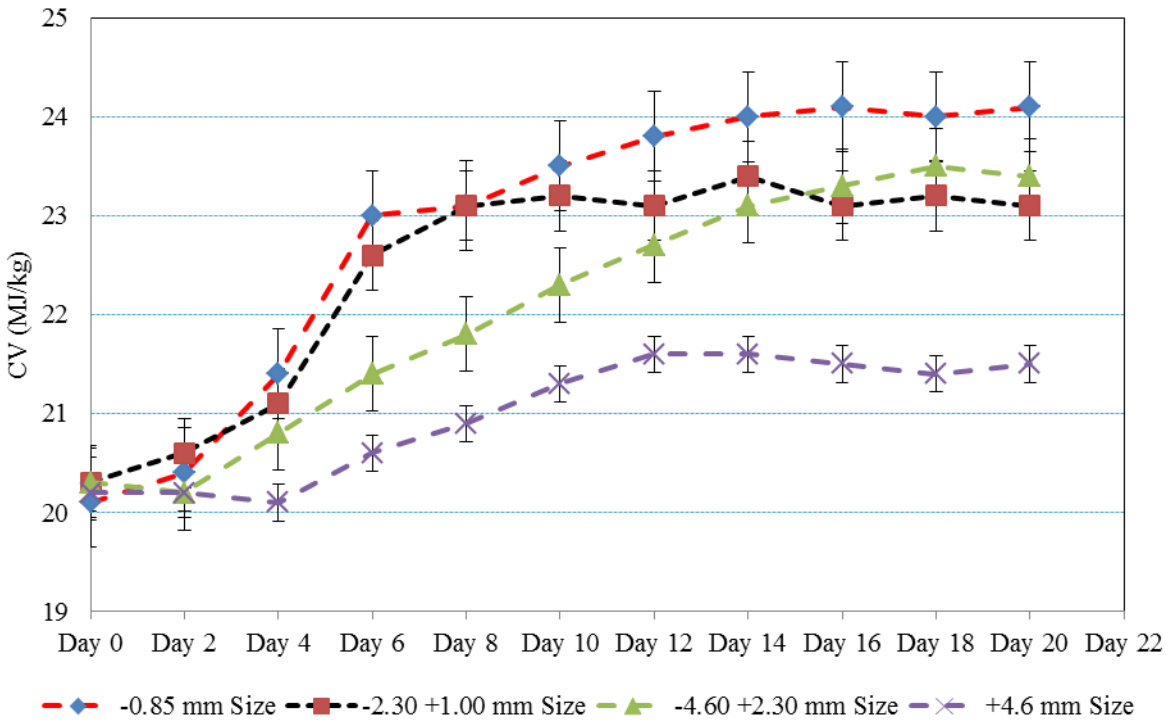

Figure 5.6: The effect of biodesulphurization on calorific value at various reaction time for inoculated (23 ± 3 °C)

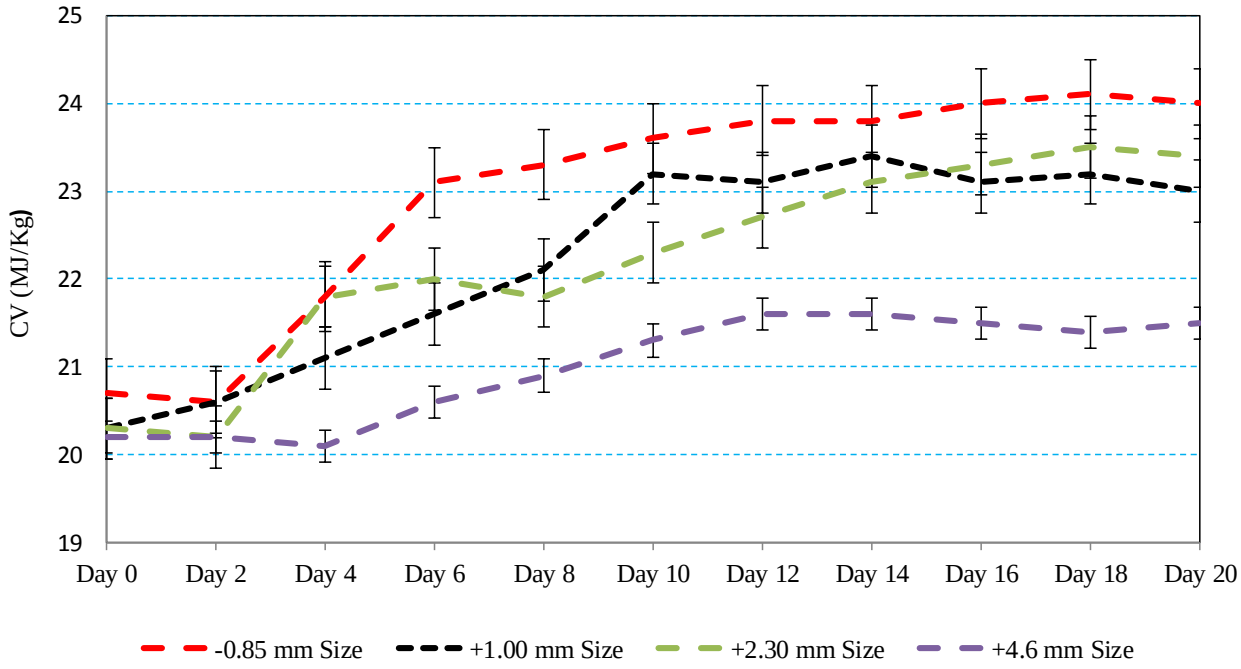

Figure 5.7: The effect of biodesulphurization on calorific value at various reaction time for uninoculated (30 ± 2 °C)

Fig. 5.8 presents the calorific value increase rate at various reaction time for inoculated (23 ± 3 °C) and uninoculated (30 ± 2 °C) conditions. The insignificant impact due to the temperature increase on the CV values was demonstrated by monitoring daily CV increase for various particle sizes studied. For both conditions under consideration, the extent to which the CV increase rate was in the particle size distribution order of – 0.85 mm, +1.00 mm, +2.30 mm and +4.60 mm respectively. Hence, only graph suffice to represent both scenarios. For both coal particle sizes studied, CV increase was the highest at Day 6th. The overall increase in CV is the sum of the individual CVs for each day. Therefore, similar to the sulphur reduction rate and ash reduction, CV increase rate was found to be coal particle size – dependent.

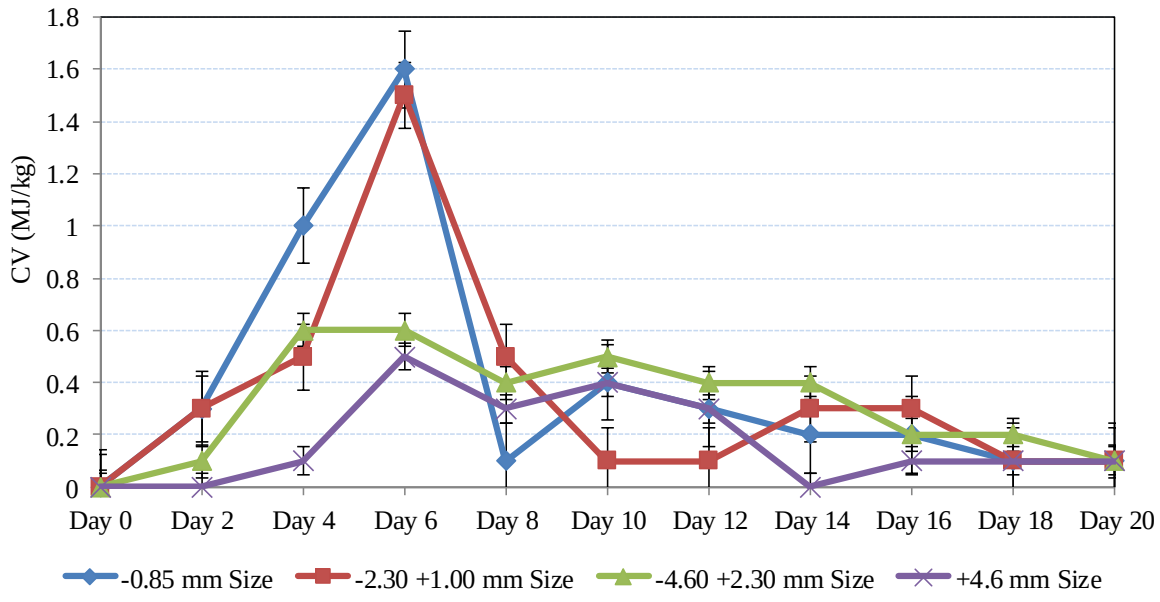

Figure 5.8: Calorific value at different reaction time

CV of coal samples studied can be calculated based on its carbon, hydrogen, sulphur, and ash as per Eq. (5.4):

$$CV = 0.47C + 1.30H + 0.190S + 0.107A + 8.80 \quad (5.4)$$

where: C = Carbon, H = Hydrogen, S = Total Sulphur, and A = Ash

Using corresponding measured values for elemental composition of eight coal samples on Eq. 5.4, calculated CV values and coefficient of variation (σ) values with measured CV values were obtained as reported in Table 5.1 σ values are quite acceptable in the range of up to 3 unit increase which indicates that Eq. 5.4 hold for Waterberg coalfield.

Table 5.1: Calorific value analyses

PSD (mm)	Measured CV(MJ/kg)	Calculated CV (MJ/kg)	σ (MJ/kg)
− 0.85	24.1	24.2	0.1
	24.0	24.2	0.2
−2.30 +1.00	23.2	25.9	-2.7
	23.1	25.9	-2.8
−4.60 +2.30	23.5	24.6	-1.1
	23.4	23.3	0.1
+4.60	21.4	24.4	-3.0
	21.5	24.4	-2.9

Saikia *et al.* (2014a) undertook a detailed study on the effect of desulphurization on coal heat value. Their work established that the CV changes after desulphurization might depend on the ratio of microbial desulphurization and demineralization that is also observed in our present study. Therefore, for any microbial desulphurized coal similar to the conditions studied, the CV should be able to be estimated given that carbon, hydrogen, sulphur, and ash content has been analyzed for those samples.

5.2.3 The effect of microbial desulphurization treatment on microbial solution pH

A number of authors have pointed out the effect of biodesulphurization treatment on microbial solution pH. As pointed out previously by Acharya *et al.* (2001), who also showed that the value of the pH variations during the microbial desulphurization treatment are known to have a great effect on the rate of the reactions. In order to investigate the effect of pH on coal biodesulphurization, experiments were carried out by observing pH changes over biodesulphurization period without any pH adjustment. Fig. 5.8 and Fig. 9 represent variation in pH by microbial desulphurization process for time for inoculated (23 ± 3 °C) and uninoculated (30 ± 2 °C) conditions respectively. It must be noted that for experimental conditions evaluated, the variations in microbial solution pH results were found to be within the error of repeatability, hence figures are appearing to be the sameand can always be

represented as one. In summary, for all conditions under consideration, it can be seen from that by decreasing pH from 6.73 to 3.23 for various coal particles, both total sulphur and ash content of the treated coal decreased while CV increased. In addition, it should be noted that the pH of a biodesulphurization system significantly affects the growth and activity of acidophilic microorganisms and the dissolution rate of acid-soluble minerals. Tang *et al.* (2009) observed that a mixed acidophilic SRB culture was able to grow at a pH of 3.0, supporting the view that mixed SRB cultures are more tolerant of extreme conditions when compared with pure cultures. According to Tang *et al.* (2009), some microorganisms responded differently at different levels of pH. These bacteria use elemental sulphur as an energy source, oxidizing it to sulphate under aerobic conditions with oxygen as the electron acceptor (reaction 5.5):

$$S^{o} + 1.5O_2 + H_2O \rightarrow H_2SO_4 \qquad (5.5)$$

This reaction produces 530 kJ of heat per mole of S oxidized to sulphate and one tonne of sulphuric acid per 327 kg of S_0 oxidized (de Oliveira *et al.*, 2014). Şenera *et al.* (2018) have reported similar results of acid tolerances for these microbes to range from pH 5.0 to 1.02 and these results agreed with those Şenera and co-worker observations. Therefore, sulphur-reducing microbes are known to flourish in the environments with pH in the range of 6.73 to 3.23 pH values of which outside this range usually results in reduced desulphurization activity. Lastly, oxidation of reduced sulphur compounds generates significant acidity and thus several species used are therefore acidophilic.

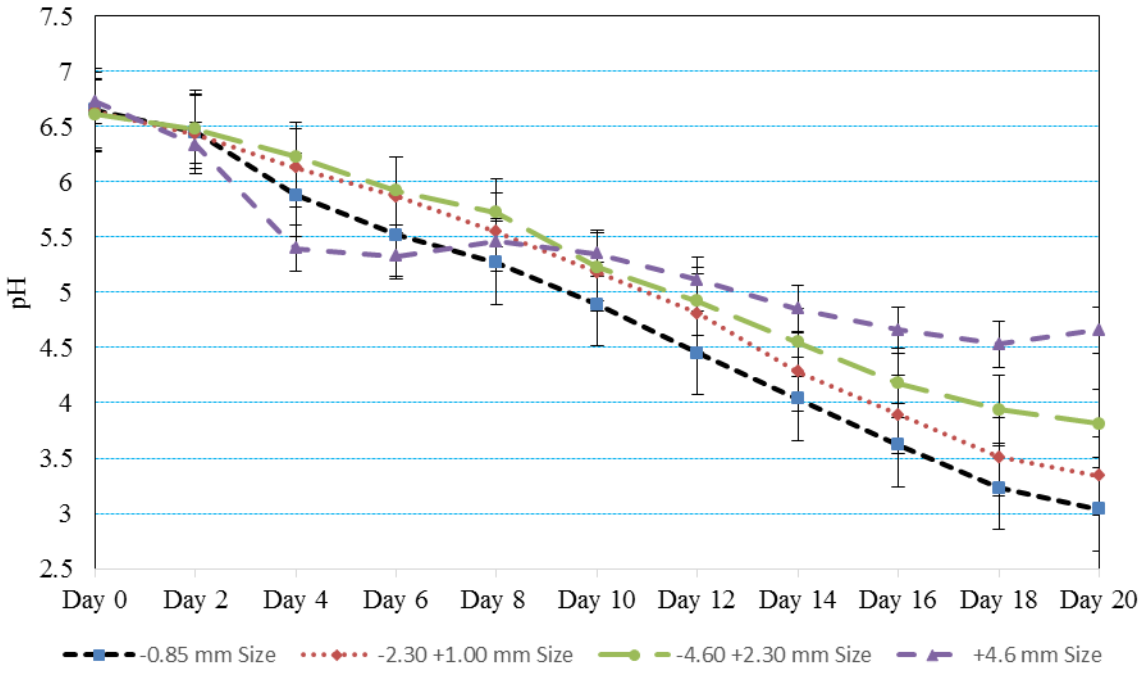

Figure 5.9: Variation in pH by microbial desulphurization process for Inoculated (23 ± 3 °C) and Uninoculated (30 ± 2 °C)

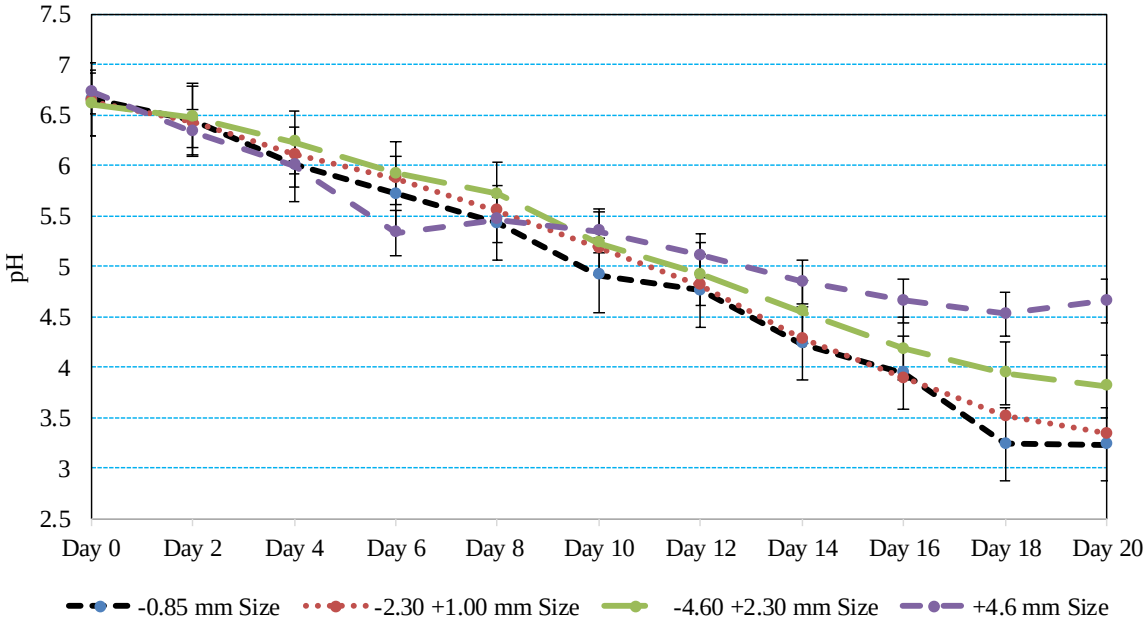

Figure 5.10: Variation in pH by microbial desulphurization process for uninoculated (30 ± 2 °C)

5.2.4 The effect of microbial desulphurization treatment on redox potential

The redox potential (Eh) of a bacterial desulphurization medium affects the rate of metal sulphide oxidation by microorganisms. Similar to pH microbial solution, it must be noted that various experimental conditions were evaluated and the variations in redox potential results were found to be within the error of repeatability, hence only one figure is presented for all conditions. The effect of biodesulphurization treatment on redox potential is depicted in Figs. 5.11 and 5.12 for inoculated (23 ± 3 °C) and uninoculated (30 ± 2 °C) conditions. The changes noted on both graphs is on significant figures, hence both graphs looks the same. In general, the Eh increased from +1.4 mV to +13.1 mV over 20 days period as shown in Figs. 5.11 and 5.12. The oxidation of metal sulphides by microbes is both pH and coal particle size – dependent. As can be seen in both Fig. 5.11 and 5.12 that as the pH decreased, the redox potential increased. Figure 5.13 depicts the relationship between Eh–pH diagrams for sulphur species at 40 °C. These Eh results are consistent with the data obtained by Ochoa-González et al. (2013) indicating that the dominant sulphate ions were stable which indicates that sulphur reduction may have happened according to the potential redox-pH diagram illustrated in Fig. 5.13. The imaginary area is marked in blue square on Fig. 5.13. The SO_3^{2-} is less stable than other sulphate.

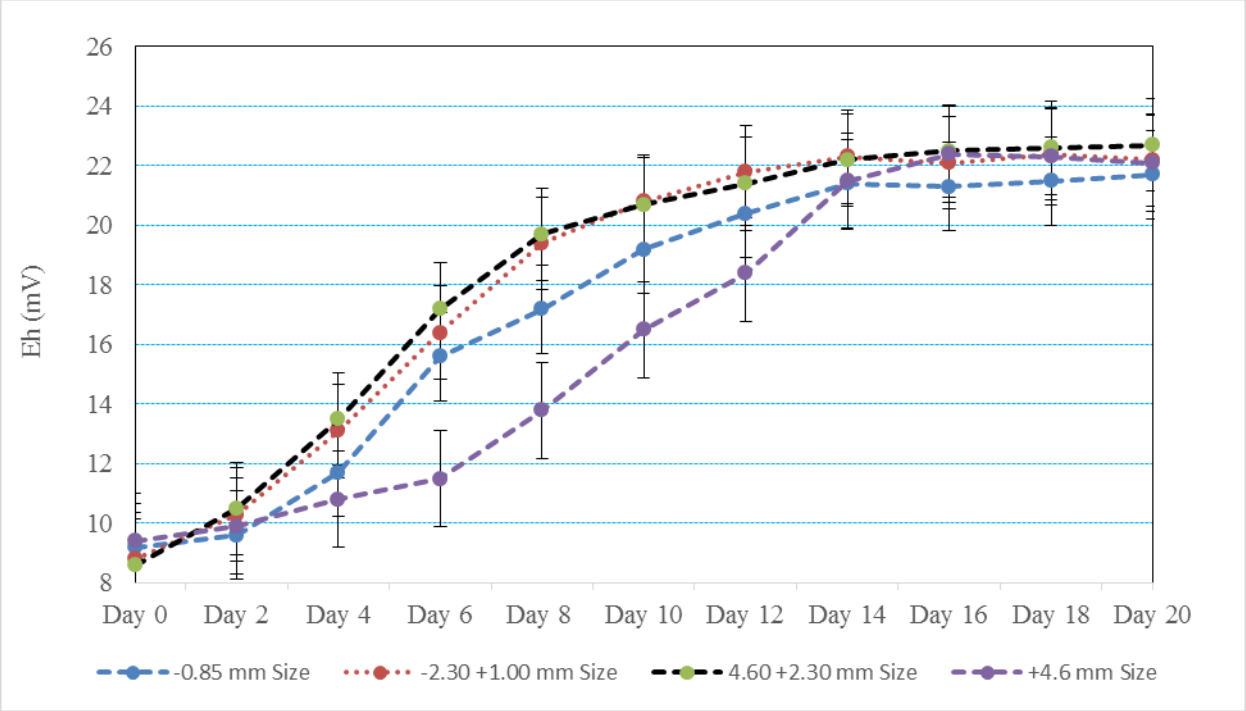

Figure 5.11: Variation in Eh by microbial desulphurization process for Inoculated (23 ± 3 °C)

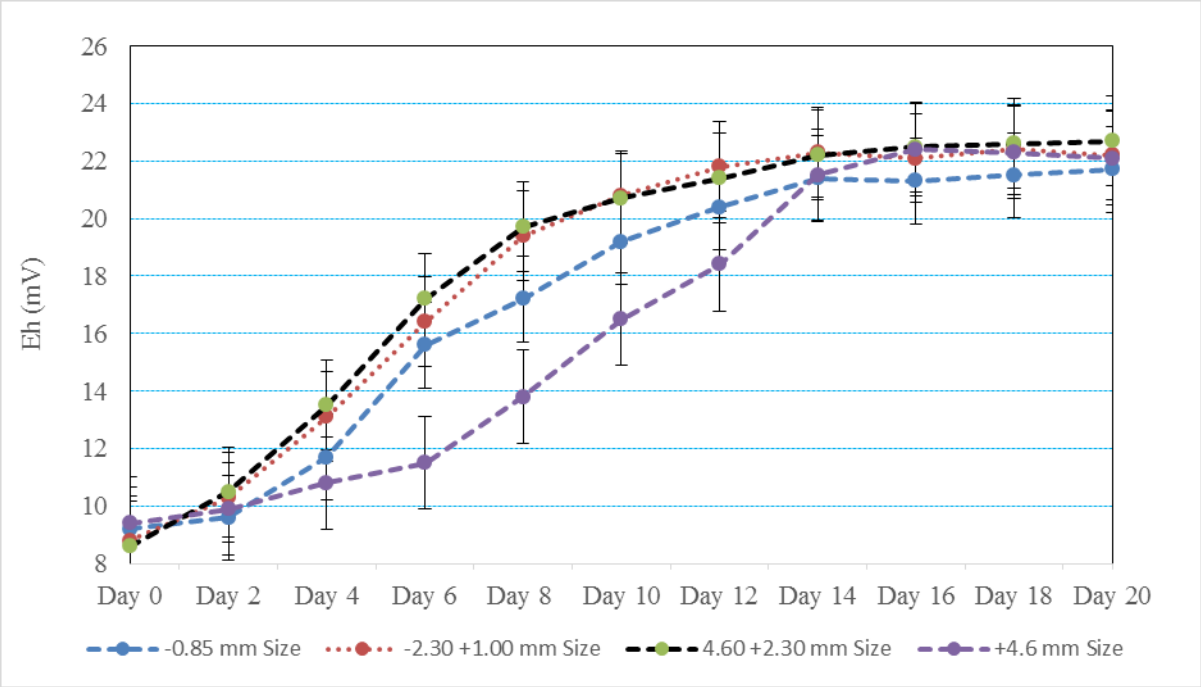

Figure 5.12: Variation in Eh by microbial desulphurization process for Uninoculated (30 ± 2 °C)

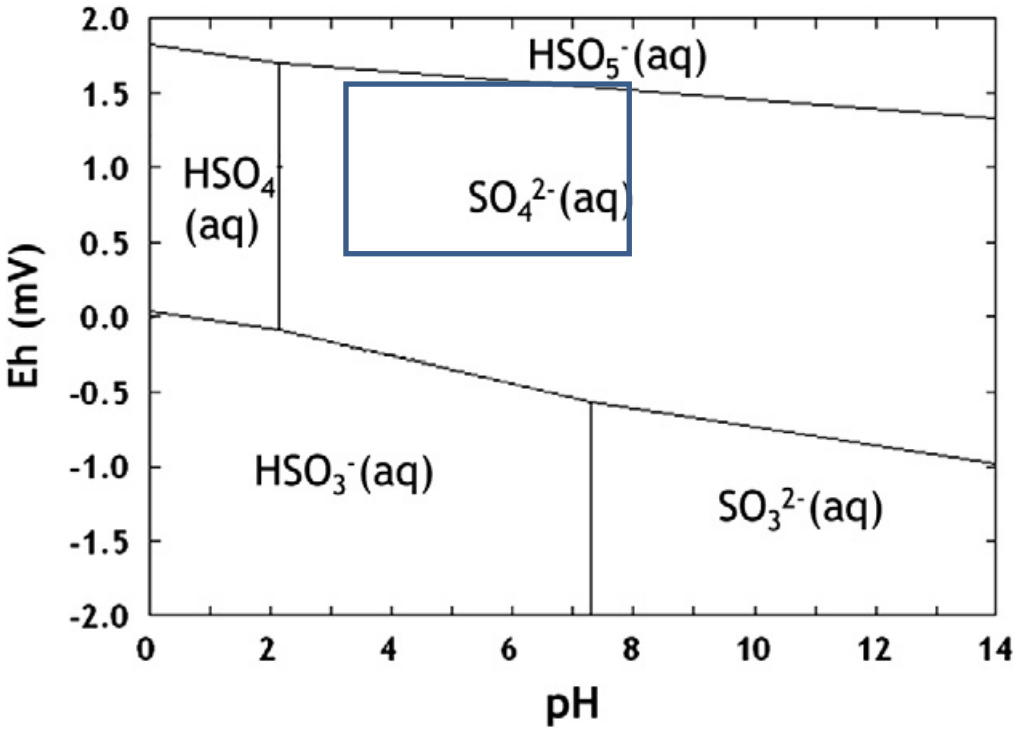

Figure 5.13: Eh–pH diagram for sulphur species at 40 °C (Ochoa-González *et al.*, 2013)

5.2.5 The effect of microbial desulphurization treatment on coal ash content

The changes in ash content of coal samples because of biodesulphurization treatment were evaluated using Eq .5.6 and the findings are as depicted in Fig. 5.14.

$$\text{Ash}_{\text{Treated coal, T,n}} = \text{Ash}_{\text{Untreated coal, T,0}} - \sum(a,T_1;b,T_2;c,T_3...k,T_{11}) \quad (5.6)$$

Where T, n = Time in any day; $\sum(a,T_1;b,T_2;c,T_3...k,T_{11})$ = sum of daily ash decrease over the biodesulphurization period

During the start-up stage (Days 0 – 6), the ash content of – 0.85 mm particle size fraction decreased gradually from 34.2 to 32.8 wt.% then linearly to 23.2 wt.% on Day 16 and it was maintained until at the end of the Day 20th period. Therefore, biodesulphurization treatment has a big effect on the reduction of coal ash content and the decrease was found to increase with HRTs. However, the large size fraction of +4.60 mm shows lower ash content reduction mainly because large size coal particles size fractions have less liberated mineral impurities as opposed to lower size fraction coal samples. The decrease in ash content observed might be owing to liberation of mineral matter from coal matrix, the loss of sulphur form (pyritic sulphur in particular) as well as some ash oxide analyses. Ken and Nandi (2019) also reported similar observations. This finding is desirable as coal ash content accumulate and act as an insulating layer, which reduces heat transfer between the furnace and the steam inside the boiler tubes impacting on the furnace boiler tubes resulting in lowering efficiency of boilers. Furthermore, ash handling, management, storage, transportation and ash disposal involves extra cost and leads to a reduction in operating efficiency and availability of thermal power plant. Therefore, it is significant to note that the ash reduction of coal due to biodesulphurization is very essential for the sustainable use of coal in thermal power plants environment.

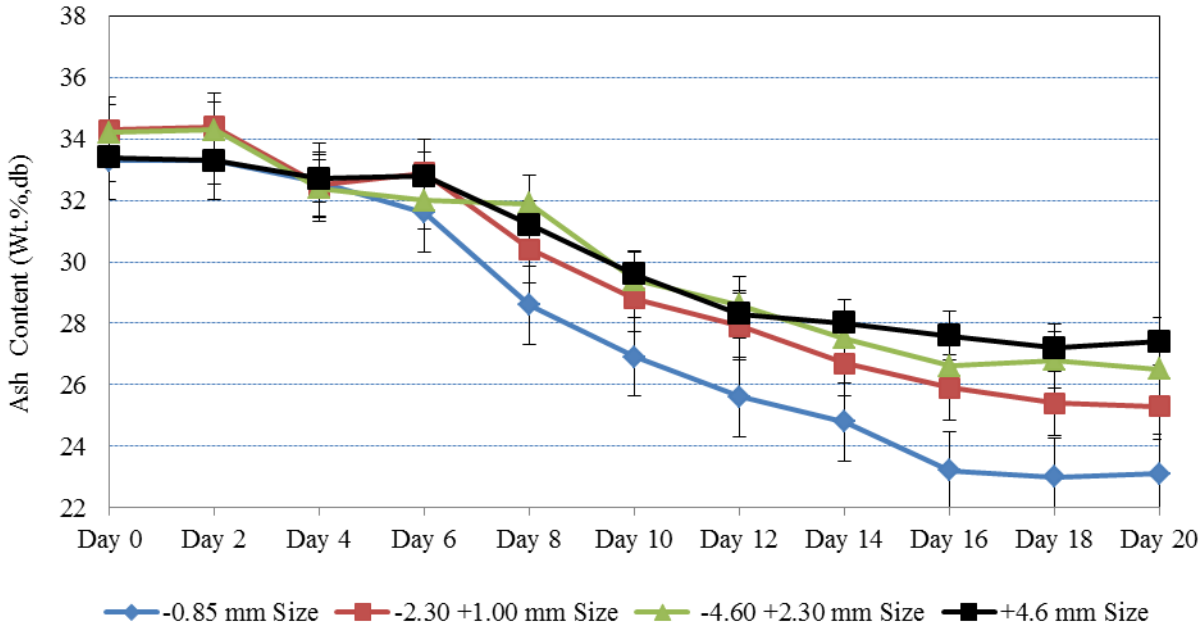

Figure 5.14: Coal ash content at various hydraulic retention times for Inoculated (23 ± 3 °C) and Uninoculated (30 ± 2 °C)

Fig. 5.15 depicts the biodesulphurization rate reduction for ash content at various particle sizes. Fig. 5.15 clearly shows that the ash reduction was gradually decreased with the greatest rate reduction at Day 12 for – 0.85 mm, +2.30 mm and +4.60 mm particle sizes were found to be 3.0 wt.%, 2.50 wt.% and 1.60 wt.% respectively. The most rate reduction of ash content for +1.00 mm particle size was found to be 2.50 wt.% at Day 10. Similar to the sulphur rate reduction, the ash rate reduction was also found to be coal particle size – dependent. Therefore, the ash content reduction rate is given by Eq.5.7:

$$-\frac{dS}{dt} = kA \qquad (5.7)$$

where A = ash content in the coal; *k* is the first-order rate constant.

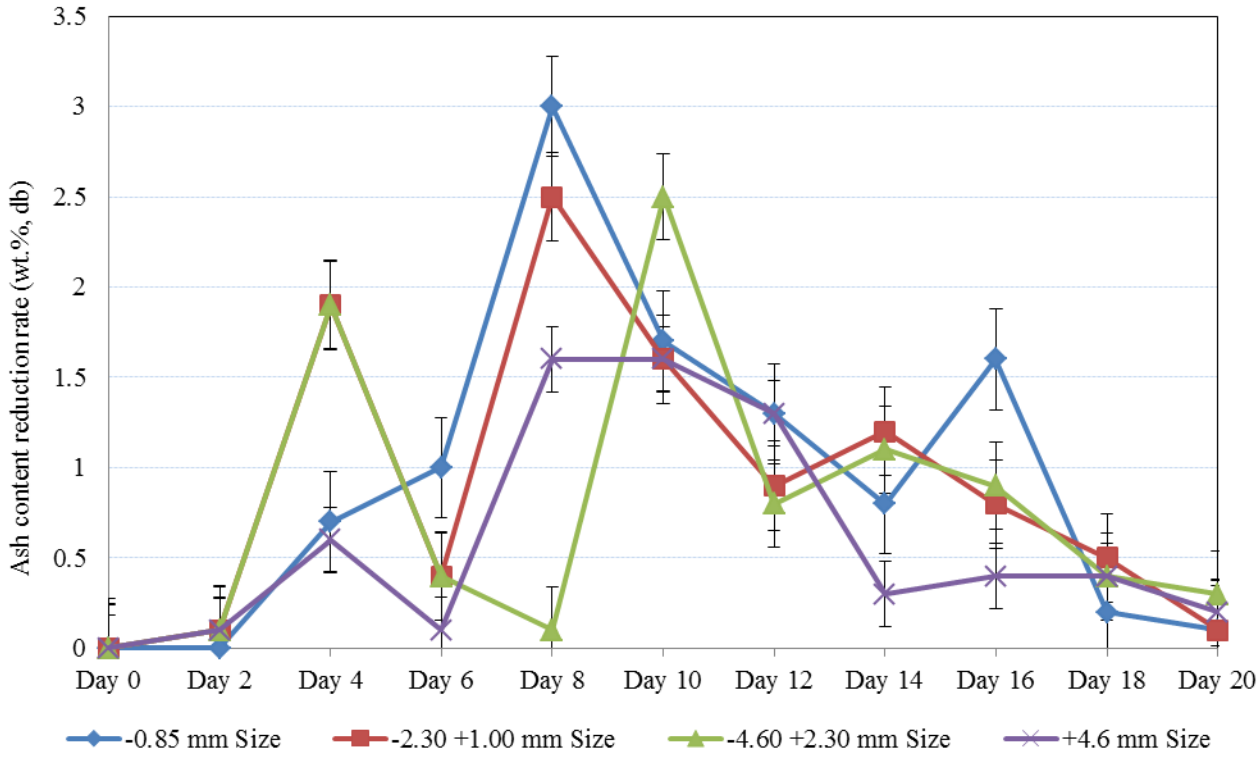

Figure 5.15: Biodesulphurization reduction rate for ash content at various particle sizes

5.2.6 The effect of microbial desulphurization treatment on sulphur forms and their transformation

Reduction in the sulphur content of the Waterberg steam coal is necessary and requires knowledge of the sulphur forms and distribution in the coal. Sulphur forms and distribution in Waterberg steam coal exists as per Eq. 5.8:

$$S_T = \sum (S_{IN} + S_{PYR} + S_S + S_{ORG}) \quad (5.8)$$

where S_{IN} = Sulphide/ mineral sulphur; S_{PYR} = Pyritic sulphur, S_S = Sulphate sulphur, S_{ORG} = Organic sulphur, S_T = Total sulphur

In order to evaluate the effect of biodesulphurization on sulphur forms, three pre and post–treated coal samples were subjected to sulphur analyses and the results are as shown in Table 5.2. These samples were taken from particle size fractions of −4.60 + 2.30 mm, −2.30 + 1.00 mm and −0.85 mm tested earlier in section 5.2.1. In general, the pre and post–treated coal samples result show significant differences except for sulphate sulphur content. The reason

for the difference in the portion of the sulphate sulphur form is attributed to sulphate sulphur occurring in smaller amounts been diluted by many other forms of sulphur which occur in larger proportion. Hence, the lack of accessibility of sulphate sulphur by bacterial consortium. It can be seen from Table 5.3 – Table 5.4 that the total sulphur content of the pre-treated Waterberg steam coal sample A, coal sample B and coal sample C were 1.37 wt%, 1.49 wt% and 1.15 wt% respectively. Post-treated by biodesulphurization of coal sample A, coal sample B and coal sample C resulted in total sulphur content been reduced to 0.65 wt%, 0.73 wt% and 0.51 wt%. Surprisingly, when the temperature was increased, the total sulphur further reduced to 0.73 wt.%, 0.66 wt.% and 0.40 wt.%. In comparison, there was a small reduction of total sulphur content from 1.43 wt.% to 1.03 wt.%, 1.10 wt.% and 1.35 wt.% for coal sample A, coal sample B and coal sample C respectively observed in the uninoculated 23 ± 3°C (control experiments), which desulphurization activity is suggested that inherent bacteria removed pyritic sulphur form in the coal (Chandra and Mishra, 1988). Sulphur forms behave differently during microbial treatment and the following sub section detail the effect of microbial treatment on each sulphur form.

5.2.6.1 Pyritic sulphur

Pyritic sulphur of the initial coal sample A, coal sample B and coal sample C was reduced from 0.64 wt.%, 0.66 wt.% and 0.51 wt.% to 0.19 wt.%, 0.24 wt.% and 0.16 wt.% respectively translating to 63.6 – 70.3% range of biodesulphurization efficiency. When the temperature was increased, a pyritic sulphur content of the initial coal sample A, coal sample B and coal sample C was reduced from 0.62 wt.% to 0.12 wt.%, 0.20 wt.% and 0.24 wt.% respectively translating to 61.2 – 81% range of biodesulphurization. Prasassarakich and Pecharanond (1992) have reported that the pyritic sulphur conversion increases as the temperature increases. In comparison, there was a significantly lesser reduction of pyritic sulphur reduction of about 29% observed in the uninoculated 23 ± 3°C (control experiments), which desulphurization activity can be attributed to the action of microbes present in the coal. Previous work undertaken by Gonsalvesh and co-workers (2012) reported a most pyritic sulphur reduction of 71.4% that is in good agreement with the finding of the current study. As pointed out previously, Dong-chen *et al.* (2009) succeeded in oxidizing 74.98% – 86.16% of the pyrite sulphur using *Thiobacillus ferrooxidans* after leaching for 24 days. The minor difference in the biodesulphurization efficiency of the pyrite sulphur form achieved from the Dong-chen *et al.* (2009)'s studies can point to the fact that specialized culture used has a

great biodesulphurization effect on pyrite sulphur than bacterial consortium used otherwise the difference is still within the margin of error. Although higher pyrite sulphur removal efficiency was noted from Dong-chen and co-workers work, it was achieved after leaching for 24 days versus 18 days reported in the current study. The desulphurization of pyritic sulphur compounds by bacterial consortium happens on the surfaces of coal particles, hence finer particle size fraction achieved better efficiency than coarse particle size. Pyrite sulphur transformation is possible in accordance with the reactions 5.9 and 5.10:

$$FeS_2 + H_2 \rightarrow FeS + H_2S \quad (5.9)$$

$$FeS\ (Fe_{1-x}S) + H_2 \rightarrow Fe + H_2S \quad (5.10)$$

5.2.6.2 Organic sulphur

Directly, there is no analytical instrument used for the measurement of organic sulphur (S_{ORG}). Therefore, it is calculated by the difference from the total sulphur (S_T) and the sum of other forms of sulphur. According to Barma (2019), strong chemical bonding holds organic sulphur (denoted as S-s, S-p and S-o) structure in coal and its removal within the coal matrix involves the destruction part of the coal. Organic sulphur of the coal sample A, coal sample B and coal sample C was reduced from 0.56 wt.%, 0.64 wt.% and 0.49 wt.% to 0.34 wt.%, 0.37wt.% and 0.24 wt.% respectively. These results have demonstrated that the extent of organic sulphur removal efficiency was found to vary widely within 37.5 – 51.0% range. When the temperature was increased, an organic sulphur content of the initial coal sample A, coal sample B and coal sample C was reduced from 0.60 wt.% to 0.20 wt.%, 0.34 wt.% and 0.37 wt.% respectively translating to 38.3 – 66.7% range of biodesulphurization. In comparison, there is no appreciable change in the reduction of organic sulphur content observed in the uninoculated 23 ± 3°C (control experiments), which desulphurization activity can be attributed to the accumulation of analytical errors during the analysis of other forms of sulphur analysis. Several groups (Liu et al., 2008; Dong-chen et al., 2009; Gonsalvesh et al., 2012) with respect to organic sulphur reduction have also reported a various range of biodesulphurization efficiency performance. Gonsalvesh and co-workers who achieved a maximum removal efficiency of 47.8% that is in good agreement with the finding of the current study revealed good correlation of organic sulphur desulphurization. In another case, Barooah and Baruah (1996) reported lower range organic sulphur removal efficiency of 26 – 46%. Organic sulphur biodesulphurization efficiency of 19.00% was reported while in

another case Liu *et al.* (2008) also showed that upon subjecting Thailand coals to biodesulphurization treatment, much lower organic sulphur removal efficiency in the range 2.6 –25.4% was achieved. The higher organic sulphur removal efficiency of 51.98% – 61.30% was noted by Dong-chen *et al.* (2009) demonstrating the biodesulphurization effect of *Thiobacillus ferrooxidans* on the organic sulphur. Therefore, the reduction of organic sulphur is complicated because of the lack of an accurate, direct instrument and reliable method of analysis.

5.2.6.3 Sulphide sulphur

The sulphide sulphur content of the initial coal sample A, coal sample B and coal sample C was reduced from 0.14 wt.%, 0.16 wt.% and 0.13 wt.% to 0.09 wt.%, 0.09 wt.% and 0.08 wt.% respectively translating to 35.8 – 43.8% range of biodesulphurization. When the temperature was increased, there was no appreciable change on sulphide sulphur removal efficiency found. It is interesting to note that beyond 0.08 – 0.09 wt.% range, no further reduction of sulphide sulphur was achieved by biodesulphurization treatment. Similarly, there was no reduction of sulphide sulphur content observed in the uninoculated 23 ± 3°C (control experiments).

5.2.6.4 Sulphate sulphur

The distribution of sulphate sulphur (SO_4^{2-}, denoted as S+6) in Waterberg steam coal studied is very low and in a lesser amount in comparison to other forms of sulphur. Inversely, biodesulphurization treatment of a sulphate sulphur content of the coal sample A, coal sample B and coal sample C of 0.03 wt.% resulted in no appreciable change implying that none of the sulphur forms got oxidized to sulphate sulphur. Although the results of sulphate sulphur reduction by biodesulphurization treatment were not as good as expected, sulphate sulphur concentration levels are not of much threat to the environment since smaller amounts of 0.03 wt.% been diluted by many other forms of sulphur, hence, the lack of accessibility of sulphate sulphur by bacterial consortium. This is consistent with previous physiological observations by Imachi *et al.* (2002) who showed that these microorganisms could not utilize sulphate sulphur as an electron acceptor. In addition, most sulphate minerals are converted into coal fly ash during coal combustion (Mketo *et al.*, 2018). This result is in agreement with a point conceded by Ge *et al.* (2017) where the sulphate sulphur of all the treated coals under their investigation remained unchanged during biodesulphurization treatment.

Table 5.2: Sulphur forms in coal samples and its distribution in pre and post biodesulphurization coal samples for inoculated (23 ± 3 °C) (wt.%, db)

Forms of Sulphur	Coal A	Coal B	Coal C	Coal A	Coal B	Coal C
	Pre – Treatment			Post – Treatment		
Sulphide sulphur	0.14	0.16	0.13	0.09	0.09	0.08
Organic sulphur	0.56	0.64	0.49	0.34	0.37	0.24
Pyritic sulphur	0.64	0.66	0.51	0.19	0.24	0.16
Sulphate sulphur	0.03	0.03	0.02	0.03	0.03	0.03
Total Sulphur	1.37	1.49	1.15	0.65	0.73	0.51

Table 5.3: Sulphur forms in coal samples and its distribution in pre and post biodesulphurization coal samples for uninoculated (30 ± 2 °C) (wt.%, db)

Forms of Sulphur	Coal A	Coal B	Coal C	Coal A	Coal B	Coal C
	Pre – Treatment			Post – Treatment		
Sulphide sulphur	0.15	0.16	0.15	0.09	0.09	0.06
Organic sulphur	0.60	0.60	0.60	0.34	0.37	0.20
Pyritic sulphur	0.62	0.62	0.62	0.20	0.24	0.12
Sulphate sulphur	0.03	0.03	0.03	0.03	0.03	0.02
Total Sulphur	1.40	1.40	1.40	0.66	0.73	0.40

Table 5.4: Sulphur forms in coal samples and its distribution in pre and post biodesulphurization coal samples for uninoculated (23 ± 3 °C) (wt.%, db)

Forms of Sulphur	Coal A	Coal B	Coal C	Coal A	Coal B	Coal C
	Pre – Treatment			Post – Treatment		
Sulphide sulphur	0.15	0.16	0.16	0.11	0.13	0.14
Organic sulphur	0.61	0.61	0.62	0.44	0.44	0.55
Pyritic sulphur	0.64	0.63	0.63	0.45	0.51	0.63
Sulphate sulphur	0.03	0.03	0.02	0.03	0.02	0.03
Total Sulphur	1.43	1.43	1.43	1.03	1.10	1.35

5.2.7 The effect of sulphur forms on microbial desulphurization treatment

A correlation between distributions of sulphur forms in untreated and treated coal samples by desulphurization process is reported in Table 5.5. It can be observed that sulphur forms in Waterberg coals reduced after biodesulphurization treatment. A mathematical expression based on the total sulphur for each sulphur form was developed to establish the effect of biodesulphurization of thermal power plant coal is shown in Eq. 5.11:

$$Y = zS_T + c \qquad (5.\ 11)$$

where, Y = form of sulphur, z = distribution factor/ gradient, S_T = total sulphur, c = constant

Table 5.5: The relationship between sulphur forms in pre- and post-treated Waterberg steam coal

Forms of Sulphur	Formula	Formula
	Pre – Treatment	Post – Treatment
Sulphide sulphur	$S_{IN} = 0.11 \times S_T$	$S_{IN} = 0.14 \times S_T$
Organic sulphur	$S_{ORG} = 0.43 \times S_T$	$S_{ORG} = 0.50 \times S_T$
Pyritic sulphur	$S_{PRY} = 0.44 \times S_T$	$S_{PRY} = 0.311 \times S_T$
Sulphate sulphur	$S_S = 0.02 \times S_T$	$S_S = 0.05 \times S_T$

S_{IN} = Sulphide/mineral sulphur; S_{PYR} = Pyritic sulphur, S_S = Sulphate sulphur (SS), S_{ORG} = Organic sulphur, S_T = Total sulphur;

The substantial variations are reflected in the increase of the proportions, *m* of sulphide sulphur, organic sulphur and sulphate sulphur. The increase of the proportions, *m* can be twofold: decomposition of pyritic sulphur during desulphurization resulted in forming sulphide sulphur and conversion of the sulphide sulphur into organic sulphur. The relationship between the distribution of sulphur forms in pre- and post-treated Waterberg steam coal indicated the reliability of the data.

5.2.8 Desulphurization mechanisms

Knowledge of bacterial cell attachment mechanisms in the coal desulphurization may lead to improving the rate of sulphur reduction. According to Prasassarakich and Thaweesri (1996), the biodesulphurization mechanism of any sulphur form requires physical contact between sulphur form particles in the coal samples and microbial solution. In summary, during the oxidation of sulphur in coal slurry, the following two steps take place: (I) Transfer of microbes media through coal pores and cracks and (II) Chemical reaction. This model is based on different rate-controlling steps in the overall desulphurization mechanism.

5.2.8.1. Transfer of microbes media through coal pores and cracks

The size of the coal particle is much larger than the size of the microbes, therefore, the surface of the coal particle can be considered as a spherical in comparison to the microbes (Vijayalakshmi and Raichur, 2003). Fig. 5.16 depicts the schematic diagram showing microbes going through coal cracks to access A: Pyritic sulphur, B: Sulphide, C: Sulphate, and D: Organic Sulphur. It is evident from Fig. 5.16 that the order in which the microbes access the sulphur forms in the coal is a function of their distribution in the parent coal. As already mentioned, the biodesulphurization mechanism of any sulphur form in the total Sulphur requires physical contact between sulphur form particles in the coal samples and microbial solution (Olson, 1994). According to Rossi (1993), the microbes – coal particle attachment normally takes place in specific locations in the coal particle such as voids, cracks and defects. The CSTR accelerated the bacterial solution through voids, cracks and defects, exposed the coal particle core with a microbial solution and then escalate desulphurization kinetics. It must be noted that bacteria – coal particle attachment is not only a function of the Sulphur form surface properties but also of the nutrient medium composition in the bioreactor (Kargi and Robinson, 1986).

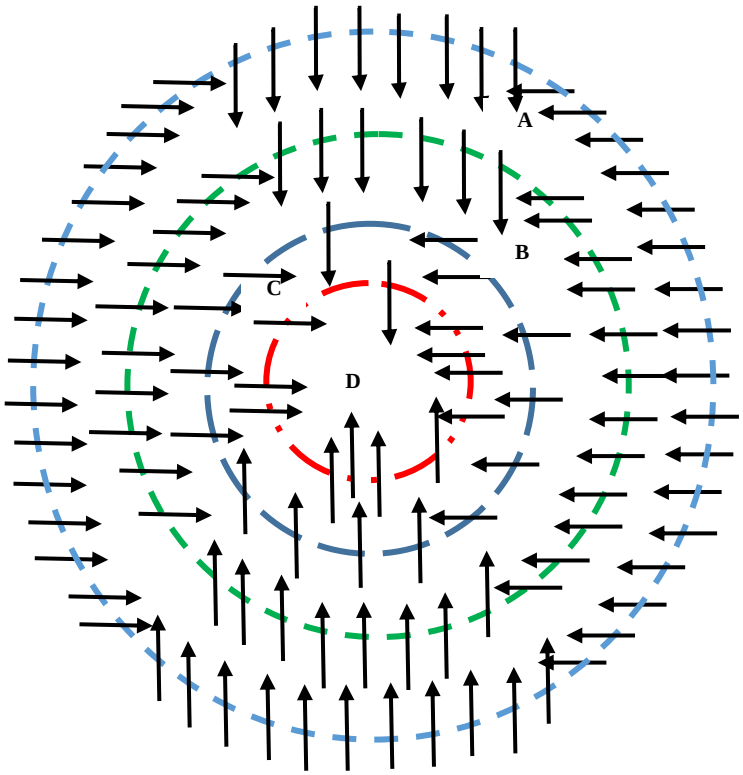

Figure 5.16: Schematic diagram showing bacteria going though coal cracks to access A: Pyritic sulphur, B: Sulphide, C: Sulphate, and D: Organic Sulphur

5.2.8.2 Chemical reaction control

Generally, sulphur occurs with three oxidation states of −2 (sulphide and reduced organic sulphur), 0 (elemental sulphur) and +6 (sulphate) being the most significant in nature (Tang et al., 2009). According to Tang et al. (2009), oxygen is a universal electron acceptor used by most sulphur containing oxidizers. The biodesulphurization mechanism of any sulphur form requires physical contact between sulphur form particles in the coal samples and microbial solution. In summary, during the oxidation of sulphur in coal slurry, the following two steps take place in electrons produced during the oxidation of sulphur forms are transferred to the dissolved oxygen supplied in the form of process air that results in dissolved oxygen giving rise to water formation. It is evident from Fig. 5.17 that the desulphurization mechanism consists of sulphur oxidation followed by microbial metabolisms. The breaking of C – C bond cleavage followed by C – S bond cleavage is regarded as an important precondition for initiating the desulphurization of coals. In the coal – microbial solution slurry state, it is much

easier for the electron transfer to interact with the sulphur forms compounds facilitated by microbial activity. In summary, the purpose of the oxidation stage for desulphurization treatment is to release the locked sulphur atoms present in the aromatic rings so that these sulphur forms are much more prone to attack by microbial culture. Release of S0 due to the breakdown of C – S bonds is possible in those sulphur- containing free electrons where the sulphur atom – containing the unshared electron is bonded to alkyl groups because in these species, the C – S bond dissociation energy (approximately 260 kJ/mol) is relatively lower than its aromatic analogues (Kerber, 1993). The following reactions (5.12 – 5.15) equations take into account forms of sulphur in the coal samples and its biocatalysis by bacteria consortium:

$$8e^- + SO_4^{2-} + 10H^+ \xrightarrow{\text{Bacteria}} H_2S + 4H_2O \quad (5.12)$$

$$6e^- + SO_3^{2-} + 8H^+ \xrightarrow{\text{Bacteria}} H_2S + 3H_2O \quad (5.13)$$

$$10e^- + S_2O_3^{2-} + 12H^+ \xrightarrow{\text{Bacteria}} 3H_2S + 3H_2O \quad (5.14)$$

$$6e^- + S^{2-} + 8H^+ \xrightarrow{\text{Bacteria}} H_2S + 3H_2O \quad (5.15)$$

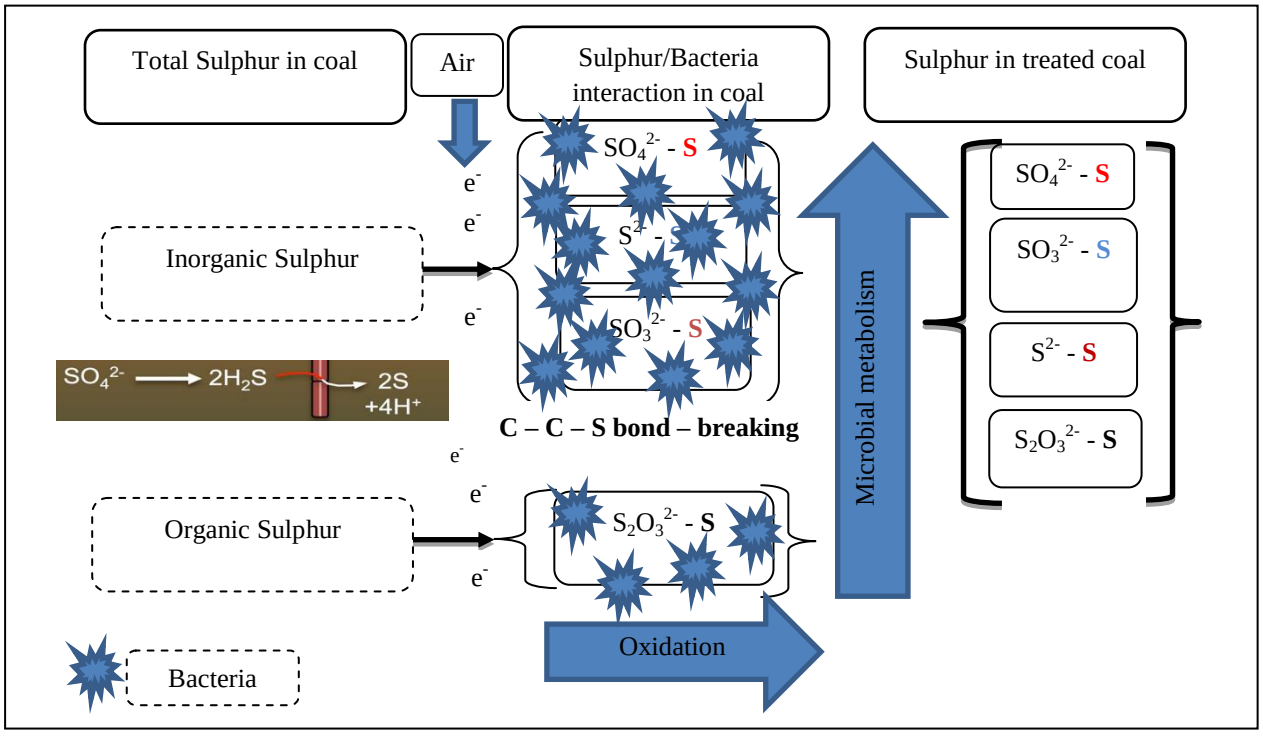

Figure 5.17: Biodesulphurization mechanism

5.2.9 Overall Process Efficiencies

To shed more light on the biodesulphurization treatment process performance, biodesulphurization efficiency, (η) was calculated based on total sulphur content using Eq. 5.16 and the results are recorded in as shown in Fig. 5.18 to Fig. 5.21 respectively:

$$\eta = \frac{(S_{\text{Untreated coal}} - S_{\text{Treated coal}})}{S_{\text{Untreated coal}}} \times 100 \qquad (5.16)$$

Where η is the biodesulphurization efficiency; $S_{\text{Untreated coal}}$ = the total sulphur, an ash content of untreated coal; $S_{\text{Treated coal}}$ = is the total sulphur, an ash content of treated coal.

Figs. 5.18 clearly shows overall process efficiency for –0.85 mm size, +1.00 mm size, +2.30 mm size and +4.6 mm size is 65.4%, 53.8%, 49.2% and 23.6% respectively. More importantly, the current study shows that an acceptable efficiency of 65.4% for total sulphur biodesulphurization from thermal power plant coal samples. Thus, biodesulphurization efficiency also increased with the decrease of coal particle size. Comparatively, previous work undertaken by Dong-chen *et al.* (2009) points out that total sulphur can reach biodesulphurization efficiency of 51.98% – 61.30% while Gonsalvesh *et al.* (2012) undertook biodesulphurization efficiency study of low – rank coals. This work showed that maximum removal of total sulphur of 57.8% could be achieved that really support the finding of the current study.

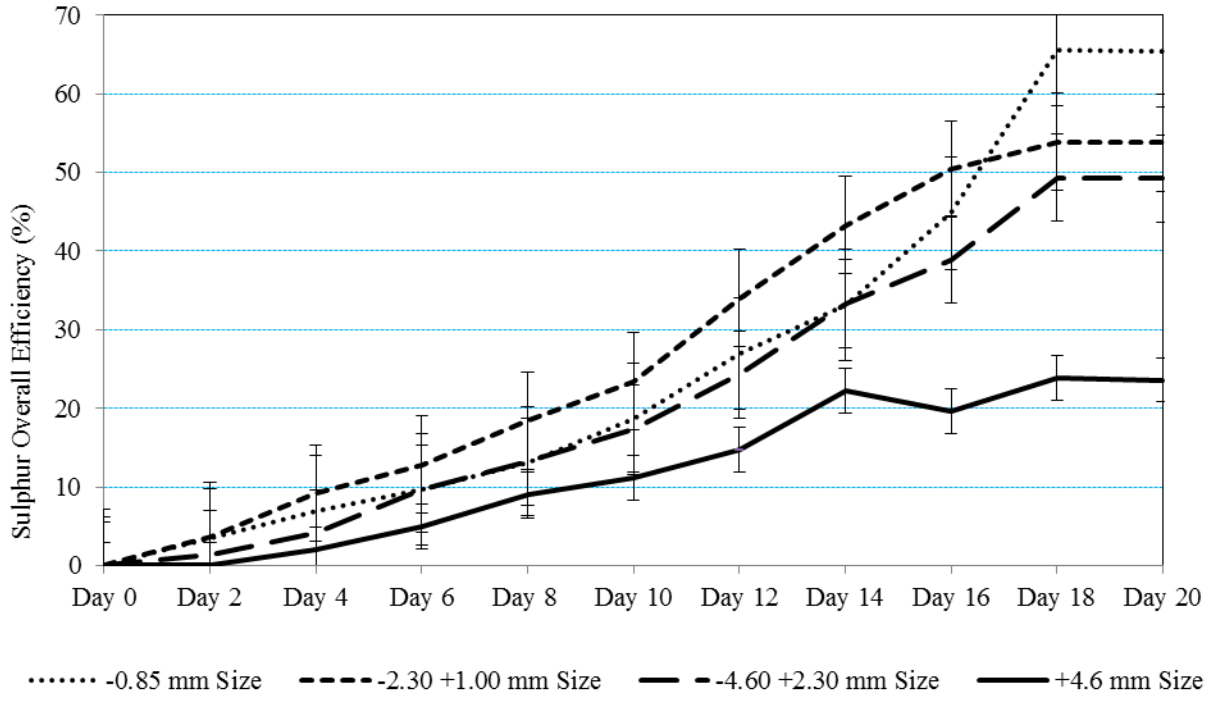

Figure 5.18: Sulphur overall efficiency at various reaction contact time for inoculated (23 ± 3 °C)

In comparison, Fig. 5.19 shows small process efficiency for –0.85 mm size, +1.00 mm size, +2.30 mm size and +4.6 mm size is 12.40%, 9.72%, 8.51% and 5.92% respectively. There was a minor reduction of total sulphur content to 1.29 wt.% observed in the uninoculated 23 ± 3°C (control experiments), which confirm the microbial action of microbes present in the coal.

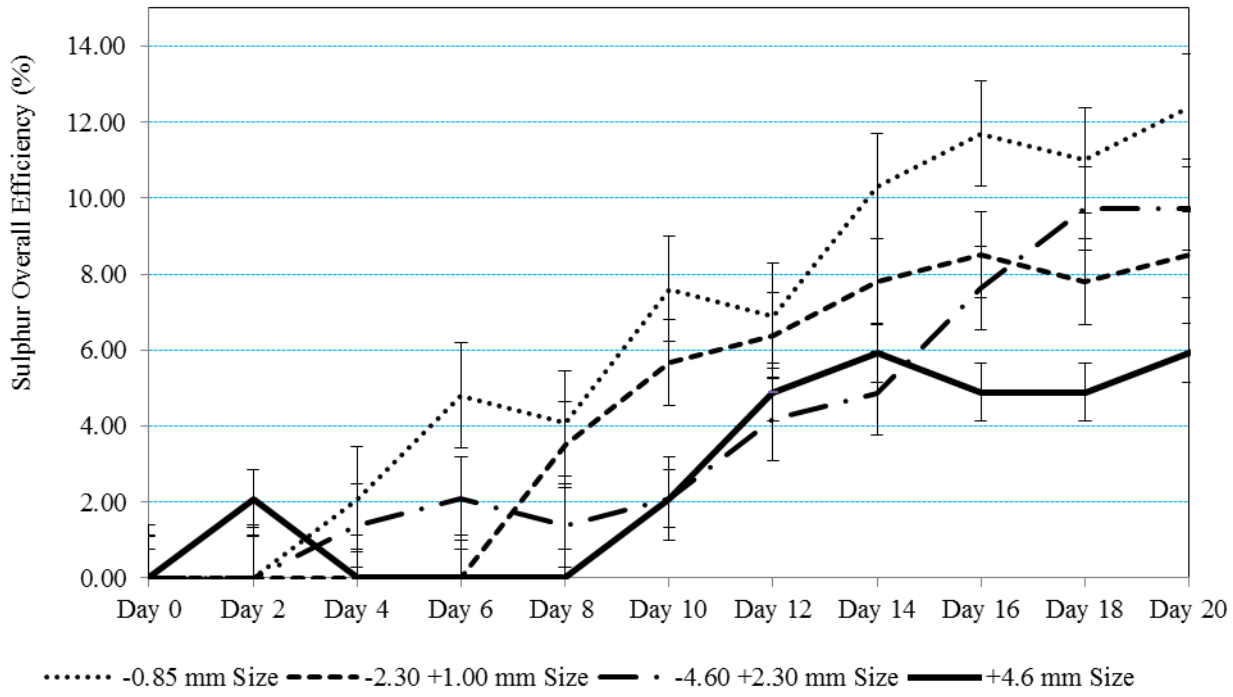

Figure 5.19: Sulphur overall efficiency at various reaction contact time for uninoculated (23 ± 3 °C)

Fig. 5.20 clearly shows an acceptable degree of sulphur content overall efficiency for – 0.85 mm size, +1.00 mm size, +2.30 mm size and +4.6 mm size is 72.4 %, 57.4 %, 54.2 % and 27.9% respectively. It was therefore clear that a minor reduction of total sulphur content of 1.29 wt.% was observed in the uninoculated 23 ± 3°C (control experiments), which confirm the microbial action of microbes present in the coal.

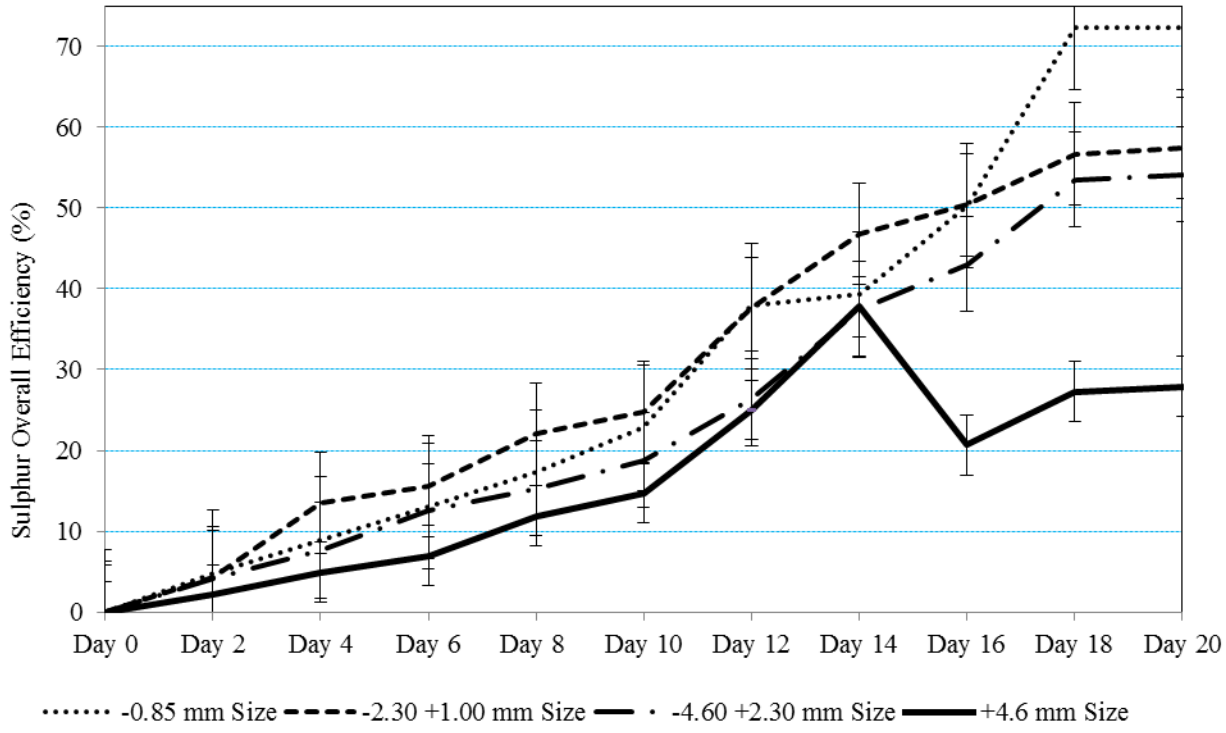

Figure 5.20: Sulphur overall efficiency at various reaction contact time for uninoculated (30 ± 2 °C)

Similar to sulphur content, biodeashing efficiency, (η) was calculated based on total ash content using Eq. 5.17 and the results are recorded in as shown in Fig. 5.21.

$$\eta = \frac{(A_{Untreated\ coal} - A_{Treated\ coal})}{A_{Untreated\ coal}} \qquad (5.17)$$

where η = the biodesulphurization efficiency; $A_{Untreated\ coal}$ = the ash content of untreated coal; $A_{Treated\ coal}$ = the ash content of treated coal.

Fig. 5.21 clearly shows ash content overall efficiency for – 0.85 mm size, +1.00 mm size, +2.30 mm size and +4.6 mm size is 30.6%, 26.2%, 22.5% and 17.96% respectively. This is quite an outstanding finding and is desirable.

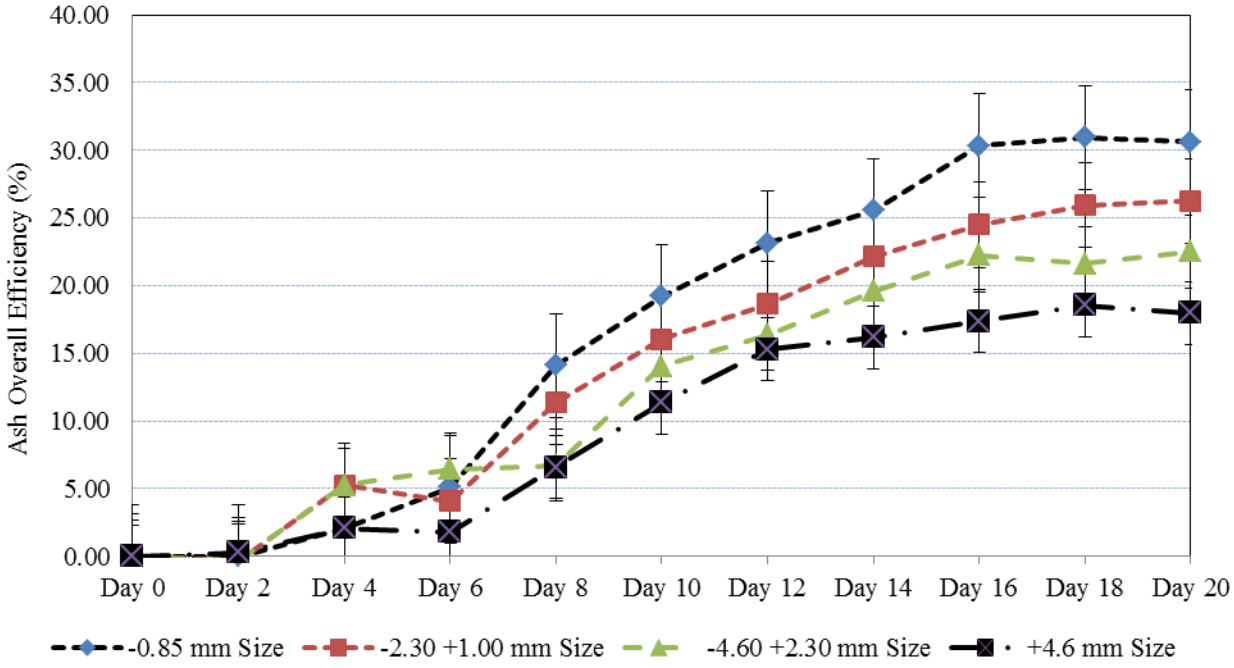

Figure 5.21: Ash overall efficiency at various reaction contact time

5.2.10 Variation of biomass concentration during microbial desulphurization

The use of different forms of sulphur content in coal as the preferred source for bacterial growth was monitored with time for different scenarios studied. Fig. 5.22 depicts the growth curves for inoculated (23 ± 3 °C), uninoculated (23 ± 3 °C), uninoculated (30 ± 2 °C) and sterilized coal. Generally, the bacteria's growth curve composed of four separate phases of growth including the lag phase, the exponential or log phase, the stationary phase, and the death or decline phase (Rolfe et al., 2012). The lag phase is an adaptation period, where the bacteria are adjusting to their new conditions and the lag phase's length can vary considerably depending on the microorganisms. In the current study, there was no lag phase as the condition that the bacteria came from did not differ, hence already acclimatized to the coal environment. It can be seen from Fig. 5.22 that the growth curves for inoculated (23 ± 3 °C) at Days 0 – 6, the bacterial population increased from 34 to 45 (viable cells/mL) due to more essential nutrients and enough space. The bacteria reached the stationary phase after Day 6th and lasted until Day 14th. At a stationary phase, the number of new cells being produced is equal to the number of cells dying off as such growth has entirely ceased. The bacteria concentration in the reactor started decreasing considerably from Day 14th to Day 20th due to low essential nutrient content reduction and an inhibitory by-product of sulphur oxides content concentrations. At the end of Day 14th, the death or decline phase start until Day 20th

where the number of viable cells decreases from 45 to 28 viable cells/mL in an exponential way. The steepness shape of the slope corresponds to how fast these bacterial are losing viability. Similarly, uninoculated (23 ± 3 °C) enters the exponential growth phase immediately after Day 0 until Day 8th at 28 viable cells/mL. It was found that the stationary phase lasted between Day 8th and Day 14th followed by death phase starting just after Day 14th at 28 viable cells/mL decreasing to 12 viable cells/mL. Furthermore, uninoculated (30 ± 2 °C) enters the exponential growth phase immediately after Day 0 until Day 8th at 38 viable cells/mL. The observed growth was faster for uninoculated (30 ± 2 °C) mainly because coal samples were treated at the same condition as the culturing condition. It was found that the stationary phase lasted between Day 8th and Day 14th followed by death phase starting just after Day 14th at 40 viable cells/mL decreasing to 23 viable cells/mL. The sterilized coal (control) was also considered in order to assess that indeed the bacterial consortium was derived from the coal. It can be observed from Fig. 5.22 that no viable cells were detected. The difference between sterilized and unsterilized microbial consortium is mainly due to more microbial population coming out for un-sterilized coal sample. Therefore, working with unsterilized coal seems more suitable due to the need to ease the study on an industrial scale.

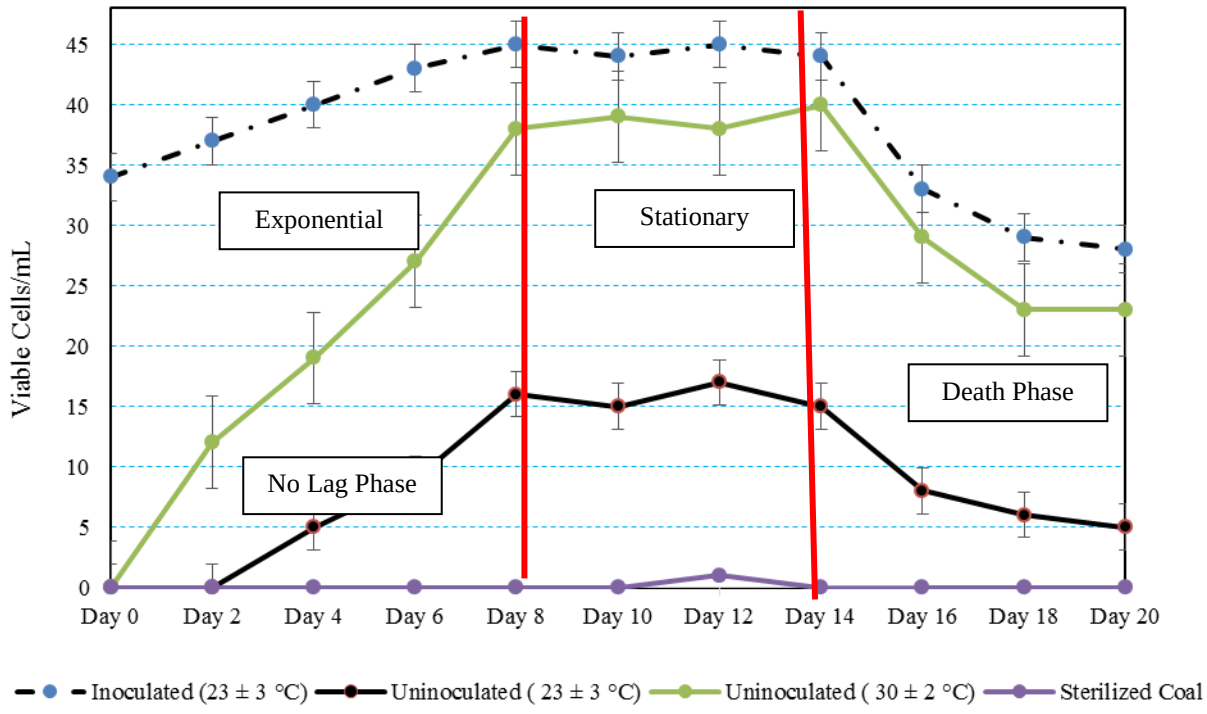

Figure 5.22: Growth curves for variation of biomass concentration

The difference between sterilized and unsterilized microbial consortium is mainly due to more microbial population coming out for un- sterilized coal sample. Therefore, working with unsterilized coal seems more suitable due to the need to ease the study on an industrial scale that appears to in the future.

5.2.11 Bacterial identification

During the desulphurization treatment process, the microbial community were monitored substantially from day 0 to day 20th. At the end of desulphurization treatment, microorganism's comparisons were completed over the 20 days period. Fig. 5.23 shows purification of the most dominant colonies and to better understand the microbial community after day 20, phylogenetic trees of isolates culture were constructed based on the results of the Blast search of the GenBank (NCBI) as shown in Fig. 5.24. Only seven dominant microbial communities were visible in the phylogenetic trees mapped to major genera. These seven isolates represented in the Table 5.6 and phylogenetic tree by A – G are known as *Pseudomonas sp, Pseudomonas aeruginosa, Pseudomonas putida; Pseudomonas stutzeri, Bacillus sp., Pseudomonas rhizosphaerae and Pseudomonas alcaligenes*. *Pseudomonas sp* have the ability to reduce sulphur but can also use oxygen and other terminal electron acceptors. According to Liu *et al.* (2017), *Pseudomonas putida* is reported for the ability to reduce pyritic sulphur and organic sulphur from the lignite coals. According to Gonsalvesh *et al.* (2012), *pseudomonas putida* bacterium is an effective microbial culture capable to decrease coal organic sulphur. *Pseudomonas sp*. is reported to have a capacity of removing sulphur from coal by Guo *et al.* (2014). The works of Klein et al. (1994) have reported oxidative desulphurization of benzylmethylsulphide by *Pseudomonas aeruginos*a. According to Klein *et al*. (1994), several *pseudomonas species* have been isolated and used for the removal of organic sulphur from oil. Some of these organisms (e.g. *Pseudomonas alcaligenes)* were reported for the first time in sulphur content reduction. In short, these groups of seven microbes identified function at a near room temperature range of 23 – 30 °C and are capable of oxidizing reduced sulphur species including SO_4^{2-}, SO_3^{2-}, $S^{2-}$and $S_2O_3^{2-}$.

Figure 5.23: Colony morphologies present on a typical plates

Table 5.6: Characterization of bacteria culture using 16S rRNA fingerprint

Result	Query Cover (%)	Inoculated (23 ± 3 °C)	Uninoculated (23 ± 3 °C)	Uninoculated (30 ± 2 °C)
A.*Pseudomonas putida*	100	X	X	X
B.*Pseudomonas aeruginosa*	100	X	X	X
C.*Pseudomonas sp.*	99	X	X	X
D.Pseudomonas stutzeri	99	X	N	X
E .*Pseudomonas rhizosphaerae*	99	X	X	N
F. *Pseudomonas alcaligenes*	99	X	N	X
G. *Bacillus sp.*	98	X	X	N

X = Present, N = Not found

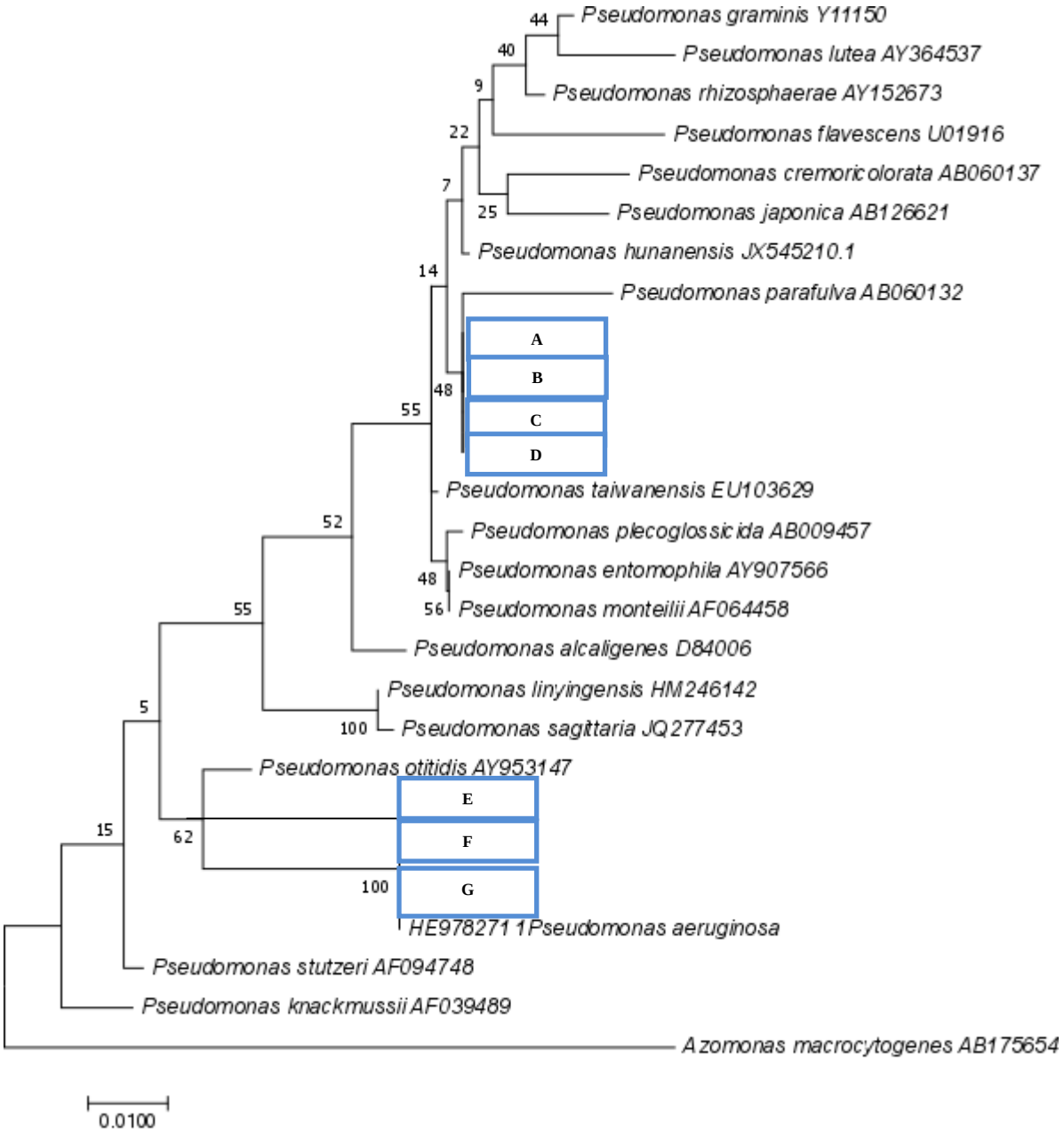

Figure 5.24: phylogenetic tree mapped to major genera

5.2.12 The effect of microbial desulphurization treatment on coal ash oxide

Coal ash oxide is a function of basic and acidic oxides and is as expressed in Eq.5.18.

$$\text{Ash Oxide} = f\sum(\text{Basic compounds; Acidic compounds})\text{oxides} \quad (5.18)$$

Table 5.7 shows ash oxide analysis of pre – and post– biodesulphurization treatment of coal samples. The sum of ash oxides approximates to 100% and analytical errors of these oxides are found to be statistically insignificant. The most important changes in ash oxide are that basic compounds or water-soluble structures (viz. Na_2O, MgO and CaO) reduced after biodesulphurization treatment while basic compounds or less soluble structure (SiO_2, Al_2O_3, Fe_2O_3, TiO_2, P_2O_5 and K_2O) increased. In addition, the significant increase in P_2O_5 occurring during combustion is less desirable especially given that phosphorus is detrimental to boiler equipment. The extent of changes in water-soluble structures and less soluble structure are shown in Table 5.7. Reduction in basic compounds can be due to the decomposition of hydrocarbon chains of coal structure because of an acidic media generated during the biodesulphurization treatment process. Furthermore, the increase can be explained by the decrease in the ash content. However, for trace oxides such as MnO, there was insignificant change because of the desulphurization treatment process. Similar findings have been reported by Şenera et al. (2018) who mentioned a reduction in water-soluble structures and increase on less – soluble structures due to desulphurization treatment.

Table 5.7: Ash oxide analyses of pre – and post –biodesulphurization treatment (wt.%.db)

Condition	Sample	SiO_2	Al_2O_3	Fe_2O_3	TiO_2	P_2O_5	CaO	MgO	Na_2O	K_2O	SO_3	MnO
Before Desulphurization	Sample 1	57.5	27.6	4.00	1.20	0.40	5.44	2.60	0.20	0.90	1.30	0.03
	Sample 2	57.6	27.8	4.00	1.30	0.38	5.40	1.10	0.50	1.10	1.80	0.02
	Sample 3	57.4	27.7	4.70	1.30	0.50	5.20	0.90	0.20	0.80	1.40	0.02
After Desulphurization	Sample 1	58.9	29.4	5.16	2.04	0.81	2.60	0.83	0.12	1.08	0.80	0.03
	Sample 2	58.1	29.7	5.19	2.08	0.80	2.38	0.88	0.13	1.13	0.84	0.02
	Sample 3	58.6	29.5	5.14	2.10	0.90	2.69	0.78	0.15	1.11	0.82	0.02

Phosphorus, essential to plant life, is an intrinsic mineral in coal, which cannot be easily removed by beneficiation. South African coals contain varying concentrations of phosphorus, which can have a number of detrimental effects on downstream usage, and the phosphorus content is one of the important specifications in terms of coal quality used in the metallurgical industry (Hancox and Götz, 2014). Hancox and Götz (2014) were also able to observe a low phosphorous results (less than 0.010%) coals which is suitable for the metallurgical industry occur in the Witbank, Ermelo, Klip River, Utrecht, Nongoma, Sonkhele, Waterberg, Soutpansburg, Limpopo coalfields and Kangwane coalfield.

5.2.13 The effect of microbial desulphurization on petrographic study

The science of coal petrography and coal petrology has evolved over the years, particularly post-World War II, to the extent that coal organic constituents, called macerals, are reasonably well known for their properties. Initially, the properties of macerals in cokemaking for the steel industry were the prime focus of investigation, and this was later followed by the study of their combustion characteristics. There are three main coal group macerals, namely vitrinite, liptinite and inertinite –Table 5.8 reports the maceral and mineral group composition of the coal samples studied. Inertinite is the dominant maceral (up to 47.8 vol.%), whereas vitrinite and liptinite occurred in lesser proportions. Some variation as expected between the different coal size fractions feed and product may be related to the heterogeneous nature of coal and the way the coal was sampled and prepared through all steps. However, the variations are within the error of repeatability. These results appear to be in good agreement with previous work undertaken by various authors (Hagelskamp and Snyman, 1988; Kruszewska, 1989) who reported that South Africa Gondwana coals are naturally enriched in inertinite. A correlation exists between coal petrographic properties and steam output, the flame shape and stability, an amount of unburnt carbon and thermographic data and combustion efficiency. According to Cloke et al. (2002), inertinite maceral group have often been affiliated with burnout problems. On the other hand, vitrinite has been reported to burn readily, although the rate of burnout decrease as its reflectance increases (Cloke et al., 2002). Falcon and Ham (1988) recognized a considerable variation in the petrography of coals within the Waterberg Coalfield. For example, the coals of the Grootegeluk Formation have been reported by Faure et al. (1996) and separately by Dreyer (2006) to be higher in vitrinite (especially near the top of the sequence) and are very high in mineral matter. According to these authors, the vitrinite reflectance of the Gootegeluk

Formation is 0.72% (mean random) which correspond to the Medium Rank C bituminous coal following the ECE-UN in seam coal classification system. According to Dreyer (2006), this Permian Coalfield typically contains high vitrinite, high ash coals in the Kungurian Grootegeluk Formation and high inertinite as opposed to low ash coals in the Artinskian Vryheid Formation. However, given the high degree of variability exhibited by the major maceral differences in the Grootegeluk Formation, the amount of vitrinite and inertinite macerals and their discrepancy appears to be based on a manifestation of different degrees of maceral group degradation. According to Falcon and Ham (1988), this variation tied to changing climatic, tectonic and sedimentary settings with time.

XRD results show that quartz is the feed is in the range of 17.1 – 19.8 and it was not impacted by biodesulphurization treatment as shown in the product samples. According to Faure et al. (1996), the average grain size of quartz improves toward the top of the formation, where the grains are silt size on average. Similar to quartz, carbonates results are also scattered everywhere in both the feed and products coal samples and there was an insignificant effect of the biodesulphurization treatment. It is important to note that according to Faure et al. (1996), four types of carbonites are present in the Waterberg Coalfield. The finer fraction reported a higher proportion of clays, as expected. Some secondary mineralization was observed, typical of weathered coal.

Questions to address in this section included: Does pyrite occur in all macerals groups? Did the desulphurization process reduce syngenetic and/or epigenetic pyrite? Lastly, did the original particle size have an impact on pyrite reduction? The mode of occurrence of pyrite (epigenetic or syngenetic) was determined microscopically to provide information regarding whether pyrite is present and in which maceral groups. Results show that pyrite was observed in vitrinite and inertinite, both syngenetically and epigenetically. However, the pyrite content differed significantly between the feed and product samples, with the product reporting significantly lower amounts of pyrite. This observation confirms the effectiveness of the biodesulphurization treatment on the total sulphur content reduction.

Table 5.8: Maceral Group Analyses (Vol.%)

Maceral Group	−0.85 mm Feed	−0.85 mm Product	−2.30 +1.00 mm Feed	−2.30 +1.00 mm Product	−4.60 +2.30 mm Feed	−4.60 +2.30 mm Product	+4.60 mm Feed	+4.60 mm Product
Vitrinite	20.4	18.7	19.8	15.1	24.4	21.7	21.9	20.6
Liptinite	1.8	2.4	2.4	4.4	4.3	3.3	3.8	3.8
Inertinite	34.3	39.9	46.2	43.8	40.9	43.3	47.8	44.8
Mineral Group								
Clays	16.3	11.1	2.7	9.4	8.7	7.6	5.8	8.3
Quartz	19.8	20.9	7.1	20.5	18.7	18.4	17.3	18.9
Carbonate	3.9	3.9	4.2	4.0	4.4	4.1	4.6	4.4
Pyrite	2.6	0.4	2.6	0.6	2.6	1.2	2.6	1.8
Other Minerals	1.8	1.2	0.2	0.8	0.4	0.4	0.2	0.4

5.2.14 The effect of microbial desulphurization on maceral distribution

Table 5.9 shows macerals distribution in the feed and products at various particle size distributions. Pyrite occurred in vitrinite and inertinite macerals, in syngetetic and epigenetic structures. Vitrinite consists of telinite (4.1%), collotelinite (69.6%), collodetrinite (16.4%), corpogelinite (4.1%) and pseudovitrinite (6.1%). O'Keefe et al. (2013) support the vitrinite categorization results found in the current study. Liptinite consists of sporinite (100%). O'Keefe *et al.* (2013) established that liptinite macerals include sporinite, composed of plant spores, pollen and cutinite. Furthermore, liptinite composed of plant cuticles, uticular layers and resinite. Inertinite consists of fusinite (13.5%), reactive semifusinite (0.5%), inert semifusinite (35.4%), micrinite (1.9%), secretinite (0.5%), inertodetrinite I (5.6%) and inertodetrinite I (42.9%). Roberts (1988) who provided atlas for categorization of inertinite macerals support the latter results. According to Roberts (1988), the inertinite maceral group includes semifusinite, fusinite (pyrofusinite, degradofusinite, rank, and primary fusinite), funginite (including hyphae and mycelia; part of what was previously named sclerotinite), secretinite (part of what was previously named sclerotinite), macrinite, micrinite, and inertodetrinite. In another case, Hower *et al.* (2012) provide an overview of the inertinite pathway as follows: fusinite, semifusinite, secretinite and inertodetrinite; funginite, macrinite, secretinite and micrinite. Fig. 5.25 depicts petrographic plates of Waterberg coal samples.

Table 5.9: Macerals distribution

		Feed (inc.mm) (vol.%)	−0.85 mm (inc.mm) (vol.%)	−2.30 +1.00 mm (inc.mm) (vol.%)	−4.60 +2.30 mm (inc.mm) (vol.%)	+4.60 mm (inc.mm) (vol.%)
Vitrinite	Telinite	1.0	0.8	0.6	0.9	0.8
	Collotelinite	14.2	13.0	10.5	15.1	14.3
	Collodetrinite	3.3	3.1	2.5	3.5	3.4
	Corpogelinite	0.8	0.8	0.6	0.9	0.8
	Pseudovitrinite	1.2	1.1	0.9	1.3	1.3
Liptinite	Sporinite	1.8	2.4	4.4	3.3	3.8
Inertinite	Fusinite	4.6	5.4	5.9	5.8	6.0
	Reactive semifusinite	0.2	0.2	0.2	0.2	0.2
	Inert semifusinite	12.1	14.1	15.5	15.3	15.8
	Micrinite	0.6	0.7	0.8	0.8	0.8
	Secretinite	0.2	0.2	0.2	0.2	0.2
	Inertodetrinite I	1.9	2.2	2.4	2.4	2.5
	Inertodetrinite I	14.7	17.1	18.7	18.5	19.2

inc. mm = including mineral matter

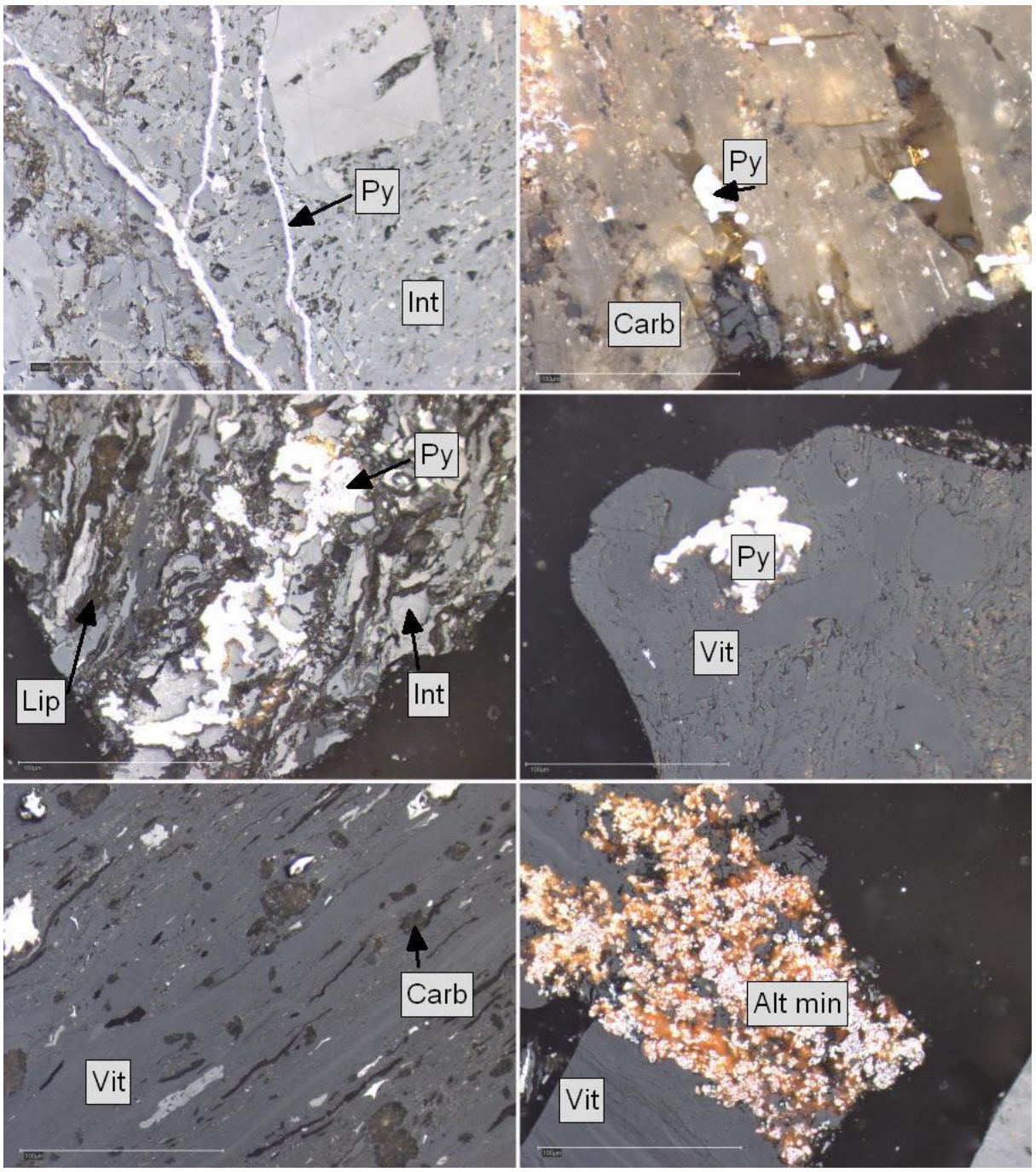

Vit = vitrinite; Int = inertinite; Py = pyrite; Lip = Liptinite; Carb = carbonates; Alt min = alteration, or secondary mineralization

Figure 5.25: Petrographic plates of Waterberg coal samples

5.2.15 The effect of microbial desulphurization treatment on SO_2 emissions

The data on SO_2 emissions are important for analyzing and understanding three important environmental problems: local air pollution and smog, acid rain and dry deposition as well as global climate change (Stern, 2005). In this section, the effect of coal biodesulphurization treatment on SO_2 emissions is presented in this section. Waterberg steam coal contains quite a large amount of sulphur and upon combustion, it leads to total sulphur dioxide (SO_2) emissions as per the following reactions 5.19 to 5.22:

$$\text{Organic Sulphur} + O_2 \rightarrow SO_2 \quad (5.19)$$

$$\text{Sulphide} + O_2 \rightarrow \text{Oxides} + SO_2 \quad (5.20)$$

$$\text{Sulphate Sulphur} + \tfrac{1}{2}O_2 \rightarrow \text{Oxides} + SO_2 \quad (5.21)$$

$$\text{Pyritic Sulphur} + 2H^+ + O_2 \rightarrow Fe^{2+} + H_2S + SO_2 \quad (5.22)$$

The current minimum emission standards in South Africa limit SO_2 emissions to below 3500 mg/Nm^3 and will even be stricter to below 500 mg/Nm^3 in the future. Test results of the SO2 emissions presented in this section are not just a forecast but are based on observed data in the running power plant. These data used in this study comprised of average 2 daily interval concentrations of SO_2 emissions for the period 0 and 20th Days. To check the validity of the approach for estimating SO_2 emissions, the emissions calculation formulae were developed, compared with observed SO_2 emissions data in the running power plant for a specific period, verified and applied. Developed emissions formulae were used to predict SO_2 emissions over various particle sizes studied using Eqs. 5.23 – 5.26 and the results are as given in Figs. 5.26 – 5.29.

$$SO_2 = \left(\frac{m \times \left(\frac{S}{100} \times \frac{1000}{32.064} \right)}{(1000 \times 64.0628)} \right) \text{kg/kg Coal}_{\text{dry}} \quad (5.23)$$

where: m = coal burnt mass flow rate (kg/h), S = Sulphur content in the coal (wt.%)

$$SO_{2\ \text{Formed}} = \left(\frac{m \times \left(\frac{S}{100} \times \frac{1000}{32.064} \right)}{(1000 \times 22.4)} \right) \text{Sm}^3/\text{h} \quad (5.24)$$

$$SO_{2\ Emission} = \left(\frac{m \times SO_{2\,Formed} \times 10^6}{\left(\sum F(a,b,c...n) \right)} \right) \text{mg/Nm}^3 \quad (5.25)$$

where $\sum F(a,b,c...n)$ equals to the sum of Flue Gas products (in Sm^3/h)

$$SO_{2\ Emission} = \left(\frac{\text{SO}_{2\,\text{Emission}} \times (21-10)}{(21-6)} \right) \text{mg/Nm}^3 \text{ (At 10\% O}_2\text{)} \quad (5.26)$$

The effect of biodesulphurization on SO_2 emissions over −0.85 mm particle size are shown in Fig. 5.26. The bold black line shows the target limit of sulphur dioxide emissions. Taking the case of inoculated (23 ± 3 °C), it is clear from Fig. 5.26 that exceedances of the 3500

mg/Nm^3 limit to be 3716 mg/Nm^3 and 3533 mg/Nm^3 for Day 0 and Day 2 respectively. However, with the steady and rapid decrease in sulphur content on Day 4th, SO_2 emissions spikes decreased steadily until Day 18th at 1280 mg/Nm^3. A decrease in SO_2 emissions in Days 18 suggests that sulphur value is reduced and couldn't reduce further in Day 20th. Quite clearly, during the control stage (uninoculated, 23 ± 3 °C), the exceedance of the 3500 mg/Nm^3 limit was prolonged to Day 8th at 3502 mg/Nm^3 and then there was a slight decrease in SO_2 emission between Day 10th and 18th due to a small reduction of sulphur content in the coal samples. Considering the uninoculated (30 ± 2 °C), it is interesting to find that SO_2 emission exceedance level of 3716 mg/Nm^3 at Day 0th reduced gradually to 1024 mg/Nm^3 at Day 18th which is in proportion with the lowered sulphur content present in the coal samples achieved.

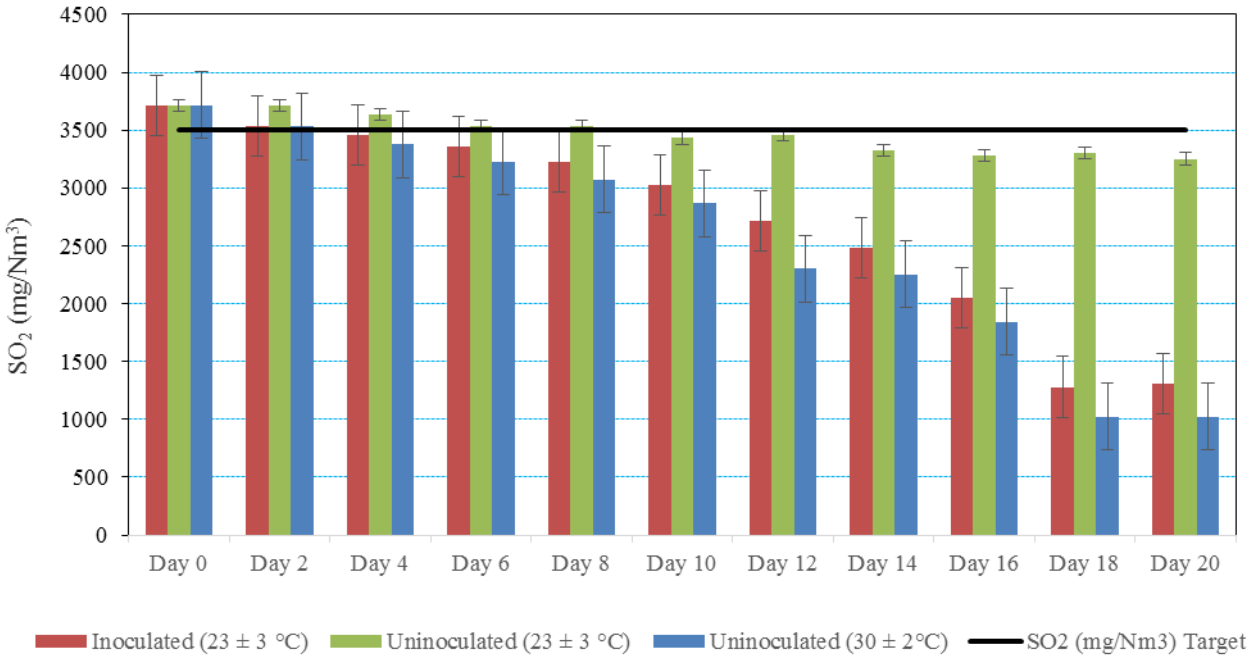

Figure 5.26: The effect of biodesulphurization on SO_2 emissions over −0.85 mm particle size

The effect of biodesulphurization on SO_2 emissions over −2.30 +1.00 mm particle size are shown in Fig. 5.27. Taking the case of inoculated (23 ± 3 °C), it is clear from Fig. 5.27 that exceedances of the 3500 mg/Nm^3 limit to be 3613 mg/Nm^3 and 3533 mg/Nm^3 for Day 0 and Day 2 respectively. Nevertheless, with the steady and rapid decrease in sulphur content on Day 4th, SO_2 emissions spikes decreased steadily until Day 18th at 1664 mg/Nm^3. Consequently, during the control stage (uninoculated, 23 ± 3 °C), the exceedance of the 3500 mg/Nm^3 limit was prolonged to Day 8th then there was a slight decrease in SO_2 emission between Day 10th and 18th mainly attributed to a small reduction of sulphur

content in the coal samples. Taking the case of an uninoculated (30 ± 2 °C), it is attractive to note that SO_2 emissions exceedance level of 3587 mg/Nm^3 at Day 0 gradually reduced to 1536 mg/Nm^3 at Day 18th was achieved which is in proportion with the lowered sulphur content present in the coal.

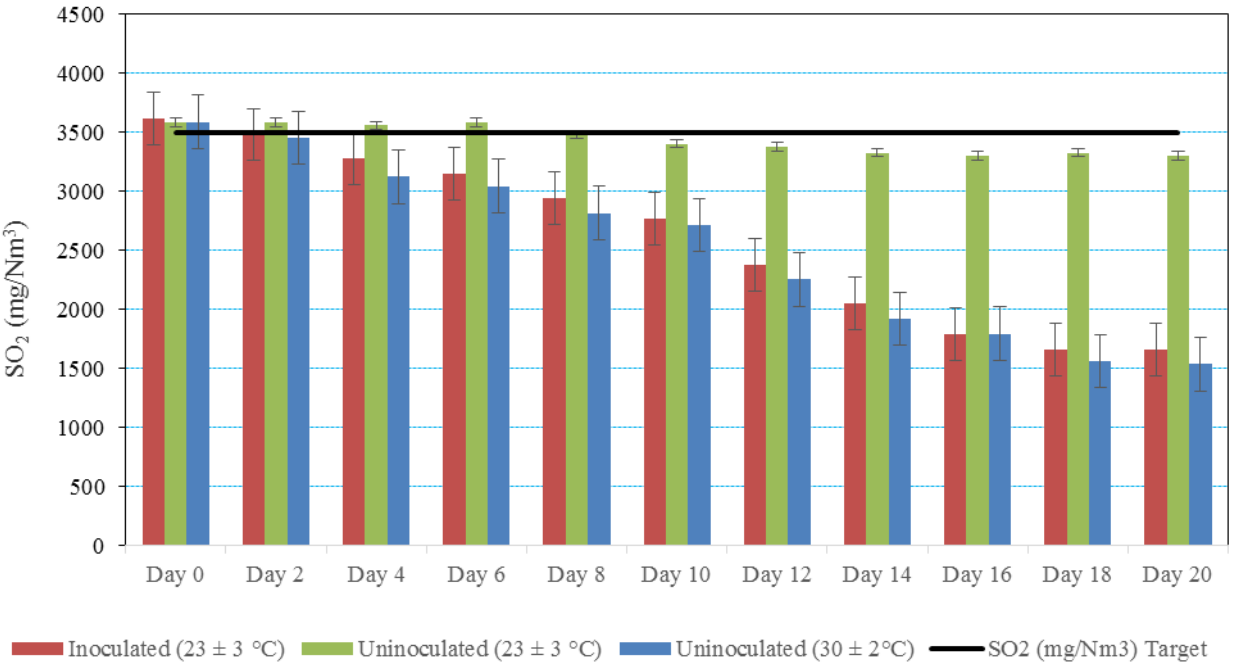

Figure 5.27: The effect of biodesulphurization on SO_2 emissions over −2.30 +1.00 mm particle size

The effect of biodesulphurization on SO_2 emissions over −4.60 +2.30 mm particle size are shown in Fig. 5.28. Taking the case of inoculated (23 ± 3 °C), it is clear from Fig. 5.28 that exceedances of the 3500 mg/Nm^3 limit to be 3690 mg/Nm^3, 3686 mg/Nm^3 and 3661 mg/Nm^3 for Day 0, Day 2 and Day 4 respectively. Nevertheless, after Day 6, a spike of SO_2 emissions reduces compatibly to 1868 mg/Nm^3 in line with sulphur content reduction. Consequently, during the control stage (uninoculated, 23 ± 3 °C), the exceedance of the 3500 mg/Nm^3 limit was prolonged to Day 12th then there was a slight decrease in SO_2 emission between Day 14th and 18th mainly attributed to a small reduction of sulphur content in the coal samples. Taking the case of an uninoculated (30 ± 2 °C), it is engaging to note that SO_2 emissions exceedance level of 3690 mg/Nm^3 at Day 0 gradually reduced to 1689 mg/Nm^3 at Day 18th was achieved which is in proportion with the lowered sulphur content present in the coal.

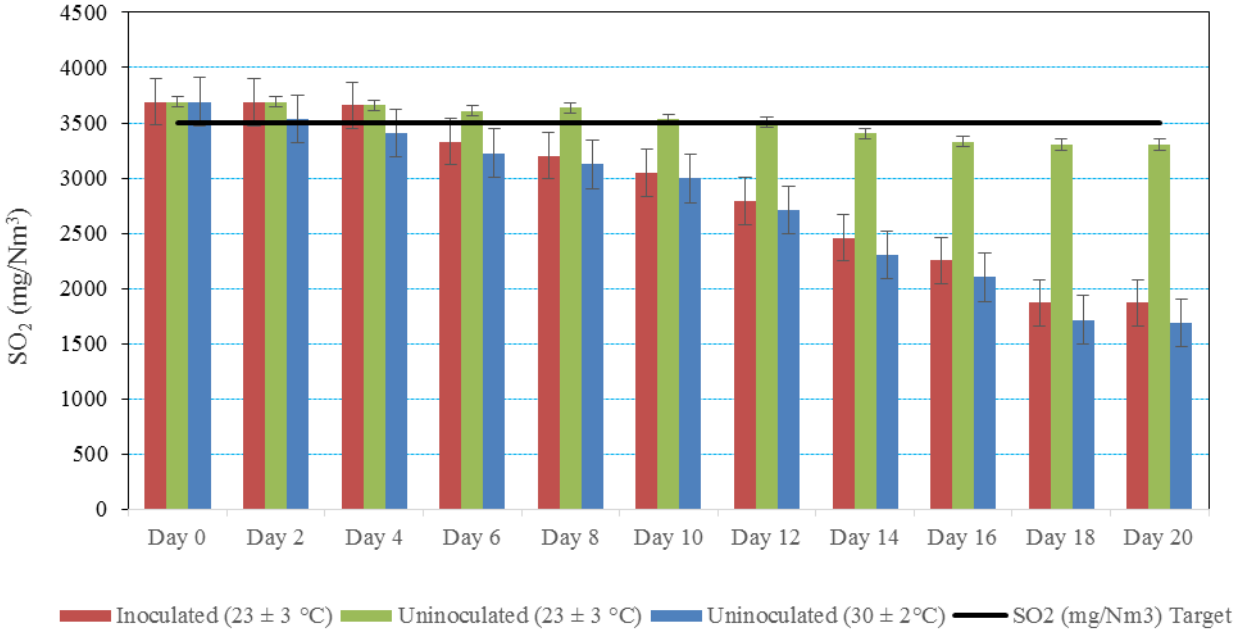

Figure 5.28: The effect of biodesulphurization on SO_2 emissions over −4.60 +2.30 mm particle size

The effect of biodesulphurization on SO_2 emissions over +4.60 mm particle size are shown in Fig. 5.29. Taking the case of inoculated (23 ± 3 °C), it is clear from Fig. 5. 29 that exceedances of the 3500 mg/Nm^3 limit to be 3664 mg/Nm^3, 3686 mg/Nm^3 and 3686 mg/Nm^3 for Day 0, Day 2 and Day 4 respectively. Nonetheless, after Day 6, a spike of SO_2 emissions reduces compatibly to 2790 mg/Nm^3 in line with sulphur content reduction. Consequently, during the control stage (uninoculated, 23 ± 3 °C), the exceedance of the 3500 mg/Nm^3 limit was prolonged to Day 12th then there was a slight decrease in SO_2 emission between Day 14th and 18th mainly attributed to a small reduction of sulphur content in the coal samples. Taking the case of an uninoculated (30 ± 2 °C), it is engaging to note that SO_2 emissions exceedance level of 3664 mg/Nm^3 at Day 0 gradually reduced to 2637 mg/Nm^3 at Day 18th was achieved which is in proportion with the lowered sulphur content present in the coal samples. In overall, there is a positive correlation between sulphur content in the coal and the corresponding SO_2 emission concentration. Therefore, coal with higher sulphur content leads to greater SO_2 emissions than coal with lower sulphur content. Hence, it is unquestionable that the tightened emissions standards for SO_2 emissions will strongly affect the demand for low-sulphur coal. It is expected to be so for combustion plants not equipped with FGD. Therefore, desulphurization of Waterberg steam coal using bacteria derived from coal as a pre-combustion technique in power plants that are reaching their end of life is a reasonable way to reduce SO_2 emissions to meet the environmental regulations.

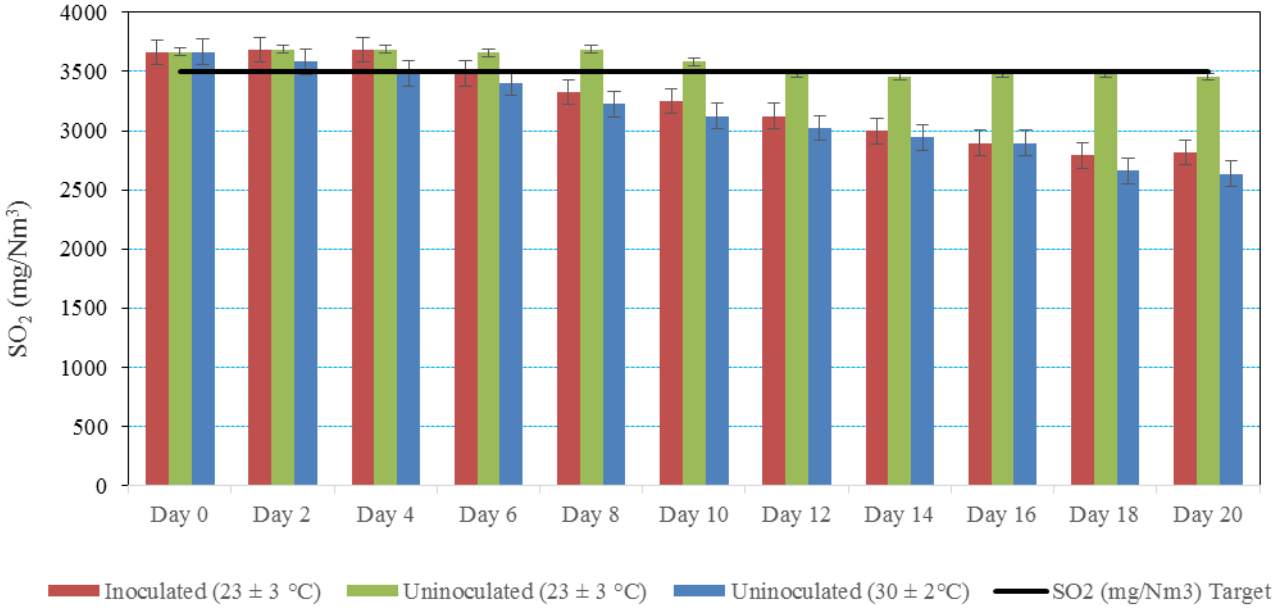

Figure 5.29: The effect of biodesulphurization on SO_2 emissions over +4.60 mm particle size

5.2.16 Processing plant sizing and operating challenges

The required size of the biodesulphurization processing plant takes into account about millions of tonnes of Waterberg coal being consumed on an annual basis per unit over the number of units per power station (For example, 1500 Tons × 6 = 9000 Tons/day), the 18 days that the successful biodesulphurization process took and the available coal of 2.1 Million Tons in the stockpile to be biodesulphurized. In summary, the processing plant will consist of 3 × Bacterial Reactor (600 kL) with associated pumps around the system, conveyor belt to each reactor and final product to the stockpile and 3 × filtration system per unit resulting in 4380 Ton production over 18 days period as shown in Fig. 5.30. The total cost equals to 6 × 1.9 Million USD = 11 Million USD. In comparisons with post – combustion technology like FGD, the requirement for bioreactors with reaction times of 18 days does not fit into the normal coal power generation industry's current operation. Therefore, biodesulphurization activities of the current coal – based bacteria are still too low for implementation on an industrial scale given the volume of tonnes of coal to be burnt but it would only be competitive with other advanced coal preparation treatments technologies if coal is stockpiled for months prior to combustion. Alternatively, biodesulphurization process could be conducted during coal preparation after coal mining other than on a product fraction obtain from coal processing product that is supplied to the power stations. However, for power stations that are almost at their end of life and to those running on reserves, biodesulphurization is competitive with a slightly lower sulphur content coal that has to be shipped from greater distances (Olson, 1994). Therefore, more research is required

along the lines of reducing the biodesulphurization duration by at least a quarter so that it can be competitive with other commercial technologies. Table 5.10 shows the business case assessment for desulphurized coal used in the current study.

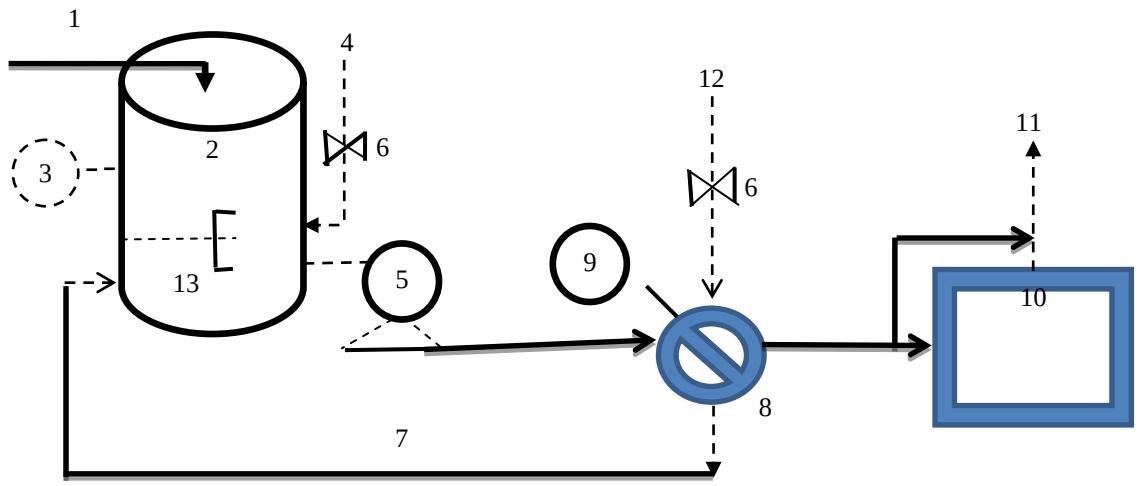

No	Description
1	Coal conveyor belt
2	Bacterial Reactor
3	Online pH Meter
4	Compressed Air
5	Pumps
6	Non-return valve
7	Recycled filtrate
8	Filter
9	Pressure Gauge
10	Drying Ovens
11	Conveyor belt to stockpile
12	Washing water
13	Stirrer

Figure 5.30: Schematic representation of the microbial desulphurization process

Table 5.10: Business case assessment for desulphurized coal

Description	Lab Unit	Processing Plant	Unit Requirements	Stockpile Volume
Reactor Volume	500 mL	18 × 600 kL	37 × 600 kL	-
Coal used	200 g	4, 380 Ton	1500 Tons/Unit	2.1 Million Tons
Bacterial consortium	250 mL	150, kL	37 × 75 kL	-
Days Stock	-	-	9 kTons/ Station	7.8 Months
Processing Days	20	20	-	-
Annual Running	365/20	18.25 Times	3 Million Tons	-
Annual production	18.25	79,935 Tons	-	-

5.2.17 Investment cost and operating cost

The biodesulphurization technology is not yet available for largescale industrial applications. However, for a more realistic investment and operating costs comparisons, the biodesulphurization technology systems were evaluated compared with other technologies that have reached full largescale application. The total cost of investment includes four aspects: equipment cost, operation and maintenance cost and well as project cost. The details of the investment costs can be described as per Eq. 5.26:

$$\text{Total cost} = \sum_{t=0}^{t=f}(I_i + O_c + M_i + I_e) \quad (5.26)$$

where:

I_i is the cost of the initial investment at t, in units of \$. O_c is the operation costs for t, in units of \$. M_i is the maintenance costs for t, in units of \$. F is the interest expenditures for t, in units of \$. Table 5.11 shows the estimated investment costs for microbial desulphurization technology per unit. In order to evaluate the plant cost, the price of each equipment has been firstly assessed assuming mild steel as construction material in order to withstand acidic solutions generated during the desulphurization process. The resulting cost has been subsequently multiplied with corrective factors taking into account the right material and operating conditions. The combined costs of each equipment provided the so – called purchased equipment with the addition of extra-costs of transportation. Therefore, the assessment of the annual fee is based on the Eq. 5.27:

$$\sum_{z=1}^{n} \frac{1}{(1+j)^z} \quad (5.27)$$

where: n: number of years of depreciation, j: discount rate, z: reference year.

A full economic cost-benefit analysis of biodesulphurization technique would require detailed information on alternative strategies and their associated costs of reducing SO_2 emissions. Table 5.12 shows the various desulphurization technologies capability and investment cost. Biodesulphurization process appears to come out cheaper than chemical desulphurization methods. Furthermore, its performance evaluation is competitive with sorbent injection technique. The finding is consistent with the view by Eligwe (1989) who highlighted that biodesulphurization is fairly cheaper than chemical desulphurization. Another alternative method to reduce SO_2 emission is by washing the coal prior to combustion (You and Xu, 2010). According to You and Xu (2010), this low investment and operating costs washing method could only reduce pyritic sulphur content by 40%. However, the water requirements, water pollution and associated drying issues are major concerns. Furthermore, the fact that one form of sulphur distribution is being targeted limits its application in cases where other forms of sulphur also occur in large proportion. Therefore, more scenarios analyses must be conducted to confirm if it is economically practical to implement and practice biodesulphurization technology at an industrial scale.

Table 5.11: Estimated investment costs for microbial desulphurization technology per unit

	No	Item Description	2019 Cost (USD)
I. Equipment	1.	Coal conveyor belt × 3	107, 985.00
	2.	Bacterial Reactor (600 kL) × 3	20, 040.00
	3.	Online pH Meter × 3	11, 835.00
	4.	Compressed Air	N/A
	5.	Pump × 6	85, 3194.00
	6.	Non-return valve × 6	5,922.00
	7.	Recycled Filtrate	N/A
	8.	Filter × 3	49, 093.00
	9.	Pressure Gauge × 6	2,448.00
	10.	Drying Oven × 3	49, 083.00
	11.	Conveyor belt to stockpile× 3	107,985.00
	12.	Washing water	N/A
	13.	Stirrer × 12	76,968.00
	14.	Piping Work	80,000.00
		Total I	**284,543.00**
II. Project Costs		Construction cost	265,602.00
		Total II	**265,602.00**
III. Operations		Chemicals costs	562, 500.00
Costs/Year		Coal costs for culturing	9, 000.00
		Labour cost	299,057.00
		Insurance premium	16,944.00
		Miscellaneous	9,550.00
		Total III	**897,051.00**
IV. Maintenance Costs		Spares cost	29,250.00
		Preventative maintenance cost	19,633.00
		Total IV	**48,883.00**
Grand Total USD			**1.9 Million**

Wet Scrubber that is the most installed emissions control units in the new power station built cost almost 6 times the proposed microbial process. According to Eligwe (1988), the desulphurization process is also cheaper than chemical desulphurization. You and Xu (2010), suggested washing the coal prior to combustion as another alternative method to reduce SO_2 emission. The distinction between You and Xu (2010) proposal and the current

study is based on low investment and operating costs washing method by You and Xu (2010) which could only reduce pyritic sulphur content to 40%. However, the water requirements, water pollution and associated drying issues are major concerns. Furthermore, the fact that one form of sulphur distribution is being targeted limits implementation of this technology in the power generation environment.

Table 5.12: The various desulphurization technologies

Technology	SO_2 Removal Capability	Investment Cost	Reference
Spray-Dry Scrubber	70 – 90%	$37 Million	Dimitrijevic´ and Tatic (2012)
Dry-CFB Scrubber	93 – 97%	$31 Million	Dimitrijevic´ and Tatic (2012)
Wet Scrubber	90 – 99%	$66 Million	Dimitrijevic´ and Tatic (2012)
Sorbent Injection	30 – 60%	$66 Million	Dimitrijevic´ and Tatic (2012)
Microbial Process	72.4%	$2 Million	Current Study

5.3. Summary

In the current study, biodesulphurization of Waterberg steam coal was investigated in the batch operated scale using a bacterial consortium isolated from coal. The overall biodesulphurization efficiencies for – 0.85 mm, – 2.30 +1.00 mm, – 4.60 +2.30 mm and +4.60 mm particle sizes were found to be 65.4%, 53.8%, 49.2% and 23.6% respectively being reached after 18 days. When the temperature increased from 23 ° to 30 °C, overall process efficiency for –0.85 mm improved further to 72.4 %. The process of biodesulphurization reduced the ash by 33% and concomitantly improved the CV by 19%. The decrease in ash content due to biodesulphurization treatment is desirable given that improved combustion of the coal would be expected, and a lower amount of ash will need to be discarded, thus imparting a positive impact on the environment, and a reduction in operational costs such as the transportation of ash to dump site. Sulphur forms reduction efficiency were found to be in the order Pyritic sulphur > Organic sulphur > Sulphide sulphur > Sulphate sulphur. Ash oxide of waster-soluble structures reduced after biodesulphurization treatment while less soluble structure increased. Growth pH varies in the range from 6.5 to 3.0. Seven isolates after purification of the most dominant colonies, viz: *Pseudomonas sp, Pseudomonas aeruginosa, Pseudomonas putida; Pseudomonas stutzeri, Bacillus sp., Pseudomonas rhizosphaerae and Pseudomonas alcaligenes* have been identified. Preliminary investment and operating costs for microbial desulphurization process were conducted. The basis for sulphur forms biodesulphurization of coal depends on coal particle size, percentage distribution, initial sulphur content and the concentration of

the bacterial consortium solution. Key coal macerals found included vitrinite, liptinite and inertinite. The latter maceral group, inertinite is the dominant maceral (up to 47.8 vol.%), whereas vitrinite and liptinite occurred in minor proportions as 20.4 vol.% and 4.4 vol.% respectively. Pyrite occurred in vitrinite and inertinite macerals, in syngetetic and epigenetic structures. XRD results show that quartz is the feed is in the range of 17.1 – 19.8 and it was not impacted by biodesulphurization treatment. Some results that have been independently confirmed by various laboratories suggest that biodesulphurization technique can serve as a pre-combustion technique for the power generation industry where SO_2 emissions levels have been legislated, particularly on coal-fired power plants that have passed their half-life. Should such processing become economically practical to implement and practice, it should contribute significantly to the reduction of sulphur in the coal, and ultimately a reduction in the sulphur emissions from the process of combustion.

CHAPTER 6

KINETICS STUDY AND MODELLING OF MICROBIAL DESULPHURIZATION OF COAL USED IN POWER PLANTS

6.1 Introduction

The supply of energy in South Africa continues to depend heavily on coal and will continue to do so the near future. Further deployment of renewable energy technologies in the region is hindered by concerns over high cost and unreliable electricity generation capacity. In South Africa, coal still stands as the most reliable, cheap and abundantly available energy source. Almost 95% of electricity generation in the country is from coal-fired power plants. However, the use of coal in electricity generation has attracted attention due to its sulphur content. Upon combustion, sulphur in the coal leads to sulphur dioxide which has serious negative effects on plant and animal health, metallurgical and environment which may give rise to global warming (Mketo *et al.*, 2016), acid rain (Hu *et al.* 2018) and water pollution. Additional issues including human health such as chronic respiratory illnesses (Mketo *et al.*, 2016), sulphate aerosols from S (0)/S (-2) oxidation causing corrosion, abrasion, fouling and slagging of metal bodies which result in boiler tubes leaks. Therefore, the removal of all sulphur forms in coal is essential to protect the environment and community properties. Several pre-combustion processes (viz. biological treatment, chemical and physical processes) and post-combustion desulphurization technologies have been reported in the literature. Among the variety of pre-combustion processes mentioned, biodesulphurization arises as a clean, efficient and environmentally friendly technique that is having low capital and operating costs as well as being less – energy intensive.

Chemical kinetics is a discipline that quantitatively describes the progress of reactions on a large range of different scales: from interactions between atoms and electrons in chemical bonds to production rates in chemical reactors. Kinetics on the level of individual molecules describes the modifications that the reactants undergo to form the products. In other words, knowledge of microbial kinetics is essential for microbial desulphurization system design and optimization of operational conditions. For a process design and to optimize the appropriate biodesulphurization treatment process, it is important to obtain a kinetic expression for the principal reaction occurring during microbial desulphurization. The chemical kinetics of coal has relevance to a wide range of coal utilization processes (Giri and Sharmar, 2000). A summary of previous literature on kinetic modelling of biodesulphurization and biokinetic coefficients is presented in Table 6.1 and Table 6.2. A variety of mathematical models have been proposed to describe the dynamics of metabolism

of compounds exposed to pure cultures of microorganisms or microbial populations of natural environment. However, most of the published literature in this area has taken into account only the first reaction in the 4S metabolic pathway – i.e. the disappearance of the model substrate dibenzothiophene in a reaction mixture using only pure cultures (as shown in Table 6.1). Secondly, dibenzothiophene is recognized to behave differently to the actual sulphur content in the coal.

It is apparent from the literature survey that microbial desulphurization treatment is very difficult to model because very little is understood about the mechanism by which calorific value, ash content and sulphur content are affected by the process itself. This may require detailed analyses of both proximate and ultimate analyses. Besides the interaction of solid, liquid and gas phase interaction, microorganisms is introduced to the system. However, most models that have been reported in literature have assumed ideal conditions, related only growth rate and oxidation rate descriptions. Comprehensive models are constructed in an attempt to compile every piece of information available from both empiricism and theoretical development (Milioli and Foster, 1995). The result is a huge number of parameters and coefficients to be set, and mathematical complexities of difficult treatment. This makes the comprehensive models very difficult to apply, and limited to particular cases.

Table 6.1: Equations for the biodesulphurization kinetic model (Agarwal *et al.*, 2016)

Reaction	Rate expression	Kinetics type
$DBT + ½O_2 \xrightarrow{r_1(FMNH_2)} DBTO + H_2O$	$r_1 = \frac{k_1 C_{DBT}}{K_1 + C_{DBT}}$	Michaelis–Menten
$DBT + ½O_2 \xrightarrow{r_2(FMNH_2)} DBTO_2 + H_2O$	$r_2 = \frac{k_2 C_{DBTO}}{K_2 + C_{DBTO}}$	Michaelis–Menten
$DBT + ½O_2 \xrightarrow{r_3(FMNH_2)} HBPS^- + H_2O$	$r_3 = \frac{k_3 C_{DBTO2}}{K_3 + C_{DBTO2}}$	Michaelis–Menten
$HBPS^- + H_2O \xrightarrow{r_4} HBP + SO_3^{2-} + H^+$	$r_4 = \frac{k_4 C_{HBPS}}{K_4\left(1 + C_{HBP/K_I}\right) + C_{HBPS}}$	Product competitive inhibition

In this study, a model was developed on simultaneous disappearance of medium sulphur type coal due to biodesulphurization treatment in a batch system. Moreover, ash content and

calorific value desulphurization data were analyzed in order to determine the relationship between them and the effect of the desulphurization process.

Table 6.2: Various models used so far to determine biokinetic coefficients

Model	Equation	Reference
Michalis-Menten	$v = \frac{V_m C_s}{K_m + C_s}$	Brandis – Heep *et al.* (1983)
Kinetic model	$r_s = \left\{\frac{\mu_{max} S}{K_S S_0 X + S} - k_d\right\}\frac{X}{Y}$	Moosa *et al.* (2005)
Monod	$\mu = \frac{\mu_{max} S}{K_S + S}$	Monod (1949)
Stover–Kincannon model	$\frac{V}{Q(S_i - S_e)} = \frac{K_B S_i}{U_{max} V Q} + \frac{1}{U_{max}}$	Kosioska and Miśkiewicz (2009)
Contois	$\mu = \frac{\mu_{max} S}{K_S X + S}$	Contois (1959)
First Order Growth model	$\ln(x) = \mu t - B$	Medircio (2006)
Chen and Hashimoto	$\mu = \frac{\mu_{max} S}{K_S S_0 + (1 - K_S) S}$	Chen and Hashimoto (1980)

6.2 Materials and Methods

6.2.1 Experimental set-up

The desulphurization experiments were conducted in 500 mL continuously stirred Erlenmeyer flask. The reactor was inoculated with 250 mL of bacterial consortium from primary enrichment batch reactors and 200 g of the coal sample. A magnetic stirrer operating at a rate of 200 rpm in order to maintain a completely stirred tank reactor (CSTR) conditions homogenized the medium. Four different size fractions (+4.60 mm, −4.60 +2.30 mm, −2.30 +1.00 mm and − 0.85 mm) were considered to ensure an adequate representation. For experiments with sterilized coal (to remove inherent bacteria), sterilization was done by autoclaving at 103 Pa (gauge) for 15 min. At the end of biodesulphurization experiments, peristaltic pump was used to introduce the treated coal samples to vacuum filtration followed by vigorous wash to dissociate bacteria that may be attached to coal particles. Treated coal samples were dried overnight in a Protea Drying Oven at 30 ± 2 °C and analyzed. Figure. 6.1 Schematic representation of microbial desulphurization reactor system

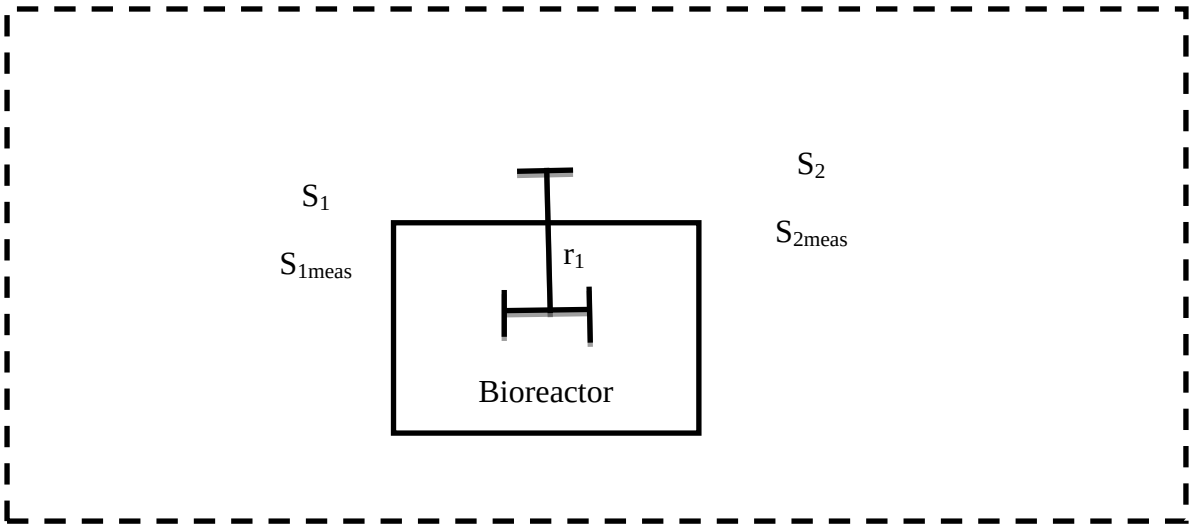

Figure 6.1: System volume representation of microbial desulphurization reactor

6.2.2 Simulation analysis using AQUASIM 2.0 Software

Data simulation with Aquasim uses the DASSL algorithm, which is based on the implicit (backward differencing) variable-step, variable-order Gear integration technique (Petzold, 1983; Gear, 1971; Reichart, 1998). This technique makes use of a numerically integrating system of ordinary and partial deferential equations in time and simultaneously solves the algebraic equations. Spatial discretization of partial deferential equations is done using conservative finite deference schemes (Le Veque, 1990; Reichart, 1998). From differential conservation law, the equation below was derived and developed in Aquasim. Also, the implementation of the DASSL algorithm allows the use of full or branded Jacobian matrix Equation 6.1, in solving the nonlinear system of algebraic equation (Reichart, 1998).

$$\frac{\partial \hat{p}}{dt} = \frac{\partial \hat{j}}{\partial z} + \hat{r} \tag{6.1}$$

Equation 6.1 is discretised as 6.2

$$\frac{d}{dt}\hat{p}(x_i,t) = \frac{\hat{j}_{num}(x_{i+0.5},t) - \hat{j}_{num}(x_{i-0.5},t)}{x_{i+0.5} - x_{i-0.5}} + \hat{r}(x_i,t) \tag{6.2}$$

$$\underline{\underline{J}} = \frac{\partial F}{\partial y} \tag{6.3}$$

$$\underline{\underline{J}} = \begin{bmatrix} \frac{\partial f_1}{\partial x_1} \cdots \frac{\partial f_1}{dy} \\ \frac{\partial f_2}{\partial x_2} \cdots \frac{df_2}{dy} \end{bmatrix} \tag{6.4}$$

6.2.3 Parameter estimation

In AQUASIM 2.0, the mass balance was evaluated numerically by the forth order Runge-Kutta method (RK-4). The parameters were obtained by minimizing the Chi-square ($\chi 2$) values between the model data and the actual data using a simplex method built within AQUASIM (Reichert, 1998). Aquasim estimate model parameters are represented by constant variables by minimizing equation 6.5 with the constraints ($\ell_{\min,i} \le \ell_i \le \ell_{\max,i}$) (Reichart, 1998). This equation is described as the sum of the squares of the weighted deviations between measurements and calculated model results (Reichart, 1998). The various authors (Nelder and Mead, 1965; Ralston and Jennrich, 1978; Reichart, 1998)) concut that minimization of equation 6.22 uses simplex algorithm or secant algorithm.

$$x^2(\ell) = \sum_{i=1}^{n} \left[\frac{U_{meas,i} - U_i(\ell)}{\alpha_{meas,i}} \right]^2 \tag{6.5}$$

where: $U_{meas,i}$ = i-th measurement, $\alpha_{meas,i}$ = standard deviation, $U_i(\ell)$ = calculated value of the model variable corresponding to the i-th measurement and evaluated at the time and location of this measurement, $\ell = (\ell_i, .., \ell_m)$ = model parameters, $\ell_{miin,i}, \ell_{\max,i}$ = minimum and maximum constant variable representing ℓ_i n = number of points and x^2 = the sum of the deviation for all the fit targets.

6.2.4 Sensitivity analysis of the estimated parameters

Sensitivity analysis in Aquasim is solved by combined identifiable analysis and uncertainty analysis (Reichart, 1998). The aim of identifiability analysis with Aquasim is to determine if the model parameters can be uniquely determined with the aid of available data and to estimate the uncertainty of the parameter estimates. This is done by estimating the standard error and correlation coefficient of the parameters during parameter estimation (Reichart, 1998). Equations 6.25 – 6.28 are distinguished by Aquasim.

$$\delta_{y,\ell}^{a,a} = \frac{\partial y}{\partial \ell} \tag{6.6}$$

$$\delta_{y,\ell}^{r,a} = \frac{1}{y}\frac{\partial y}{\partial \ell} \tag{6.7}$$

$$\delta_{y,\ell}^{a,r} = p\frac{\partial y}{\partial \ell} \tag{6.8}$$

$$\delta_{y,\ell}^{r,r} = \frac{p}{y}\frac{\partial y}{\partial \ell} \tag{6.9}$$

where:

y = arbitrary variable calculated by Aquasim, and ℓ = model parameter by a constant.

$$\delta_y = \sqrt{\sum_{i=1}^{m}\left(\frac{\partial y}{\partial \ell_i}\right)^2 \delta_{\ell_i}^2}$$

(6.10)

where: ℓ_i = uncertainty model parameter, δ_i = standard deviations, $y(\ell_i,...,\ell_m)$ = solution of the model equations for a given variable at a given location and time, δ_y = approximate standard deviation of the model result. The error contribution of each parameter is given as;

$$\delta_{y\ell}^{err} = \frac{\partial y}{\partial \ell}\delta_\ell$$

(6.11)

Aquasim calculate equation 6.6 – 6.28, 6.9 and 6.11 by using the derivatives as follows:

$$\frac{\partial y}{\partial \ell_i} \approx \frac{y(\ell_i + \Delta\ell_i) - y(\ell_i)}{\Delta\ell_i} \tag{6.12}$$

Where: $\Delta\ell_i$ = 1% of the standard deviation δ_{ℓ_i}, of the parameter ℓ_i.

6.2.5 Standard Error of Estimate

The standard error of estimate (SEE) is a measure of the accuracy of predictions or model and is defined by Kellogg and Spence (1931) as in Eq. 6.13:

$$E = \sqrt{\frac{\sum(z-z')}{N}}$$

(6.13)

where:

Z = the experimental value,

Z’ = the predicted

6.2.6 AQUASIM

Software process

1. Edit Variables

S_{meas}

k_d

k_{ms}

K_s

t

t_0

X

X_0

3. Edit Compartments

Bioreactor

Active variables: S_2

Active processes: Biodesulphurization

Initial Condition: $S_2 = S_{2meas}$
Input: $S_2 = kS_1$

2. Edit Process

Biodesulphurization

$$\text{Rate} = \frac{k_{ms}\, SX}{K_c + S}$$

4. Edit Name :

Biodesulphurization reactor

5. Edit Plot definition

Name : Plot1
Abscissa: Time (h)
Ordinate : S (mg/L)
Curves :Smeas

7. Parameter Estimation

Calculation Active:

Fit1:

Data: S_{2meas} Variable: S_2

Compartment: Bioreactor
Time/Space: 0

6. Parameter Estimation

Parameters Active:

k_d

k_{mc}
K_c
X_0

k

t_0

6.3 Results and Discussions

6.3.1 Mass balance around a bioreactor

In this study, sulphur content, ash content and calorific value desulphurization data were analyzed in order to determine the relationship between them and the effect of the desulphurization process. In general, mass balance around a reactor is described by Eq. 6.14

$$[\text{Input}] - [\text{Output}] + [\text{Generation}] - [\text{Consumption}] = [\text{Accumulation}] \quad (6.14)$$

According to Fogler (1999), a sulphur species S_T at any instant time, t yields the following Eq. 6.15:

$$\left\{\begin{matrix}\text{Rate of}\\ \text{mass}\\ \text{in}\end{matrix}\right\} - \left\{\begin{matrix}\text{Rate of}\\ \text{mass}\\ \text{out}\end{matrix}\right\} + \left\{\begin{matrix}\text{Rate of}\\ \text{mass}\\ \text{generated}\end{matrix}\right\} - \left\{\begin{matrix}\text{Rate of}\\ \text{mass}\\ \text{consumed}\end{matrix}\right\} = \left\{\begin{matrix}\text{Rate of}\\ \text{mass}\\ \text{accumulated}\end{matrix}\right\} \quad (6.15)$$

Revising Eq. (6.15) in the context of targeted pollutant gives Eq. 6.16: (6.16)

$$\left\{\begin{matrix}\text{Rate of}\\ \text{flow of } S_T\\ \text{in}\end{matrix}\right\} - \left\{\begin{matrix}\text{Rate of}\\ \text{flow of } S_T\\ \text{out}\end{matrix}\right\} + \left\{\begin{matrix}\text{Rate of } S_T\\ \text{generated}\end{matrix}\right\} - \left\{\begin{matrix}\text{Rate of}\\ S_T\\ \text{consumed}\end{matrix}\right\} = \left\{\begin{matrix}\text{Rate of}\\ S_T\\ \text{accumulated}\end{matrix}\right\}$$

The Eq. (6.16) is best suited for continuous processes and may be written more precisely in continuous processes applications. According to Fogler (1999), a batch reactor is a non-continuous and perfectly mixed closed vessel where a reaction takes place. Therefore considering that a batch reactor has neither inflow nor outflow of reactants or products while the reaction is being carried out: $F_{ST},0 = F_{ST} = 0$. Furthermore, given its volume V and the initial sulphur content, $S_{T,0}$, the total mass will be $M = V. S_{T,0}$. In the unit time, the sulphur content will be able to change only in virtue of a chemical reaction. Therefore, the mass balance reduces to Eq. 6.17:

$$[F_{ST,0}] - [F_{ST}] + [G_{ST}] - [C_{ST}] = \left[\frac{dm_{ST}}{dt}\right] \quad (6.17)$$

By taking the appropriate limits (i.e. let $M \rightarrow \infty$ and $\Delta V \rightarrow 0$) and making use of the definition of the integral, we can rewrite the foregoing Eq. 6.18 in the form:

$$G_{ST} = \int r_{ST}\, dV \tag{6.18}$$

We can replace G_{ST} in the Eq. 6.17 equation:

$$[F_{ST,0}] - [F_{ST}] + [G_{ST}] - [C_{ST}] = \left[\frac{dm_{ST}}{dt}\right]$$

$$[F_{ST,0}] - [F_{ST}] + \int r_{ST}\, dV - [C_{ST}] = \left[\frac{dm_{ST}}{dt}\right] \tag{6.19}$$

Where *r* is the rate of generation (+) or depletion (-). Since the assumption of no flow in and out of the reactor volume, Q = 0, and the constant volume V, If the reaction mixture is perfectly mixed so that there is no variation in the rate of reaction throughout the reactor volume, we can take r_{ST} out of the integral and write the mass balance in the form of Eq. (6.20):

$$\frac{dm}{dt} = \frac{d(c.V)}{dt} = V.\frac{dc}{dt} = V.r \tag{6.20}$$

Where c = c (t) is the concentration at any given time inside the reactor, then,

$$\frac{dc}{dt} = r \tag{6.21}$$

The above differential equation is the characteristic equation of a batch reactor. Therefore considering a first order reaction ($r = -k.c$)

$$\frac{dc}{dt} = -k.c \tag{6.22}$$

Solving ,

$$\ln\frac{c}{c_0} = -k.t \tag{6.23}$$

or

$$c = c_0.\, e^{-k.t}$$

6.3.2 Sulphur content reduction parameters estimation

In order to simplify the model, the desulphurization reaction proceeds with the initial formation of activated complex (Coal – S.Oxidant) which is an associated intermediate as per reaction 6.24.

$$\text{Coal –S + Oxidant} \underset{k_2}{\overset{k_1}{\rightleftharpoons}} \text{Coal – S.Oxidant} \xrightarrow{k_3} \text{Sulphur loss} \qquad (6.24)$$

The Coal – S.Oxidant is in equilibrium with the reactants. Being a transient intermediate, Coal – S.Oxidant decomposes either into the products resulting to sulphur loss or revert to the reactants as shown in reaction 6.24.

To simplify reaction 6.24 for the modelling purposes, we suggest that a single representative enzyme reduces sulphur content as a result of the overall biodesulphurization treatment process. The simplified sulphur content reduction equation can thus be written as reaction 6.25:

$$\text{Coal –}S_T + E \underset{k_2}{\overset{k_1}{\rightleftharpoons}} E^*\text{Coal} - S_T \xrightarrow{k_3} E + S_T \qquad (6.25)$$

where: S_T = Total sulphur content

E = S_T reductase as a biocatalyst,

E*Coal – S_T = The transitional bacteria-S_T complex,

k_1 = Reaction rate constant for the forward reaction

k_2 = Reaction rate constant for the reverser reaction

k_3 = Reaction rate constants of the third reaction

If the S_T content is represented by S and the bacteria – S_T complex by E*. Eq. 6.25 can represent the overall rate of reduction:

$$\frac{dE}{dt} = k_1 . S_T . E \qquad (6.26)$$

$$\frac{dE^*}{dt} = k_2 . S_T . E^* \qquad (6.27)$$

Therefore,

$$\frac{dE^*}{dt} = \frac{dS_T}{dt} = k_3.E^* \quad (6.28)$$

Combining Equation 6.26, 6.27 and 6.28 gives the rate of E* formation represented as:

$$\frac{dE^*}{dt} = k_1(E - E^*)(S_T) - k_2(E^*) - k_3\,(E^*) \quad (6.29)$$

In Eq. 6.29 above, steady –state conditions can be assumed to prevail as long as E* is formed and destroyed spontaneously such that d (E*)/dt ≈ 0. Therefore the mass balance represented in Eq. 6.29 can thus be written as:

$$0 = k_1(E - E^*)(S_T) - k_2(E^*) - k_3\,(E^*) \quad (6.30)$$

$$k_1S_T(E - E^*) = k_2(E^*) + k_3\,(E^*)$$

$$(k_1ES_T) - (k_1E^*S_T) = k_2(E^*) + k_3\,(E^*)$$

$$(k_1ES_T) = (k_1E^*S_T) + k_2(E^*) + k_3\,(E^*)$$

$$(k_1ES_T) = (k_1S_T + k_2 + k_3)E^* \quad (6.31)$$

So after rearranging Eq. 6.6, E* can be expressed as:

$$E^* = \frac{S_T.E}{\left(S_T + \frac{(k_2+k_3)}{k_1}\right)} \quad (6.32)$$

Thus, the sulphur reduction rate in Eq. 6.32 becomes:

$$r = -\frac{dS_T}{dt} = \frac{k_3S_T.E}{\left(S_T + \frac{(k_2+k_3)}{k_1}\right)} \quad (6.33)$$

In Eq. 6.33, k_1, k_2 and k_3 are constants. The group of constants in Eq.(6.33) can be replaced by a meaningful symbols from enzyme kinetics as follows: $(k_2+k_3)/k_1$ can be replaced by half velocity concertation K_c (ML^{-3}) and k_3 can be replaced by the maximum specific sulphur content reduction rate coefficient k_{mc} (T^{-1}) such that:

$$r = -\frac{dS_T}{dt} = \frac{k_{mc}S_T.E}{(S_T + K_c)} \quad (6.35)$$

The rate of sulphur content reduction in the biological system is highly dependent on the number of active cells present in the reactor and the capacity of cells to produce enzymes that can reduce sulphur content under various particle size fractions. According to

Nkhalambayausi-Chirwa and Wang (2001), viable biomass can be used to determine the level of biological activity during the entire period of operation. Therefore, for any amount of cells X, the amount of enzyme produced will be proportional to the cell concentration such that the enzyme E can be replaced by the total cell biomass term *X* if cells are being harvested during the log growth phase. This gives a Monod type equation

$$r = -\frac{dS_T}{dt} = \frac{k_{mc} S_T . X}{(S_T + K_c)} \qquad (6.36)$$

where: S_T = Sulphur content at time t (ML^{-3}), k_{mc} = maximum specific S_T reduction rate coefficient (T^{-1}), K_c = half velocity constant (ML^{-3}), *X* = concentration of viable cells at time t (ML^{-3}), and t = time (T)

In this model, only k_{mc} and K_c are the unknown parameters and can assume a stationary phase with respect to *X* since the experiments were performed under very high biomass concentration. Cells were concentrated in the ration 1/5, screening performed in growth condition and therefore assumption can be made that *X* is constant. ($X = X^0$). In order to determine kinetic parameters, the analytical solution could be used. This was expressed as a function of time as shown in the Eq 6.11:

$$t = \frac{K_c}{X^0 . k_{mc}} \ln\left(\frac{S_{T,0}}{S_T}\right) + \frac{1}{X^0 . k_{mc}} \left(S_{T,0} - S_T\right) \qquad (6.37)$$

where: X^0 = initial biomass concentration (ML^{-3}), initial $S_{T.0}$ concentration (ML^{-3}) and S_T is the final concentration (ML^{-3}).

Since the coal particles were very small, it was assumed that all the coal particles were spherical in shape.

Eq. 6.10 can be solved numerically. It may also happen that an equally good fit is accomplished by more than one model therefore the choice was guided most importantly by convenience. The parameters were estimated by optimization of Eq. 6.37 against batch experimental data using the AQUASIM 2.0 Software. The values of the kinetic parameters (K_C and k_{mc}) in the batch study determined from the experimental data are shown in Table 6.3. These results are statistical correct since the regression coefficients *R* are above 97 % and

all R^2 are above 95 %. However, the biodesulphurization rate coefficient, k_{mc} was determined to be very low. This indicates that sulphur reduction happened faster during exponential phase. However, these parameters could not generate a unique representative model for all studied coal particle sizes. The results also show that *Kc* values obtained from the non-linear regression were not constant and were shown to be much higher than S_T values ($Kc >> S_T$). According to Brey (1958) the reaction rate approaches first order when the half velocity coefficient K_c is much greater than S_T. Table 6.4 shows Applied K_c and k_{mc} parameter on the Monod type equation

Table 6.3: Parameter estimation obtained for Monod type equation

Parameters	–0.85 mm	–2.30 +1.00 mm	–4.60 +2.30 mm	+4.60 mm
K_c	76465.760	114328.310	71271.225	98731.441
k_{mc}	17.474	14.660	13.304	11.105
R	0.998	0.987	0.979	0.973
R^2	0.997	0.976	0.956	0.962
SEE	0.052	1.450	1.465	2.342

**SEE: Standard Error of Estimates

Table 6.4: Applied K_c and k_{mc} parameter on the Monod type equation

Parameters	Kinetic Equation showing parameters k_{mc} and K_c
– 0.85 mm	$t = 1.039423 \times \ln\left(\frac{S_{T,0}}{S_T}\right) + 1.35933E-05 \times \left(S_{T,0} - S_T\right)$
–2.30 +1.00 mm	$t = 1.8524125 \times \ln\left(\frac{S_{T,0}}{S_T}\right) + 1.620261E-05 \times \left(S_{T,0} - S_T\right)$
–4.60 +2.30 mm	$t = 1.272476 \times \ln\left(\frac{S_{T,0}}{S_T}\right) + 1.78543E-05 \times \left(S_{T,0} - S_T\right)$
+4.60 mm	$t = 2.111809 \times \ln\left(\frac{S_{T,0}}{S_T}\right) + 2.13894E-05 \times \left(S_{T,0} - S_T\right)$

6.3.4 Ash content reduction parameters estimations

$$\text{Coal} - A + \text{Oxidant} \underset{k_2}{\overset{}{\rightleftharpoons}} \text{Coal} - A.\text{Oxidant} \xrightarrow[k_3]{} \text{Ash loss} \qquad (6.38)$$

The Coal – A.Oxidant is in equilibrium with the reactants. Being a transient intermediate, Coal – A.Oxidant decomposes either into the products resulting to ash content loss or revert to the reactants as shown in reaction 6.38.

To simplify reaction 6.38 for the modelling purposes, we suggest that a single representative enzyme reduces sulphur content as a result of the overall biodesulphurization treatment process. The simplified sulphur content reduction equation can thus be written as reaction 6.39:

$$\text{Coal} - A + E \underset{k_2}{\overset{k_1}{\rightleftharpoons}} E^{*}\text{Coal} - A \xrightarrow{k_3} E + A \qquad (6.39)$$

where: A = Ash content (wt.%,db),

E = A reductase as a biocatalyst,

E*Coal – A = The transitional bacteria-A complex,

k_1 = Reaction rate constant for the forward reaction

k_2 = Reaction rate constant for the reverser reaction

k_3 = Reaction rate constants of the third reaction

If the ash content in the coal is represented by A and the bacteria – A complex by E*. Eq. 6.40 can represent the overall rate of reduction:

$$\frac{dE}{dt} = k_1.A.E \qquad (6.40)$$

$$\frac{dE^*}{dt} = k_2.A.E^* \qquad (6.41)$$

Therefore,

$$\frac{dE^*}{dt} = \frac{dA}{dt} = k_3.E^* \qquad (6.42)$$

Combining Equation 6.40, 6.41 and 6.42, gives the rate of E* formation represented as:

$$\frac{dE^*}{dt} = k_1(E - E^*)(A) - k_2(E^*) - k_3\ (E^*) \quad (6.43)$$

In Eq. 6.43 above, steady –state conditions can be assumed to prevail as long as E* is formed and destroyed spontaneously such that d (E*)/dt ≈ 0. Therefore the mass balance represented in Eq. 6.43 can thus be written as:

$$0 = k_1(E - E^*)(A) - k_2(E^*) - k_3\ (E^*) \quad (6.44)$$

$$k_1A(E - E^*) = k_2(E^*) + k_3\ (E^*)$$

$$(k_1EA) - (k_1E^*A) = k_2(E^*) + k_3\ (E^*)$$

$$(k_1EA) = (k_1E^*A) + k_2(E^*) + k_3\ (E^*)$$

$$(k_1EA) = (k_1A + k_2 + k_3)E^*$$

So after rearranging Eq. 6.45, E* can be expressed as:

$$E^* = \frac{A.E}{\left(A + \frac{(k_2+k_3)}{k_1}\right)} \quad (6.45)$$

Thus, the sulphur reduction rate in Eq. 6.46 becomes:

$$r = -\frac{dA}{dt} = \frac{k_3A.E}{\left(A + \frac{(k_2+k_3)}{k_1}\right)} \quad (6.46)$$

In Eq. 6.46, k_1, k_2 and k_3 are constants. The group of constants in Eq.(6.46) can be replaced by a meaningful symbols from enzyme kinetics as follows: $(k_2+k_3)/k_1$ can be replaced by half velocity concertation K_c (ML^{-3}) and k_3 can be replaced by the maximum specific sulphur content reduction rate coefficient k_{mc} (T^{-1}) such as Eq. 6.47:

$$r = -\frac{dA}{dt} = \frac{k_{mc}A.E}{(A+K_c)} \quad (6.47)$$

The rate of sulphur content reduction in the biological system is highly dependent on the number of active cells present in the reactor and the capacity of cells to produce enzymes that can reduce sulphur content under various particle size fractions. According to Brey (1958), viable biomass can be used to determine the level of biological activity during the entire period of operation. For any amount of cells X, the amount of enzyme produced will be proportional to the cell concentration such that the enzyme E can be replaced by the total cell

biomass term *X* if cells are being harvested during the log growth phase. This gives a Monod type equation as shown in Eq. 6.48.

$$r = -\frac{dA}{dt} = \frac{k_{mc}A.X}{(A+K_c)} \qquad (6.48)$$

where: S_T = Sulphur content at time t (ML^{-3}), k_{mc} = maximum specific S_T reduction rate coefficient (T^{-1}), K_c = half velocity constant (ML^{-3}), X = concentration of viable cells at time t (ML^{-3}), and t = time (T)

In this model, only k_{mc} and K_c are the unknown parameters and can assume a stationary phase with respect to X since the experiments were performed under very high biomass concentration. Cells were concentrated in the ration 1/5, screening performed in growth condition and therefore assumption can be made that X is constant. ($X = X^0$). In order to determine kinetic parameters, the analytical solution could be used. This was expressed as a function of time as shown in the Eq. 6.49:

$$t = \frac{K_C}{X^{0}.k_c}\ln\left(\frac{A_0}{A}\right) + \frac{1}{X^0 k_{mc}}(A_0 - A) \qquad (6.49)$$

where: X^0 = initial biomass concentration (ML^{-3}), initial $S_{T.0}$ concentration (ML^{-3}) and S_T is the final concentration (ML^{-3}).

Since the coal particles were very small, it was assumed that all the coal particles were spherical in shape.

Eq. 6.69 can be solved numerically. It may also happen that an equally good fit is accomplished by more than one model therefore the choice was guided most importantly by convenience. The parameters were estimated by optimization of Eq. 6.49 against batch experimental data using the AQUASIM 2.0 Software. The values of the kinetic parameters (K_C and k_{mc}) in the batch study determined from the experimental data are shown in Table 6.5. These results are statistical correct since the regression coefficients R are above 97 % and all R^2 are above 96 %. However, the biodesulphurization rate coefficient, k_{mc} was determined to be very low. This indicates that sulphur reduction happened faster during exponential phase. However, these parameters could not generate a unique representative model for all studied coal particle sizes. The results also show that *Kc* values obtained from the non-linear regression were not constant and were shown to be much higher than S_T values ($Kc >> S_T$). According to Brey (1958), the reaction rate approaches first order when the half velocity

coefficient K_c is much greater than S_T. Table 6.6 shows applied K_c and k_{mc} sulphur content parameters on the Monod type equation

Table 6.5: Sulphur contents parameter estimation obtained for Monod type equation

Parameters	–0.85 mm	–2.30 +1.00 mm	–4.60 +2.30 mm	+4.60 mm
K_c	87334.11	90409.473	98465.558	111306.32
k_{mc}	22.681	23.782	27.149	25.876
R	0.999	0.988	0.987	0.979
R^2	0.999	0.987	0.968	0.965
SEE	0.078	1.230	1.332	1.954

**SEE: Standard Error of Estimates

Table 6.6: Applied K_c and k_{mc} sulphur content parameters on the Monod type equation

Parameters	Kinetic Equation showing parameters k_{mc} and K_c
–0.85 mm	$t = 0.9578 \ln\left(\frac{A_0}{A}\right) + 1.09676\,E-05 \times (A_0 - A)$
–2.30 +1.00 mm	$t = 0.9457 \ln\left(\frac{A_0}{A}\right) + 1.04599\,E-05 \times (A_0 - A)$
–4.60 +2.30 mm	$t = 0.9022 \ln\left(\frac{A_0}{A}\right) + 9.16263\,E-06 \times (A_0 - A)$
+4.60 mm	$t = 0.0700 \ln\left(\frac{A_0}{A}\right) + 9.613400E-06 \times (A_0 - A)$

6.3.5 Calorific values parameters estimations

$$\text{Coal –CV +Oxidant} \underset{k_1}{\overset{k_2}{\rightleftharpoons}} \text{Coal – CV.Oxidant} \xrightarrow{k_3} \text{CV gain} \qquad (6.50)$$

The Coal – CV.Oxidant is in equilibrium with the reactants. Being a transient intermediate, Coal – CV.Oxidant decomposes either into the products resulting to CV gain or reverts to the reactants as shown in reaction Eq. 6.50. To simplify reaction 6.50 for the modelling purposes, we suggest that a single representative enzyme increases CV values as a result of

the overall biodesulphurization treatment process. The simplified CV increase equation can thus be written as reaction 6.51:

$$\text{Coal} - \text{CV} + \text{E} \underset{k_2}{\overset{k_1}{\rightleftharpoons}} \text{E}^*\text{Coal} - \text{CV} \xrightarrow{k_3} \text{E}+\text{CV} \qquad (6.51)$$

where: CV = calorific value

E = CV increase by a biocatalyst,

E*Coal – CV = The transitional bacteria-CV complex,

k_1 = Reaction rate constant for the forward reaction

k_2 = Reaction rate constant for the reverser reaction

k_3 = Reaction rate constants of the third reaction

If the calorific value in the coal is represented by CV and the bacteria – CV complex by E*. Eq. 6.52 can represent the overall rate of reduction:

$$\frac{dE}{dt} = k_1.CV.E \qquad (6.52)$$

$$\frac{dE^*}{dt} = k_2.CV.E^* \qquad 6.53)$$

Therefore,

$$\frac{dE^*}{dt} = \frac{dCV}{dt} = k_3.E^* \qquad (6.54)$$

Combining Equation 6.52, 6.53 and 6.54, gives the rate of E* formation represented as:

$$\frac{dE^*}{dt} = k_1(E - E^*)(CV) - k_2(E^*) - k_3\,(E^*) \qquad (6.55)$$

In Eq. 6.55 above, steady –state conditions can be assumed to prevail as long as E* is formed and destroyed spontaneously such that d (E*)/dt ≈ 0. Therefore the mass balance represented in Eq. 6.56 can thus be written as:

$$0 = k_1(E - E^*)(CV) - k_2(E^*) - k_3\,(E^*) \qquad (6.56)$$

$$k_1CV(E - E^*) = k_2(E^*) + k_3\,(E^*)$$

$$(k_1ECV) - (k_1E^*CV) = k_2(E^*) + k_3\,(E^*)$$

$$(k_1ECV) = (k_1E^*CV) + k_2(E^*) + k_3\,(E^*)$$

$$(k_1ECV) = (k_1S_T + k_2 + k_3)E^*$$

So after rearranging Eq. 6.56, E* can be expressed as:

$$E^* = \frac{CV.E}{\left(CV + \frac{(k_2+k_3)}{k_1}\right)} \tag{6.57}$$

Thus, the sulphur reduction rate in Eq. 6.57 becomes:

$$r = -\frac{dCV}{dt} = \frac{k_3 CV.E}{\left(CV + \frac{(k_2+k_3)}{k_1}\right)} \tag{6.58}$$

In Eq. 6.58, k_1, k_2 and k_3 are constants. The group of constants in Eq.(6.58) can be replaced by a meaningful symbols from enzyme kinetics as follows: $(k_2+k_3)/k_1$ can be replaced by half velocity concertation K_c (ML^{-3}) and k_3 can be replaced by the maximum specific sulphur content reduction rate coefficient kmc (T^{-1}) such that:

$$r = -\frac{dCV}{dt} = \frac{k_{mc} CV.E}{(S_T + K_c)} \tag{6.59}$$

The rate of sulphur content reduction in the biological system is highly dependent on the number of active cells present in the reactor and the capacity of cells to produce enzymes that can reduce sulphur content under various particle size fractions. According to Nkhalambayausi-Chirwa and Wang (2001), viable biomass can be used to determine the level of biological activity during the entire period of operation. For any amount of cells X, the amount of enzyme produced will be proportional to the cell concentration such that the enzyme E can be replaced by the total cell biomass term X if cells are being harvested during the log growth phase. This gives a Monod type equation

$$r = -\frac{dCV}{dt} = \frac{k_{mc} CV.X}{(CV + K_c)} \tag{6.60}$$

where: CV = calorific value at time t (ML^{-3}), k_{mc} = maximum specific S_T reduction rate coefficient (T^{-1}), K_c = half velocity constant (ML^{-3}), X = concentration of viable cells at time t (ML^{-3}), and t = time (T)

In this model, only k_{mc} and K_c are the unknown parameters and can assume a stationary phase with respect to X since the experiments were performed under very high biomass concentration. Cells were concentrated in the ration 1/5, screening performed in growth condition and therefore asdsumption can be made that X is constant. ($X = X^0$). In order to

determine kinetic parameters, the analytical solution could be used. This was expressed as a function of time as shown in the Eq 6.61:

$$t = \frac{K_C}{X^{0} \cdot k_c} \ln\left(\frac{CV_0}{CV}\right) + \frac{1}{X^{0} k_{mc}} (CV_0 - CV) \qquad (6.61)$$

where: X^0 = initial biomass concentration (ML^{-3}), initial $S_{T.0}$ concentration (ML^{-3}) and S_T is the final concentration (ML^{-3}).

Eq. 6.61 can be solved numerically. It may also happen that an equally good fit is accomplished by more than one model therefore the choice was guided most importantly by convenience. The parameters were estimated by optimization of Eq. 6.61 against batch experimental data using the AQUASIM 2.0 Software. The values of the kinetic parameters (K_C and k_{mc}) in the batch study determined from the experimental data are shown in Table 6.7. These results are statistical correct since the regression coefficients *R* are above 97 % and all R^2 are above 95 %. However, the biodesulphurization rate coefficient, k_{mc} was determined to be very low. This indicates that sulphur reduction happened faster during exponential phase. However, these parameters could not generate a unique representative model for all studied coal particle sizes. The results also show that *Kc* values obtained from the non-linear regression were not constant and were shown to be much higher than S_T values ($Kc >> S_T$). According to Nkhalambayausi-Chirwa and Wang (2001), the reaction rate approaches first order when the half velocity coefficient K_c is much greater than S_T. Table 6.8 shows applied K_c and k_{mc} Calorific values parameter on the Monod type equation.

Table 6.7: Calorific values parameters estimation obtained for Monod type equation

Parameters	–0.85 mm	–2.30 +1.00 mm	–4.60 +2.30 mm	+4.60 mm
K_c	101221.790	112478.932	113405.334	123445.101
k_{mc}	10.234	11.223	12.201	15.235
R	0.987	0.998	0.990	0.977
R^2	0.987	0.996	0.987	0.965
SEE	1.452	1.789	1.342	1.301

**SEE: Standard Error of Estimates

Table 6.8: Applied K_c and k_{mc} Calorific values parameter on the Monod type equation

Parameters	Kinetic Equation showing parameters k_{mc} and K_c
0.85 mm	$t = 0.9578 \ln\left(\frac{CV_0}{CV}\right) + 1.09676\ E-05 \times (CV_0 - CV)$
–2.30 +1.00 mm	$t = 0.9457 \ln\left(\frac{CV_0}{CV}\right) + 1.04599\ E-05 \times (CV_0 - CV)$
–4.60 +2.30 mm	$t = 0.9022 \ln\left(\frac{CV_0}{CV}\right) + 9.16263\ E-06 \times (CV_0 - CV)$
+4.60 mm	$t = 0.0700 \ln\left(\frac{CV_0}{CV}\right) + 9.613400E-06 \times (CV_0 - CV)$

In Tables 6.9 – 6.11, the coefficient, $k_{m.t}$ in the second part of equation are insignificant compared to numerical coefficients in the logarithmic part. They are over 100 less than logarithmic coefficients. Therefore, if insignificant values are neglected, reduction rates are shown to correspond to a first order reduction equation Eq. 6.62.

$$S = S_0 e^{-km.t} \tag{6.62}$$

where *km.t* is a representative first order sulphur reduction rate coefficient

Table 6.9: Parameter obtained for the first order equation – sulphur content

Parameters	–0.85 mm	–2.30 +1.00 mm	–4.60 +2.30 mm	+4.60 mm
k_{mt}	0.974	0.561	0.0813	0.045
R	0.998	0.993	0.999	0.996
R^2	0.970	0.978	0.987	0.981

Table 6.10: Parameter obtained for the first order equation – ash content

Parameters	–0.85 mm	–2.30 +1.00 mm	–4.60 +2.30 mm	+4.60 mm
k_{mt}	0.353	0.267	0.178	0.179
R	0.988	0.979	0.988	0.979
R^2	0.969	0.989	0.977	0.968

Table 6.11: Parameter obtained for the first order equation – calorific value

Parameters	–0.85 mm	–2.30 +1.00 mm	–4.60 +2.30 mm	+4.60 mm
k_{mt}	1.256	2.561	1.135	3.343
R	0.983	0.977	0.997	0.986
R^2	0.980	0.988	0.974	0.973

6.4 Model Validation

6.4.1 Determination of order of reaction for sulphur content and ash content

The kinetic model of sulphur content and ash content were validated using several sets of experimental data available. To cross validate the proposed model structure with its estimated parameters, experimental data, obtained from batch scale study experiments were used. Figs. 6.2 – 6.9 shows that the parameter obtained by using the first order equation fitted quite well in the defined model.

6.4.2 Determination of order of reaction for calorific values model validations

To validate the proposed model structure with its estimated parameters, experimental data obtained from experiments were used. The correlation between the experimental data and the model-simulated data of the microbial desulphurization treatment are illustrated in Figs 6.10 – 6.13. The kinetic parameters were obtained through fitting experimental data to the kinetic model and minimizing the χ^2 values between the model data and the actual data. From these results, it can be noticed that the fitting between the model-simulated and the experimental data is satisfactory except for Fig. 6.6 where the model could not track well the CV profile. However, different from the sulphur and the ash contents, the experimental data for CV

values were found to correlate well with a second-order rate equation of the following Eq. 6.63:

$$\frac{dC}{dt} = kC^2 \qquad (6.63)$$

where k is the intrinsic kinetic rate constant whose value will depend upon the sulphur content.

The experimental data were found to correlate well with a second-order rate equation.

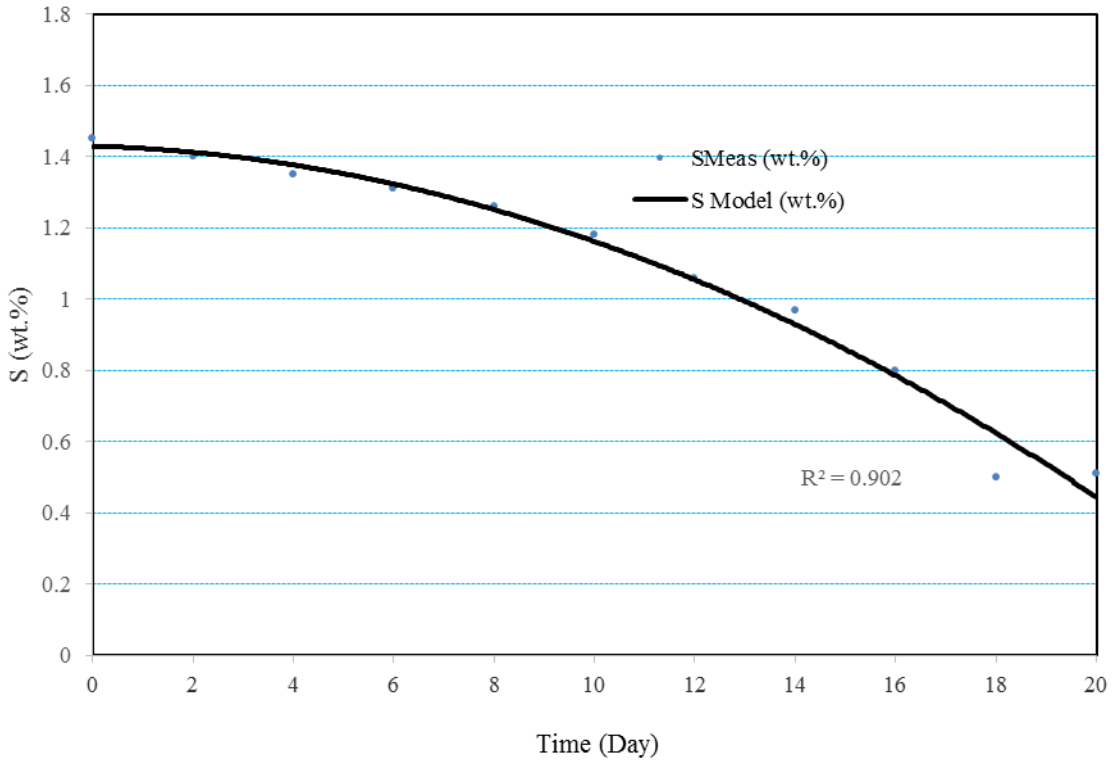

Figure 6.2: Sulphur model validation for coal particle size of – 0.85 mm

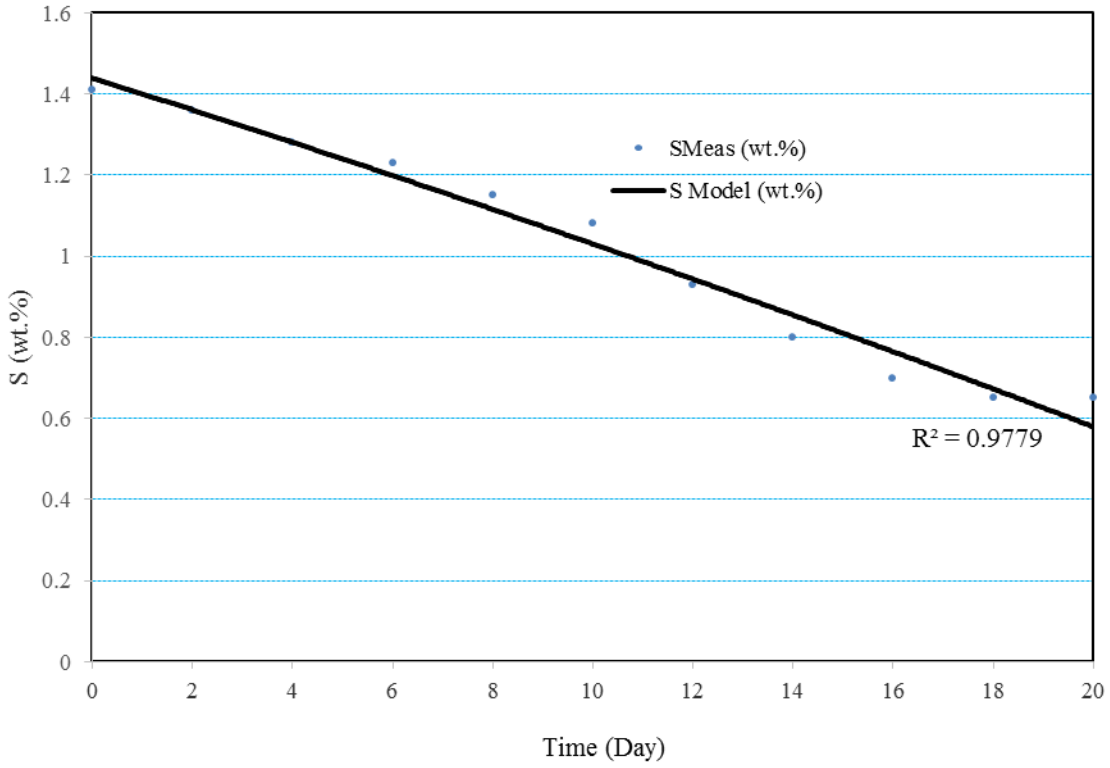

Figure 6.3: Sulphur model validation for coal particle size of −2.30 +1.00 mm

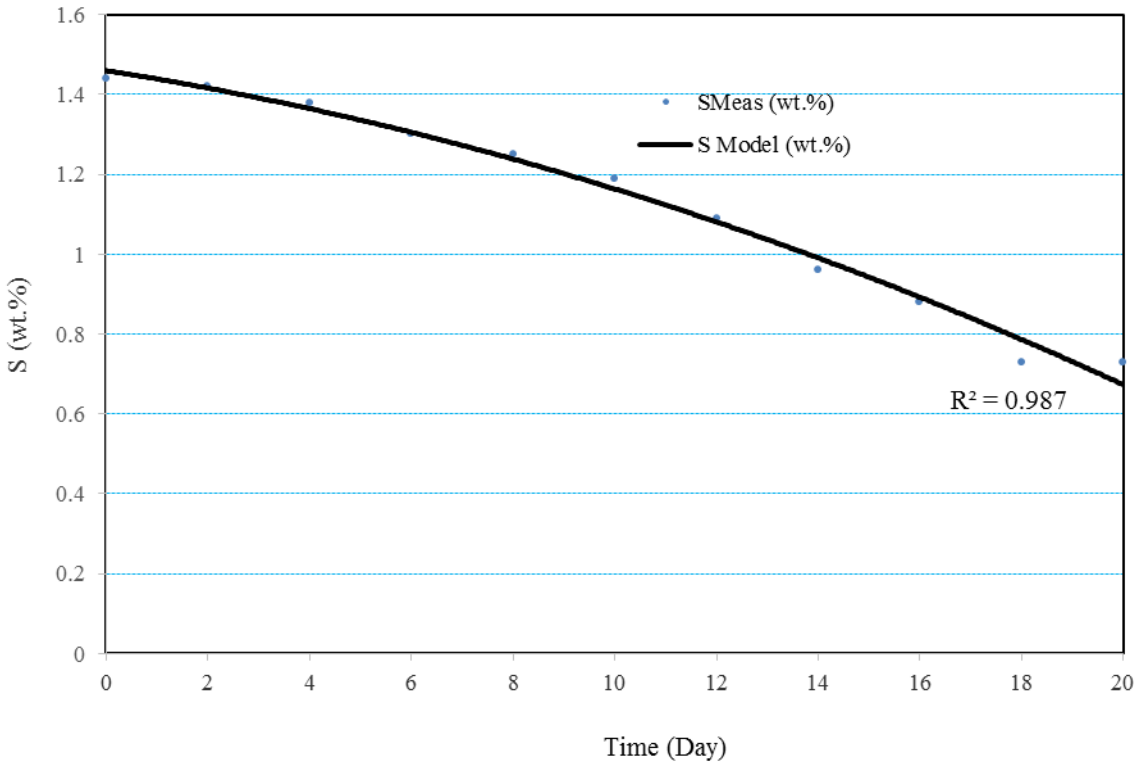

Figure 6.4: Sulphur model validation for coal particle size of −4.60 +2.30 mm

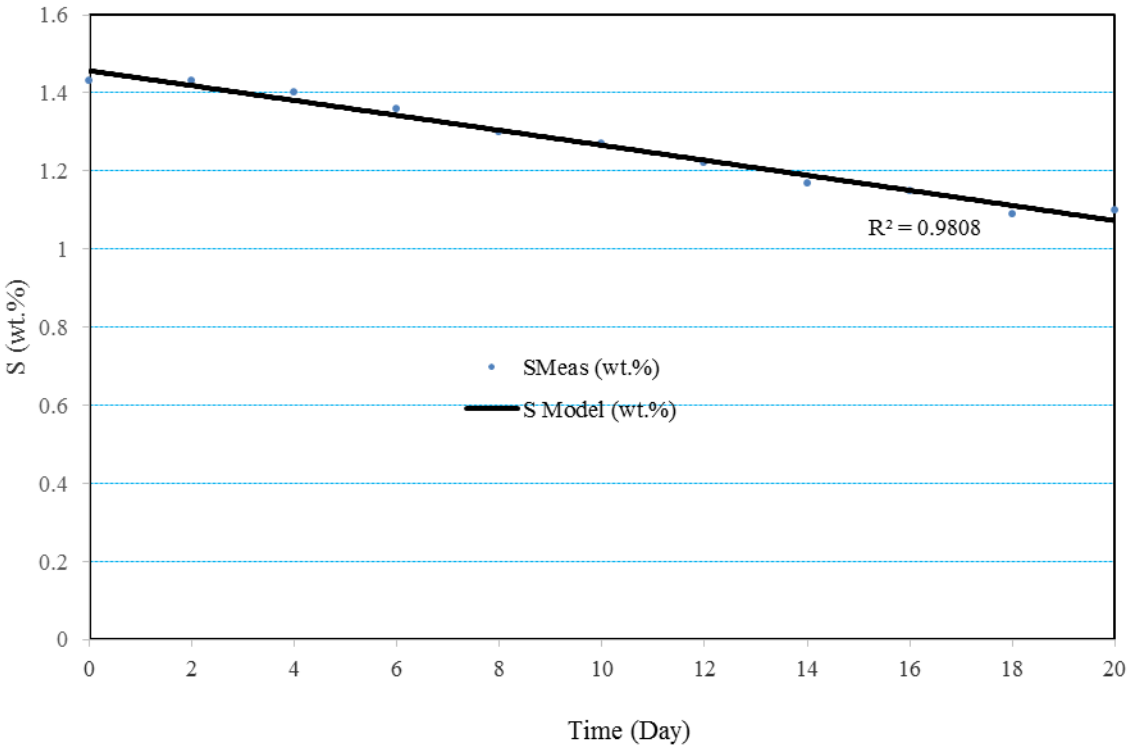

Figure 6.5: Sulphur model validation for coal particle size of +4.60 mm

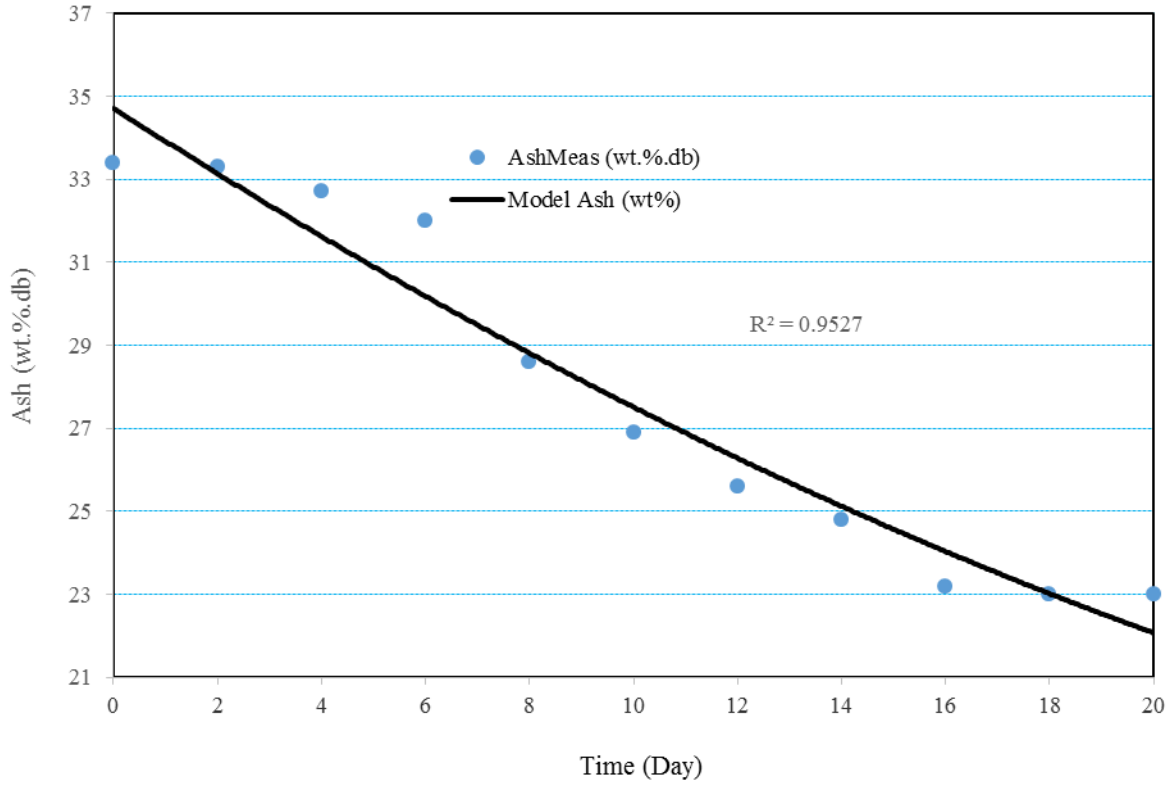

Figure 6.6: Ash content model validation for coal particle size of – 0.85 mm

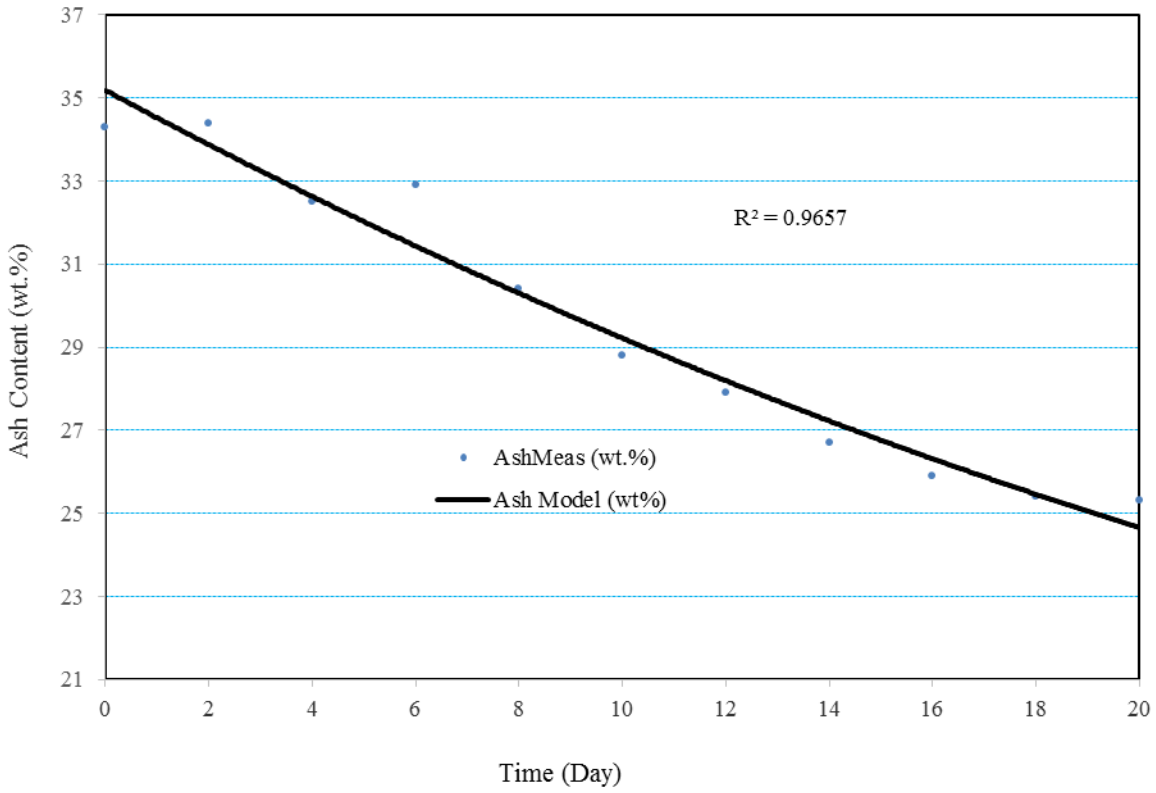

Figure 6.7: Ash content model validation for coal particle size of −2.30 +1.00 mm

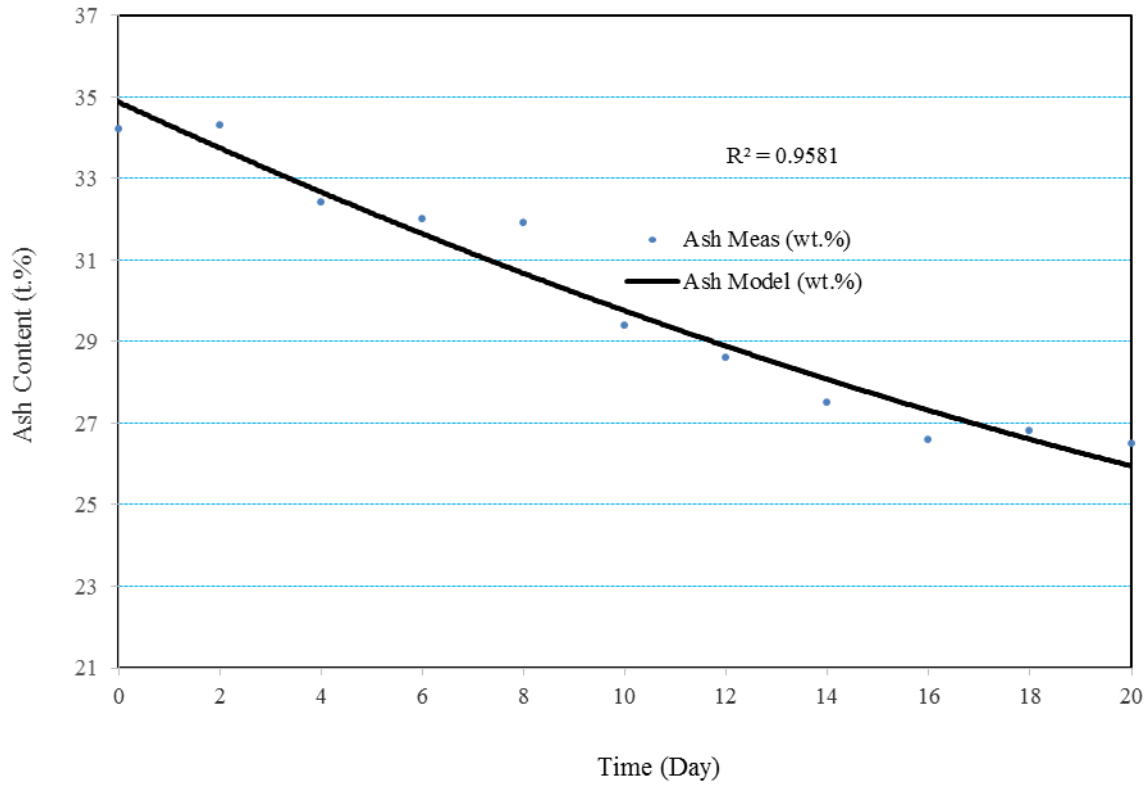

Figure 6.8: Model validation for coal particle size of −4.60 +2.30 mm

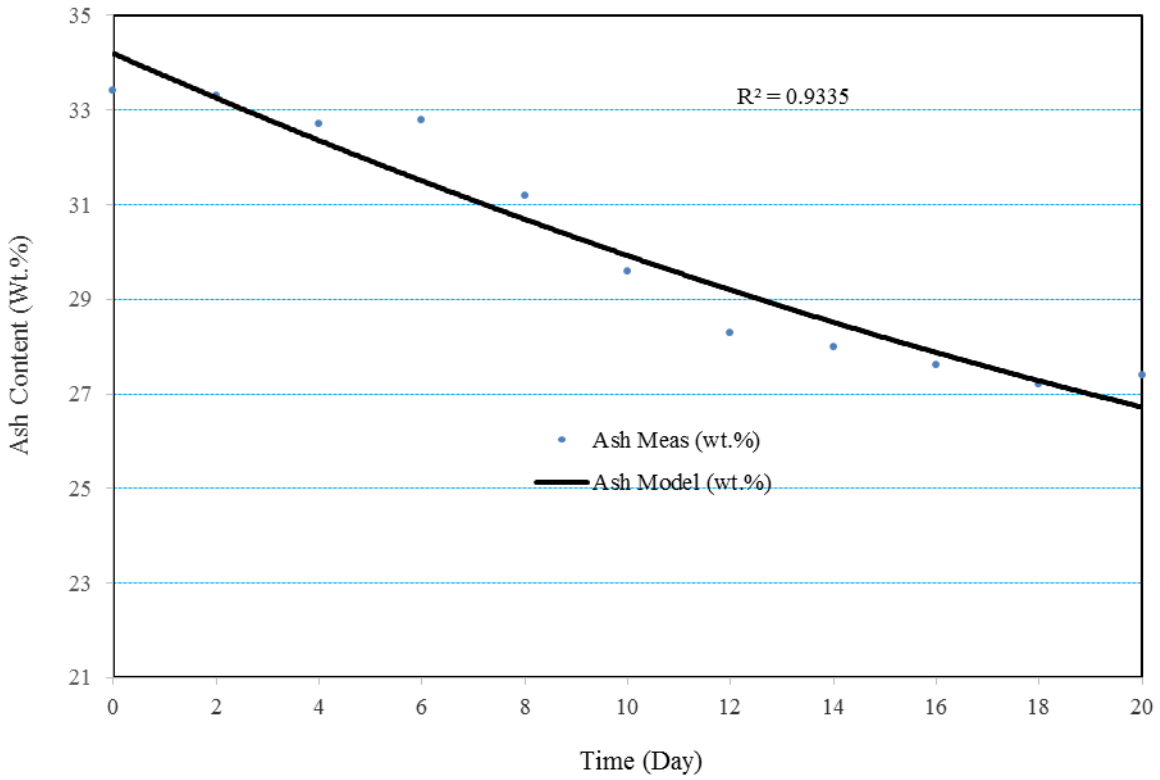

Figure 6.9: Ash content model validation for coal particle size of +4.60 mm

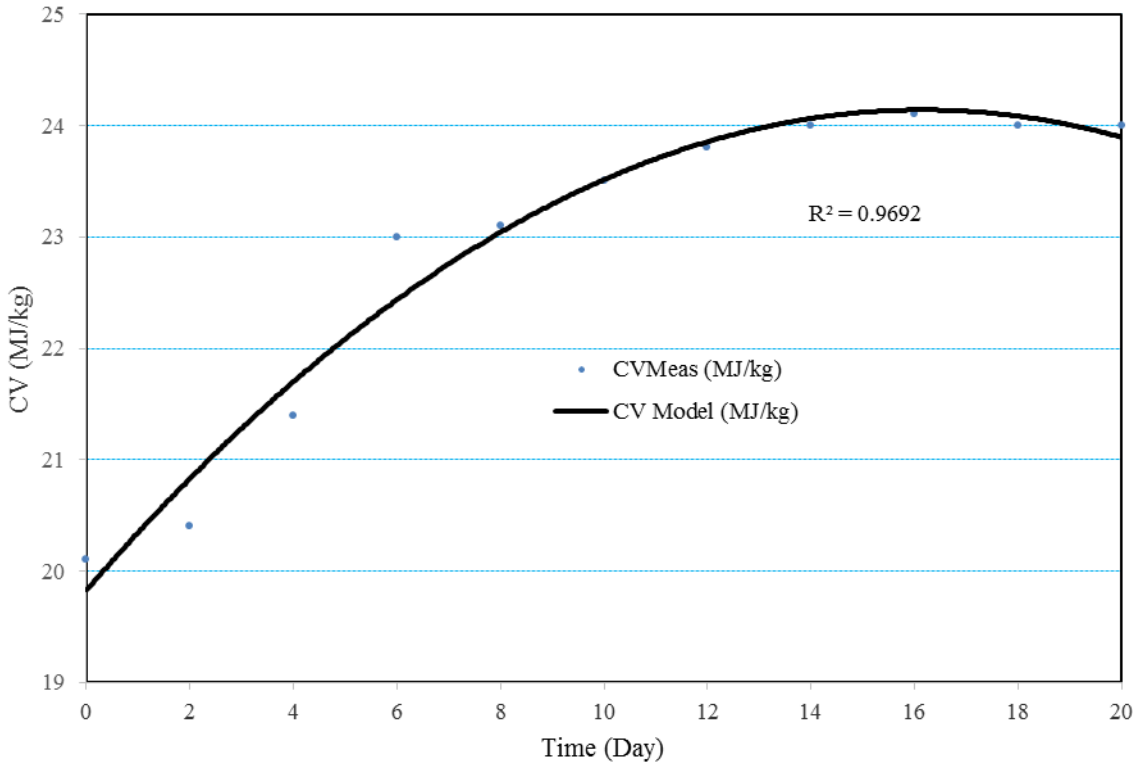

Figure 6.10: CV model validation for coal particle size of – 0.85 mm

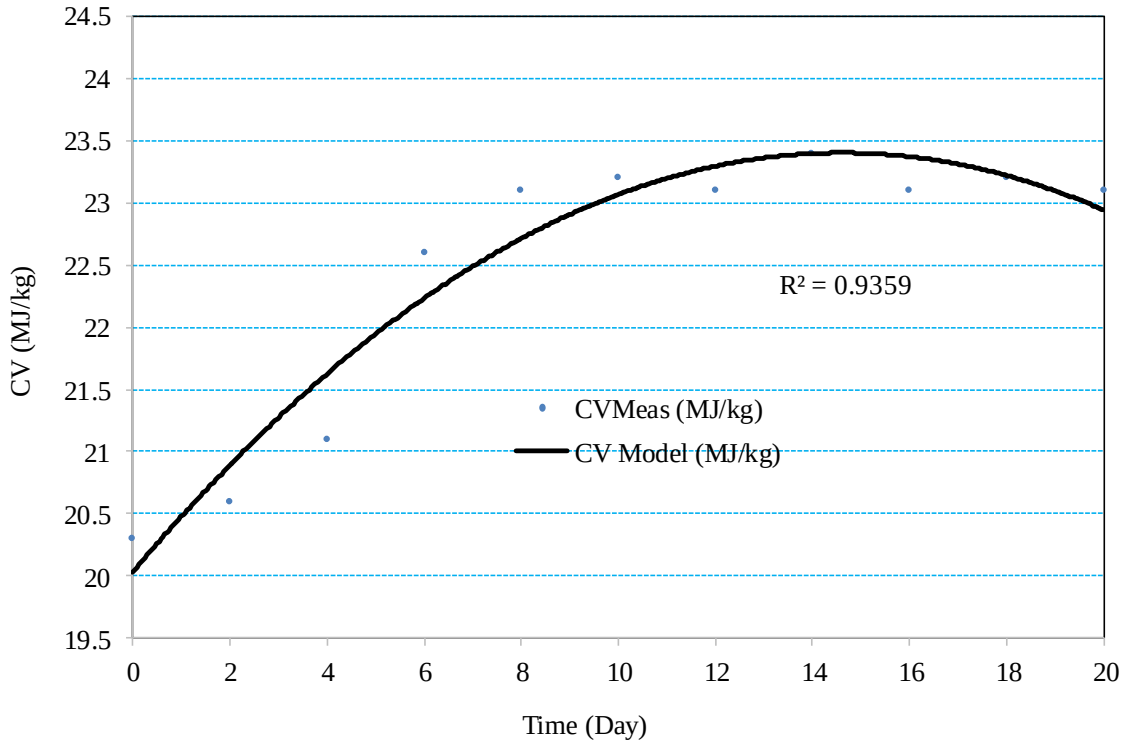

Figure 6.11: CV model validation for coal particle size of −2.30 +1.00 mm

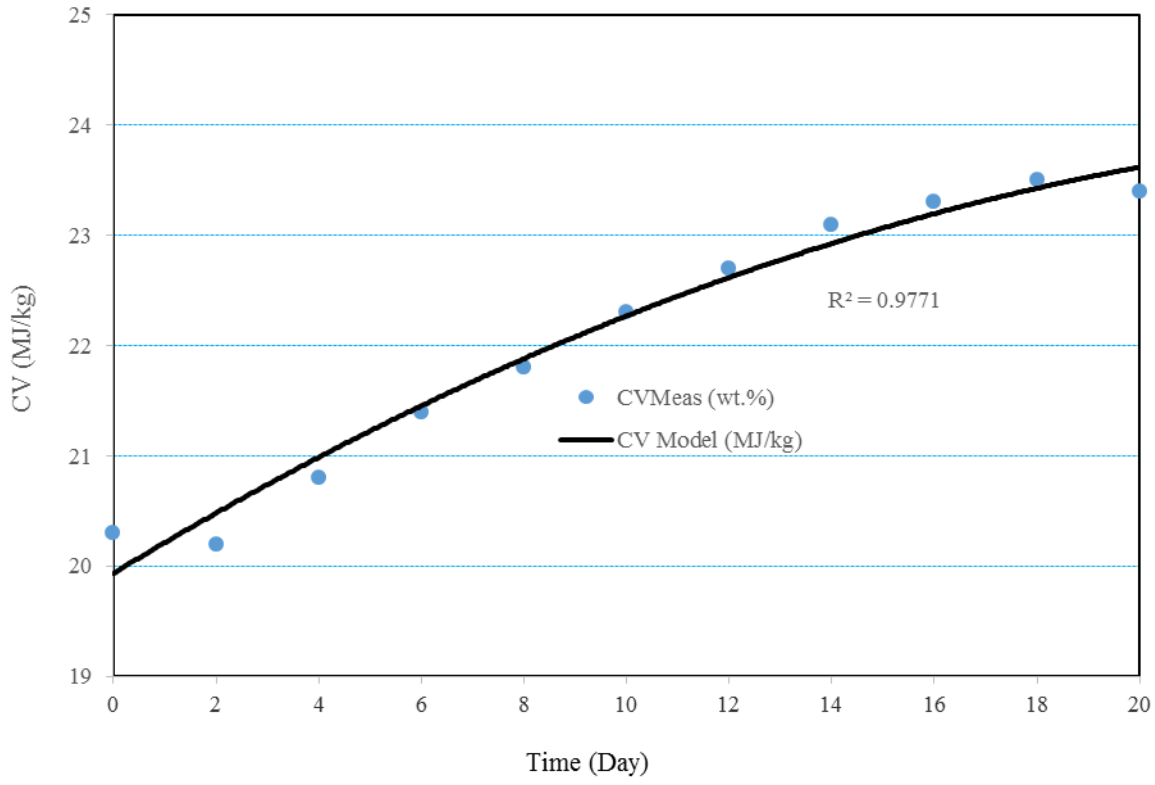

Figure 6.12: CV model validation for coal particle size of −4.60 +2.30 mm

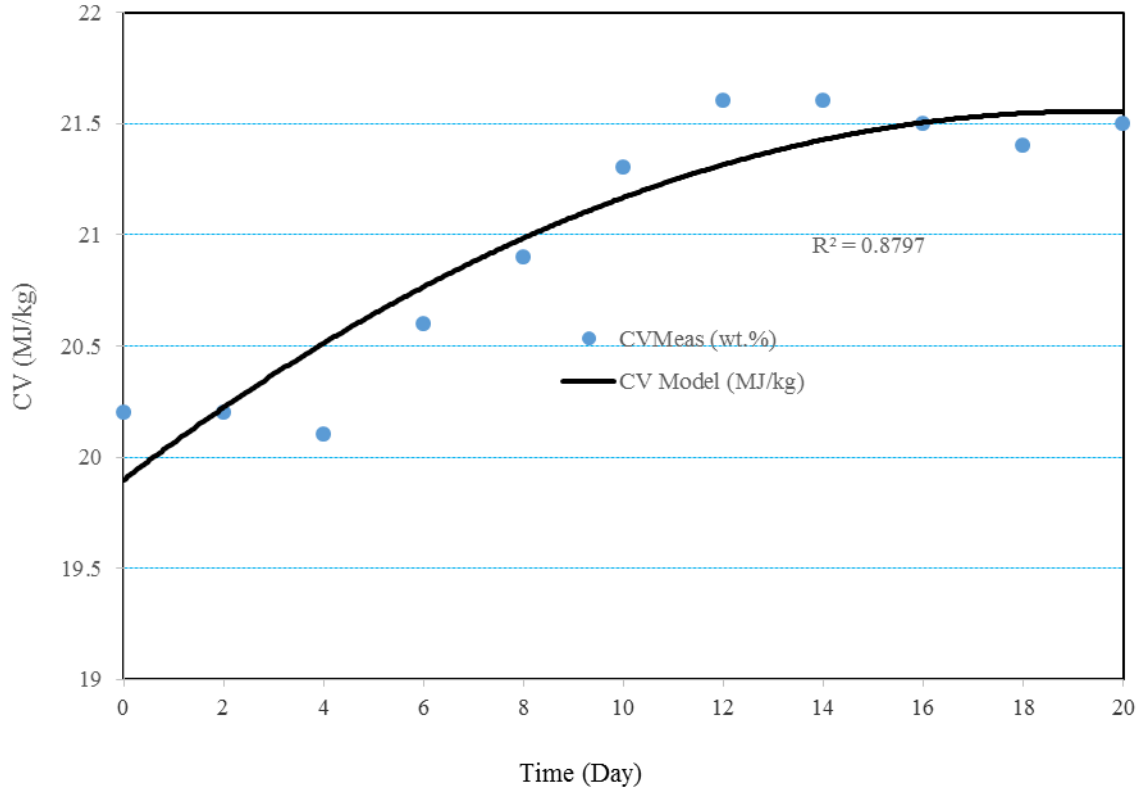

Figure 6.13: CV Model validation for coal particle size of +4.60 mm

6.5 Summary

The current section dealt with developing a model based on reaction kinetics, simulate microbial desulphurization process in a CSTR system and validate the model under various experimental conditions. The values of the kinetic parameters (K_s *and* k_{mc}) in the batch study were determined from the experimental data are shown in Table 6.3. These results are statistical correct since the regression coefficients R are above 97 % and all R^2 are above 95 %. However, the biodesulphurization rate coefficient, k_{mc} was determined to be very low. This indicates that sulphur reduction happened faster during exponential phase. These kinetic parameters could not generate a unique representative model for all studied coal particle sizes. The results also show that K_c values obtained from the non-linear regression were not constant and were shown to be much higher than S_T values ($K_c >> S_T$). From these results, it can be noticed that the fitting between the model-simulated and the experimental data is satisfactory. Though different from the sulphur and the ash contents, the experimental data for CV values were found to correlate well with a second-order rate equation. For the

conditions covered in the current study, the various parameters of the logistic model for sulphur content, ash content and calorific values analyses were established. The developed logistic model is able to accommodate all the characteristics that coal samples have during batch desulphurization. However, more research work needs to be done to establish more relationship covering the entire petrography, proximate and ultimate analyses.

CHAPTER 7

REDUCTION IN COAL FINES AND EXTENDED COKE PRODUCTION THROUGH RECYCLING CARBONIZATION TAR: ENVIRONMENTALLY CLEAN PROCESS

7.1 Introduction

Coke production plays an essential role in the South African national economy and will continue to increase in importance in the near future. In South Africa, coke making plants produce both metallurgical and market coke which is used by the steel plants and the ferroalloy industry respectively. Coke quality has been a topic of intense research for a long time and previous efforts attempted to develop best techniques for the production of good quality coke. Many researches and experiments that are well documented and commonly known to improve coke quality include coal pre-treatment (Jackman and Helfinstine, 1979); diesel and tar to coal blends (Chatterjee and Prasad, 1981); addition of petroleum coke to coal blends (Forrest and Marsh, 1981); oil (Kestner *et al.*, 1981); petroleum pitch (Gonzalez – Cimas and Patrick, 1986; Collin and Bujnowaska, 1994); pitch (Lin and Hong, 1986); breeze addition (Taylor and Coban, 1987); addition of aluminum metal in scrap form (Alvarez *et al.*, 1989); substitution of coking coals by non-coking coals (Das *et al.*, 2002); formed coke (Plancher *et al.*, 2002); chemical additives such as hydrochloric acid (Shevkoplyas, 2002); plastic addition (Nomura and Kato, 2006; Melendi *et al.*, 2011); stamped charging (Saxena *et al.*, 2010); coal-tar pitch (Benk, 2010; Benk and Coban, 2011); steam treated coking coals (Shui *et al.*, 2011) and briquetting charging (Díez *et al.*, 2013) have been carried out. Predicted operational challenges associated with most of these techniques include carryover of fines, explosion hazards, increased charging and pushing frequencies, thus limiting the full scale of application of these techniques. Moreover, other shortcomings surrounding the implementation included high cost of reagents, insufficient additives stock and cost of converting current top-charged coke oven batteries to include different charging is so high that is not economically viable to pursue.

In the coke – making set up, oven charging process generates significant amounts of waste in the form of coal fines that ends up being discarded. The use of coal fines is becoming an issue due to high Quinoline Insoluble (QI) formation during the carbonization process, additional coal loses and to the greater likelihood of spontaneous combustion and acid mine

drainage as well as carryover or enhancement of carbon deposition in the upper parts of coke ovens (Nakagawa *et al.,* 1998). This will not only endanger coke – making personnel through occupational diseases as well as fatalities but also bring about possible coke – making plant closures. According to various authors (Krebs *et al.,* 1996; Nakagawa *et al.,* 1998), carbon deposition brings about high resistance of pushing the coke, narrowing of the cross – section of the ascension pipes, giving rise to numerous complications in oven maintenance. Furthermore, depletion of coking coal deposits, the comparatively high price of prime coking coals and their scarcity worldwide generate the need to develop new clean coal technologies to maintain coke production levels for years to come. The earlier statement is supported by another case mentioned by Nomura and Arima (2017) who mentioned that one of the most significant focuses for the coke making industry today is the future depletion of coking coals that forms good quality coke.

Carbonization tar is a kind of toxic hazardous industrial solid waste produced in the process of coke making. Carbonization tar is currently being used in chemistry and refractory material industry, production of synthetic carbon materials or electrodes for the metallurgy and in carbon composites technology (Mikociak *et al.,* 2014). The off-specification carbonization tar is usually reported pertaining to QI and MIT values and has significant implications on its use as binder material. The off-specification carbonization tar poses storage requirements, plant availability complications and landfill disposal that require some premium budget. Therefore, partial substitution of more expensive coking coals with carbonization tar in order to lower coal blend cost and minimize carbonization tar waste disposal is becoming more critical to the successful coke production in a competitive market.

The addition of carbonization tar into coal blend was chosen in the current study, as it is one of the by-products of the coke making process, hence readily available and a relatively inexpensive hazardous material. Even though the possibility of using tar as an additive in coal blends has been studied, its influence on coal blending not only based on coke properties but also from the point of view of proximate analysis has not been discussed. Additionally, its environmental pollution impact analysis coupled with economic assessment has not yet been precisely evaluated. The principal aims of the present study were to assess the effect of adding carbonization tar to an industrial coal blend. Special emphasis was placed on carbonization tar recycling, coal fines reduction, coal blend cost analysis, extended coke production and improved coke quality.

7.2 Results and Discussion

7.2.1 Characterization of blend coking coals

The coal blends used comprised mainly of New Zealand (NZ), United States of America (USA), South African (RSA) and Australian coals. Table 7.1 shows the results of the coking coal samples characterization. The coal blends contained between 0.65 – 1.08 wt.% sulphur content, 3.8 – 10 wt.% ash, and 24.5 – 37.2 wt.% volatile matter. The coal blend compositions were comprised of 35% RSA coal, 19% USA coal, 38% Australian coal and 8% NZ coal. Considering the results shown in Table 7.1, it can be seen that RSA coking coal (Coal A) is a low – rank non-coking Bituminous C coal with a Vitrinite Reflectance (RoVr%) of 0.71. The rank of both the NZ coking coal (Coal B) and the USA coking coal was classified as Bituminous B with the vitrinite reflectance of 1.10 to 1. 30 RoVr% respectively. The Australian coking coal C falls within the borderlines of Bituminous B and C (RoVr% = 0. 90). i.e. marginally out of the prime coking category and just like NZ coking coal (Coal B). The vitrinite reflectance (RoVr %) of these coking coals are commonly accepted as a rank parameter indicating the rank or the degree of coalification of the coal, which controls the coking capacity in the vitrinite macerals in the coal (i.e. the properties of swell, plasticity and fusion).

Table 7.1: Coking coals origin and proximate properties

Coal	Origin	Blend %	FC (wt.% db)	VM (wt.% db)	Ash (wt.% db)	Moisture (wt.% db)	R_oVr (%)	SD (δί) RoVr (%)	FSI (ISO)	S (Pyritic)	S (SO_4)	Total S
Coal A	RSA	35	47.0	37.2	10.0	5.8	0.71	0.028	6.0	0.12	0.01	1.06
Coal B	NZ	8	57.3	32.0	3.8	6.9	1.12	0.034	9.6	0.12	0.01	1.00
Coal C	Australia	38	58.9	24.5	9.8	6.8	0.90	0.042	8.3	0.10	0.01	0.65
Coal D	USA	19	60.0	26.7	6.9	6.4	1.32	0.036	8.5	0.13	0.01	1.08

VM: volatile matter; db: dry basis; FSI: Free Swelling Index; FC: Fixed Carbon; S: Sulphur; R_oVr: Reflectance; SD: Standard Deviation of Reflectance; NZ = New Zealand;

RSA: Republic of South Africa; USA: United States of America

The coal macerals detected in the coking coal samples are comprised of vitrinite, liptinite, semifusinite, inertinite and pseudovitrinite, as shown in Table 7.2. The significant of macerals in the context of this study is that vitrine and liptinite groups of coking coals behave as reactive macerals during carbonization process (Varma, 2002). The vitrinite maceral group is grey in colour, with a reflectance that is between that of liptinite and inertinite. Generally, the coal rank is directly proportional to the volatile matter and carbon content in European and USA coals but due to the heterogeneous nature of RSA coals, rank in RSA is more reliably determined by vitrinite reflectance (Falcon and Ham, 1988). The liptinite macerals occur as fine particles embedded in a matrix of vitrinite components (Fig. 7.1). The coking coal from Coal C is rich in vitrinite followed by Coal D. Coal A has a low vitrinite content followed by Coal B. The coal A liptinite content of 4.6 vol. % is higher than the rest of the coking coals. According to Teichmüller (1989), liptinites were derived from hydrogen-rich plant organs and from decomposition products. A high inertinite content was detected in Coal B. Coal D has a high semifusinite content, 15.1 vol. %.

Table 7.2: Maceral analyses of individual coking coals

Maceral	Coal A	Coal B	Coal C	Coal D
Vitrinite [vol.%]	78.4	70.2	88.0	84.0
Liptinite [vol.%]	4.6	1.2	2.4	0.0
Semifusinite [vol.%]	3.5	5.1	5.0	15.1
Pseudovitrinite [vol.%]	8.0	0.8	1.4	0.0
Inertinite [vol.%]	5.5	13.0	3.0	0.0

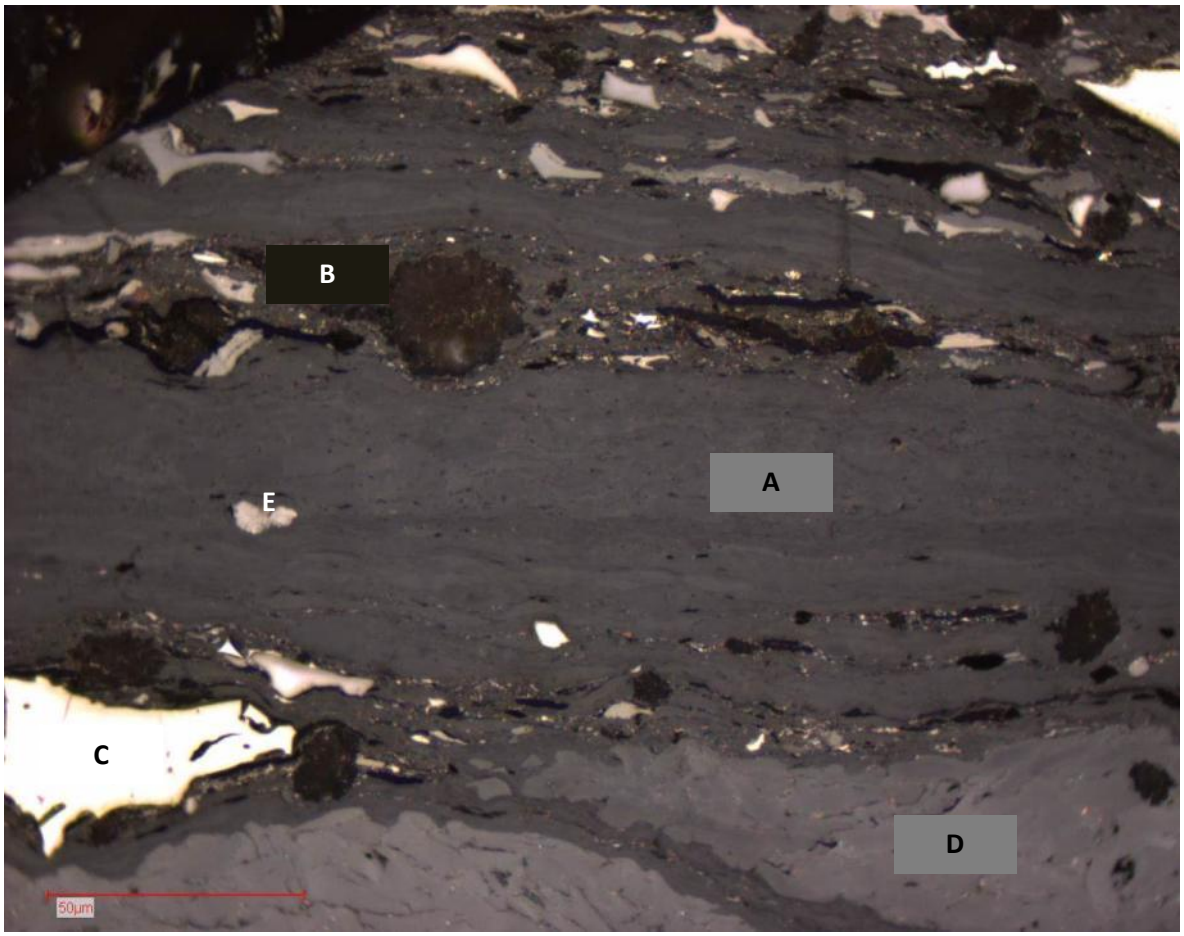

Figure 7.1: Typical macerals found in coking coal include A: Vitrinite, B: Liptinite, C: Semifusinite, D: Pseudovitrinite, E: Inertinite

7.2.2 Characterization of carbonization tar

Table 7.3 shows the properties of the carbonization tar used in this investigation. From the analyses, it was determined that the moisture content was 3.1 wt.% and 3.4 wt.%, against a target of ≤ 5 wt.%. Low moisture content in carbonization tar is considered acceptable as high moisture content brings about bulk density effects on the coal blend. Low ash content of 0.04 wt.% was observed against a target of 0.16 wt.%. Ash content in carbonization tar is necessary as it may cause reduced ash content when added to a high ash content coal blend. The specific gravity (SG) of 1.12 g.cm^{-3} and 1.15 g.cm^{-3}, against a target of 1.20 gcm^{-3} was reported. Furthermore, the flue temperature of 1230 °C and 1233 °C were observed against a target of 1233 °C.

Table 7.3: Properties of Carbonization tar with various moisture content

	H_2O (%)	MIT (wt.%)	Ash (wt.% db)	QI (wt.%)	SG (gcm^{-3})	Flue Temperature (°C)
Target	5.0	6.0	0.16	6.0	1.20	1233
Sample 1	3.4	7.3	0.04	7.8	1.12	1230
Sample 2	3.1	7.2	0.04	7.4	1.15	1233

MIT – Matter Insoluble in Tar; db – dry basis; QI - Quinoline-Insoluble; SG –Specific Gravity

QI is used to determine the quantity of solid and high molecular weight material in Carbonization tar. According to Patrick *et al.*, (1983), the presence of inert QI particles influences the anisotropy present in the carbonised tar, and the current work reveals that the rank of the coal from which the carbonization tar was obtained also has a marked influence. High QI values of 7.4 wt.% and 7.8 wt.% against a target of 6.0 wt.% are reported. These values are in agreement with classification made by Panaitescu and Predeanu (2007), who reported QI values in the precursor carbonization tar in the range of 5 – 8 wt.%, also in accordance with the study of Díez *et al.* (1994) who characterised coal tar as follows: Ash (0.04%), SG (1.17), mean flue temperature (1230) and QI (2.9). Matter Insoluble in Tar (MIT) of 7.2 wt.% and 7.3 wt.% against a target of 6.0 wt.% was also recorded.

The carbonization tar characterisation required the use of a specialised analytical tool that can work over a range of molecular masses such as a GC-MS. Fig. 7.2 depicts the typical hydrocarbons found in carbonizationtar as indicated by GC-MS analyses. Table 7.4 shows about sixteen (16) predominant hydrocarbons were detected by GC-MS analyses.

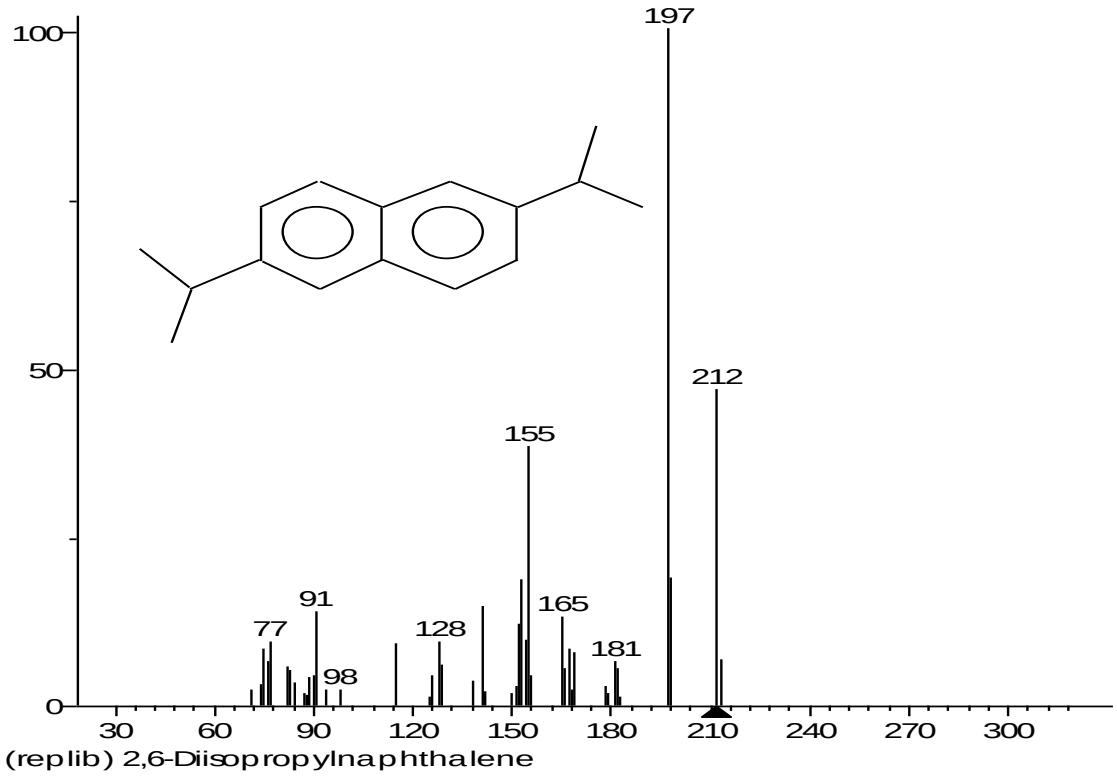

Figure 7.2: Typical hydrocarbons found in carbonization tar

Many investigators have studied the characteristics of coal tar. The results as shown in Table 7.4 are also in good agreement with those reported by other authors (Benk and Coban, 2011; Wang *et al.*, 2013; and Si *et al.*, 2017). The results obtained for these hydrocarbons are significant, confirming carbonization tar characteristics regarding its influence on coal blend binder quality.

Table 7.4: Qualitative data from GC-MS analysis of carbonization tar samples

No	RT(min)	Compound	MF	MW (g/mol)
1	18.01	Benzene	C_6H_6	78
2	19.50	Thiophene	C_4H_4S	84
3	21.45	Phenol	C_6H_6O	94
4	22.00	o-cresol	C_2H_8O	108
5	23.09	Xylenol	$C_8H_{10}O$	120
6	25.38	Naphthalene	$C_{10}H_8$	128
7	25.51	Quinoline	C_9H_7N	129
8	26.26	Methylquinoline	$C_{10}H_9N$	143
9	29.13	biphenyl	$C_{12}H_{10}$	154
10	30.22	Phenylpyridine	$C_{11}H_9N$	155
11	32.02	Carbazole	$C_{12}H_9N$	167
12	33.24	Dibenzofuran	$C_{12}H_8O$	168
13	34.10	Anthracene	$C_{14}H_{10}$	178
14	36.00	Benzoquinoline	$C_{13}H_9N$	179
15	36.44	Fluorenol	$C_{13}H_{10}O$	181
16	38.07	Pyrene	$C_{16}H_{10}$	202

RT = Retention Time; MF = Molecular Formula; MW = Molecular Weight

7.2.3 Effect of carbonization tar addition on coal proximate analyses

The effect of carbonization tar addition on the proximate analyses of coal blends was evaluated and the results are shown in Table 7.5. Ash content, sulphur content and volatile matter content of individual coking coal values are additive properties which means the value of the coal blend will be the average value of the individual coking coals within the blend. The rule of the mixture is the simplest way of predicting a coal property from its coal blend using Eq. (7.1):

$$Z_i = \sum_{i=1}^{n} x_i Z_a \qquad (7.1)$$

where:

Z_i = the property such as ash content, sulphur content and volatile matter content of the coal blend,

Z_a and x_i = the property and the percentage mass fraction of coal *i* respectively

n = the number of coals blended.

Eq. (7.1) makes the implicit, but a reasonable assumption, that volume fractions and mass fractions of the blend components are the same, i.e. that all coals have the same density.

Coking coal is commonly distinguished from thermal coal in having lower contaminants of ash content. Varma (2002) published typical values of low ash content ranges. Prior to carbonization tar addition, the measured coal blend ash content of 9.20 wt.% was reported as opposed to 8.84 wt.% calculated using Eq. 7.1. A small standard deviation of 0.36 can be observed for the ash content in the coal blend. After addition of 2.0 wt.% carbonization tar, the ash content was significantly reduced to 8.55 wt.%. The ash content remained constant with further increase in carbonization tar addition up to 8 wt.%. The reduction in ash content and constant values of ash content with further carbonization tar addition can be attributed to the low ash content available in the carbonization tar and low percentage of carbonization tar added to the coal blend respectively. These findings were as expected since coal charge is one of the most important parameters that influence the coke size.

The volatile matter content of the coal blend affects both coke quantity and coke quality. In this study, as the carbonization tar increased to 2 wt.%, the coal blend volatile matter decreased from 31.1 to 30.0 wt.%. On the other hand, as the carbonization tar increased from 4 wt. % to 8 wt. %, the volatile matter content remained constant. The volatile matter content obtained for the carbonization tar addition was in the same range of 30.0 – 30.4 wt.%. The volatile matter of the coal blends was expected to decrease with carbonization tar addition because coking coals with high volatile matter content are being replaced by carbonization tar, which has low volatile matter content. Conclusively, the ash content, sulphur content and volatile matter content for the coal blends under consideration were found to be additive.

Table 7.5: Proximate Analyses

Coal Blend	Ash (wt.% db) Measured	Ash (wt.% db) Eq.1	Sulphur (wt.% db) Measured	Sulphur (wt.% db) Eq.1	VM (wt.% db) Measured	VM (wt.% db) Eq. 1
0 wt.% Tar	9.20	8.84	0.87	0.90	31.1	30.0
2 wt.% Tar	8.55	8.66	0.99	n.a	30.0	n.a
4 wt.% Tar	8.63	8.66	0.98	n.a	30.1	n.a
6 wt.% Tar	8.62	8.66	0.97	n.a	30.2	n.a
8 wt.% Tar	8.66	8.66	0.99	n.a	30.4	n.a

n.a: not available; VM: volatile matter; db: dry basis

7.2.4 Effect of carbonization tar addition on coke sulphur content

Table 7.6 shows coal – coke sulphur relationship as a function of carbonization tar addition. Prior to carbonization tar addition, the measured coal blend sulphur content of 0.87 wt.% was reported as opposed to 0.90 wt.% calculated using Eq. 7.1. Therefore, the sulphur content of individual coking coals confirmed to be additive with a low standard deviation of 0.03 as per the standard statistical procedure. The sulphur content increased from 0.87 to 0.99 wt.% at carbonization tar addition of 2 wt.% and remained constant at 0.99 wt.% with further carbonization tar addition. Although the coal blend sulphur content increased, it is still within the acceptable range of <1 wt.%. The sudden increase in sulphur content with carbonization tar addition might be due to hydrogen sulphide (H_2S) and sulphur in the carbonization tar. According to a study by Hou *et al.* (2018) who investigated transformation of sulphur and nitrogen during pyrolysis of Shenmu coal found that 43.7 wt.% of coal blend sulphur was transferred into coal tar with main forms of benzothiophene (52 wt.%), dibenzothiophene (41%), thiophene (0.15 wt.%) and the other (6.85 wt.%). About 56.2 wt.% of coal blend sulphur was transferred into retorting gas with main forms of H_2S, carbonyl sulphur and a small amount of SO_2,(Hou *et al.*, 2018). The remaining 0.1% sulphur was possibly lost during the carbonization process. Sulphur is the single most influential chemical component in coal that affect coke CSR, therefore, it is undesirable that carbonization tar increases coal blend sulphur although the increase was within the acceptable margin of < 1 wt.%.

Coke sulphur content was not affected by carbonization tar addition. The constant sulphur content in the coke with an increasing carbonization tar addition is attributed to no increase of organic sulphur in the parent coal blend. It is an established fact that coke sulphur content is dependent upon sulphur content of the precursor coal blend as revealed in Eq. 7.2 that shows the empirical relationships between sulphur content of cokes and those of precursor coals:

$$\text{Coke Sulphur} = 0.66\ (\text{Coal Sulphur}) + 0.184 \qquad (7.2)$$

When coal sulphur content was applied on Eq. 7.2, Ndaji & Imobighe Model gave averaged 0.5 wt.% error as shown in Table 7.6. This error can be attributed to the differences in the quality of the individual coals in the blends. The analyses all fall within acceptable margins of error according to the standard deviation for that particular analysis.

Table 7.6: Coal – coke sulphur relationship as a function of tar addition

	Coal Sulphur (wt.% db)	Coke Sulphur (Actual)	Coke Sulphur (Ndaji & Imobighe Model)	Error
0 wt.% Tar	0.87	0.90	0.76	0.14
2 wt.% Tar	0.99	0.89	0.84	0.05
4 wt.% Tar	0.98	0.87	0.83	0.04
6 wt.% Tar	0.97	0.91	0.82	0.09
8 wt.% Tar	0.99	0.89	0.84	0.05

db: dry basis

7.2.5 Effect of carbonization tar addition on ash content of cokes

Coke ash content is the most important parameter which influences the resultant coke size. Table 7.7 shows the ash content of coal blend and cokes over a range of 0 – 8 wt. % carbonization tar addition. The ash content of cokes decreased from 12.5 at 0 wt. % and 2 wt. % to 11.8 over 4 – 8 wt.% carbonization tar addition range. This finding was expected as low ash content in the carbonization tar is substituting coking coals with high ash content. Therefore, it is desirable that carbonization tar addition decrease ash content of cokes to an acceptable range. According to Ndaji and Imobighe (1989), an excessive ash (> 12. 5 wt.%) in metallurgical coke gives rise to high slag volume, result in high coke rate that arises from the accelerated oxidation of coke by CO_2 and O_2 which is caused by the catalytic activities of the numerous metallic oxides that are contained in the coke ash as well as low efficiency of the blast furnace. It is well established that coke ash content is dependent upon coal blend ash content as revealed in Eq. 7.3 that shows the empirical relationships between ash content of cokes and those of precursor coals:

$$\text{Coke Ash} = 1.32\ (\text{Coal Ash}) + 0.53 \qquad (7.3)$$

When coal ash was applied on Eq. 7.3 Ndaji & Imobighe Model gave error of 0.10 wt.% as shown in Table 7.7 below. This error can be attributed to the differences in the quality of the individual coals in the blends. The analyses all fall within acceptable margins of error according to the standard deviation for that particular analysis.

Table 7.7: Ash content of cokes as tar increases

	Coal Ash	Coke Ash	Coke Ash (Ndaji & Imobighe Model	Error
0 wt.% Tar	9.2	12.5	12.6	0.10
2 wt.% Tar	8.5	12.3	11.8	-0.50
4 wt.% Tar	8.6	11.8	11.9	0.10
6 wt.% Tar	8.6	11.8	11.9	0.10
8 wt.% Tar	8.6	11.8	11.9	0.10

7.2.6 Effect of carbonization tar addition on coal Roga

Roga index is determined as a measure for the swelling performance and coking power of coals and their associated blends (Collin and Bujnowaska, 1994). Fig. 7.3 depicts the relationship between Roga and carbonization tar addition. As carbonization tar addition increases, Roga increases exponentially with a good correlation factor of the variance of 81.3%. The results are in good agreement with the view that the higher the Roga index, the better the caking properties of coals.

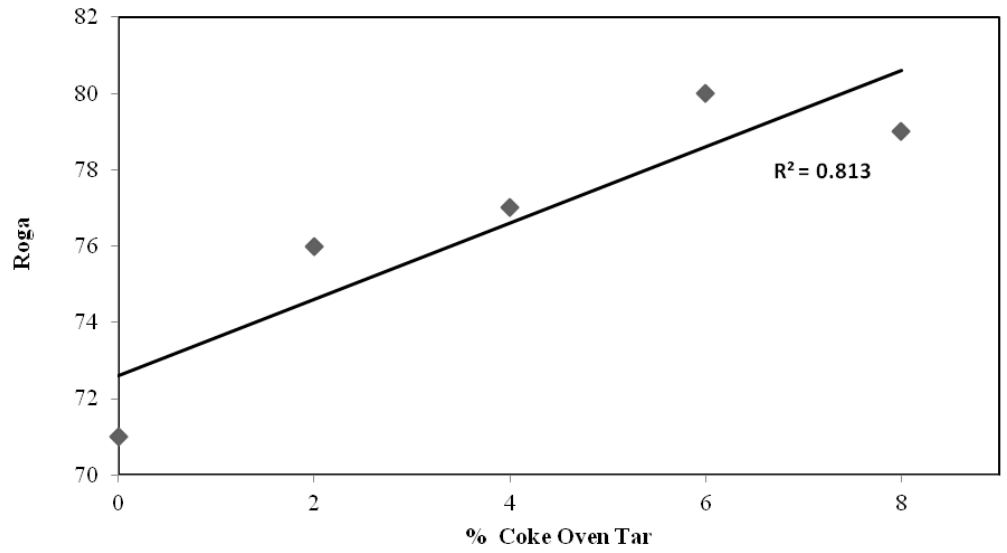

Figure 7.3: Relationship between Roga and carbonization tar addition

7.2.7 Effect of carbonization tar addition on ash composition and phosphorus in coal blend

Table 7.8 shows the effect of carbonization tar addition on ash composition. It can be seen from Table 7.8 that the rest of ash composition with the exception of phosphorus showed no significant change with carbonization tar addition. However in the case of phosphorus, as carbonization tar addition increases, phosphorus content decreases from 0.038 wt.% to 0.024 wt.% against a target of P ≤ 0.036 wt.%. It is desirable that carbonization tar addition reduced phosphorus content to an acceptable level.

Table 7.8: Ash composition in various coal blends (wt.%, db)

Coals	Na_2O	MgO	Al_2O_3	SiO_2	P	Fe	K_2O	CaO	TiO_2	Mn
0 wt.% Tar	0.05	0.04	2.5	5.0	0.038	0.50	0.12	0.16	0.21	0.006
2 wt.% Tar	0.05	0.06	2.6	4.6	0.035	0.60	0.13	0.18	0.22	0.008
4 wt.% Tar	0.04	0.04	2.6	5.8	0.028	0.70	0.14	0.15	0.21	0.010
6 wt.% Tar	0.03	0.04	2.2	5.0	0.024	0.60	0.13	0.17	0.20	0.009
8 wt.% Tar	0.04	0.05	2.1	5.2	0.023	0.60	0.14	0.13	0.21	0.009

7.2.8 Effect of carbonization tar on basicity and catalytic Index

Basicity Index (BI) within the ash composition is defined as the ratio of the sum of the fraction of the basic compounds in the ash (CaO, MgO, K_2O, Na_2O and Fe_2O_3) to the fraction of the acidic compounds (SiO_2 and Al_2O_3) in the ash. Hattingh *et al.* (2011) reported the BI of the ash as the ratio of non-catalytic constituents, i.e.: Al_2O_3 to SiO_2 present in the ash. As shown in Table 7.9, BI decreased from 0.35 to 0.43 at 2.0 wt.% carbonization tar addition and stays uniform up to 8.0 wt.%. On the other hand, Catalytic Index (CI) was calculated using the information provided in Table 7.9 above and the obtained values were reported in Table 8.9. Different from BI, CI decreased from 0.35 to 0.25 at 2.0 wt.% carbonization tar addition and stays constant up until to 8.0 wt.%. This is good results because the catalytic index has a significant influence on the coke quality and then lower it is, the better. The difference between CI and BI can be attributed to the fact that BI calculated in this study just give an indication and is not comprehensive as CI calculated from Eq. 7.4.

$$CI = \left(\frac{Fe_2O_3 + CaO + MgO + K_2O + Na_2O}{SiO_2 + Al_2O_3} \right) \quad (7.4)$$

Table 7.9: Basicity Index versus carbonization tar addition

Coal Tar	Eq. 3. CI	Hattingh *et al.* BI
0 wt.% Tar	0.35	0.37
2 wt.% Tar	0.26	0.43
4 wt.% Tar	0.26	0.43
6 wt.% Tar	0.25	0.43
8 wt.% Tar	0.26	0.43

7.2.9 Effect of carbonization tar addition on Free Swelling Index (FSI) and G values

Free Swelling Index (FSI) test is used to determine the agglomeration or swelling properties of coal and its blend. Therefore, FSI indicates the caking ability of coal blend through swelling behaviour. The effect of carbonization tar addition on FSI is shown in Table 7.10. As shown in Table 7.10, there was no change in FSI of 8.1 with carbonization tar addition. The analyses all fall within acceptable margins of error according to the standard deviation for that particular analysis. According to Collin and Bujnowaska (1994), FSI greater than 4 means well – coking coals and FSI greater than 7 indicates high – quality coking coal.

On the other hand, the *G* factor is one of the predicting tools used to determine coke quality. The effect of carbonization tar addition on *G* values is shown in Table 7.10. There was an insignificant change in G values of 1.01 with carbonization tar addition. According to Collin and Bujnowaska (1994), prime coking coals have *G* values between 1.02 and 1.1, and the current study results are in good agreement with Collin and Bujnowaska (1994) findings.

G –values can be calculated using Eq. 7.5 below:

$$G = \left(\frac{T_1 + T_3}{2}\right) \times \left(\frac{C + D}{C \times T_3 + D \times T_1}\right) \tag{7.5}$$

where, T_1 = Softening Temperature; T_3 = Maximum Dilatation Temperature; C = Maximum Contraction; D = Maximum Dilatation. Taking the case of 0 wt.% Carbonization tar addition, *G*

Value calculation is as follows:

$$G = \left(\frac{T_1 + T_3}{2}\right) \times \left(\frac{C + D}{C \times T_3 + D \times T_1}\right)$$

$$G = \left(\frac{381 + 426}{2}\right) \times \left(\frac{27.5 + 36.0}{27.5 \times 426 + 36 \times 381}\right)$$

$$G = 1.01$$

Similarly, all the other G - values were calculated using Eq.7.5 and results are recorded as shown in Table 10. Table 10 shows that G-values did not changer with carbonization tar addition and the analyses all fall within acceptable margins of error according to the standard deviation for that particular analysis. According to Collin and Bujnowaska (1994), good coking coals have *G* values between 1.02 and 1.1 that support the results of the current study.

7.2.10 Effect of carbonization tar addition on maximum contraction and dilatation

Maximum dilatation percentage specifies the coking properties of coking coal. Fig. 7.4 depicts the relationship between maximum dilatation and carbonization tar addition. It can be observed that as carbonization tar increased from 2.0 wt.% to 8.0 wt. %, maximum dilatation increased from 36.0 wt.% to 55.1 wt.%, respectively. According to (North *et al.*, 2018), the observed dilatation values for the coal blend confirm that it is necessary to obtain a completely fused coke structure of minimum M10, and therefore a high value of tensile strength.

The degree of maximum contraction of the coal blend charge seems to be one of the vital factors for coking pressure since on this project the final volume of coke relative to the initial coal blend charge. Fig. 7.5 depicts the effect of carbonization tar on the maximum contraction of coal blend. In the event of maximum contraction, at 2.0 wt.% to 8.0 wt.% carbonization tar addition, maximum contraction increased from 27.5 at 0 wt.% to 29.8 at 2 wt.% and remained constant with the further addition of carbonization tar up to 8 wt.%. The acceptable range for maximum contraction during coking is between 25 and 30 wt.%. The degree of maximum contraction of the coal blend charge seems to be one of the vital factors for coking pressure since this directs the final volume of the carbonised mass relative to the initial coal blend charge. Therefore, from a process safety perspective, the addition of carbonization tar did not increase the maximum contraction of coal blend beyond the acceptable range.

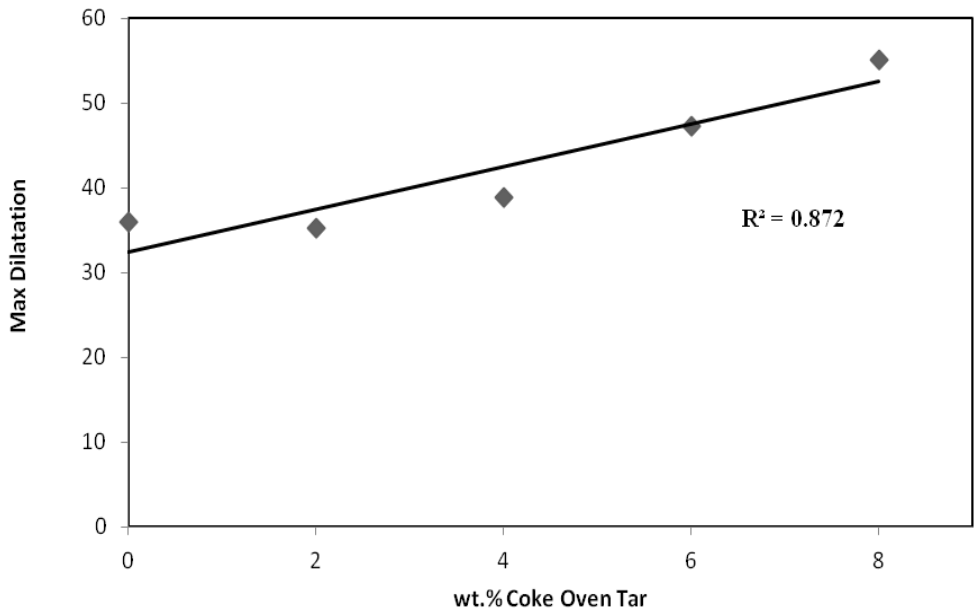

Figure 7.4: Relationship between Maximum Dilatation and carbonization tar addition

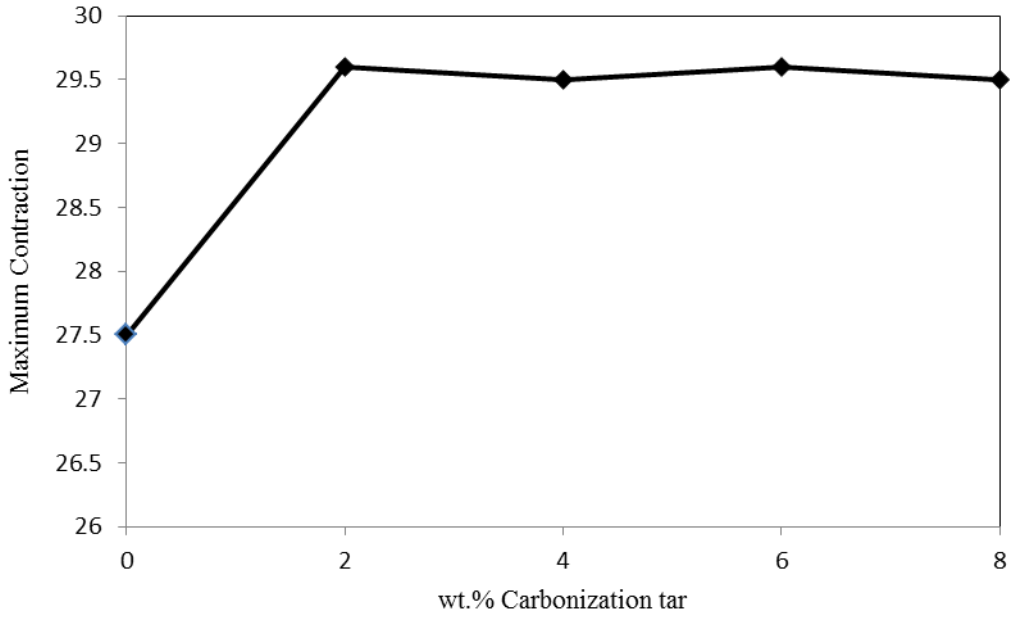

Figure 7.5: Relationship between Maximum Contraction and carbonization tar addition

Table 7.10: Coal blend Rheological properties

Plasticity	0 wt.% Tar	2 wt.% Tar	4 wt.% Tar	6 wt.% Tar	8 wt.% Tar
T_1 (°C)	381	381	375	360	372
T_2 (°C)	411	414	411	413	417
T_3 (°C)	426	465	462	483	474
Max Fluidity (ddpm)	466	476	488	489	491
Max Fluidity Temp. °C	357	360	367	388	397
Plastic Range °C	78	81	84	86	90
G value	1.01	1.01	1.01	1.03	1.04
FSI	8.1	8.1	8.2	8.2	8.3

T_1 = Softening Temperature; T_2 = Maximum Contraction Temperature; T_3 = Maximum Dilatation Temperature; FSI = Free Swelling Index,

7.2.11 Effect of carbonization tar addition on plasticity and fluidity

The fluidity of coal is considered one of the important parameter in the coke formation and in determining the quality of the coke produced. In order to ensure optimum coal particle interaction, it is important that the temperature intervals of the plastic state of each coal constituting a blend should overlap. The effect of carbonization tar addition on plasticity and fluidity was investigated and the results are reported in Table 7.10. Coal blend fluidity effects due to carbonization tar addition showed a linear increase from 466 ddpm at 0 wt. % to 491 ddpm at 8 wt. %. It is well known, that coal blend fluidity is a non-additive property and is considered as the superposition of the fluidities of the individual components at a specific temperature (Fernández *et al.*, 2012). The phenomena occurring in the plastic stage are influenced by the carbonization tar and are indicated by an increase in the plastic temperature range of 357 °C (0 wt. %) to 397 °C (8 wt. %). The results are in good agreement with the findings by Lin and Hong (1986) who noted the significance of pitches to improve the fluidity of coal blends. The results are further supported by an additional case, reported by Chatterjee and Prasad (1982), whose results reported an increase in maximum fluidity due to tar addition. The escalation in the maximum fluidity of most coal blends due to tar addition

plainly points out the improvement of the intrinsic coking characteristics of such blends due to carbonization tar additions. These results are consistent with the view that during heating through the thermoplastic range, the development of Gieseler fluidity is strongly dependent on a source of transferable hydrogens to cap radical species and thereby generate the low molecular weight 'solvating' species favourable to fluidity development.

7.2.12 Effect of carbonization tar addition on coal fines

In order to quantify the effect of carbonization tar addition on particle size distribution, crushed coal blend samples were collected and analysed. Table 7.11 shows the influence of carbonization tar addition on coal fines (– 0.106 mm). The coal blend with the carbonization tar addition of 2 wt.% reduced coal fines from 19 wt.% to 16 wt.%. As the carbonization tar increased to 4.0 wt.%, the coal fines were further reduced to 12 wt.%. With further carbonization tar addition to 6.0 wt.%, coal fines substantially reduced to 8.0 wt.%. Lastly, with the carbonization tar addition of 8.0 wt.%, the coal fines reduced to 6.0 wt.%. The overall percentage reduction in coal fines (powder) due to carbonization tar addition over a range of 2 wt.%, 4 wt.%, 6 wt.% and 8 wt.% was found to be 16%, 37%, 58%, 68% respectively.

The decrease in coal fines by means of carbonization tar addition may be attributed to the carbonization tar serving as a binder, wetting coal fine particles (which may cause suppressing of coal fines), which subsequently bind to larger particles. These results are important because more coal fines are less desirable owing to high dust, high QI formation, carbon deposits and bulk density increase. Yu et al. (1995) who mentioned that the bulk density is strongly affected by the particle size distribution support the latter. By reducing coal and coke fines, there is a considerable reduction in coal dust that personnel are exposed to, and a reduction in acid mine drainage when storing the discarded coal fines as well as a decreased likelihood of spontaneous combustion. In addition, coal dust being particulate in nature is a significant hazard factor that can cause explosions, pneumoconiosis and other health – related conditions. Therefore, coal fines reduction is a major plus for the industries concerned. Alternatively, using water as an additive to lower the coal fines dust is generally unfavourable for the coke quality. Nomura and Arima (2008) reported that a large amount of vaporized coal moisture (moisture content 20 wt.%) could break through the plastic layer and cause at the thin and uneven plastic layer in the case of wet coal charging, which can seriously affect the coking property. Secondly, as climate change takes effect, many countries

are facing serious water scarcity and many others will face severe water shortages within a short period.

Table 7.11: Effect of carbonization tar on coal fines

Coal Screens	0 wt.% Tar	2 wt.% Tar	4 wt.% Tar	6 wt.% Tar	8 wt.% Tar
– 0.106 mm (%)	19.0	16.4	12.3	8.2	6.0
	19.2	16.1	12.0	8.0	6.2

7.2.13 Coke hot and cold strength properties: Comparative study

In assessing coke quality, many parameters are used such as coke size, ASTM stability, CSR, CRI, grindability, hardness and various drum indices. Table 7.12 shows for blast furnaces the physical and chemical properties of coke produced at optimum conditions of 6 wt.% Carbonization tar addition compared together with those reported by other operation for European, Australian BHP Port Kembla, American and Japanese blast furnaces as reported by Díez *et al.* (2002). It should be noted that the abrasion resistance, M10 of 7.0 is greater than for Australian Port Kembla where a value of 6.5 was reported and falls within the European range. The lowest coke fragmentation, M40 of 67 is reported, compared to other furnaces operations that are reported. On the other hand, I20 of 80 is reported which is in good agreement with European Range of > 77.5.

Although the lower I40 of 51 is reported in the current study as compared with European range of 53 – 55, this value is still inside the usual range for coke quality used in coke making.

Coke size depends on fissured occurring in the coke. The mean coke size of 58 mm is however very much within the range of both Japan and European Range. The Australian Port Kembla and American Range reported lower mean coke size values than in the current study. It is well known that coke oven flue temperature is one of the factors controlling coke size (Nomura and Arima, 2013) which was found to be stable in the current study.

As shown in Table 7.12, the stability of 56 reflecting the load carrying strength or impact resistance of the coke for the current study was shown. Although the current study reported

less coke stability among other blast furnaces operations, the reported value has improved from the base coal blend and meets the requirement for the current blast furnace operation in the country (Mangena and du Cann, 2007). These results were in agreement with those reported by DuBroff *et al.* (1985), who mentioned that the stability index of about 50 to 60 is preferred for an acceptable strength metallurgical coke.

Table 7.12: Physical properties requirements of blast furnace coke in current operation

Properties	European Range[a]	Australian Port Kembla[a]	American Range[a]	Japan Range[a]	South African [Current Study]
Mean size (mm)	47 – 70	50	50	45 – 60	58
M40	> 78 – > 88	85	n.a	n.a	67
M10	< 5 – < 8	6.5	n.a	n.a	7.0
I40	53 – 55	n.a	n.a	n.a	51
I20	> 77.5	n.a	n.a	n.a	80
ASTM Stability	n.a	63.6	60	n.a	56
CRI	> 60	74.1	61	50 – 65	65
CSR	20 - 30	17.7	23	n.a	20

n.a: not available; [a]Díez *et al.* (2002).

The CSR and CRI are valuable parameters used to evaluate the behaviour of coke in a blast furnace. Therefore, CSR and CRI were also determined for all the samples. Fig. 7.6 shows the relationship between CRI and CSR of cokes produced as a function of the amount of carbonization tar added to the blend. A CRI of 65 against a target of CSR of 60 was achieved at the optimum 6 wt.% carbonization tar addition. Therefore, the coke from the carbonization tar addition follows the general trend observed for the CRI and CSR of the blast-furnace cokes: i.e. the lower the CRI, the higher the CSR index. Fig. 7.6 shows a high degree of correlation (i.e. R^2 = 0.986) between CSR and CRI indices achieved with carbonization tar addition. The results are in good agreement with the previous findings by MacPhee *et al.* (2009), who stated that the CSR drop is accompanied, as expected, by a concomitant rise in CRI. Even though CSR values for the current study indicated lower values as opposed to

other regions as reported by Díez *et al.* (2002), this value is within the usual range of coke of acceptable quality.

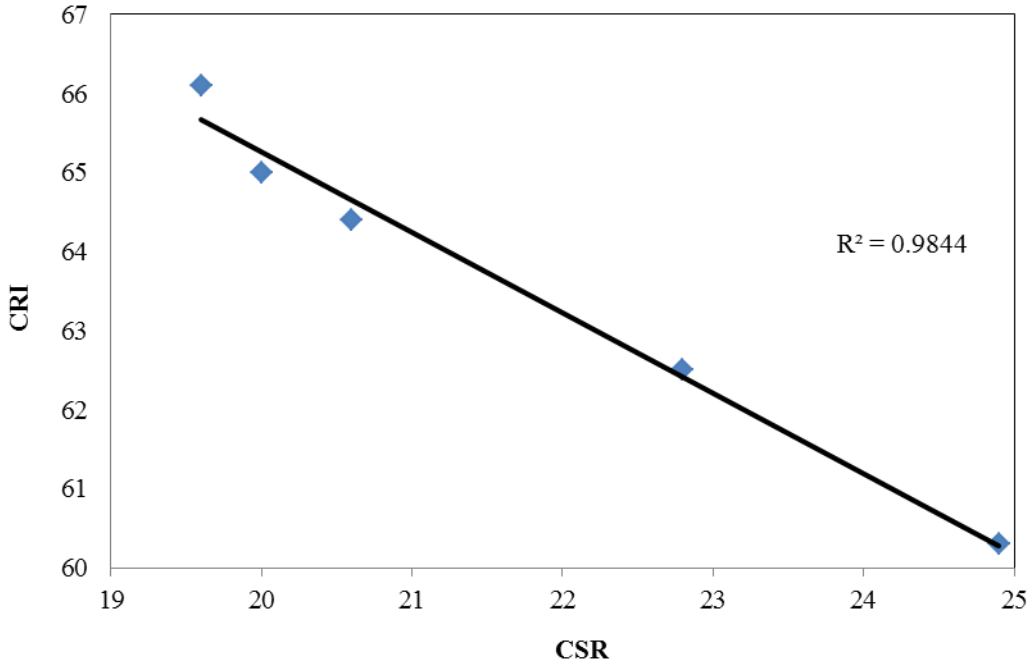

Figure 7.6: The relationship between CSR and CRI indices

7.3 An Economic Evaluation of Carbonization Tar Addition

In order to assess the economics of carbonization tar addition, a schematic layout of the process was designed, based on the required steps to facilitate metallurgical coke production from the carbonization tar addition technology, as shown in Fig. 7.7. The manufacturing process involves equipment such as carbonization tar storage tank (1), carbonization tar filters (10), and canopy with sparing nozzles (22) and coal conveyers system (23) as well as associated connecting pipes.

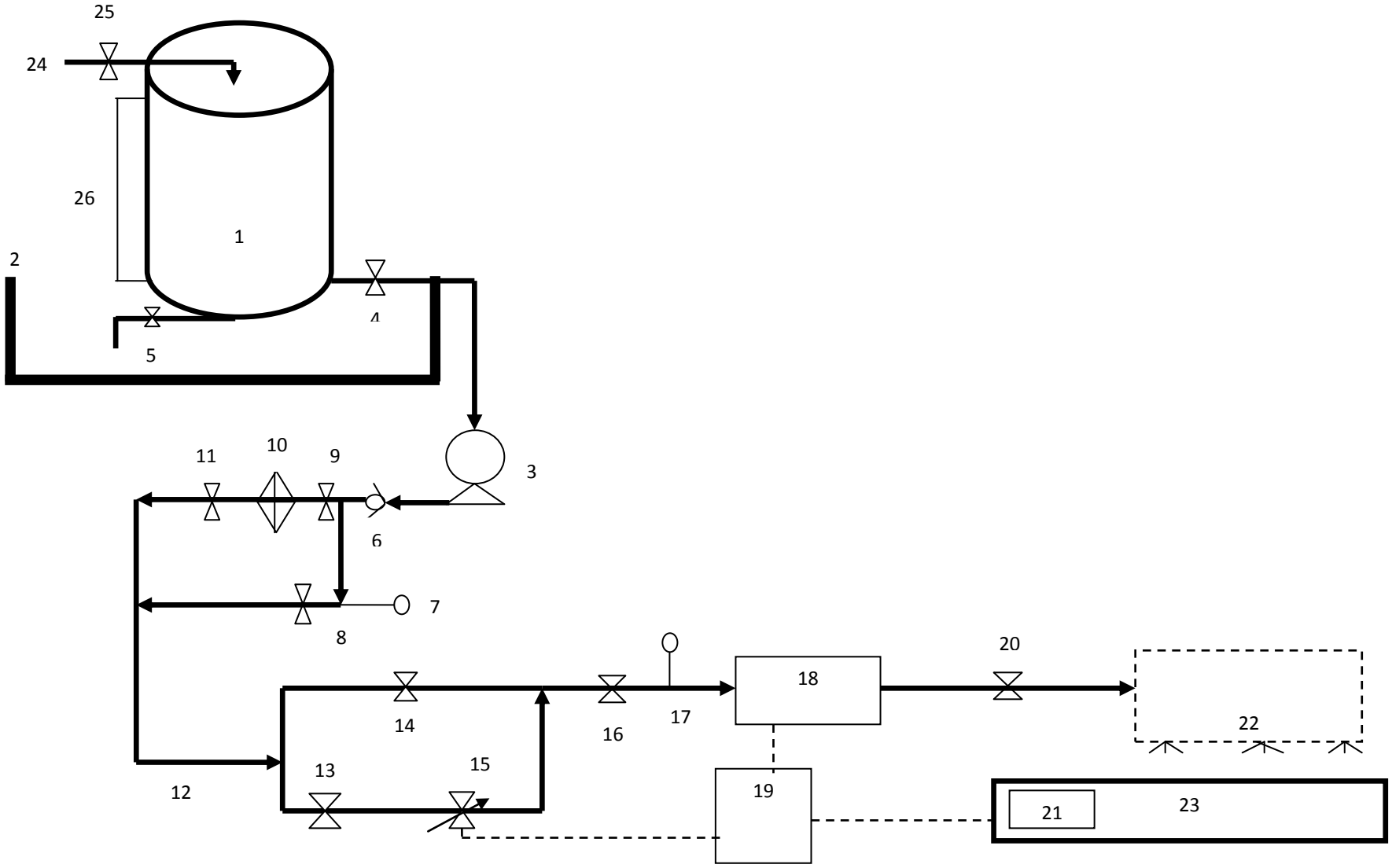

Figure 7.7: Schematic layout for carbonization addition plant

Table 7.13 shows the initial investment costs for the carbonization tar addition plant. The costs of the equipment used were estimated based on South African market prices. The equipment was not scaled up or down since, they were not different from the required size of the process. The total capital investment of almost USD 370 000 includes all costs incurred to purchase the equipment needed for the control system (purchased equipment costs), the costs of labour and materials for installing that equipment (direct installation costs) and certain other costs (indirect installation costs). Operational costs were broken into maintenance costs – which include the cost of keeping equipment in good working condition by undertaking regular repairs as needed, training and miscellaneous. The major costs of coke production through carbonization tar addition related to site preparation, carbonization tar storage, and transportation and capital costs, such as equipment to be used.

Table 7.13: Initial investment costs for carbonization tar addition plant set-up

No	Item Description
1.	Carbonization tar storage tank
2.	Bund Wall
3.	Motor-pump unit
4.	Hand Shut-off valve
5.	Drain valve
6.	Non-return valve
7.	Pressure gauge
8.	By-pass valve
9.	Hand valve
10.	Filters
11.	Hand valve
12.	32 mm pipe
13.	Auto-shut off valve
14.	By-pass valve
15.	Flow control valve
16	Manual control valve
17.	Pressure gauge
18.	Flow meter
19.	Programmable Logistic Controller
20.	Manual shut off valve
21.	Weighing scale
22.	Canopy with nozzles
23.	Tar resistant Conveyor Belt
24.	From Carbonization tar Storage
25.	Hand valve
26.	Level Indicator

The financial viability inputs were summarized and shown in Table 7.14. The international bulk coking coal prices are usually quoted by independent media organisations in USD/T, representing spot prices for loading or delivery within 90 days, with standardise specifications relating both to cargo size and location (Australia, China, India, Japan, Colombia, Europe, and the USA) and also for coal qualities (Matyjaszek *et al.*, 2018). The costs of imported coals were weighed against coke yield. Carbonization tar yield is another important factor in assessing the feasibility of adopting this method, as it would have a marked effect on the overall economics. It is shown in a study that for the optimum condition achieved, the coke yield decreased by 2 wt%. Since raw material prices vary greatly with the international market fluctuations, the production costs were determined in a range according to the maximum and minimum values of the annual average raw material over the last ten years (from 2008 to 2018). Prices quoted for coking coals are as delivered prices, whereas the price quoted for coke, excludes transport. Scholtz *et al*. (2006) mentioned that the coke manufacturing process is a continuous production operation and as such, costs related to carbonization tar addition were calculated using this basis. The capacity of the plant was estimated to be 950 tons/ day (Scholtz *et al*. 2006), when operating 85% of the time which then corresponds to (365-day x 85%) 310 days per year. Each coke oven was found to produce approximately 18.62 tons of coke (Scholtz *et al.* 2006) and the production was planned for 22 days per month excluding planned maintenance. It was determined that the plant would produce 245,784.00 ton/year, resulting in considerable savings per month estimated, as indicated in Table 7.14.

Table 7.14: Coke production 2018 investment annual operating costs

Description	Unit Cost	0 wt.% Tar		6 wt.% Tar	
	USD/Ton	Composition	Weight (Ton)	Composition	Weight (Ton)
Coal B	231.25	8%	92	7.3%	83.95
Coal C	225.00	38%	437	34.5%	396.75
Coal D	218.75	19%	218.5	17.2%	197.80
Coal A	118.75	35%	402.5	35%	402.50
Carbonization Tar	120.00				
Carbonization Tar Added	61.62	0%	0	6%	69.00
Coal Blend per Oven			23.00		23.00
Coal Blend per 50 Ovens			1150		1150
Coal Blend Cost USD		215,193.75		203,999.60	
Blend Saving USD		-		11,194.16	
Coke per Oven			19.00		18.62
Coke Yield		69%		67%	
Coke Production/Day			950		931
Coke USD	237.50	225,625.00		221,112.50	
Production Lost USD		-		4,512.50	
Savings/Day USD		-		6,681.66	
Saving/Month USD		-		146,996.47	

7.3.1 Net present value

The sum of discounted net cash flows derives the Net Present Value (NPV). The NPV allows for simulations in which multiple uncertainties and risk factors are taken into account. In other words, it calculates the NPV of all cash flows in a carbonization tar addition project and focuses directly on the profitability of a project instead of only its costs. The NPV is one criterion by which to simultaneously examine costs (cash outflows) and revenue (cash inflows). Estimated daily profit of USD 7,000.00 is made due to the difference in blend saving (USD 11, 194.16) and decrease in coke throughput (USD 4,512.50) because of carbonization tar addition. Carbonization tar addition results in savings of USD 150,000.00 per month, amounting to USD 1,7 million per year. The reported price was the minimum at which the coke production investment could make optimal profits. Although coke yield decrease of about 2% was reported, major savings have risen because of carbonization tar addition to coal blend. Given that the initial investment of USD 370,000.00 was used and an additional saving of USD 150,000.00 per month was realized.

7.3.2 Break-even

Break-even (BE) analysis is used to determine the minimum level of coke sales that ensure the project is not experiencing any loss. According to Tsorakidis *et al.* (2000), break-even is the analysis of the level of sales and can be calculated using Eq. (7.6):

$$BE = \frac{F_C}{(S_P - V_P)} \tag{7.6}$$

where BE = Break-even; F_C = fixed cost, S_P = Selling price, V_P = variable price

The results are presented in Table 7.15. Table 7.15 shows that as long as coke production and sales are above 6.3 months, coke-making industry will experience profit and the returns on investment will be within the same period.

Table 7.15: Profit/Loss margin for different coke volume sold

Range	1 Month	6.2 Month	6.3 Month
Coke sold (237.50 USD)	619 (Ton)	3 837 (Ton)	3 899.70 (Ton)
Total coke Sales (USD)	146,996.52	911,477.50	926, 178.75
V_P (USD)	88,197.91	546,886.50	555,707.25
Contribution Margins	58,798.61	364,591.00	370, 471.00
FC (USD)	369,225.00	369,225.00	369,225.00
Profit/Loss (USD)	(-310,426.39)	(-4,634)	(1 246)

V_P = variable cost; USD = United States Dollar; F_C = Fixed carbon

7.3.3 Discounted payback period

The discounted payback period is the number of years that will pass before the investment cost is recovered; it is calculated while accounting for the time-value of money. The discounted payback period works as a quick assessment of the time during which an investor's capital is at risk (Short *et al.*, 1995). Eq. 7.7 determines the discounted payback period:

$$NPV = \sum_{j=0}^{N} \frac{S_j}{(1+c)^j} \tag{7.7}$$

where j = analysis year

NPV = net present value of the capital investment,

S_j = cash flows received at time j,

c = rate that equates the present value of positive and negative cash flows, when used as a discount rate.

Approximately, 2.5 months payback period is required to recover the initial investment cost used for carbonization tar addition project. In addition, it is expected that a maximum of up to 50% of carbonization tar added be recovered after carbonization (Chatterjee and Prasad, 1982).

7.3.4 Sensitivity analysis

Sensitivity analysis was performed to understand the influence of the uncertain variables on the NPV value of the three-carbonization production processes. In this study, variations in the purchase price of carbonization tar and the selling price of coke were investigated based on a 20 – year plant life. The prices of all these parameters were varied between – 50% and 50% of the original values and the results are as shown in Table 7.16.

Table 7.16: Sensitivity analysis values

Range	0 %	50%	– 50%
Saving/Month USD	146,996.47	220494.69	73498.23

7.4 Summary

Carbonization tar addition over a 2 – 8 wt.% range was studied as a possible route for recycling tar waste into a coal blend. The use of carbonization tar for coal blends is posed as an alternative to its disposal. Effects of carbonization tar addition on the coal blend proximate analyses were evaluated. The ash content, sulphur content and volatile matter content of individual coals making a blend under consideration were additive. Carbonization tar addition

reduced the ash content in the coal blend from 9.20 to 8.63 wt.%. A 56.8% reduction in coal fines (powder) was observed which consequently resulted in less coal dust pollution to the environment. Good coke qualities, competitive with other blast furnaces across the world, were obtained. This occurred even when lower quality coking coal of up to 35% addition was included in the blend. The coke quality results are comparable to international benchmarks and mathematical models used to calculate the cost-effectiveness of such a project. Savings of up to USD 1,7 million per year were postulated and supported by the results. Recycling carbonization tar has a great realistic significance in saving coal resources and protecting the environment. Therefore, future work should focus on quantifying the impact of coke oven gas emissions because of carbonization tar addition.

CHAPTER 8

CONCLUSIONS AND RECOMMENDATIONS

8.1 Conclusions

Currently, the minimum emissions standards that are being applied in several countries have put combustion, carbonization and gasification coal users under enormous pressure to decrease high SO_2 emissions level in their operations. Therefore, with the adoption of clean air act amendments of 1990 in the USA and recently with legislated stringent minimum emissions standards for SO_2 levels in South Africa, developing methods to remove sulphur from fossil fuels has become even more critically important. For this purpose, South African electricity public utility, Eskom resolved to install FGD technology for new boilers and wherever necessary to retrofit on the existing boilers. However, implementation of the FGD is subject to a number of challenges including waste disposal, being too costly regarding capital and operating cost as well as technically difficult to install. Furthermore, using FGD requires that limestone be brought in from Northern Cape mines that are situated about thousand km away from Eskom's power plants. Furthermore, retrofitting FGD to old units is not always possible not only because of the high capital cost involved but also due to space limitations. On the other hand, most of the coal-fired power plants are close to the end of their expected lifetime while many will reach their end of life between now and the year 2045. In spite of all these operational concerns, stringent limits for sulphur levels have to be implemented in order for these plants to remain in operation for the remaining of their design life. After taking all of these points into consideration, the current study was undertaken to investigate the feasibility of various forms of sulphur content desulphurization as a pre-combustion technique.

Much academic research has not been undertaken on the effect of desulphurization on various forms of sulphur content, petrographic properties, ultimate and proximate analysis in the coal. Waterberg steam coal is unique in various aspects on high sulphur coals dominating the literature. Furthermore, the Waterberg steam coal is one of the remaining large resources of South Africa's remaining coal reserves. Therefore, biodesulphurization of Waterberg steam coal is a new contribution to clean coal technologies research with the intention to reduce high sulphur pollutants in the coal leading to undesirable high SO_2 emissions. To fill up the knowledge gaps mentioned, the present study evaluated the feasibility of biodesulphurization treatment as a pre-combustion technique to reduce high SO_2 emissions spikes from the power

plant. This was successfully achieved through an electron transfer pathway process where sulphur is reduced by accepting electrons from oxygen through a microbial treatment process with bacteria isolated from coal. Therefore, the novelty of the current study compared to the state of the art consists of bacteria isolated from coal been used for the first time towards biodesulphurization of Waterberg coalfield steam coal.

The second part of the study dealt with the impact of coke making plants on environmental and personnel safety. In the coke – making setting, oven charging process generates significant amounts of waste in the form of coal fines. The use of coal fines is becoming an issue due to high Quinoline Insoluble (QI) formation during the carbonization process, additional coal loses and to the greater likelihood of spontaneous combustion and acid mine drainage as well as carry over or enhancement of carbon deposition in the upper parts of coke ovens. This will not only endanger coke – making personnel through occupational diseases as well as fatalities but also bring about possible coke – making plant closures. Furthermore, depletion of coking coal deposits, the comparatively high price of prime coking coals and their scarcity worldwide generate the need to develop new clean coal technologies to maintain coke production levels for years to come while complying with environmental requirements.

8.1.1 Conclusions on the microbial desulphurization study

For the main objectives of microbial desulphurization study, the results obtained can be interpreted and summarised as follows:

Coal was classified as medium sulphur coal when the sulphur content was detected in the range of 1.15 – 1.49 wt.%. Four forms of sulphur - pyrite, mineral/sulphide sulphur, inorganic sulphates and organic sulphur are present in Waterberg coal with pyritic sulphur (≥ 0.51 wt.%) and organic sulphur (≥ 0.49 wt.%) accounted for the bulk of the total sulphur in coal. Maceral analyses of coal showed that inertinite was the dominant maceral (up to 48 vol.%), whereas vitrinite and liptinite occurred in proportions of 22 vol.% and 4 vol.% respectively. Theoretical calculations were developed, verified at the existing plant and used to predict the resultant SO_2 emissions from the combustion of the Waterberg coal in a typical power plant. The sulphur content requirements for Waterberg coal to comply with the minimum emissions standards of 3500 mg/Nm^3 and 500 mg/Nm^3 were found to be ≤1.37 wt.% and ≤0.20 wt.%, respectively. The overall process efficiency for –0.85 mm, +1.00 mm, +2.30 mm and +4.6 mm particle size to be 65%, 54%, 49% and 24% respectively with a plateau was reached in

18 days. Increasing temperature from 23 ± 3 °C to 30 ± 2 °C resulted in further improvement in an overall process efficiency to 72 %. The results show that both forms of sulphur are removed by biodesulphurization treatment. Biodesulphurization efficiencies of 70%, 44%, and 51% were achieved for pyritic sulphur, sulphide sulphur and organic sulphur form respectively. Furthermore, as the temperature increased from 23 ± 3 °C to 30 ± 2 °C, further microbial desulphurization efficiencies of 81%, 44%, and 67% were achieved for pyritic sulphur, sulphide sulphur and organic sulphur form respectively. Therefore, sulphur forms reduction efficiency were found to be in the order Pyritic sulphur > Organic sulphur > Sulphide sulphur > Sulphate sulphur. Interestingly, the order of sulphur forms reduction was consistent with the distribution of sulphur forms in the coal emphasizing the important factor of limited availability to microorganisms. Moreover, ash content reduced by 33% and CV improved by 19% that suggests that microbial desulphurized coal could produce more heat than the untreated coal. Therefore, the current study established that sulphur content and ash content in the coal reduce the heating value of the coal, hence after both sulphur and ash contents simultaneously reduced, CV improved. Microbial growth solution pH varied in the range of 3.0 – 6.5. Seven isolates after purification of the most dominant colonies, viz: *Pseudomonas sp, Pseudomonas aeruginosa, Pseudomonas putida; Pseudomonas stutzeri, Bacillus sp., Pseudomonas rhizosphaerae and Pseudomonas alcaligenes* have been identified.

The other part of this study dealt with developing a model based on reaction kinetics, simulate microbial desulphurization process in a CSTR system and validate the model under various experimental conditions. The values of the kinetic parameters (K_s *and* k_{mc}) in the batch study were determined from the experimental data. These results are statistical correct since the regression coefficients R are above 97 % and all R^2 are above 95 %. However, the biodesulphurization rate coefficient, k_{mc} was determined to be very low. This indicates that sulphur reduction happened faster during exponential phase. These kinetic parameters could not generate a unique representative model for all studied coal particle sizes. The results also show that K_c values obtained from the non-linear regression were not constant and were shown to be much higher than S_T values ($K_c >> S_T$). From these results, it can be noticed that the fitting between the model-simulated and the experimental data is satisfactory. Though different from the sulphur and the ash contents, the experimental data for CV values were found to correlate well with a second-order rate equation.

8.1.2 Conclusions on Coking coal

Coke oven tar addition within the 2 – 8 wt.% loading range was studied as a possible route for recycling coke oven tar waste into a coke making process. Based upon the results, the following conclusions can be drawn. Coke oven tar addition reduced ash content in coal blend from 9.20 to 8.63 wt.%. The ash content usually results in slag volume reduction and possibly affects the oxidation rate of coke by carbon dioxide and oxygen in the furnace. A 56.8%reduction in coal fines (powder) was achieved which consequently resulted in less coal dust pollution to the environment. The decrease in coal fines by means of coke oven tar addition was attributed to coke oven tar serving as a binder – which actively wetted and suppressed coal fines – subsequently agglomerating into larger particles. Apart from reducing environmental impacts such as air and water pollution, the reduction of coal fines reduces the long-term formation of acid rain and the likelihood of spontaneous combustion into the atmosphere. Coke quality results were comparable to international benchmarks and mathematical models used to calculate the cost-effectiveness of such a project. Savings of up to USD 1.7 million per year were postulated and supported by the results. Recycling carbonization tar has a great realistic significance in saving coal resources and protecting both the environment. Researchers can use the obtained results for coking coal blend qualities within the range of the current study. For different coal properties outside the scope of the current study, further assessments would be required to validate the results.

8.2 Recommendations

It must be stated that, whilst all the objectives in this research were accomplished, there is further work to be undertaken in up scaling the microbial treatment process for commercial purposes. There is a need for faster growing, stable, and more active biodesulphurization microbial culture than those that have been developed up to the present time. To this end, there is a need for a structured and systematic programme of strain selection and improvement through molecular genetics, and a need for a thorough understanding of the coal biodesulphurization metabolism as well as its associated metabolic pathways. The long residence time required for bioprocessing is also a major obstacle to the usefulness of this technology. Low biodesulphurization rate, slow bacterial growth, and low process yield may all contribute to limit future application of biodesulphurization. Therefore, coal porosity, bacteria size and coal particle size - bacteria interaction beyond the 18th day need to be further evaluated for process improvement.

REFERENCES

Acharya, C., Kar, R.N., Sukla, L.B., 2001. Bacterial removal of sulphur from three different coals. *Fuel* 80, 2207 – 2216.

Acharya, C., Sukla, L.B., Misra, V.N., 2005. Biological elimination of sulphur from high sulphur coal by Aspergillus-like fungi. *Fuel* 84, 1597–1600.

Agarwal, M., Dikshit, P.K., Bhasarkar, J.B., Borah, A.J., Moholkar, V.S., 2016. Physical insight into ultrasound-assisted biodesulfurization using free and immobilized cells of Rhodococcus rhodochrous MTCC 3552. *Chemical Engineering Journal* 295, 254 –267.

Aller, A., Martinez, O., de Linaje, J.A., Mendez, R., Moran, A., 2001. Biodesulphurisation of coal by microorganisms isolated from the coal itself. *Fuel Processing Technology* 69, 45 –57.

Alvarez, R., Menendez, R., Marsh, H., Miyar, E.A., Canga, C.S., 1989. Improving coke strength by co - Carbonization of aluminium with high volatile Spanish coal. *Fuel* 68, 1325 –1329.

Araya, P.E., Badillaohlbaum, R., Droguett, S.E., 1981. Study of the Treatment of Subbituminous Coals by Naoh Solutions. *Fuel* 60, 1127 – 1130.

Aytar, P, Gedikli, S, Şam, M, Ünal, A, Çabuk, A, Kolankaya, N, Yürüm, A, 2011. Desulphurization of some low-rank Turkish lignites with crude laccase produced from Trametes versicolor ATCC 200801. *Fuel Processing Technology* 92, 71–76.

Aytar, P., Sam, M., Çabuk, A., 2008. Microbial desulphurization of Turkish lignites by white rot fungi. *Energy Fuels* 22, 1196 –1199.

ASTM D2014, 2010. Standard Test Method for Expansion or Contraction of Coal by the Sole-Heated Oven.

ASTM D3682–13: Standard Test Method for Major and Minor Elements in Combustion Residues from Coal Utilization Processes.

ASTM D4239–14: Standard Test Method for Sulphur in the Analysis Sample of Coal using High-Temperature Tube Furnace Combustion.

ASTM D5341 – 99, 2004. Standard Test Method for Measuring Coke Reactivity Index (CRI) and Coke Strength After Reaction (CSR).

ASTM D6316–09be1: Standard Test Method for Determination of Total, Combustible and Carbonate Carbon in Solid Residues from Coal and Coke. ASTM D4239 – 14: Standard Test Method for Sulphur in the Analysis Sample of Coal using High-Temperature Tube Furnace Combustion.

ASTM D3682 – 13: Standard Test Method for Major and Minor Elements in Combustion Residues from Coal Utilization Processes.

Barma, S.D., 2019. Ultrasonic-assisted coal beneficiation: A review. *Ultrasonics Sonochemistry* 50, 15 – 35.

Barooah, P.K., Baruah, M.K., 1996. Sulphur in Assam coal. *Fuel Processing Technology* 46, 83 – 97.

Brey, W.S., Jr., 1958. Principles of physical chemistry. New York: Appleton-century-Crofts.

Barreira, A, Patierno, M, Bautista, C,R, 2017. Impacts of pollution on our health and the planet: the case of coal power plants. *Perspect* 28, 1–10.

Baruah, M.K., 1992. The chemical structure of secondary sulfur in Assam coal. *Fuel Processing Technology 31*, 115 – 119.

Benk, A., 2010. Utilisation of the binders prepared from coal tar pitch and phenolic resins for the production of metallurgical quality briquettes from coke breeze and the study of their high temperature Carbonization behaviour. *Fuel Processing Technology* 91, 1152–1161.

Benk, A., Coban, A., 2011. Molasses and air blown coal tar pitch binders for the production of metallurgical quality formed coke from anthracite fines or coke breeze. *Fuel Processing Technology* 92, 1078 –1086.

Benko, T., Teichmann, C., Mizsey, P., Jacob, D., 2007. Regional effects and efficiency of flue gas desulphurization in the Carpathian Basin. *Atmospheric Environment* 41, 8500 – 8510.

Beyer, M., Ebner, H.G., Assenmacher, H., Frigge, J., 1987. Elemental sulphur in microbiologically desulphurized coals. *Fuel* 66, 551 – 555.

Borah, D. 2006. Desulfurization of Organic Sulfur from a Subbituminous Coal by Electron-Transfer Process with $K_4[Fe(CN)_6]$. *Energy Fuels* 20, 287–294.

Borah, D., Baruah, M.K., 1999. Electron transfer process 1. Removal of organic sulphur from high sulphur Indian coal. *Fuel 7*8, 1083 –1088.

Brandis-Heep, A., 1983. Anaerobic acetate oxidation to CO_2 by Desulfobacter postgatei. *Archives of Microbiology* 136, 222 – 229.

Cairncross, B., 1990. Tectono-sedimentary settings and controls of the Karoo Basin Permian coals, South Africa. *International Journal of Coal Geology* 16, 175 –178.

Cairncross, B., 2001. An overview of the Permian (Karoo) coal deposits of southern Africa. *African Earth Sciences* 33, 529 – 562.

Calkins, W.H. 1994. The chemical forms of sulfur in coal: a review. *Fuel* 73, 475 – 484.

Cara, J., Carballo, M.T., Mora´na, A., Bonilla, D., Escolanoc, O., Garcı´a Frutos, F.J. 2005. Biodesulphurisation of high sulphur coal by heap leaching. *Fuel* 84, 1905–1910.

Cara, J., Vargas, M., Moran, A., Gomez, E., Martinez, O., Garcia Frutos, F.J., 2006. Biodesulphurization of a coal by packed-column leaching. Simultaneous hermogravimetric and mass spectrometric analysis. *Fuel* 85, 756 –1762.

Chandra, D., Mishra, A.K., 1988. Desulfurization of coal by bacterial means. *Resources, Conservation & Recycling* 1, 293 –308.

Chandra, D., Roy, P., Mishra, A.K., Chakrabarti, J.N. and Sengupta, B., 1979. Microbial removal of organic sulphur from coal. *Fuel* 58, 549 – 550.

Charleson, L.R., Juerg Weber, E., 1993. Energy forecasts for Western Australia 1992–2010. *Energy Economics* 15, 111–122.

Chatterjee, A., Prasad, H.N., 1982. Possibilities of tar addition to coal as a method of improving coke strength. *Fuel* 62, 591– 600.

Chen, Y.R., Hashimoto, A.G., 1980. Substrate utilization kinetic model for biological treatment process. *Biotechnology and Bioengineering* 22, 2081 – 2095.

Cheng, J., Zhou, J., Liu, J., Zhou, Z., Huang, Z., Cao, X., Zhao, X., Cen, K., 2003. Sulphur removal at high temperature during coal combustion in furnaces: A review. *Progress in Energy and Combustion Science* 29, 381– 405.

Chikkatur, A.P., Sagar, A.D., Sankar, T.L., 2009. Sustainable development of the Indian coal sector. *Energy* 34, 942 – 953.

Chou, C.L., 2012. Sulphur in coals: A review of geochemistry and origins. *International Journal of Coal Geology* 12, 1–13.

Choudhury, N., Biswas, S., Sarkar, P., Kumar, M., Ghosal, S., Mitra, T., Mukherjee, A., Choudhury, A., 2008. Influence of rank and macerals on the burnout behavior of pulverized Indian coal. *International Journal of Coal Geology* 74, 145 –153.

Cloke, M., Lester, E., Thompson, A.W., 2002. Combustion characteristics of coals using a drop-tube furnace. *Fuel* 81, 727 – 735.

Coenye, T., Falsen, E., Vancanneyt, M., Hoste, B., Govan, J. R. W., Kersters, K., Vandamme, P., 1999. Classification of Alcaligenes faecalis-like isolates from the environment and human clinical samples as Ralstonia gilardii sp. nov. *International Journal of Systematic and Evolutionary Microbiology* 49, 405 – 413.

Collin, G., Bujnowaska, B., 1994. Co-Carbonizationof Pitches with coal mixtures for the production of Metallurgical cokes. *Carbon* 32, 547–552.

Contois, D.E., 1959. Kinetics of Bacterial Growth: Relationship between Population Density and Specific Growth Rate of Continuous Cultures. *Microbiology* 21, 40 – 50.

Cortés, C.G., Tzimas, E., Peteves, S.D., 2009. Technologies for Coal based Hydrogen and Electricity Co-production Power Plants with CO_2 Capture. *JRC Scientific and Technical Reports*, 1 – 72.

Cypionka, H., 2006. Grundlagen der Microbiologie. Heidelberg: Springer-Verlag.

Dahiya, S., Myllyvirta, L. 2019. Global SO2 Emission Hotspot Database – Ranking the World's Worst Sources of SO_2 Pollution. *Greenpeace Environment Trust*, 1 – 13.

Davidson, R.M., 1994. Quantifying organic sulfur in coal: A review. *Fuel* 73, 994 – 1005.

Das, S., Sharma, S., Choudhury, R., 2002. Non-coking coal to coke: use of biomass based blending material. *Energy* 27, 405 – 414.

de Korte, G.J. Beneficiation of Weathered Coal. 2001. COALTECH 2020, 1 – 26.

de Oliveira, D. M., Sobral, L.G.S., Olson, G.J., Olson, S.B., 2014. Acid leaching of a copper ore by sulphur-oxidizing microorganisms. *Hydrometallurgy*, 147–148.

Dimitrijević, Z., Tatić, K. The economically acceptable scenarios for investments in desulphurization and denitrification on existing coal-fired units in Bosnia and Herzegovina. *Energy policy* 49, 597- 607.

Díez, M.A., Alvarez, R., Barriocanal, C., 2002. Coal for metallurgical coke production: predictions of coke quality and future requirements for coke making. *International Journal of Coal Geology* 50, 389 – 412.

Díez, M.A., Alvarez, R., Cimadevilla, R.L.G., 2013. Briquetting of carbon-containing waste from steelmaking for metallurgical coke production. *Fuel* 114, 216 – 223.

Díez, M.A., Alvarez, R., Gonzilez, A.I., Menendez, R., Moinelo, S.R., Bermejo, J., 1994. Characterisation of coal tars produced under different carbonization conditions by FT-i.r. spectroscopy and extrography. *Fuel 73*, 139 –142.

Dreyer, J.C., 2006. An overview of the geology of the Waterberg Coalfield, implications for future exploitation. Presented at the Fossil Fuel Foundation of South Africa Conference: The Waterberg Coalfield 2006 and beyond – quo vadis? Lephalale (previously Ellisras), 22 – 23 August 2006.

Dong-chen, Z., Ming-xu, Z., Qing-ru, C., 2009. Study on coal bio-magnetizing desulphurization. *Procedia Earth and Planetary Science* 1, 673 – 678.

Duan, L., Sun, H., Jiang, Y., Anthony, E.J., Zhao, C., 2016. Partitioning of trace elements, As, Ba, Cd, Cr, Cu, Mn and Pb, in a 2.5MWth pilot-scale circulating fluidised bed

combustor burning an anthracite and a bituminous coal. *Fuel Processing Technology* 146, 1 – 8.

DuBroff, W., Kaegi, D.D., Knoerzer, J.J., Spearin, E.Y., 1985. Solvent pretreatment of coal to improve coke strength, Patent Number 4, 528, 069.

Eberhard, A., 2011. The future of South African coal: Market, Investment and Policy Challenges. *Program on Energy and Sustainable Development*, 1– 44.

Efthimiadou, A., Nikolaides, I. P., Tourlidakis, A., 2015. A proposal for SO_2 abatement in existing power plants using rich in calcium lignite. *Applied Thermal Engineering* 74, 119 – 127.

Eligwe, C.A., 1988. Microbial desulphurization of coal. *Fuel* 67, 451 – 458.

Falcon, R., Ham, A.J., 1988. The characteristics of Southern African coals. *Journal of the Southern African Institute of Mining and Metallurgy* 88, 45 – 161.

Faure, K., Armstrong, R.A., Harris, C., Willis, J.P., 1996. Provenance of mudstones in the Karoo Supergroup of the Ellisras basin, South Africa: geochemical evidence. *Journal of African Earth Sciences* 23, 189 –204.

Faure, K., Willis, J.P., Dreyer, J.C., 1996. The Grootegeluk Formation in the Waterberg Coalfield, South Africa: facies, palaeoenvironment and thermal history evidence from organic and clastic matter. *International Journal of Coal Geology* 29, 147–186.

Fecko, P., Pectova, I., Cablik, V., Riedlova, S., Ovcari, P., Tora, B. 2006. Bacterial Desulphurization of coal. *Górnictwo i Geoinżynieria • Rok* 30: 47 – 65.

Fernández, A.M., Barriocanal, C., Alvarez, R., 2012. The effect of additives on coking pressure and coke quality. *Fuel* 95, 642 – 647.

Fogler, H.S. 1999. Elements of Chemical Reaction Engineering. Prentice Hall of India, New Delhi.

Forrest, M., Marsh, H., 1981. Effects of additions of petroleum coke in coals upon strengths of resultant cokes. *Fuel* 60, 429 – 433.

Fourie, C.J.S., Henry, G., 2009. New airborne geophysical data from the Waterberg Coalfield (PositionIT July 2009) www.csir.co.za/nre/mineral_resources/pdfs/CPO-0024.pdf2009 (PDF file Date accessed 12 January 2018).

Franco, A., Diaz, A.R., 2009. The future challenges for "clean coal technologies": joining efficiency increase and pollutant emission control. *Energy* 34, 348 – 354.

Gao, H., Li, C., Zeng, G., Zhang, W., Shi, L., Fan, X., Zeng, Y., Wen, Q., Shu, X., 2011. Experimental study of wet flue gas desulphurization with a novel type PCF device. *Chemical Engineering and Processing* 50, 189 –195.

Ge, S., Liu, Z., Li, R., Furuta, Y., Peng, W., 2017. Biodesulphurization characteristics of bamboo charcoal from sulfur solution. *Saudi Journal of Biological Sciences* 24, 127–131.

Gear, C., 1971. The automatic integration of ordinary differential equations, Communication ACM, 14: 176 – 179.

Ghosh, W, Dam, B, 2009. Biochemistry and molecular biology of lithotrophic sulfur oxidation by taxonomically and ecologically diverse bacteria and archaea. *FEMS Microbiology* 33, 999 –1043.

Giri, C.C., Sharma, D.K. 2000. Kinetic studies and shrinking core model on solvolytic extraction of coal. *Fuel Processing Technology* 52, 97 – 109.

Gökcay, C.F., Yurteri, R.N., 1983. Microbial desulfurization of lignites by a thermophilic bacterium. *Fuel* 62, 223 –1224.

Gonsalvesh, L., Marinov, S.P., Stefanova, M., Carleer, R., Yperman, J., 2012. Organic sulphur alterations in biodesulphurized low rank coals. *Fuel* 97, 489 – 503.

Gonzalez – Cimas, M.J., Patrick, J.W., Walker, A., 1986. Influence of Pitch additions on coal carbonisation. *Fuel* 66, 1019 –1023.

Government Notice No.248. 31 March 2010. NATIONAL ENVIRONMENTAL MANAGEMENT: AIR QUALITY ACT, 2004 (ACT NO. 39 OF 2004), Page 11.

Greenwood, N.N., Earnshaw, A., 1997, Chemistry of the Elements (2nd ed.), Oxford: Butterworth-Heinemann, ISBNÄ0080379419.

Gryglewicz, G., Boudou, J.P., BouUgue, J., Machnikowska, H., Jasieirko, S., 1995. Sulfur characterization of Polish coals, their lithotypes and macerals. *Fuel* 74, 349 – 355.

Guo, H., Chen, C., Lee, D.J., Wang, A., Gao, D., Ren,N., 2014. Coupled carbon, sulfur and nitrogen cycles of mixotrophic growth of Pseudomonas sp. C27 under denitrifying sulfide removal conditions. *Bioresource Technology* 171, 120 –126.

Gómez, F., Amils, R., Marin, I., 1997. Microbial ecology studies for the desulfurization of Spanish coals. *Fuel Processing Technology* 52, 183 – 189.

Göckay, C.F., Yurteri, R.N., 1983. Microbial desulfurization of lugnites by a thermophilic bacterium. *Fuel* 62, 1223 –1224.

Hagelskamp, H.H.B., Snyman, C.P., 1988. On the origin of low-reflecting inertinites in coals from the Highveld Coalfield, South Africa. *Fuel* 67, 307–313.

Hall, T.A., 1999. BioEdit: A User-Friendly Biological Sequence Alignment Editor and Analysis Program for Windows 95/98/NT. *Nucleic Acids Symposium Series* 41, 95 – 98.

Han, Y, Zhang, Y, Xu, C, Hsu, C S, 2018. Molecular characterization of sulfur-containing compounds in petroleum. *Fuel* 221, 144 –158.

Hancox, P.J., Götz, A.E., 2014. South Africa's coalfields — A 2014 perspective. *International Journal of Coal Geology* 132, 170 –254.

Handayani, I., Paisal, Y., Soepriyanto, S., Chaerun, S.K., 2017. Biodesulfurization of organic sulfur in Tondongkura coal from Indonesia by multi-stage bioprocess treatments. *Hydrometallurgy* 168, 84 – 93.

Hao, Y., Wu, S., Pan, Y., Li, Q., Zhou, J., Xu, Y., Qian, G., 2016. Characterization and leaching toxicities of mercury in flue gas desulphurization gypsum from coal-fired power plants in China. *Fuel* 177, 157–163.

Hattingh, B.B., Everson, R.C., Neomagus, H.W.J.P., Bunt, J.R., 2011. Assessing the catalytic effect of coal ash constituents on the CO_2 gasification rate of high ash, South African coal. *Fuel Processing Technol*ogy 92, 2048 – 2054.

Helle, S., Gordon, A., Alfaro, G., Garcı´a, X., Ulloa, C., 2003. Coal blend combustion: link between unburnt carbon in fly ashes and maceral composition. *Fuel Processing Technology* 80, 209 – 223.

Hippo, E.J., Crelling, J.C., 1991. Desulphurization of single coal macerals. *Fuel Processing Technology* 27, 287 – 305.

Hou, J., Ma, Y., Li, S., Shi, J., He, L., Li. J., 2018. Transformation of sulfur and nitrogen during Shenmu coal pyrolysis. *Fuel* 231, 134 –144.

Hower, J.C., Wagner, N.J., O'Keefe, M.K., Drew, J. W., Stucker, J.D., Richardson, A.R., 2012. Maceral types in some Permian southern African coals. *International Journal of Coal Geology* 100, 93 –107.

http://www.eskom.co.za/IR2015/Documents/Eskom_fact_sheets_2015.pdf. Accessed 19 August 2019.

Hu, X., Liu, Y., Yang, L., Shi, Q., Zhang, W., Zhong, C., 2018. SO_2 emission reduction decomposition of environmental tax based on different consumption tax refunds. *Journal of Cleaner Production* 186, 997 – 1010.

Huifang, Z., Yagin, L., 1993. Microorganisms desulphurization of coal. *Chinese Journal of Environmental Science* 5, 83 – 89.

Huxtable, R.J., Lafranconi, W.M 1986. Biochemistry of Sulfur. Plenum Press, New York.

IEA – International Energy Agency, 2008. World Energy Outlook. International Energy Agency, Paris.

IEA, 2014, South Africa Role Coal Energy Security. International Energy Agency http://www.iea.org/ciab/South_Africa_Role_Coal_Energy_Security.pdf, Last accessed 13/05/2017 at 19:00.

Imachi, H., Sekiguchi, Y., Kamagata, Y., Hanada, S., Ohashi, A., Harada, H., 2002. Pelotomaculum thermopropionicum gen. nov., sp. nov., an anaerobic, thermophilic, syntrophic propionate-oxidizing bacterium. *International Journal of Systematic and Evolutionary Microbiology* 52, 1729 – 1735.

Isbister, J.D. 1985. Mutant microorganism and its use in removing organic sulfur compounds. Atlantic Research Corporation. USA Patent (4808535).

ISO 157, 1996. Coal — Determination of forms of sulphur. International Organisation for Standardization.

ISO 349, 1975. Hard coal – Audibert-Arnu dilatometer test. International Organisation for Standardization.

ISO 501, 2012. Hard coal – Determination of the crucible swelling number. International Organisation for Standardization.

ISO 562, 2010. Hard coal and coke — Determination of volatile matter. International Organisation for Standardization.

ISO 556, 1980. Coke (greater than 20 mm in size) – Determination of mechanical strength. International Organisation for Standardization.

ISO 1171, 2010. Solid mineral fuels — Determination of ash. International Organisation for Standardization.

ISO 562, 2010. Hard coal and coke — Determination of volatile matter. International Organisation for Standardization.

ISO 1928, 2009. Solid mineral fuels — Determination of gross calorific value by the bomb calorimetric method and calculation of net calorific value. International Organisation for Standardization.

ISO 7404-3, 1994. Methods for the petrographic analysis of bituminous coal and anthracite —Part 3: Method of determining maceral group composition. International Organisation for Standardization.

ISO 7404-2, 2009. Methods for the petrographic analysis of coals — Part 2: Methods of preparing coal samples. International Organisation for Standardization.

ISO 7404-5, 1994. Methods for the Petrographic Analysis of Bituminous Coal and Anthracite—Part 5: Method of Determining Microscopically the Reflectance of Vitrinite. International Organisation for Standardization.

ISO 10329, 2009. Coal – Determination of plastic properties -- Constant-torque Gieseler plastometer method. International Organisation for Standardization.

ISO 11722, 2013. Solid mineral fuels – Hard coal – Determination of moisture in the general analysis test sample by drying in nitrogen. International Organisation for Standardization.

ISO 11760, 2005. Classification of Coals. International Organisation for Standardisation. TC 27. International Organisation for Standardization.

ISO 12902, 2001. Solid mineral fuels – Determination of total carbon, hydrogen and nitrogen — Instrumental methods. International Organisation for Standardization.

ISO 23380, 2008. Selection of methods for the determination of trace elements in coal. International Organisation for Standardization.

Jackman, H.W., Helfinstine, R.J., 1970. Preheating Coal Blends As a Means of Increasing Coke Strength, Circular 453 Illinois State Geological Survey. *Circular*. 453, 1–15.

Jeffrey, L.S., 2005. Characterization of the coal resources of South Africa. *The Journal of the South African Institute of Mining and Metallurgy* 105, 95 – 102.

Kalenga, P.M. 2011. Determination and characterization of sulphur in South African coal. MSc Thesis. University of The Witwatersrand. Available online: https://core.ac.uk/download/pdf/39669062.pdf, Accessed March 2018.

Kang, Y.S., Kim, S.S., Hong, S.C., 2015. Combined process for removal of SO2, NOx, and particulates to be applied to a 1.6-MWe pulverized coal boiler. *Journal of Industrial and Engineering Chemistry* 30, 97–203.

Kargi, F., 1982. Microbiological coal desulphurization. *Enzyme and Microbial Technology* 4, 13 – 19.

Kargi F, Robinson J., 1986. Removal of organic sulphur from bituminous coal: Use of the thermophilic organism *Sulfolobus acidocaldarius*. *Fuel* 65, 397– 409.

Karaca, H., Ceylan, K. 1997. Chemical cleaning of Turkish lignites by leaching with aqueous hydrogen peroxide. *Fuel Processing Technology* 50, 19 – 33.

Karavaiko, G.I., Lobyreva, L.B., 1994. An overview of the bacteria and archaea involved in removal of inorganic and organic sulfur compounds from coal. *Fuel Processing Technology* 40, 167–182.

Kellogg. C.E., Spence, K.W., 1931. Note on the Standard error of the standard errors of estimate and measurement. *Journal of Educational Psychology* 22, 313 – 315.

Ken, B.S., Nandi, B.K., 2019. Desulfurization of high sulfur Indian coal by oil agglomeration using Linseed oil. *Powder Technology* 342, 690 – 697.

Kerber, R.C. 1993. Organoiron Chemistry: Annual survey for the year 1991. *Journal of Organometallic Chemistry* 457, 63 – 120.

Kestner, M.O., Gilewicz, S.E., Aktuna, M.E., 1981. Method of improving the bulk density and the throughput characteristics of coking coal. *United States Patent*. 4, 636.

Kiani, M.H., Ahmadi, A., Zilouei, H., 2014. Biological removal of sulphur and ash from fine-grained high pyritic sulphur coals using a mixed culture of mesophilic microorganisms. *Fuel* 131, 89 – 95.

Kilbane, J.J., 1989. Desulfurization of coal: the microbial solution. *TIBTECH* 7, 97 – 101.

Kilbane, J.J., 1990. Sulfur-Specific Microbial Metabolism of Organic Compounds. *Resources, Conservation and Recycling* 3, 69 –79.

Kılıç, O., Acarkan, B., Ay, S., 2013. FGD investments as part of energy policy: A case study for Turkey. *Energy Policy* 62, 1461–1469.

Klein, J., van Afferden, M., Pfeifer, F., Schacht, S., 1994. Microbial desulfurization of coal and oil. *Fuel Processing Technology* 40, 297 – 310.

Klubek, B., Ochman, M., Nabe, S., Clark, D., Alam, K., Abdulrashid, N., 1988. Microbial removal of organic sulphur from coal. *Mineral Matters* 10, 1– 3.

Kodama, K., 1970. Microbial conversion of petro-sulfur compounds part III. *Agricultural and Biological Chemistry* 34, 1320 – 1324.

Kolja, S.A., 1995. Desulfurization of coal by air + steam at 400°C in a fixed bed. *Fuel* 74, 1834 – 1838.

Kosioska, K., Miśkiewicz, T., 2009. Performance of an anaerobic bioreactor with biomass recycling, continuously removing COD and sulphate from industrial wastes. *Bioresource Technology* 100, 86 – 90.

Krebs, V., Furdin, G., Mareche, J.F., Dumay, D., 1996. Effects of coal moisture content on carbon deposition in coke ovens. *Fuel* 75, 979 – 986.

Kruszewska, K., 1989. The use of reflectance to determine maceral composition and the reactive-inert ratio of coal components. *Fuel* 68, 753 – 757.

Kudelko, M., 2003. The market for low-sulphur coals under the restrictive environmental standards in Poland. *Applied Energy* 74, 261– 269.

Kumar, S., Tamura, K., Nei, M., 2004. MEGA3: Integrated software for Molecular Evolutionary Genetics Analysis and sequence alignment. *Briefings in Bioinformatics* 5, 150 –163

Li, S., Xu, T., Sun, P., Zhou, Q., Tan, H., Hui, S., 2008. NO_x and SO_x emissions of a high sulfur self-retention coal during air-staged combustion. *Fuel* 87, 723 –731.

Li, W., Tang, Y., 2014. Sulfur isotopic composition of superhigh-organic-sulfur coals from the Chenxi coalfield, southern China. *International Journal of Coal Geology* 127, 3 – 13.

Lin, M.F., Hong, M.T., 1986. The effect of coal blend fluidity on the properties of coke, *Fuel* 65, 307– 311.

Lin, M.S., Premuzic, E.T., Manowitz, B., Jeon, Y., Racaniello, L., 1993. Biodegradation of coals. *Fuel* 72, 1667 – 1672.

Liu, T., Hou, J., Peng, Y., 2017. Effect of a newly isolated native bacteria, Pseudomonas sp. NP22 on desulfurization of the low-rank lignite. *International Journal of Mineral Processing* 162, 6 –11.

Liu, X., Lin, B., Zhang, Y. 2016. Sulfur dioxide emission reduction of power plants in China: current policies and implications. *Journal of Cleaner Production* 113, 133 – 143.

Liu, K., Yang, J., Jia, J., Wang, W., 2008. Biodesulphurization of coal via low temperature atmospheric alkaline oxidation. *Chemosphere* 71, 183 –188.

MacPhee, J.A., Gransden, J.F., Giroux, L., Price, JT., 2009. Possible CO_2 mitigation via addition of charcoal to coking coal blends, *Fuel Processing Technology* 90, 16 – 20.

Maffei, T., Sommariva, S., Ranzi, E., Faravelli, T., 2012. A predictive kinetic model of sulfur release from coal. *Fuel 91*, 213 –223.

Mangena, S.J., du Cann, V.M., 2007. Binderless briquetting of some selected South African prime coking, blend coking and weathered bituminous coals and the effect of coal properties on binderless briquetting, *International Journal of Coal Geology* 71, 303 – 312.

Matin, S.S., Chelgani, S.C. 2016. Estimation of coal gross calorific value based on various analyses by random forest method. *Fuel* 177, 274 – 278.

Matyjaszek, M., Wodarskib, K., Krzemieńc, A., García-Mirandad, C.E., Sánchezd, A.S., 2018. Coking coal mining investment: Boosting European Union's raw materials initiative. *Resources Policy* 57, 88–97.

Melendi, S., Díez, M.A., Alvarez, R., Barriocanal, C., 2011. Plastic wastes, lube oils and carbochemical products as secondary feedstocks for blast – furnace coke production. *Fuel Processing Technology* 92, 471– 478.

Mikociaka, D., Magieraa, A., Labojkob, G., Blazewicza, S., 2014. Effect of nanosilicon carbide on the Carbonizationprocess of coal tar pitch. *Journal of Analytical and Applied Pyrolysis* 107, 191–196.

Milioli, F.E., Foster, P.J. 1995. A model for particle size distribution and elutriation in fluidized beds. *Powder Technology* 83, 265 – 280.

Martínez, I., Mohamed, M.E., Santos, V.E., García, J.L., García-Ochoa, F., Díaz, E., 2017. Metabolic and process engineering for biodesulfurization in Gram-negative bacteria. *Journal of Biotechnology* 262, 47– 55.

Martínez, I., Dı´ez, C., Miles, N., Shah, C., Mora´n, A., 2003. Biodesulphurization as a complement to the physical cleaning of coal. *Fuel* 82, 1085 –1090.

Mastral, A.M., Calle´n, M.S., Garcia, T., 2000. Toxic organic emissions from coal combustion. *Fuel Processing Technology* 67, 1 – 10.

Matin, S.S., Chelgani, S.C., 2016. Estimation of coal gross calorific value based on various analyses by random forest method. *Fuel* 177, 274 –278.

Medircio, S.N., Leão, V.A., Teixeira, M.C., 2006. Specific growth rate of sulfate reducing bacteria in the presence of manganese and cadmium. *Journal of Hazardous Materials* 143, 593 – 596.

Meshram, P., Purohit, B.K., Sinha, M.K., Sahu, S.K., Pandey, B.D., 2015. Demineralization of low grade coal – A review. *Renewable and Sustainable Energy Reviews* 41, 745 –761.

Mishra, S., Panda, P.P., Pradhan, N., Satapathy, D., Subudhi, U., Biswal, S.K., Mishra, B. K., 2014. Effect of native bacteria *Sinomonas flava 1C and Acidithiobacillus ferrooxidans* on biodesulphurization of Meghalaya coal and its combustion properties. *Fuel* 117, 415 – 421.

Mketo, N., Nomngongo, P.N., Ngila, J.C., 2016. Evaluation of different microwave-assisted dilute acid extracting reagents on simultaneous coal biodesulphurization and demineralization. *Fuel* 163, 189 –195.

Mketo, N., Nomngongo, P.N., Ngila, J. C., 2018. Environmentally friendly microwave-assisted sequential extraction method followed by ICP-OES and ion-chromatographic analysis for rapid determination of sulphur forms in coal samples. *Talanta* 182, 567– 573.

Monod, J., 1949. The growth of bacterial cultures. *Annual Reviews in Microbiology* 3, 371 – 394.

Moosa, S., Nemati, M., Harrison, S.T.L., 2005. A kinetic study on anaerobic reduction of sulphate, part II: incorporation of temperature effects in the kinetic model. *Chemical Engineering Science* 60, 3517 – 3524.

Mukherjee, S., Borthakur, P.C., 2001. Chemical demineralization/desulphurization of high sulphur coal using sodium hydroxide and acid solutions. *Fuel* 80, 2037 – 2040.

Mukherjee, S, Borthakur, P.C., 2003. Effect of leaching high sulphur subbituminous coal by potassium hydroxide and acid on removal of mineral matter and sulphur. *Fuel* 82, 83 – 788.

Nakagawa, T., Suzukic, T., Furusawab, A., Maeno, Y., Komaki, L., Nishikawaa, K., 1998. Influence of fine particles on carbon deposition in the coke oven chamber. *Fuel* 77, 1141–1146.

Ndaji, F.E., Imobighe, G.A., 1989. Controlling effects of Ash, Total Sulphur and Chemical Forms of Sulphur in Coals on The Selection of Components of Coal Blends for Making Metallurgical Cokes. *Fuel Processing Technology* 21, 49 – 61.

Nelder, J., Mead, R., 1965. A simplex method for function minimization. *Computer Journal 7*, 308 – 313

Nkhalambayausi-Chirwa, E.M, Wang, Y.T. 2001. Simultaneous chromium(VI) reduction and phenol degradation in a fixed-film coculture bioreactor: reactor performance. *Water Research* 35, 921-32.

Nomura, S., Arima, T., 2008. The cause of the uneven carbonization process in wet coal charging in coke oven chamber. *Fuel* 87, 3240 – 3246.

Nomura, S., Arima, T., 2013. Effect of Coke Contraction on Mean Coke Size, *Fuel* 105, 176 –183.

Nomura, S., Arima, T., 2017. Influence of binder (coal tar and pitch) addition on coal caking property and coke strength. *Fuel Processing Technology* 159, 369 – 375.

Nomura, S., Kato, K., 2006. The effect of plastic size on coke quality and coking pressure in the co-Carbonizationof coal/plastic in coke oven. *Fuel* 85, 47– 56.

North, L., Blackmore, K., Nesbitt, K., Mahoney, M.R., 2018. Models of coke quality prediction and the relationships to input variables: A review. *Fuel* 219, 446 – 466.

Ochoa-González, R., Díaz-Somoano, M., Martínez-Tarazona, M.R., 2013. Effect of anion concentrations on Hg2+ reduction from simulated desulphurization aqueous solutions. *Chemical Engineering Journal* 214, 165 –171.

O'Keefe, J.M.K., Bechtel, A., Christanis, K., Dai, S., DiMichele, W.A., Eble, C.F., Esterle, J.S., Mastalerz, M., Raymond, A.L., Valentim, B.V., Wagner, N.J., Ward, C.R., Hower, J.C., 2013. On the fundamental difference between coal rank and coal type. *International Journal of Coal Geology* 118, 58 – 87.

Olson, G.J., 1994. Prospects for biodesulfurization of coal: mechanisms and related process designs. *Fuel Processing Technology* 40, 103 – 114.

Olson, G.J., Brinckman, F.E., 1986. Bioprocessing of coal. *Fuel* 65, 1638 – 1646.

Olson, G.J., Kelly, R.M., 1991. Chemical and microbiological problems associated with research on the biodesulfurization of coal. A review. *Resources, Conservation and Recycling* 5, 183 – 193.

Orsi, N., Rossi, G., Trois, P., Valenti, P.D., Zecchin, A., 1991. Coal biodesulfurization: design criteria of a pilot plant. *Resources, Conservation and Recycling* 5, 211 – 230.

Ozonoh, M., Aniokete, T.C., Oboirien, B.O., Daramola, M.O., 2018. Techno-economic analysis of electricity and heat production by co-gasification of coal, biomass and waste tyre in South Africa. *Journal of Cleaner Production* 201, 192 – 206.

Özbas Bozdemir, T., Durusoy, T., Tanyolaç, A., Yürüm, Y., 1993. The factors affecting the growth kinetics of Sulfolobus solfataricus, a sulphur removing bacterium. *Fuel Processing Technology* 33, 61–75.

Özbas Bozdemir, T., Durusoy, T., Erincin, E., Yürüm, Y., 1996. Biodesulfurization of Turkish lignites: 1. Optimization of the growth parameters of Rhodococcus rhodochrous, a sulphur-removing bacterium. *Fuel* 75, 1596 – 600.

Panaitescu, C., Predeanu, G., 2007. Microstructural characteristics of toluene and quinoline-insolubles from coal–tar pitch and their cokes. *International Journal of Coal Geology* 71, 448 – 454.

Pandey, R.A., Raman, V.K., Bodkhe, S.Y., Handa, B.K., Bal, A.S., 2005. Microbial desulphurization of coal containing pyritic Sulphur in a continuously operated bench scale coal slurry reactor. *Fuel* 84, 81– 87.

Patrick, J.W., Reynolds, M.J., walker, A., 1983. Carbonizationof coal-tar pitches: effect of rank of parent coal. *Fuel* 62, 129 –130.

Petzold, L., 1983. Adescription of DASSL: A differential/algebraic system solver. In Stepleman, R. E., editor, Scientific Computing, IMACS/North-Holland, pages 65- 68.

Pokorna, D., Zabranska, J., 2015. Sulfur-oxidizing bacteria in environmental technology. *Biotechnology Advances* 33, 1246 –1259.

Prasassarakich, P., Pecharanond, P., 1992. Kinetics of coal desulphurization in aqueous copper (II) sulphate. *Fuel* 71, 929 – 933.

Prasassarakich P., Thaweesri, T. 1996. Kinetics of coal desulfurization with sodium benzoxide. *Fuel* 75, 816 – 820.

Prayuenyong, P., 2002. Coal biodesulfurization processes. *Songklanakarin Journal of Science and Technology* 24, 493 – 507.

Plancher, H., Agarwal, P.K., Severns, R., 2002. Improving form coke briquette strength, *Fuel Processing Technology* 79, 83–92.

Qian, J., Zhang, K., 1998. China's desulfurization potential. *Energy Policy* 26, 345 – 351.

Quick, J.C., Brill, T., 2002. Provincial variation of carbon emissions from bituminous coal: influence of inertinite and other factors. *International Journal of Coal Geology* 49, 263 – 275.

Rai, C., Reyniers, J.P., 1988. Microbial desulphurization of coals by organisms of the genus Pseudomonas. *Biotechnology Progress* 4, 225 –230.

Ralston, M., Jennrich, R. 1978. DUD – a derivative-free algorithm for non-linear least squares. Technometrics, 20, 7 – 14.

Rechert, P., 1998. Computer program for the identification and simulation of Aquatic systems - AQUASIM 2.0: User Manual. Swiss Federal Institute for Environmental Science and Technology (EAWAG), CH-8600 Dübendorf, Switzerland.

Roberts, D.L., 1988. The relationship between macerals and sulphur content of some South African Permian coals. *International Journal of Coal Geology* 10, 399 – 410.

Rokni, E., Panahi, A., Ren, X., Levendis, Y.A., 2016. Curtailing the generation of sulfur dioxide and nitrogen oxide emissions by blending and oxy-combustion of coals. *Fuel* 181, 772 –784.

Rolfe, M.D., Rice, J.C., Lucchini, S., Pin, C., Thompson, A., Cameron, A.D.S., Alston, M., Stringer, M.F., Betts, R.P., Baranyai, J., Peck, M.W., Hinton, J.C.D. 2012. Lag phase is a distinct growth phase that prepares bacteria from expontential growth and involves transient metal accumulation. *The Journal of Bacteriology* 194, 686 – 701.

Rossi, G., 2014. The Microbial Desulfurization of Coal. *Advances in Biochemical Engineering/Biotechnology* 142, 147–167.

Rossi, G. 1993. Biodepyritization of coal: achievements and problems. *Fuel* 72, 1581 – 1592.

Roslev, P., Iversen, N., Henriksen, K., 1998. Direct fingerprinting of metabolically active bacteria in environmental samples by substrate specific radiolabeling and lipid analysis. *Journal of Microbiological Methods* 31, 99 – 111.

Runnion, K.N., Combi, J.D., 1990. Microbial removal of organic sulfur from coal. 2/62–2/76.

Saha, M., Dally, B.B., Medwell, P.R., Chinnici, A., 2017. Effect of particle size on the mild combustion characteristics of oulverized brown coal. Fuel Processing Technology 155, 74 – 87.

Saikia, B.K., Dalmora A.C., Choudhury R., Das T., Taffarel, S.R., Silva, L.F.O., 2016. Effective removal of sulfur components from Brazilian power-coals by ultrasonication (40 kHz) in presence of H_2O_2. *Ultrasonics Sonochemistry* 32, 147–157.

Saikia, B.K., Dutta, A.M., Saikia, L., Ahmed, S., Baruah, B.P., 2013. Ultrasonic assisted cleaning of high sulphur Indian coals in water and mixed alkali. *Fuel Processing Technology* 123, 107–113.

Saikia, B.K., Dutta, A.M., Saikia, L., Baruah, B.P., 2014a. Feasibility studies of desulphurization and de-ashing of low grade medium to high sulphur coals by low energy ultrasonication. *Fuel* 123, 12 – 18.

Saikia, B.K., Khound, K., Baruah, B.P., 2014b. Extractive de-sulfurization and de-ashing of high sulfur coal by oxidation with ionic liquids. *Energy Conversion and Management* 81, 298 –305.

SANS 11722, 2005. Solid minerals fuels — Determination of moisture in the general analysis test sample by drying in nitrogen.

Santhosh Raaj, S., Arumugam, S., Muthukrishnan, M., Krishnamoorthy, S., Anantharaman, N., 2016. Characterization of coal blends for effective utilization in thermal power plants. *Applied Thermal Engineering* 102, 9 –16.

Saxena, V.K., Varma, A.K., Kumar, G., 2010. Effect of Stamping and Binder on coke quality for LVMC coal. Proceedings of the XI International Seminar on Mineral. *Fuel Processing Technology* 489 – 497.

Scholtz, V., Magudulela, D.S., van Zyl, F., Coetzee, A., Humpel, A., Hill, C., Potgieter, A.J., 2006. Added Value Long Steel Products produced at MSSA Newcastle Works, *Journal of the Southern African Institute of Mining and Metallurgy* 151 – 170.

Scott, A.C., 2002. Coal petrology and the origin of coal macerals: a way ahead? *International Journal of Coal Geology* 50, 119 – 134.

Shah, C.L., Abbott, J.A., Miles, N.J., Xuejun, L., Jianping, X., 2002. Sulphur reduction evaluation of selected high-sulphur Chinese coals. *Fuel* 81, 519 – 529.

Shen, Y., Sun, T., Jia, J., 2012. A novel desulphurization process of coal water slurry via sodium metaborate electroreduction in the alkaline system. *Fuel* 96, 250 –256.

Shevkoplyas, V.N., 2002. Coal Carbonizationwith addition of hydrochloric acid as a way of improving coke quality. *Fuel* 81, 947– 950.

Short, W., Packey, D.J., Holt, T., 1995. A manual for the economic evaluation of energy efficiency and renewable energy technologies.

Shui, H., Li, H., Chang, H., Wang, Z., Gao, Z., Lei, Z., Ren, S., 2011. Modification of sub-bituminous coal by steam treatment: Caking and coking properties. *Fuel Processing Technology* 92, 2299 –2304.

Si, T., Cheng, J., Zhou, F., Zhou, J., Cen, K., 2017. Control of pollutants in the combustion of biomass pellets prepared with coal tar residue as a binder. *Fuel* 208, 439 – 446.

Siddhartha, R.K., 2013. Coal Characterisation and Design for Fossil Fuel Fired Boiler in Thermal Power Plants. *JOTITT* 1, 1–14.

Singleton, T.C., 2010. The decision to install flue gas desulphurisation on Medupi Power Station: Identification of environmental criteria contributing to the decision making process. MSc Thesis. University of The Witwatersrand. Available online: http://wiredspace.wits.ac.za/handle/10539/8387, Accessed March 2018.

Spörl, R., Maier, J., Scheffknecht, G., 2013. Sulphur Oxide Emissions from Dust-Fired Oxy-Fuel Combustion of Coal. *Energy Procedia* 37, 1435 – 1447.

Şenera, B., Aksoy, D.Ö., Çelika, P.A., Toptaş, Y., Koca, S., Kocad, H., Çabuke, A., 2018. Fungal treatment of lignites with higher ash and sulphur contents using drum type reactor. *Hydrometallurgy* 182, 64 – 74.

Sloss, L.L., 2014. Blending of coals to meet power station requirements. *IEA Clean Coal Centre*, 1– 68.

Snyman, C.P., 1989. The role of coal petrography in understanding the properties of South African coal. *International Journal of Coal Geology* 14, 83–101.

Srivastava, R.K., Jozewicz, W., 2001. Flue gas desulphurization: the state of the art. *Journal of the Air & Waste Management Association* 51, 1676 –1688.

Stern, D.I., 2005. Global sulfur emissions from 1850 to 2000. *Chemosphere* 58, 63 – 175.

Stevens, S.E., Burgess, W.D., 1989. Microbial desulfurization of coal. US Patent # 48511350.

Tang, K., Baskaran, V., Nemati, M., 2009. Bacteria of the sulphur cycle: An overview of microbiology, biokinetics and their role in petroleum and mining industries. *Biochemical Engineering Journal* 44, 73 – 94.

Taylor, J.W., Coban, A., 1987. Factors affecting the tensile strength of formed coke made from lignite char, *Fuel* 66, 1274 – 1280.

Teichmüller, M., 1989. The genesis of coal from the viewpoint of coal petrology, *International Journal of Coal Geology* 12, 1 – 87.

Thompson, J.D., Gibson, T.J., Plewniak, Jeanmougin, F., Giggins, D.G., 1997. The CLUSTAL_X Windows Interface: Flexible Strategies for Multiple Sequence Alignment Aided by Quality Analysis Tools. *Nucleic Acids Research* 25, 4876 – 4882.

Tsorakidis, N., Papadoulos, S., Zerres, M., Zerres, C.H., Break-even analysis, ISBN 978-87-7681-290-4.

Van Afferden, M., Schacht, S., Klein, J., Trüper, H.G., 1990. Degradation of dibenzothiophene by Brevibacterium sp. DO. *Archives of Microbiology* 153, 324 –328.

Van Niekerk, D., Pugmirec, R.J., Solum, M.S., Painter, P.C., Mathews, J.P., 2008. Structural characterization of vitrinite-rich and inertinite-rich Permian-aged South African bituminous coals. *International Journal of Coal Geology* 76, 290 – 300.

Varma, A.K., 2002. Thernogravimetric investigation in prediction of coking behaviour and coke properties derived from inertinite rich coals. *Fuel 81*, 1321–1334.

Vekemans, O., Laviolette, J.P., Chaouki, J., 2016. Co-combustion of coal and waste in pulverized coal boiler. *Energy* 94, 742 – 754.

Verma, V.K., Bram, S., Delattin, F., De Ruyck, J., 2013. Real life performance of domestic pellet boiler technologies as a function of operational loads: A case study of Belgium. *Applied Energy* 101, 357 – 362.

Vasilakos, N.P., Clinton, C.S., 1984. Chemical beneficiation of coal with aqueous hydrogen peroxide/sulphuric acid solutions. *Fuel* 63, 1561 – 1563.

Vijayalakshmi, S.P., Raichur, A.M. 2003. The utility of *Bacillus subtilis* as a bio-flocculant for fine coal. *Colloids and Surfaces B: Biointerfaces* 29, 265 – 275.

Wagner, N.J., Tlotleng, M.T., 2012. Distribution of selected trace elements in density fractionated Waterberg coals from South Africa. *International Journal of Coal Geology* 94, 225 –237.

Warzinski, R.P., Friedman, S. 1977. Chemical Cleaning of Coal. *The Journal of Engineering for Gas Turbines and Power 99*, 361– 364.

Wang, P., Jin, L., Liu, J., Zhu, S., Hu, H., 2013. Analysis of coal tar derived from pyrolysis at different atmospheres. *Fuel* 104, 14 –21.

Wagner, N.J., Tlotleng, M.T., 2012. Distribution of selected trace elements in density fractionated Waterberg coals from South Africa. *International Journal of Coal Geology* 94, 225 – 237.

Weerasekara, N.S., Garcı´a Frutos, F.J., Cara, J., Lockwood, F.C., 2008. Mathematical modelling of demineralisation of high sulphur coal by bioleaching. *Minerals Engineering* 21, 234 –240.

Xiong, T., Jiang, W., Gao, W., 2016. Current status and prediction of major atmospheric emissions from coal-fired power plants in Shandong Province, China. *Atmospheric Environment* 124, 46 –52.

Ye, J., Zhang, P., Zhang, G., Wang, S., Nabi, M., Zhang, Q., Zhang, H., 2018. Biodesulfurization of high sulfur fat coal with indigenous and exotic microorganisms. *Journal of Cleaner Production* 197, 562 – 570.

Yingzhong, T., Qin, Z., Yun, T., Yueqin, Q., Zhihong, L., Tin, H., Peiliang, Z., Xiaofen, H., Ren, S., Xiao, T. 2010. Float-Sink Desulfurization of high – sulphur coal from Puan Country, Guizhou Province, PRC. *Petroleum & Coal* 52, 249 – 253.

You, C.F., Xu, X.C., 2010. Coal combustion and its pollution control in China. *Energy* 35, 4467– 4472.

Yu, A.B., Standish, N., Lu, L., 1995. Coal agglomeration and its effect on bulk density, *Powder Technology* 82, 177 –189.

Zhao, Y., Wang, S., Duan, L., Lei, Y., Cao, P., Hao, J., 2008. Primary air pollutant emissions of coal-fired power plants in China: Current status and future prediction. *Atmospheric Environment* 42, 8442 – 8452.